Storage demand in highly renewable energy scenarios for Europe:
The influence of methodology and data assumptions in model-based assessments

A thesis accepted by the faculty of ENERGY-, PROCESS- and BIO-ENGINEERING of the University of Stuttgart
in partial fulfillment of the requirements for the degree of

DOCTOR OF ENGINEERING SCIENCE (Dr.-Ing.)

by

Felix Cebulla

born in Weimar, Germany

1. Examiner	Prof. Dr. André Thess
2. Examiner	Prof. Dr. Kai Hufendiek
Date of defense	27 November 2017

Institute of Energy Storage, University of Stuttgart

2017

DLR Deutsches Zentrum für Luft- und Raumfahrt
German Aerospace Center
Institute of Engineering Thermodynamics

University of Stuttgart
Germany

ABSTRACT

Future low-carbon energy systems are likely to rely on power generation from variable, renewable energies (VRE) sources, thus fostering an increased demand for flexibility options which can balance mismatches of power demand and supply. Electrical energy storage (EES) is a promising option to tackle this matter and its required capacity is typically studied with model-based assessments. However, such analyses barley account for uncertainties in data assumptions or the chosen methodology, and, in consequence, lack an understanding of the robustness of the derived EES capacity. Therefore, this thesis aims to shed light on the main drivers for EES demand in highly renewable European energy systems in a comprehensive approach, considering parametric and methodological uncertainty.

Using and enhancing the linear optimization model REMix, this study analyzes the required storage capacity and its utilization for northern, western, and central Europe in energy scenarios with high shares of renewable power generation (> 80%). The robustness of the storage capacity was tested against a large set of parameter variations (e.g. cost parameters or the meteorological year as input for VRE power) and methodological assumptions. The latter include different levels of technological detail (e.g. modeling approaches for thermal power plants), variations in the spatial and temporal resolution, as well as more general assumptions (e.g. restricted curtailments).

In the reference scenario an overall EES capacity of approximately 200 GW and 30 TWh for Europe was derived. These results are particularly sensitive to investment costs variations of EES and VRE technologies (I) and to assumptions regarding the transmission grid infrastructure (II).

(I) Reduced costs for storage and higher investment costs for VRE technologies increase the need for EES to 270 GW/55 TWh and to 235 GW/38 TWh, respectively.

(II) Reducing transmission grid congestions can lower the ESS demand considerably, however, the analysis also showed that—even in the scenario which favor transmission the most (i.e. low investment costs for grid expansion)—around 120 GW of storage converter power and 13 TWh of storage unit capacity is still required for temporal balancing. In this sense, grid expansion and storage are not complete substitutes, but complementing flexibility options, both essential for future energy systems with high shares of VRE power generation.

Moreover, the model-endogenously derived EES capacity mix in all scenarios is technology-diverse, underlining the necessity for a balanced storage portfolio. These findings are supported by the high dependency of the spatial capacity distribution of storage with the regionally predominant VRE technology and its temporal power generation characteristics. In this regard, significant correlations between the electricity generation from offshore and onshore wind systems with hydrogen storage charging are observed. Onshore wind power production also correlates with adiabatic compressed air storage, whereas the generation of photovoltaic systems is predominantly balanced by stationary lithium-ion batteries.

To analyze the impact of the technological detail on storage demand, a comparison of two approaches for modeling thermal power plants was carried out: a detailed, mixed-integer unit-commitment approach and a simplified economic dispatch method. The results indicate that for larger observation areas (e.g. Europe) with high VRE shares, in-depth modeling is not necessarily required, however, analyses for smaller model regions in combination with lower VRE penetration levels can greatly benefit from detailed power plant modeling.

ZUSAMMENFASSUNG

Strom aus regenerativen, fluktuierenden Ressourcen (fRE) bildet den wichtigsten Baustein für die Realisierung einer weitgehend CO_2-neutralen Energieversorgung in Europa. Die begrenzte Regelbarkeit der Stromeinspeisung erneuerbarer Erzeuger, wie insbesondere der Photovoltaik (PV) und der Windkraft, erfordert jedoch eine erhöhte Flexibilität im Energieversorgungssystem. Stromspeicher (SP) können dabei einen wichtigen Beitrag liefern und die Abschätzung ihres Bedarfs erfolgt zumeist modellgestützt. Der Einfluss von datenseitigen, als auch methodischen Annahmen wird jedoch in diesen Analysen zumeist vernachlässigt. Die vorliegende Arbeit untersucht daher die Robustheit der benötigten Speicherkapazität in europäischen Szenarien mit hohen Anteilen erneuerbarer Stromerzeugung (> 80%) und identifiziert Haupteinflussfaktoren auf den Stromspeicherbedarf.

Mithilfe des linearen optimierenden Energiesystemmodells REMix, welches im Rahmen der Dissertation erweitert wurde, wurde die Robustheit des europäischen Speicherbedarfs hinsichtlich einer Vielzahl an Parametervariationen (bspw. Kostenannahmen oder unterschiedliche Wetterjahre) und methodischen Annahmen getestet. Letztere beinhalten verschiedene Detailierungsgrade hinsichtlich der technologischen (bspw. Modellierungsansätze für thermische Kraftwerke), räumlichen und zeitlichen Auflösung.

Im Referenzszenario für Europa ergibt sich eine Gesamtkapazität an SP von circa 200 GW und 30 TWh. Diese Ergebnisse sind insbesondere sensitiv hinsichtlich der Investitionskostenannahmen für SP und fRE (I), sowie in Bezug auf Annahmen zur Übertragungsnetzinfrastruktur (II).

(I) Reduzierte Investitionskosten für SP und höhere Kosten für fRE-Technologien lassen den Speicherbedarf auf 270 GW/55 TWh beziehungsweise 235 GW/38 TWh ansteigen.

(II) Eine Reduktion von Netzengpässen im Übertragungsnetz kann den Bedarf für SP deutlich verringern. Die Analyse zeigt jedoch auch, dass Netzausbau und SP sich nicht vollständig substituieren, sondern vielmehr komplementäre Flexibilitätsoptionen sind. Selbst in Szenarien, die den Netzausbau am stärksten begünstigen (niedrige Investitionskosten), verbleibt eine SP-Kapazität von rund 120 GW und 13 TWh, um zeitliche Diskrepanzen von Strombedarf und -erzeugung auszugleichen.

Die modell-endogen errechneten SP-Kapazitäten unterstreichen zudem die Notwendigkeit ausgeglichener, diversifizierter Speicherportfolios, in denen jede Technologie ihre Nische besetzt. Die Analyse zeigt, dass eine signifikante Abhängigkeit der räumlichen Verteilung der SP-Kapazitäten von den lokalen fRE Potenzialen sowie deren zeitlichen Stromerzeugungsprofilen existiert. In diesem Sinne ergeben deutliche Korrelationen zwischen der Beladung von Wasserstoffspeichern und der Stromerzeugung aus onshore und offshore Windkraft sowie zwischen onshore Windkraft und adiabaten Druckluftspeichern. Die Stromerzeugung aus PV-Anlagen korreliert hingegen stärker mit der Nutzung von stationären Lithium-Ionen-Batterien.

Um den Einfluss von technologischen Detailierungsgraden auf den SP-Bedarf zu evaluieren, wurden zwei Ansätze zur Modellierung konventioneller Kraftwerke verglichen: eine detaillierte, gemischt-ganzzahlige Methodik (unit commitment), sowie ein vereinfachter Ansatz (economic dispatch). Die Ergebnisse zeigen, dass die vereinfachte Methodik hinreichend ist, solang der Fokus auf größeren Betrachtungsgebieten (z.B. Europa) mit hohen fRE Stromerzeugungsanteilen liegt. Analysen für kleinere Regionen in Kombinationen mit niedrigen Anteilen von fRE können hingegen stark von einer detaillierten Kraftwerksmodellierung profitieren.

Acknowledgements

This work would have not been possible without the help and support of many dedicated colleagues and friends. A very special thanks to Prof. André Thess and Prof. Kai Hufendiek for supervising my thesis and their guidance throughout this work. I would also like to thank Carsten Hoyer-Klick, Christoph Schillings, and all other colleagues of the department of Systems Analysis and Technology Assessment at DLR, providing such a stimulating research and work environment. A very special thanks to Thomas Pregger, Tobias Naegler, and Yvonne Scholz for supervising this thesis and supporting me throughout my work. My sincere thanks to Hans Christian Gils, Karl-Kiên Cao, Tobias Fichter, Denis Hess, Manuel Wetzel, and Kai von Krbek for their valuable input for this work, refreshing discussions within the REMix group, and proof-reading. Thanks also to Prof. Mark Z. Jacobson who provided me the opportunity to visit Stanford University for a research stay. Finally, I would like to especially thank my family who supported me at all times.

This research was funded by the Helmholtz Research School on Energy Scenarios. Thanks to all for supporting this research and the education in energy scenarios and modeling.

Contents

List of Tables

List of Figures

List of Acronyms

AC	Alternating current
aCAES	Adiabatic compressed air storage
BEV	Battery electric vehicle
CAES	Compressed air storage
CAPEX	Capital expenditure costs
CCGT	Combined cycle gas turbine
CHP	Combined heat and power
CSP	Concentrating solar thermal power
DC	Direct current
dCAES	Diabatic compressed air storage
DOD	Depth of discharge
E2P	Energy-to-power ratio
ED	Economic dispatch
EES	Electrical energy storage
EEX	European Energy Exchange
EnDAT	Energy Data Analysis Tool
ENTSO-E	European Network of Transmission System Operators for Electricity
EUMENA	Europe, Middle East, and North Africa
GAMS	General algebraic modeling system
GT	Gas turbine
H_2	Hydrogen
Li-ion	Lithium ion battery storage
LP	Linear programming
MILP	Mixed-integer linear programming
NaS	Sodium-sulfur battery storage
Nb	Number of power blocks within a power plant or power plant cluster
NC	Total number of storage cycles
NC_{typ}	Total number of typical storage cycles
NFC	Total number of storage full cycles
NLP	Non-linear programming
NTC	Net transfer capacity
OPEX	Operating expenditures
OptiMo	Optimization model
O&M cost	Operations and maintenance costs
PEM	Polymer electrolyte membrane
PHS	Pumped hydro storage
PtG	Power to gas storage
PV	Photovoltaic
REMix	Renewable Energy Mix model
SOC	State of charge
TES	Thermal energy storage
TYNDP	Ten Year Network Development Plan
UC	Unit-commitment
UPS	Uninterruptible power supply
VRE	Variable renewable energy
WEPP	World Electric Power Plants Database

List of Symbols

Indices

$x \in X$		Technologies
$t \in T$	[1,2,3…8760]	Time
$n \in N$		Model regions
g_x		Initial uptime periods
l_x		Initial downtime periods

Parameter

α	[-]	Annual theoretical power generation share of PV and wind power systems w.r.t. the overall theoretical power generation from VRE
β	[-]	Annual theoretical power generation share of PV systems w.r.t. the overall theoretical power generation from VRE
Δt	[h]	Length of one time-step
$P_{Wind}(t)$	[GWh_{el}/h]	Theoretical electricity generation from wind power w.r.t. annual elec. demand
$P_{PV}(t)$	[GWh_{el}/h]	Theoretical electricity generation from PV systems w.r.t. annual elec. demand
D	[GWh_{el}]	Annual electrical demand
$P'_x(t)$	[GWh_{el}/h]	Actual electricity generation from technology x
σ_x	[-]	Actual generation share of technology x
σ_x^{LP}	[-]	Technology-specific generation share in simplified merit order dispatch (LP)
σ_x^{MILP}	[-]	Generation share in unit-commitment with economic dispatch (MILP)
$\Delta \sigma_x$	[%]	Generation share difference between economic dispatch and unit-commitment
$f_x^{Annuity}$	[-]	Technology-specific annuity factor
cur_x		Technology-specific curtailment share
$P_{x,n}^{Cap\_Installed}$	[GW_{el}]	Exogenous stock of installed generation capacity
$P_{x,n}^{Cap\_Total}$	[GW_{el}]	Maximum of installable generation capacity
$p_{x,n}^{PotGen}$	[-]	Normalized, potential, technology and region-specific generation from VRE
$P_{x,n}^{Stor\_Installed}$	[GW_{el}]	Exogenous stock of installed storage converter capacity (power-related)
$P_{x,n}^{Stor\_Total}$	[GW_{el}]	Maximum of installable storage converter capacity (power-related)
$E_{x,n}^{Stor\_Installed}$	[GWh_{el}]	Exogenous stock of installed storage unit capacity (energy-related)
$E_{x,n}^{Stor\_Total}$	[GW_{el}]	Maximum of installable storage unit capacity (energy-related)
η_x^{Net}	[-]	Technology-specific net efficiency of generation technologies
η_x^{Net}	[-]	Technology-specific gross efficiency of generation technologies
$\eta_x^{Stor\_Char}$	[-]	Technology-specific charging efficiency of storage
$\eta_x^{Stor\_Dischar}$	[-]	Technology-specific discharging efficiency of storage
$\mu_x^{Stor\_Selfdischar}$	[1/h]	Technology-specific self-discharge rate of storage
c_x^{Fuel}	[€/MWh_{therm}]	Technology-specific fuel costs
$c^{W\&T}$	[€/MWh_{el}/h]	Specific costs wear and tear
c^{Slack}	[€/MWh_{el}/h]	Specific costs for artificial load or generation
f_x^{CO2}	[t CO_2/MWh_{therm}]	Specific emission factor
c_x^{CO2}	[€/t CO_2]	Specific CO_2 emission costs
c_x^{Inv}	[€/GW_{el}]	Technology-specific overnight investment costs
i	[-]	Discount rate
N_x^{AmorT}	[a]	Technology-specific amortization time
τ_x	[-]	Generation technology availability
Φ	[h/days]	Average length of a typical cycle NC_{typ}
κ_x	[1/0]	Initial commitment status of a power plant unit, cluster, or power block

δ_x	[GW_{el}]	Typical power plant block or cluster size
λ_x^{Min}	[-]	Minimum load rate of the a power plant unit, cluster, or power block
λ_x^{Part}	[-]	Part load rate of the a power plant unit, cluster, or power block
A1	[-]	Ambient temperature correction factor 1
A2	[-]	Ambient temperature correction factor 2
A3	[-]	Ambient temperature correction factor 3
A4	[-]	Ambient temperature correction factor 4
A5	[-]	Ambient temperature correction factor 5
A6	[-]	Ambient temperature correction factor 6
$\theta_{n,t}$	[°C]	Ambient temperature at model region *n* and time-step *t*
UT_x	[h]	Minimum up time of technology *x*
DT_x	[h]	Minimum down time of technology *x*

Variables

C^{Total}	[k€/a]	Annual overall system cost
C^{Inv}	[k€/a]	Annual investment costs for capacity expansion
C^{Op}	[k€/a]	Annual operating costs
C^{Slack}	[k€/a]	Annual penalty costs for artificial generation or load
C^{Op_Fuel}	[k€/a]	Annual fuel costs
$C^{O\&M\_Var}$	[k€/a]	Annual variable operations and maintenance costs
$C^{O\&M\_Fix}$	[k€/a]	Annual fixed operations and maintenance costs
$C^{Op\_W\&T}$	[k€/a]	Annual wear and tear costs
C^{Op_CO2}	[k€/a]	Annual emission certificate costs
$P_{x,n}^{Cap\_Added}$	[GW_{el}]	Capacity expansion of additional generation units
$P_{x,n}^{Stor\_Added}$	[GW_{el}]	Expansion of storage converter capacity (power-related)
$E_{x,n}^{Stor\_Added}$	[GWh_{el}]	Expansion of storage unit capacity (energy-related)
$E_{x,n}^{Stor\_Level}(t)$	[$GWh_{el\ eq}$]	Model region and technology-specific storage level
$P_{x,n}^{Gen}(t)$	[GWh_{el}/h]	Model region and technology-specific power generation
$P_{x,n}^{Stor\_Dis}(t)$	[GWh_{el}/h]	Model region and technology-specific discharging power from storage
$P_{x,n}^{Stor\_Char}(t)$	[GWh_{el}/h]	Model region and technology-specific charging power from storage
$P_{x,n}^{Grid\_Exp}(t)$	[GWh_{el}/h]	Model region and technology-specific exported electricity
$P_{x,n}^{Grid\_Imp}(t)$	[GWh_{el}/h]	Model region and technology-specific imported electricity
$P_{x,n}^{Grid\_Loss}(t)$	[GWh_{el}/h]	Model region and technology-specific grid losses
$P_n^{Slack\_Pos}(t)$	[GWh_{el}/h]	Model region and technology-specific artificial generation
$P_n^{Slack\_Neg}(t)$	[GWh_{el}/h]	Model region and technology-specific artificial load
$P_{x,n}^{W\&T\_Pos}(t)$	[GWh_{el}/h]	Model region and technology-specific positive power change in two hours
$P_{x,n}^{W\&T\_Neg}(t)$	[GWh_{el}/h]	Model region and technology-specific negative power change in two hours
$C_{x,n}^{W\&T\_Total}$	[GWh_{el}]	Model region and technology-specific total wear and tear costs
$E_{x,n}^{FuelCons}(t)$	[GWh_{el}]	Model region and technology-specific fuel consumption
$On_{x,n}(t)$	[1,2,3…n]	Number of operating power plant units, cluster, or power blocks
$Start_{x,n}(t)$	[1,2,3…n]	Start-up process of a power plant unit, cluster, or power block
$P_{x,n}^{Gen_{P1}}(t)$	[GWh_{el}/h]	Model region and technology-specific power generation in generation range 1
$P_{x,n}^{Gen_{P2}}(t)$	[GWh_{el}/h]	Model region and technology-specific power generation in generation range 2
$C_x^{Op\_RampUp}(t)$	[k€/h]	Technology-specific up ramping costs at time-step *t*
$C_x^{Op\_RampDown}(t)$	[k€/h]	Technology-specific down ramping costs at time-step *t*
$C_x^{Op\_RampTotal}(t)$	[k€/h]	Total technology-specific ramping costs at time-step *t*

1 Introduction

The reduction of anthropogenic greenhouse gas (GHG) emissions is one of the main challenges for our society to prevent climate change [1]. An increase of the atmospheric GHG concentration not only imposes the risk of severe and irreversible damage to biodiversity and human health [2] but also has negative impacts on the economic system. In this regard, GHG mitigation is cheaper than to remain in business as usual [3]. To avoid the worst impacts on nature and human systems, GHG emissions essentially have to be kept below 450 ppm CO_2 equivalent by 2100 [4]. In 2010, CO_2 emissions from fossil fuel combustion and industrial processes accounted for 65% of the worldwide CO_2 equivalent emissions (49 Gt). To achieve decarbonization in the power sector, electricity generation technologies which rely on renewable resources (e.g. wind, solar, water) are a promising option [4]. By this means, the main benefits of renewable energy (RE) technologies are threefold. First, equivalent CO_2 emissions over the lifecycle of RE systems are in the order of a magnitude lower than for thermal power generation technologies, such as coal or gas-fired power plants (see e.g. [5–8]). Second—opposed to conventional power plants which are dependent on exhaustible fossil fuels [9]—the annual flows of RE resources exceed the global energy demand significantly [10]. Apart from this supply security, RE technologies are therefore also less prone to increases in resource prices. Finally, wind and photovoltaic (PV) systems recently have been undergoing significant cost reductions (see e.g. [11–14] for PV and [15–17] for wind), making them competitive or even cheaper with other, more traditional, power generation technologies. Consequently, the worldwide capacity expansion of renewable generation technologies continues to rise, resulting in a growth of 154 GW for the year 2015, whereas non-renewable technologies grew only by 97 GW [18]. As of 2015, PV and wind installations account for 654 GW of the worldwide power generation capacity, thereby contributing 28% (1,811 GW) of the total installed generation capacity [18, 19]. In terms of global electricity generation, RE systems provided 5,660 TWh (24%) in 2015 [20], thus tying them as an indispensable part of the current and future electricity infrastructure.

Nevertheless, the power generation based on intermittent renewable resources, such as PV or wind power—hereinafter referred to as variable renewable energies (VRE)—imposes new challenges for future energy systems. Concerning this matter, particularly the question of handling potential mismatches between the electrical supply and demand caused by the limited dispatchability of VRE is subject of current research. Recent studies mutually consent that higher

shares of power generation from VRE will most likely result in an increased demand for flexibility (see [60][1]) and electrical energy storage (EES)[2] can help to balance the resulting variations in the net load. The question of EES demand[3] in highly renewable European energy systems is more pressing than ever and this thesis, therefore, delivers novel findings, as it

(I) provides a profound review of existing methods and models which quantify flexibility in energy systems, including an analysis of the resulting ranges of storage capacity (chapter 2, partially based on Haas et al. [21] and Cebulla et al. [40]),

(II) gives an overview of electrical energy storage technologies, discussing their core principals and typical classifications (chapter 3),

(III) presents an introduction to energy system modeling and the optimization framework REMix (**R**enewable **E**nergy **Mix**), including its mathematical representation and the implemented model enhancements (chapter 4),

(IV) takes a closer look in how far modeling approaches for thermal power plants affect storage demand and utilization (chapter 5, based on F. Cebulla and T. Fichter [22]),

(V) quantifies the influence of various parameter and methodological assumptions on storage demand and utilization in Europe (chapter 6, based on Cebulla et al. [23]).

To ensure traceability of the results, transparency of scientific work is a key component. For the first time, this work therefore uses the method of the *transparency list*, introduced by Cao et al. [53].

The structure of this work is summarized in Fig. 1. Chapter 5 and 6—the main contributions to current research—each consist of an abstract, a short introduction, a description of the applied methods and the data assumptions, a summary of the main findings of the analysis, a discussion of limitations, and essential future research.

[1] A more in-depth analysis of flexibility requirements in terms of storage demand is presented in Sec. 2.2.

[2] An overview of different types of EES is provided in chapter 3.

[3] Storage applications which aim to optimize the utilization of thermal power plants (e.g. through load leveling or peak shaving) or provide ancillary services (e.g. voltage and frequency control) are beyond the scope of this study.

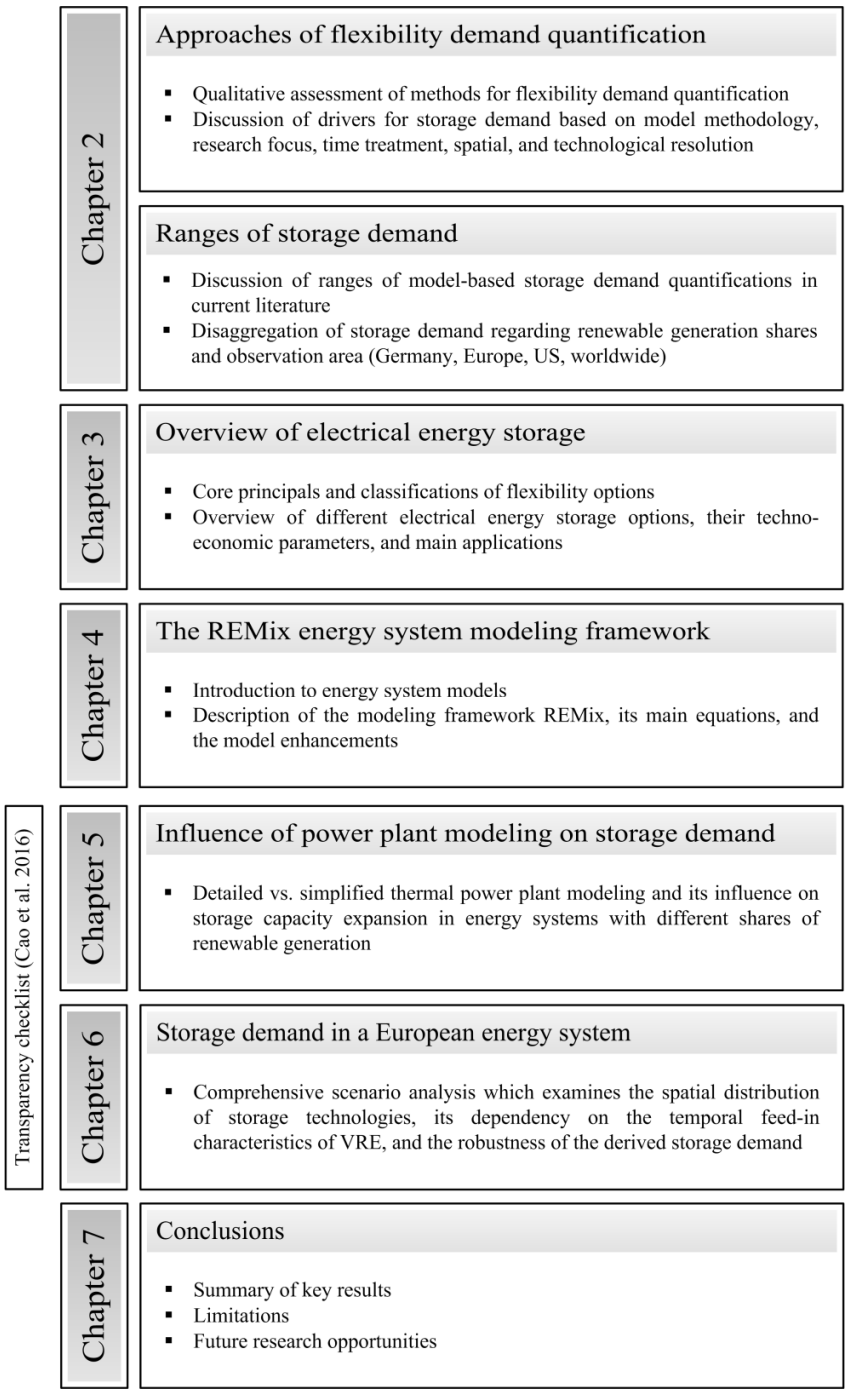

Fig. 1: Structure of this thesis.

2 State of knowledge

This chapter includes two surveys on the state of research on flexibility demand. First, Sec. 2.1 takes a closer look at existing studies which quantify flexibility demand, focusing on the underlying assumptions, methodologies, and models. Second, Sec. 2.2 discusses the ranges of derived EES demand in studies which focus on different regions, namely Germany, Europe, the U.S., and worldwide observation areas. Tab. 1 at the end of Sec. 2.2 provides a concise overview of selected flexibility demand studies, highlighting their characteristics with regard to spatial, temporal, and technological resolution. Finally, Sec. 2.3 summarizes the findings of both reviews and derives recommendations (e.g. suitable temporal or spatial resolution) for the model-based assessment of storage requirements of this study (see chapter 6).

2.1 Approaches of flexibility demand quantification[4]

Current research addresses the question of future flexibility demand typically via model-based analyses, often emphasizing the quantification of EES capacity for different energy scenarios (e.g. in [51, 132, 148, 164, 165]). These approaches, however, differ significantly in spatial, temporal, and technological resolution, modeling methodology as well as in differences in their main research focus. Subsequently, a brief discussion of each of the aforementioned aspects is provided.

2.1.1 Research focus

Two main research pillars can be identified with regard to the quantification of flexibility demand. On the one hand, studies focus on the *large-scale integration of renewable energies* and its implications on the future energy system (e.g. in terms of required generation capacity). On the other hand, various analyses evaluate *flexibility requirements* in terms of ramping (ramp magnitude and frequency) or gradients of VRE.

With respect to the first research pillar—*large-scale integration of renewable energies* or sometimes denoted as *energy management through EES*—studies typically asses the contribution of flexibility options to balance renewable power generation in time and space. These studies

[4] This section is partially based on J. Haas, F. Cebulla, K. Cao, W. Nowak, R. Palma-Behnke, C. Rahmann, and P. Mancarella, "Challenges and trends of energy storage expansion planning for flexibility provision in low-carbon power systems – a review," *Renewable and Sustainable Energy Reviews*, vol. 80, pp. 603–619, 2017.

neglect aspects of ancillary services and typically rely on temporal resolutions greater than 1 h. Moreover, they mostly focus on a number of selected flexibility technologies. In this sense, the role of flexibility through demand response and flexible operation of combined heat and power (CHP) plants in a European supply system, was studied by Gils [146]. The contribution of controlled charging of battery electric vehicles (BEV) has been assessed by Luca de Tena [191], Dallinger [24, 25], Verzijlbergh et al. [26], or Babrowski et al. [133]. Martínez-Anido et al. [152] and Steinke et al. [151] analyze the role of the electricity grid as a flexibility option. Finally, a number of studies (e.g. [119, 120, 132, 164, 190]) analyze EES demand for the large-scale integration of RE technologies.

Moreover, such studies typically emphasize in how far flexibility technologies are substitutable or complementary options. By this means, Verzijlbergh et al. [26] compare controlled BEV charging with transmission grid expansion for a European power system over various shares of VRE generation. The authors find that, in the case of similar electricity prices between model regions (*low arbitrage*), controlled charging of BEV is able to substitute grid expansion to a certain amount. Increasing the share of VRE generation, however, thus higher demand for arbitrage, will foster complementing effects of the two flexibility options. The authors argue that while transmission grid capacity is required for spatial decoupling of power demand and supply, BEV can function as an absorber of electricity. Moreover, controlled charging can flatten the net load through intertemporal arbitrage. Babrowski et al. [133] find that, for a German scenario with 46% VRE share (overall RE share of 60%) by 2040, EES capacities are not required and flexibility can solely be provided by controlled charging of BEV, the transmission grid, and dispatchable generators.

A comparison of EES and the electricity grid as flexibility options is provided by Martínez-Anido et al. [152] and Steinke et al. [151]. While the former analyze the interaction of EES and grid at relatively low VRE shares[5], the latter study examines 100% VRE scenarios. Both studies conclude that grid and EES are complement flexibility options, and, especially at higher shares of VRE penetration, a combination of both or a higher share of backup capacity (in [151] as high as the peak load) is required.

The second research pillar—*flexibility requirements* for ramping or power gradients of VRE—typically relies on hourly or sub-hourly temporal resolutions. Heide et al. [109], for example,

[5] The study analyzes the years 2010 and 2025. For 2025 wind capacities account for 13.4% of the generation mix, while PV provides approximately 3%. Dispatchable and partially dispatchable renewable power generation is considered through biomass and hydropower which account for 16.6% and 2.9% respectively.

analyze minimum EES requirements (converter power, storage capacity) in a fully renewable European power system. Huber et al. [122] investigate demand for flexibility in terms of ramp magnitude, frequency, and response, emphasizing the region's Ireland, Germany, and Italy. Weitemeyer et al. [121] analyze the impact of different shares of renewable generation as well as wind-to-PV-ratios and furthermore discuss the economic implications of three storage scenarios.

2.1.2 Model methodology

Different model methodologies are used to quantify future flexibility demand (a more general introduction to different types of energy system models is provided in Sec. 4.1). Some of the most prominent approaches are optimizations and simulations which are briefly introduced subsequently.

Optimizations typically consist of an objective function subject to a number of constraints. These constraints can be of technical (e.g. technology-specific power plant ramp up gradient), structural (e.g. district heating), or social nature (e.g. social acceptance). In addition, some model constraints also represent certain policy measures (e.g. CO_2 emission targets, limited curtailments of VRE). In the context of flexibility demand, main differences between optimization approaches particularly exist with regard to the formulation of objective functions. On the one hand, a large number of studies (e.g. [134, 145, 146, 165, 190, 191]) quantifies flexibility demand using a model which minimizes the total system costs. These approaches usually optimize the dispatch of generation units as well as investment decisions for capacity expansion. On the other hand, some methods—such as the models presented in Solomon et al. [119] or Krüger et al. [27]—include objective functions that aim to achieve high penetration rates of VRE. Solomon et al. [119] maximize the RE penetration in combination with minimized EES and backup requirements. The study uses an existing transmission grid infrastructure and tests the influence of further flexibility options, namely curtailment (*energy dumping*) and EES. Economic considerations, i.e. the cost-efficient dispatch or expansion of utilities and flexibility options, are not included. Krüger et al. [27] use a non-linear, quadratic target function to minimize the sum of the positive net load. This approach aims for efficient integration of RE through the optimized dispatch of the flexibility options.

Simulation models—as for example presented in [100, 109, 110, 120–125]—have a predictive or explorative view (i.e. forecasts) on energy scenarios [87]. They primarily rely on energy balance accounting methods, dispatch strategies (merit order), or time-series analyses to match generation and demand. Similar to optimization models, most simulations rely on weather-based

time-series as an input to generate technology-specific VRE dispatch. The main differences within simulation approaches can be found in the level of technological detail as well as in their spatial and temporal resolution. The model of Inage [123], for example, uses a simplified technology modeling with two synthetic electric load profiles (daily, annual), constant base load generation and weather-based feed-in time-series for PV and wind generation. However, the low degree of detail on the technology side enables a greater temporal resolution (0.1 h) compared to other approaches. Another simulation approach can be found in Denholm and Hand [120]. Here, a dispatch model is used to quantify the necessary grid and EES flexibility in the U.S. ERCOT system with VRE shares up to 80% of the annual demand.

Often, simulations and optimizations are not used solely but integrated into a sequence of different model applications (*soft links*). In the case of Wrobel and Beyer [124], a simulation model first determines the energy balancing demand of each of the 146 regions and then iterates the net load for Germany. In a next step, a detailed fossil-fired power plant dispatch is derived, and, finally, an optimization model calculates the total EES demand including a grid simulation as well as an optimized load and generation flow.

2.1.3 Time treatment

In the context of this study, time treatment includes two aspects of the model methodology. First, it can refer to the time interval or temporal resolution of the optimization or simulation. If flexibility is understood as an option for large-scale integration of RE, simulation as well as optimization models typically rely on hourly calculation steps. For flexibility in terms of ancillary service to maintain transmission grid stability and power quality, sub-hourly approaches are essential.

Deane et al. [126] carry out an analysis where the impact of different time intervals (5 min, 15 min, 30 min, 60 min) in a cost-minimizing optimization approach for the Irish power system is evaluated. The work supports the assumption that higher resolutions are especially beneficial for the assessment of ramp flexibility. If system costs are the main evaluation criterion, a 30 min resolution seems sufficient. In contrast, Pandzzic et al. [127] compare different unit-commitment (UC) methods using a 1 h and 15 min temporal resolution for day-ahead utility scheduling in the 24 model region IEEE reliability test system. They show that a 15 min resolution is superior in terms of a more efficient day-ahead unit-commitment, resulting in lower operational costs. O'Dwyer and Flynn [128] use mixed-integer UC modeling for the dispatch of thermal power plants and storage technologies, comparing an hourly with a 15 min temporal resolution with

regard to power plant operation and the associated costs. Again, the analysis shows the importance of sub-hourly modeling, especially in smaller energy systems with VRE shares lower than 50%. In this context, the conflict between computational effort and solution accuracy has to be stressed, leading to the conclusion that some UC approaches with 15min resolution might be impracticable for day-ahead planning due to high calculation times. The examples of [126–128] illustrate that the selection of the temporal resolution is strongly depending on the research question. However, data availability, computing times, and the required solution accuracy should also be taken into account.

The second aspect of time treatment refers to the methodology of capturing the temporal variability of VRE technologies (I) as well as to the time horizon of the analysis (II).

(I) Haydt et al. [188] introduce three concepts of modeling the intermittent nature of VRE generation: *integral*, *semi-dynamic*, and *fully dynamic* methods. *Integral* methods are typically based on accounting frameworks to balance annual power demand and supply. Temporal aspects are incorporated via load duration curves or dispatch strategies. One of the most prominent models is LEAP (**L**ong-range **E**nergy **A**lternatives **P**lanning System) [28]. *Semi-dynamic* methods, on the other hand, divide the time frame of the analysis (e.g. one year) into a number of representative time periods (e.g. day/night, typical days, weeks or seasons, see [31, 137, 138]). Typical models are TIMES (**T**he **I**ntegrated **M**ARKAL-**E**FOM **S**ystem), MARKAL (**Mark**et **Al**location), or LIMES (**L**ong-term **I**nvestment **M**odel for the **E**lectricity **S**ector). Finally, *fully dynamic* approaches represent power generation and load in a sequential order over the time frame of the analysis. Typically, time-steps are in hourly or higher resolutions. An example can be found in the REMix model (see Sec. 4.2).

(II) Within *fully dynamic* and *semi-dynamic* time treatment methods, models can either rely on *static*, *sequential* (myopic), or *path optimizing* approaches. A *static* model only considers a single time period (e.g. one year) and does not take into account any events preceding or following the simulated period. *Sequential* methods, in contrast, define a time frame which is then divided into a number of intervals. The results of the previous interval serve as input for the next interval ($t_{n-1} \rightarrow t_n \rightarrow t_{n+1}$). In cost minimizing dispatch and investment models, this is often the case for the capacity expansion of utilities and flexibility options. At last, *path optimization* solves a problem over a whole time frame which generally considers several years. As such methods can require a lot of computation time, models usually rely on simplified temporal resolution using *semi-dynamic* methods.

A comparison of a static and a myopic approach can be found in Babrowski et al. [29]. They conclude that, with steady input parameters from each previous optimization interval, results of the static and myopic approach do not differ significantly. However, if high jumps of the exogenous parameters occur, distinct variations between both methodologies can be observed.

Krey [90] carries out a comparison of path and myopic optimization, while Keppo and Strubegger [30] discuss the influence of perfect foresight in such models. Ludig et al. [31] and Nicolosi et al. [32] analyze the influence of different temporal resolutions of time slices in *semi-dynamic* methods. While the former look at climate mitigating strategies in scenarios until 2100, the latter examine capacity dispatch and expansion for the Texas ERCOT system until 2030. Furthermore, the influence of temporal resolution for utility dispatch in energy scenarios with high shares of RE generation is analyzed in Poncelet et al. [129] as well as in Nahmmacher et al. [130]. Additionally, Poncelet et al. [129] compare the impact of technological detail in power plant modeling against the temporal resolution.

2.1.4 Spatial examination area and resolution

Spatial examination area refers to the geographical region of interest of an analysis, whereas the resolution provides information with respect to the spatial level of disaggregation within the observation area. In the literature, calculations for flexibility demand exist for various observation areas (regions). The spatial resolution, i.e. the number of model regions, plays an important role, as it defines the distribution of capacities, generation, electricity load, and transmission grid topology within the observation area. Tab. 1 provides information with regard to spatial examination areas and resolution in different studies.

To the knowledge of the author, a comprehensive analysis of the influence of spatial resolution on flexibility demand has not been carried out so far. For the influence of spatial resolution on high-voltage electric grids, however, examples can be found in Shi and Tylavsky [33] and Shawhan et al. [34]. Both studies construct simplified representations of actual grid infrastructures through a reduced number of model regions. An analysis of the effects of various spatial aggregations of electric loads for the U.S. power system is conducted by Corcoran et al. [35]. Metzdorf [36] applies a spectral clustering algorithm for a German energy system where he aggregates—based on locational marginal pricing—the initial system with 500 model regions merely to 6 model regions. Though computational efficient, the results indicate that—compared to the 500 model regions reference system—large cluster (e.g. 6 model regions) will lead to deviations in system costs by around -20%.

2.1.5 Technological resolution

First, technological resolution refers to the abstraction level or technological representation in the modeling approach to characterize the technologies relevant for the analysis. In energy system modeling, this usually concerns generation units (power, heat), the load (e.g. electricity or heat/cooling demand), or the flexibility options.

Oh [131] describes an abstraction level in his modeling approach which is common for the representation of EES in power system optimizations. The EES technology—in the case of Oh [131] only one generic type—is described by its rated power, energy as well as the charge and discharge efficiencies, sometimes expressed as round-trip efficiency. Some approaches also include self-discharge rates for the storage unit, as in the model of Bussar et al. [132, 164].

Other examples for technological resolution are different degrees of detail in power plant or transmission grid modeling. The influence of power plant modeling on marginal costs is tackled by Abrell et al. [104] and Langrene et al. [105]. Its impact on long-term capacity expansion and utility dispatch is analyzed in Palmintier [168], Poncelet et al. [129], and Stoll et al. [149]. They conclude the detailed power plant modeling (e.g. discrete investment decisions and unit-commitment dispatch) can have a great influence on capacity expansion planning. However, these effects have not been analyzed for storage expansions and systems with high shares of renewable energy.

Munoz et al. [37] study the importance of transmission constraints as well as different investments approaches for additional grid capacity (discrete vs. continuous). The authors highlight that strong abstractions can lead to significant errors with regard to the derived investment costs for transmission and generation capacities. However, the analysis studies only a rather small power system (six bus/model region system) with renewable energy shares up to 50%.

Yet—to the best knowledge of the author—a systematic analysis of the influence of the applied technological resolution in order to quantify flexibility demand has not been carried out so far.

Recently, model-based expansion and dispatch planning started to include an increasing number of flexibility options. The technological diversity can be illustrated for the example of EES. For non-technology-specific calculations of storage demand, generic representations of one single technology are presented in [116, 123, 131]. Other studies introduce generic EES classes (e.g. short, mid, long-term) where techno-economic parameters are roughly based on today's

available technologies (see [132]). Finally, numerous approaches include representations of actual EES technologies, as in [134, 148, 190].

Second, technological diversity also refers to the considered energy sectors in the model-based analysis. Most of the mid to long-term energy system optimizations which emphasize the integration of renewable energies, analyze only the power sector. Inter-dependencies between the power sector and other sectors—such as transportation, heating, or cooling—are mostly neglected. If sector coupling is considered, these approaches typically rely on accounting frameworks on an annual basis which neglect intra-annual effects (see e.g. [135]). Moreover, such approaches do not provide any information on cost optimal capacity expansion and utilization. Optimizations which do consider all energy sectors usually rely on a simplified temporal resolution in terms of representative time periods (see [137, 138]).

2.2 Ranges of storage demand[6]

As shown in Sec. 2.1 various differences in modeling power system flexibility exit. In consequence, the derived demand for flexibility in the literature, especially for the required EES capacities, shows broad ranges, depending on the underlying assumptions. An overview in that regard is given by Droste-Franke et al. [39], Kondziella and Bruckner [60], and, for global, continental, as well as transcontinental scenarios, by Koskinen and Breyer [38]. For a fully renewable European power system, Droste-Franke et al. [39] identify a demand in storage converter power ranging from 500 GW up to 900 GW (no differentiation between charge and discharge power) and a storage capacity up to 520 TWh. In comparison to the upper values of these estimates, todays installed EES capacity in the EU-28 (mainly provided by pumped hydro storage) is roughly ten times lower for storage converter power (45 GW) and almost 900 times lower for energy-related storage capacity (602 GWh) [72]. This indicates a potentially high importance of long-term storage with high energy capacities in fully renewable energy scenarios.

In the literature review of Kondziella and Bruckner [60], furthermore, a differentiation between theoretical, technical, economic, and market potential for EES is provided. In terms of EES capacity for 100% VRE scenarios, Kondziella and Bruckner [60] identify values ranging from 60 TWh to 260 TWh (technical potential) for Europe, depending on the underlying scenario assumptions for storage (e.g. types of EES considered or conventional backup capacities in the

[6] This section partially is based on F. Cebulla, J. Haas , J. Eichman, W. Nowak, and P. Mancarella, “How much electrical energy storage do we need? A synthesis for the U.S., Europe, and Germany,” *Journal of Cleaner Production*, vol. 181, pp. 449–459, 2018.

associated publication). With respect to the required converter power in Europe, Kondziella and Bruckner [60] only provide numbers for VRE shares up to 60%, which result in ≈ 65 GW.

Following, additional recent literature that addresses storage demand is provided, emphasizing Europe, Germany, the U.S., and worldwide observation areas. A more in-depth discussion of this matter is provided by Cebulla et al. [40].

2.2.1 Europe

For the EU-27 region (27 model regions), Bertsch et al. [145] use the electricity market model DIMENSION to analyze flexibility requirements up to the year 2050. The model consists of two sub-models: (a) a detailed, hourly dispatch optimization and (b) a capacity expansion planning model relying on daily, weekly, and seasonal patterns for VRE integration. Sub-model (a) considers fossil-fired power plants in a detailed way (mixed-integer unit-commitment), also including firm capacity requirements. Sub-model (b) delivers the derived long-term capacities to sub-model (a). The capacities of renewable energies technologies are exogenously pre-defined. The analysis includes the following flexibility options: storage (pumped hydropower, compressed air storage), VRE curtailments, demand side management, and flexible operation of fossil-fired power plants. For a European energy system where renewable capacities provide 75% of the gross electricity generation (around 50% are provided by VRE systems), the authors derive a demand for storage power of 64 GW in scenario A and 68 GW in scenario B (higher CO_2 emission costs). Assuming a fixed storage energy-to-power ratio of 8 h [41], the study results in a storage capacity of 512 GWh and 812 GWh, respectively.

Bussar et al. [164] take a closer look on storage demand in a fully renewable energy system for Europe, the Middle East and North Africa, (EUMENA), using the power system model GENESYS. The analysis relies on a greenfield approach where all generation and flexibility capacities have to be derived model endogenously. The observation area consists of 21 model regions. Moreover, the authors analyze to what extent the temporal balancing of storage can be substituted by the spatial balancing of the transmission grid. The model includes the storage technologies pumped hydropower, stationary battery systems, and hydrogen storage. The latter assumes a conversion of surplus power to hydrogen (H_2) via electrolyzer and a reconversion of electricity via a combined cycle gas turbine (CCGT). Bussar et al. [164] also include a model constraint which fosters that at least 80% of each country's electricity demand is supplied by

national resources. The model derives an overall storage power[7] of 1,060 GW and an energy-related storage capacity of approximately 806 TWh. The latter can be mainly attributed to seasonal storage through H_2. The storage unit capacity of pumped hydro and battery storage only accounts for around 4 TWh. Additionally, Bussar et al. [164] test the influence of transmission grid restrictions, the sensitivity of storage demand to technology constraints, and variations in the investment costs. The latter decrease storage requirements to around 480 TWh (compared to 806 TWh in the reference scenario) in case of reduced investment costs for wind turbines and, in contrast, increases storage demand to 116 TWh when high investment costs for wind power are assumed. The study also finds that storage, to a certain amount, can be substituted by transmission capacity. For example, in the scenario that restricts the net transfer capacity (NTC) of a transmission grid line to 2.5 GW, the overall converter power is around 36% (+378 GW) higher compared to the reference scenario (which does not limited the line NTC), whereas the storage unit capacity is increased by 76% (+609 TWh). The EES capacities for all scenarios are shown in Tab. A 1 of Appendix A.

Finally, Scholz et al. [190] use the cost minimizing dispatch and expansion planning model REMix (see Sec. 4.2), analyzing, among others, the required power, and energy-related storage capacity over different scenarios. The latter differ in their theoretical share (before curtailments and storage losses) of VRE generation and the ratio of solar (PV and concentrating solar thermal power, CSP) to wind power generation, ranging from 0% to 140% for the VRE share and 20% to 80% of PV share. Moreover, the authors test the influence of CO_2 emission cost scenarios on storage demand. The observation area comprises most of the European countries, aggregated to 15 model regions. The analysis includes three storage technologies: hydrogen (reconversion via CCGT), pumped hydro storage, and redox-flow batteries. Scholz et al. [190] derive a demand of storage power of 4 GW to 114 GW for a theoretical VRE share of 60%, 10 GW to 200 GW for a share of 80%, and 12 GW to 235 GW for a share of 100%. In terms of the energy-related storage capacity, the model results in 266 GWh to 814 GWh for a theoretical VRE share of 60%, 266 GWh to 10,480 GWh for a share of 80%, and 272 GWh to 22,026 GWh for a share of 100%.

Fig. 2 summarizes the ranges (i.e. spreads) of storage converter power and storage unit capacity over different shares of renewable generation of six analyzed studies ([42, 123, 145, 148, 190][8]) and 73 scenarios for a European observations area. Furthermore, the violin plots show

[7] This includes short, mid, and long-term storage, but excludes the capacity of the electrolyzer (882 GW). The latter operates as the charging unit of the storage converter in the hydrogen storage.

[8] Including the results presented in this study.

the median, minimum, and maximum values. Moreover, the plots illustrate the frequency distribution of the storage capacity in the current literature, as they include a kernel density estimation function. The latter is closely related to histograms, does, however, include smoothing and harmonization of the sample data (i.e. storage converter power or storage unit capacity).

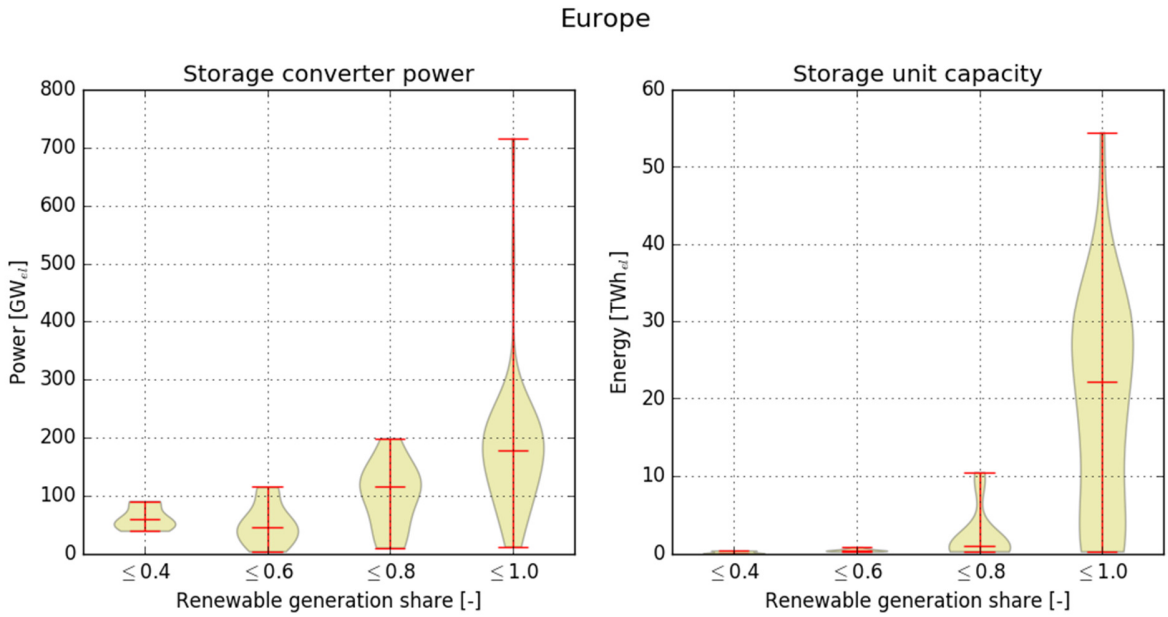

Fig. 2: Review of storage demand in Europe. Distribution of converter power and storage unit capacity over different shares of renewable generation. The figure depicts median, minimum, maximum values, and the frequency distribution of storage capacity.

The conclusions from Fig. 2 are twofold. First, in current literature, model endogenous derived storage demand does not increase proportionally with increasing renewable generation shares, but shows a more exponential growth, especially for the storage unit capacity. Second, the derived ranges or spreads of storage demand increase significantly with growing renewable generation share. This again could be interpreted as increasing uncertainty and hence decreasing robustness of the results. In that sense, storage demand could be understood as more sensitive to model assumptions at higher renewable generation shares.

2.2.2 Germany

For an isolated German observation area (no power exchange with the neighboring countries through the transmission grid), a few studies exist.

Hartmann [47] analyzes storage demand using the dispatch and capacity expansion planning model E2M2. The considered storage technologies include pumped hydro storage (PHS),

diabatic, adiabatic compressed air storage (dCAES, aCAES), and BEV. For balancing the power system—i.e. excluding the required storage capacities for BEV—Hartmann [47] derives a storage power of 27 GW (367 GWh) for a renewable generation share of 50% (with regard to the annual gross electricity demand), 78 GW (6,300 GWh) for 80%, and 139 GW (83,000 GWh) for 100%. The analysis applies a greenfield approach (no capacities installed at the beginning of the observation year) and assumes no transmission restrictions within Germany ("copper plate"). Moreover, in the base scenario, the author does not allow curtailments of VRE power generation. In further sensitivity cases, the influence of unconstrained curtailments is shown. For the 50% scenario, storage demand decreases from 27 GW to 11 GW, whereas the storage capacity (GWh) remains identical. In the case of 80% renewable generation, the storage power of the base scenario (79 GW) is reduced to 66 GW; storage capacity decreases from 6,300 GWh to 5,400 GWh. In the 100% scenario, 106 GW of storage power and 57,000 GWh storage capacity are required.

Kühne [167] quantifies the required storage demand under various shares of renewable generation, including different ratios of wind (onshore and offshore) to PV power. Moreover, the study evaluates the influence of methodological and input data assumptions—such as cost variations (investment or operating costs) or the influence of an overall emission target—on the required capacity of H_2 storage, aCAES, and PHS. The methodology is based on the optimization framework IMAKUS, including sub-models for capacity expansion and dispatch of thermal power plants (MOWIKA), storage (MESTAS), and a consideration of required firm capacity (MOGLIE). Renewable generation capacities as well as the installed power of CHP, in contrast, are exogenously pre-defined. The work relies on a single node representation of Germany, assuming no transmission grid restriction within the observation area ("copper plate"). Import and export of electricity to neighboring countries is not considered, however, electricity surplus can be sold at a fixed price. Furthermore, the optimization differentiates between charging and discharging capacity of storage as well as the storage unit capacity. Within the reference scenario, the year 2050 is characterized by a share of renewable power generation of 80% (with regard to the gross electricity consumption). The endogenously derived storage power capacity results in 36.3 GW for charging and 15.9 GW for discharging, while the storage unit capacity reaches 5.2 TWh[9]. The latter can mostly be attributed to H_2 storage (4.7 TWh) and aCAES (0.5 TWh);

[9] These storage capacities exclude already existing capacities of PHS. Charge and discharge power are assumed to be 6.2 GW and 6.5 GW respectively; the storage capacity is 77 GWh.

converter capacity in terms of discharging power is more equally distributed over the technologies, where PHS provides 2.4 GW, aCAES 9.8 GW, and H_2 storage 3.7 GW. The results for all scenarios with regard to storage power (charge and discharge) and storage unit capacity are shown in Appendix A.

Zerrahn and Schill [165] apply the hourly dispatch and capacity expansion model DIETER (**D**ispatch and **I**nvestment **E**valuation **T**ool with **E**ndogenous **R**enewables) and analyze the role of EES and demand side management (DSM). The baseline scenarios differ by their minimum share of renewable generation between 60% and 100%. The analysis relies on a greenfield approach where the model can invest into different generation and flexibility options. The former comprise coal-fired thermal power plants, CCGT's, two types of open cycle gas turbines, biomass power plants, onshore and offshore wind as well as PV systems. The flexibility options, in contrast, include seven storage technologies and DSM. It is assumed that capacity expansion of nuclear and lignite power plants, as well as of run-of-the-river hydroelectricity, is not possible. The baseline scenarios result in storage power ranging from 10 GW to 34 GW with a storage capacity of 42 GWh to 436 GWh. Moreover, numerous sensitivity calculations are performed, including variations of costs and availability of storage and VRE, different DSM potentials as well as requirements for reserves. The authors find that the required storage capacity is significantly influenced by the availability of other flexibility options, such as dispatchable biomass or DSM. The study, however, does not consider transmission grid as an option of spatial balancing and assumes unlimited transmission within Germany ("copper plate"). The results for all scenarios with regard to storage power and storage unit capacity are shown in Tab. A 2 in Appendix A.

For lower shares of renewable generation (i.e. 50% in 2030 and 60% in 2040) Babrowski et al. [133] take a closer look at the role of short-term (daily) battery storage and the influence of controlled charging of BEV. For the German observation area, the hourly, deterministic dispatch and capacity expansion model PERSEUS-NET-ESS uses a spatial resolution of 440 model regions. PERSEUS-NET-ESS relies on a mixed-integer (MIP), myopic approach which uses time slices of representative days and seasons (semi-dynamic approach, see Sec. 2.1.3). Apart from battery storage, other flexibility options are curtailments of VRE as well as spatial balancing via a given transmission grid infrastructure. While the renewable capacities are exogenously pre-defined (based on [143]), model endogenously derived investments into new capacities of CCGT, open cycle gas turbines (GT), battery storage, coal, and lignite-fired thermal power plants are possible. The study results in 3.2 GW/16 GWh of battery storage in the

reference scenario. However, these capacities can be substituted completely through controlled charging of BEV (scenario *LSP*).

Fig. 3 summarizes the ranges (i.e. spreads) of storage converter power and storage unit capacity over different shares of renewable generation of seven analyzed studies ([42, 47, 51, 133, 199][10]) and 62 scenarios for Germany.

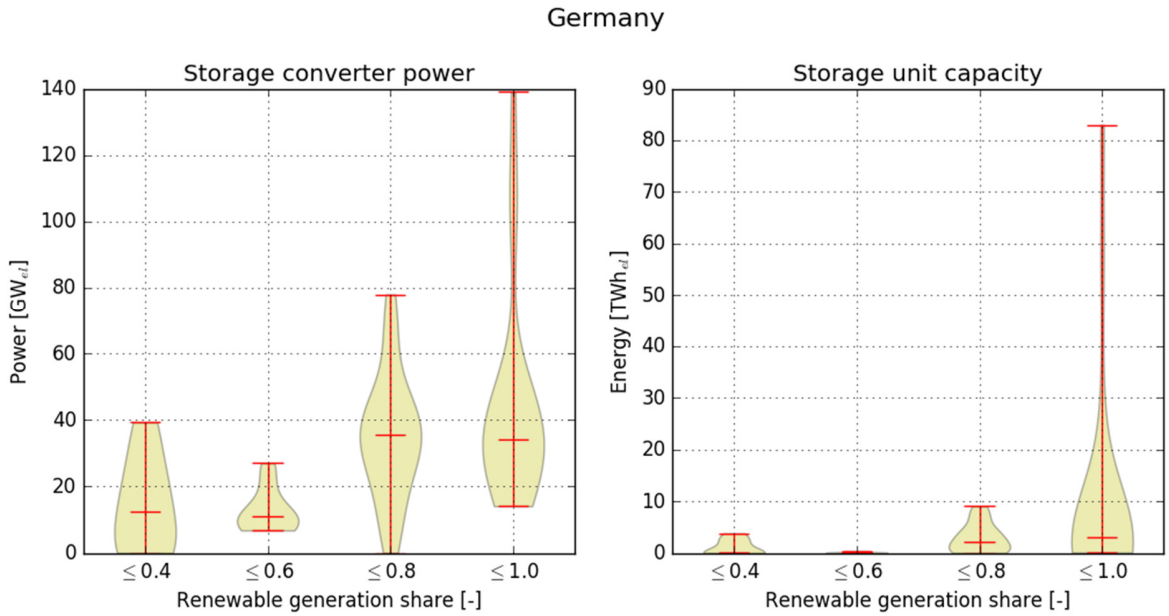

Fig. 3: Review of storage demand in Germany. Distribution of storage converter power and storage unit capacity over different shares of renewable generation. The figure depicts median, minimum, maximum values, and the frequency distribution of storage capacity[11].

Similar to the European perspective (see Fig. 2), the reviewed literature for storage demand in Germany shows broad ranges, particularly when considering higher shares of renewable generation. Again, the growth of storage demand over increasing shares of renewable generation is non-linear, in particular for the storage capacity.

2.2.3 United States

For the U.S. Western Electricity Coordinating Council (WECC) area, Mileva et al. [166] carry out an analysis of required flexibility options with an emphasis on the role of power storage. WECC comprises of 14 U.S. states, the Canadian provinces Alberta and British Columbia as well as the northern part of Baja California in Mexico. This observation area again is disaggregated

[10] Including the results presented in this study.

[11] The outliers in this figure at renewable shares of 80-100% (140 GW/83 TWh) belong to a study where all VRE power generation has to be completely integrated (no curtailment allowed).

into 50 model regions ("load zones"). The study is based on the SWITCH model (**S**olar and **wi**nd energy integrated with **t**ransmission and **c**onventional sources) which optimizes dispatch and capacity expansion under the premise of least system costs and greenhouse gas emission reduction of 85% by 2050 compared to the level of 1990. The study conducts different scenarios (i.e. sensitivity cases), assuming, for example, decreased costs of battery storage. With exceptions of the sensitivity case *nuclear*, all scenarios assume that no nuclear power and fossil-fired capacities can be built. Almost all scenarios are characterized by large shares of dispatchable CSP (enabled through thermal storage) in order to provide flexibility. Exceptions can be found in the scenarios with low costs for battery storage (*Low-Cost Batteries*, *SunShot/Low-Cost Batteries*) and load shifting (including controlled charging of BEV, scenario *Load-Shifting/Flexible EV Charging*). Here, flexibility is provided by a larger share of battery storage and by DSM. The former results in storage capacities of 82 GW/549 GWh and 129 GW/883 GWh, whereas the latter is characterized by 18 GW/80 GWh. In comparison, the model derives storage capacities of 24 GW/184 GWh in the reference scenario. The results for all scenarios with regard to storage power and storage unit capacity are shown in Tab. A 3 in Appendix A.

2.2.4 Worldwide

The number of worldwide analyses for storage or flexibility demand is very limited. Pleßmann et al. [43] for example, use the model MRESOM (**M**ulti-**R**egion **E**nergy **S**ystem **O**ptimization **M**odel) to optimize capacity expansion and hourly dispatch for a 100% renewable power system. The study considers 163 countries; each modeled isolated with no transmission grid to other regions and no grid restrictions within the countries (isolated "copper plates"). For generation technologies, the model includes PV, wind, and CSP with a thermal storage. Flexibility can be provided via stationary battery storage (lead-acid and sodium-sulfur), renewable methane (power to gas), or high-temperature thermal storage for steam turbines enabled through CSP plants or heating rods. Hydropower, biomass, or geothermal power generation, as well as CO_2 intensive technologies (e.g. fossil-fired power plants), are not considered. The results show a power system where almost half of the annual electricity generation (46%) is provided by wind power systems. PV contributes by 33%, CSP by 21%. In terms of flexibility, the largest amount is provided by thermal storage of CSP or heating rods with 4,800 TWh of the annual power generation. Electricity from power to gas accounts for almost 2,000 TWh, whereas battery storage provides only 420 TWh annually. This translates into capacities of 73.6 TWh of thermal storage and 1.5 TWh of battery storage. Concerning the gas

storage for power to gas applications, the authors include only the thermal storage capacity of 1,690 TWh. Information with regard to the power-related installed capacity is only provided for the re-conversion via CCGT in the power to gas process (2,360 GW) and the power block of the CSP plant, but not for the battery storage.

Inage [123] introduces a simulation model for worldwide required storage capacity from 2010 to 2050. The underlying scenario is based on the BLUE map scenario of the International Energy Agency (see [44]) in which the renewable power generation rises from 19% in 2010 to 46% in 2050 worldwide. The model calculates the energy balance between electric load and generation on a 0.1 h time-step basis (6 minutes), using a simplified consideration of load and generation. One key finding of the study is that the storage demand heavily depends on the variability of the wind power generation. Assuming wind variation ratios from 15% to 30% storage capacities between 189 and 305 GW are required.

Tab. 1: Overview of storage studies.

Source	Year	Publication type			Model name	Model type		Time resolution	Spatial scope	Regions	Storage technologies	Grid	Other flexibilities
		Thesis	Report	Article		Opt.	Sim.						
[199]	2012		●		N/A	●		1 h	Germany	1	Short and long-term EES	Copper plate, w/o imports/exports	DSM[a], curtailment
[133]	2016			●	PERSEUS-NET-ESS	●		1 h	Germany	440	PHS, generic battery	Exogenous, w/o imports/exports	DSM, curtailment, controlled charging of battery electric vehicles (BEV)
[145]	2016			●	DIMENSION	●		1 h	Europe/ Germany	27	aCAES, PHS	Exogenous, based on scenario B of [45]	DSM, curtailment, controlled charging of BEV
[148]	2016			●	PLEXOS	●		1 h	Europe	6	aCAES, PHS[b]	Exogenous, six different cases analyzed	DSM[a], curtailment
[46]	2013			●	RREEOM	●		1 h	U.S. PJM	1	Generic battery, H_2	Copper plate, w/o imports/exports	Curtailment, vehicle to grid
[132, 164]	2016/ 2015			●	GENESYS	●		1 h	Europe/ Middle East/ North Africa	21	PHS, generic battery, H_2	Endogenous	Curtailment
[134, 153]	2016/ 2014	●		●	POWER	●		1 h	U.S.	10	PHS, generic battery	Endogenous, additionally to existing grid	DSM[a], curtailment, controlled charging of BEV, CSP
[47]	2013	●			E2M2	●		1 h	Germany	1	PHS, CAES, aCAES	Copper plate, w/o imports/exports	Curtailment[c]
[123]	2009		●		N/A		●	6 min	U.S./Europe	12	Generic EES	Copper plate	N/A
[167]	2016	●			MESTAS	●		1 h	Germany	1	PHS, aCAES, H_2	Copper plate, w/o imports/exports[d]	Curtailment
[166]	2016			●	SWITCH	●		1 h	U.S. WECC	50	PHS[b], CAES, generic battery	Endogenous, additionally to existing grid	DSM[a], curtailment, controlled charging of BEV[e]
[48]	2014/ 2012		●		ReEDs	●		1 h	U.S.	11	PHS, generic battery, CAES	Endogenous, additionally to existing grid	DSM, CSP, controlled charging of BEV
[49]	2014		●		SCOPE	●		1 h	Europe/ Germany	20	PHS, Lead-acid battery (PbB)[e], H_2	Endogenous, additionally to existing grid based on [50]	DSM[a], curtailment, cBEV[f], flexible CHP
[190]	2016			●	REMix	●		1 h	Europe	15	Redox-flow battery (RFB)[e], PHS, H_2	Endogenous	Curtailment, CSP
[51, 62]	2013/ 2012			●	N/A	●		1 h	Germany	1	PHS	Copper plate, w/o imports/exports	DSM[g]
[52]	2016			●	REMIND/ DIMES	●		1 h	U.S./Europe	8	Generic short-term storage	Copper plate	Curtailment
[165]	2015		●		DIETER	●		1 h	Germany	1	PHS, aCAES, H_2, lithium-ion battery (Li-Ion), sodium-sulfur battery (NaS), PbB, redox-flow battery (RFB)	Copper plate, w/o imports/exports	DSM[a], curtailment

[a] In some model runs DSM is not included (or only partially) to analyze its influence on EES requirements.
[b] Only existing PHS capacities.
[c] Some sensitivity cases restrict curtailment.
[d] Electricity surplus can be sold at a fixed price to the neighboring countries.
[e] Different configurations of fixed energy-to-power ratios are used; i.e. no independent dimensioning of power and energy capacity of the EES.
[f] In some model runs controlled charging BEV is not included (or only partially) to analyze its influence on EES requirements.
[g] Load reduction in super-peak hours.

2.3 Findings from the state of knowledge

2.3.1 Limited comparability of storage demand quantifications

Model-based flexibility and storage demand quantifications result in large ranges (see Sec. 2.2) due to different conceptual, methodological, and input data assumptions. In this context, the output is only valid within the assumption framework of the study, thus hindering the comparability of the results.

Additionally, long-term energy system models rely on a number of assumptions which are associated with uncertainty. According to Kann et al. [56], uncertainty can be classified into two types: *parametric uncertainty*, which exists due to limited knowledge about the future (e.g. development of techno-economic parameters of a certain technology), and *stochasticity*, which refers to the intrinsic variability of specific processes (e.g. volatile solar irradiation or wind speeds for PV and wind power). Additional to the categorization of Kann et al. [56], the author of this study proposes the concept that uncertainty also exists with regard to the chosen modeling approach[12] as suggested by Cao et al. [53], hereinafter referred to as *methodological uncertainty*. While in theory different methodologies should lead to similar results, the lack of knowledge about the future imposes the risk that some approaches might capture specific effects incorrectly. In this sense, certain methods are more applicable than others when it comes to the assessment of future developments.

Parametric uncertainty can be tackled by sensitivity analysis and, in optimization approaches, can be supported by the interpretation of marginal values based on the duality theory [54] (see e.g. Remme [55]). While a sensitivity analysis validates the response to a single input value change (*ceteris paribus assumption* or *single-value deterministic*, [56]) or to a combination of several input parameters (*joint sensitivity analysis*, [56]), in other words, tests the robustness of the modeling result[13], the author of this study argues that the main purpose is, in fact, the assessment of inter-dependencies of model assumptions and results. To overcome parametric uncertainty for future storage demand, broad sensitivity analyses have been carried out, e.g. by Zerrahn and Schill [57, 165] and Kühne [167] for Germany, or Mileva et al. [166] for the U.S. Western Electricity Coordinating Council.

[12] This could also refer to chosen system boundaries or to model simplifications.

[13] Not to be mistaken with robustness analysis, which, in contrast to a sensitivity analysis, investigates plausibility of results through different models.

Uncertainty caused by the variability of certain processes (s*tochasticity*) can be captured through stochastic modeling. Naturally—due to the intermittency of VRE power—such approaches can be found in research which studies renewable energy systems, such as recently in Soares et al. [58]. The authors perform a day ahead optimization of the utility dispatch, including generation from VRE sources (PV, wind) and balancing through storage as well as demand response. The analysis is carried out for a 201 bus distribution grid system where about 30% of the installed capacity is provided by PV and 22% by wind power systems (other generation units comprise of hydro, biomass, and cogeneration systems). Especially if flexibility options (e.g. demand response) are scarce within the energy scenario, stochastic modeling was found to be superior in comparison to deterministic approaches. However, stochastic modeling is typically applied for smaller energy systems, short time periods, or simplified technology representation as the computational burden for large-scale, long-term optimizations is too high. In consequence, complex deterministic optimizations deal with stochasticity of the VRE generation through extensive scenario analyses, varying, for example, the underlying weather years.

To the best knowledge of the author, *methodological uncertainty* in the context of storage expansion has only been analyzed in Zerrahn and Schill [165], Bussar et al. [164], and Kühne [167]. All three studies test the dependency of storage demand on general assumptions (e.g. transmission capacity limits or restricted long-term storage), but, however, do not analyze the effect of different modeling approaches. The latter has been studied for the impact of thermal power plant modeling on marginal costs (see [104, 105]) as well as on long-term capacity expansion and utility dispatch (see [129, 149, 168]), but never for storage demand.

2.3.2 Possible drivers for long-term storage demand

Although a substantial amount of research in energy system planning has been conducted, results for storage demand are broad, as these flexibility requirements have been analyzed under various conditions, including aspects of different RE shares, wind-to-PV ratios, weather years, different observation areas as well as the influence of cost assumptions in cost optimizing approaches. In this sense, Sec 2.1 provides indicators in how far storage demand is sensitive to certain assumptions and implications on the modeling approach. With regard to the role of storage for *large-scale integration* of VRE power generation the follow conclusions can be drawn and are helpful for the model development and setup:

(I) In the European context, storage demand has been studied extensively with regard to different PV-to-wind ratios and VRE power generation shares (e.g. in [110, 112, 121, 190]). Concerning the latter, research agrees that the importance of storage will rise significantly with higher shares of VRE power (e.g. > 80%) and analyses, therefore, should emphasize such systems.

(II) Transmission grid and storage can be substitute or complement flexibility options, mainly influenced by the share of power generation from VRE [121, 151, 152].

(III) For an appropriate representation of the dynamics of VRE power generation, hourly resolutions are required (for wind) or desirable (for PV) [188]. Moreover, the benefits of sub-hourly modeling are marginal and such temporal resolutions are only essential when assessing ramp flexibility or in short-term analyses [122, 126–128].

(IV) Despite their computational advantages, *semi-dynamic* methods are unsuitable for the analysis of storage options in long-term scenarios, thus *fully dynamic* approaches have to be used [129, 130].

(V) *Sequential* (myopic) or *path optimizing* methods are not essential, as the emphasis of this study is to analyze inter-dependencies within the system with respect to a range of assumptions, not to develop transition scenarios. In this sense, a *static* approach, considering only one year (i.e. 2050) is adequate.

(VI) To the best knowledge of the author, a comprehensive analysis of the influence of spatial resolution on flexibility demand has not been carried out so far.

(VII) Co-optimization of several flexibility options for large-scale VRE integration incorporating an adequate temporal, spatial, and technological resolution has not been presented so far. Moreover, current research lacks analyses which quantify the influence of different technological abstractions levels on storage demand.

2.4 Novelty and contributions

Despite the manifold analyses discussed in the state of knowledge, several aspects of storage demand have been omitted to date. Particularly, in the light of increasing uncertainty of the required storage capacity at high shares of renewable generation (see Sec. 2.2), a comprehensive analysis of the matter seems promising. This study, therefore, expands the existing state of knowledge by tackling the subsequent research foci.

2.4.1 Robustness of storage demand[14]

As discussed in Sec. 2.3, results for storage demand in model-based approaches are only valid within the assumption framework of the study. To assess the robustness of storage demand against *parametric* and *methodological uncertainty*, a holistic analysis is essential. To the best knowledge of the author, such analyses have only been presented in a limited number of studies [164–167]. Moreover, for a European scope, only Bussar et al. [164] provide an assessment of the sensitivity of storage demand. Though extensive in terms of analyzing the influence of certain data input and more general assumptions (e.g. limited transmission grid capacity), the study relies on simplified technology representations, strongly aggregates model regions, and neglects the aspect of *methodological uncertainty*. Thus, this thesis contributes to the matter as follows.

- *The question of storage demand and utilization for a European observation area is tackled, including an adequate temporal, technological, and spatial resolution.*

- *To ensure the validity against parametric and methodological uncertainty the analysis incorporates a systematic consideration of different modeling approaches and data assumptions to identify the main drivers for storage demand.*

[14] Assumptions for long-term energy scenarios are inherently associates with uncertainties. By this means, the author highlights that this thesis is not intended to forecast future energy scenarios, but rather to analyze cause and effect of different parametric and methodological assumptions on the future demand for electrical energy storage.

2.4.2 Drivers of spatial storage capacity distribution

Recent research rarely studies in-depth the reasons for the "optimum" spatial distribution of storage expansion and its dispatch but takes the optimization model results as granted. Only one recent working paper which takes on this aspect was found. While this study of Belderbos et al. [97] provides a methodological framework to analyze the interdependency between the temporal characteristics of electricity generation (and demand) and the storage capacity, the work does not discuss the implications for large-scale European energy systems with high shares of VRE generation. By this means, this thesis contributes to the matter as follows.

- *The optimal spatial, technology-specific distribution of storage capacity in Europe is derived.*

- *The main drivers for the resulting storage distributions over the different model regions are assessed.*

3 Electrical energy storage

Electrical energy storage is one option to tackle increased flexibility requirements in energy scenarios. While various definitions of flexibility exist (see [98, 99, 120]), in this work, it is defined as the ability of technical devices to decouple electricity demand and supply in order balance variations in the net load, sometimes referred to as *residual load*. The latter is defined as the remaining electricity demand after power generation from VRE sources, or, in other words, the electrical load minus the generation from VRE. Lund et al. [59] as well as Kondziella and Bruckner [60] give a broad overview of types of flexibility options, including demand response in combination with new loads (heating, cooling, battery electric vehicles, and power-to-gas), grid ancillary services, supply-side flexibility (flexible power plants, curtailments of power generation from VRE), grid extension (transmission and distribution level), and EES. While the latter provides flexibility on a temporal level, i.e. allows shifting of energy from one point in time to another, the transmission grid can be considered as a spatial flexibility option, as it allows large-scale balancing of generation and demand between different regions which otherwise have to balance internal mismatches themselves.

As the main research focus of this thesis lays in the assessment of the possible role of EES in future energy scenarios, subsequently a review of selected EES technologies is provided (for an explanation why these technologies were selected, see Sec. 6.2.2). Other flexibility options will not be covered; a profound overview is provided by Luo et al. [202]. The subsequent review of EES includes their principal functionality, the main techno-economic characteristics, advantages and drawbacks as well as typical applications.

3.1 Principals and classifications

EES allow a temporal decoupling of electricity demand and supply, or, in other words, to time-shift electricity. The principal process is depicted in Fig. 4. The figure illustrates the hourly dispatch of VRE technologies, thermal power plants, and stationary Li-ion batteries for a hypothetical energy system. In times of VRE over-generation (a), surplus electricity is used to charge a storage unit (b). If electricity is necessary to reliably cover the electrical load (c), the storage unit is discharged.

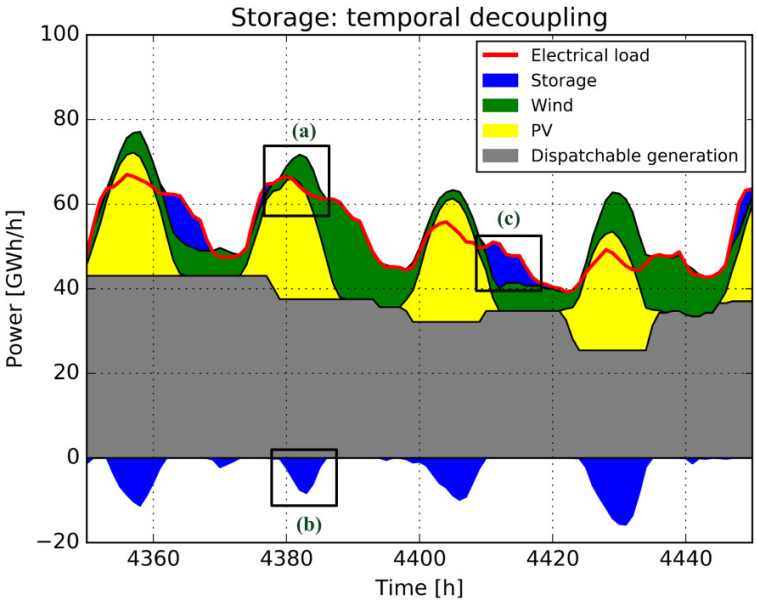

Fig. 4: Inter-temporal decoupling of power supply and demand through storage. In times of VRE over-generation (a), charging and storing (b) allows shifting energy to a later point in time when energy is required to satisfy the electrical demand (c). Storage charging is depicted as negative y-values; storage discharging as positive y-values.

Absorbing electricity with the help of storage is enabled through the charging converter unit which is characterized by its converter power and charging efficiency. Typical examples for the charging converter unit are the pumps of a PHS or the compression unit of compressed air storage (CAES). Following, the electrical energy is stored in a storage unit which is affected by self-discharging. Typical examples are evaporation in the water reservoir of a PHS or leakage of the tanks in a redox-flow battery. Storage losses are time dependent and either linear, as depicted in Fig. 5, or exponential (e.g. for flywheels) [61]. Lastly, the energy is reconverted into electricity through the discharging converter which again is affected by the discharging efficiency. The combination of charging and discharging efficiency (excluding self-discharging), i.e. the ratio of the overall electricity output to the electricity input, is sometimes referred to as cycle or round-trip efficiency.

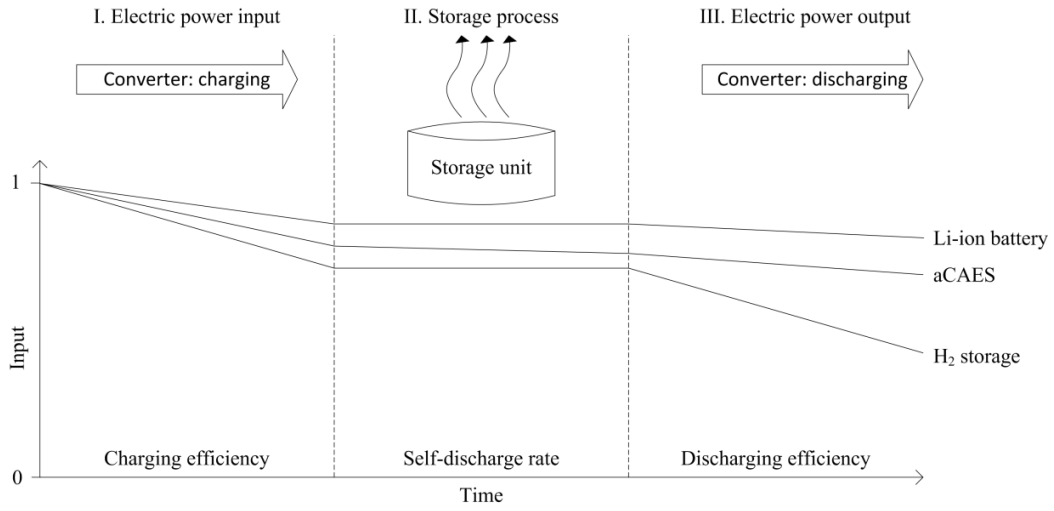

Fig. 5: Schematic illustration of the storage process. Figure adapted from [61].

EES can be classified in different ways. Chen et al. [198] for example categorize by function (a) and form (b) of EES.

(a) A higher storage capacity allows EES to respond to longer mismatches of electricity demand and supply, while a higher power capacity allows responding to mismatches of higher magnitude. First, EES which provide high power but small storage capacity are typically used for ancillary services, such as power quality or frequency control in electric grids as well as for uninterruptible power supply (UPS). Their higher power capacity enables balancing mismatches of high power [202]. Typical examples are superconductive magnetic EES, super capacitors, flywheels, and batteries. In terms of storing larger amounts of energy over a longer period of time (> 1 h)—referred to as *large-scale integration of VRE* or *energy management through EES*—PHS, CAES, H_2, electro-chemical (e.g. Li-ion, lead-acid), or redox-flow batteries are suitable, as the greater storage capacity allows to balance longer mismatches [202]. In terms of EES application, the size (i.e. volume) of an EES system is a crucial metric, mainly influenced by the power (converter) and energy density (storage unit).

(b) The second classification of EES is based on the mode of operation in EES and in which way the electricity is stored in the storage unit. Surplus electricity either can be stored directly (electricity-to-electricity) or indirectly (electricity-to-x-to-electricity) (see Fig. 6).

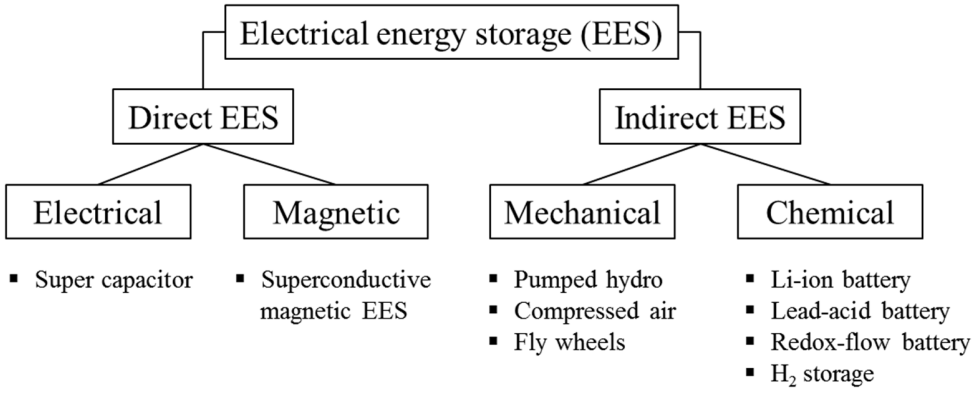

Fig. 6: Classification of electrical energy storage and examples. Figure is adapted from [66, 198, 200, 202].

Direct storage of electricity can be achieved in magnetic fields in superconductive magnetic EES or in a static electric field in super capacitors. Indirect EES can be further categorized into mechanical and chemical EES. Examples of the former are PHS or CAES; the latter include Li-ion, lead-acid, and redox-flow batteries as well as hydrogen storage.

3.2 Pumped hydro storage

Pumped hydro storage (PHS) use the gravitational energy potential through the difference in elevation of an upper and lower water reservoir. Both reservoirs are connected via a penstock through which water can be pumped from the lower to the upper reservoir in times of electricity surplus (charging). Typically, the penstock is connected to a Francis turbine which is able to pump and turbine water (reversible machine). In discharging mode and when electricity is required, the water is released through the turbines which again are connected to a generator.

The efficiency of a PHS is limited by the maximum efficiencies of the pumps and turbines. The cycle efficiency today (excluding self-discharging) typically ranges from 0.70 to 0.80 [65, 75, 198, 200, 207]. Additional to the high cycle efficiency, advantages of PHS include long lifetimes, low operating and maintenance costs, low capital costs per unit of energy, and fast response times [75]. As of today, PHS can be considered as one of the most mature storage technologies. Worldwide, about 164 GW of converter power and 1.314 GWh[15] of storage unit capacity are installed [73]. However, some shortcomings exist, including high capital costs, difficult and long approval procedures owing to public acceptance issues (see e.g. [62]), and

[15] The Global Energy Storage Database of the U.S. department of energy provides installed converter capacity as well as a duration. The latter is defined as the amount of time the PHS can discharge at the rated power capacity. However, for some sites the discharge duration is not provided. Therefore, a value of 8 h is assumed to conclude from power-related to energy-related capacity.

evaporation losses. Moreover, the potential of future PHS systems is dependent on the availability of suitable sites (in terms of topology). Capacity expansion potentials for PHS in Europe are subject of the work of van de Vegte and Huibers [63] as well as of Gimeno-Guitiérrz and Lacal-Arántegui [64, 205]. The latter derive a theoretical PHS potential of 54 TWh for Europe. In a more restrictive scenario (*realizable potential*) which includes further constraints, such as protected natural areas, this potential is reduced to 29 TWh.

3.3 Compressed air energy storage

In compressed air energy storage (CAES) the ambient air is compressed and stored in pressure tanks or underground geological formations, such as salt and hard rock caverns, depleted gas fields, or aquifers [65]. In discharging mode the pressurized air is released and expands in an air turbine connected to a generator which provides electricity [204]. In principle, two types of CAES exist: diabatic (dCAES) and adiabatic CAES (aCAES). The main difference between the two concepts lies in the way the produced heat during compressing phase is used. Diabatic systems waste the compression heat and require co-firing during discharging to avoid condensation and icing in the expansion components. Therefore, dCAES typically include a heat source to preheat the pressurized air before the expander. Adiabatic systems, in contrast, store the generated heat during the compression phase in thermal energy storage (TES). The working principle of an aCAES is depicted in Fig. 7.

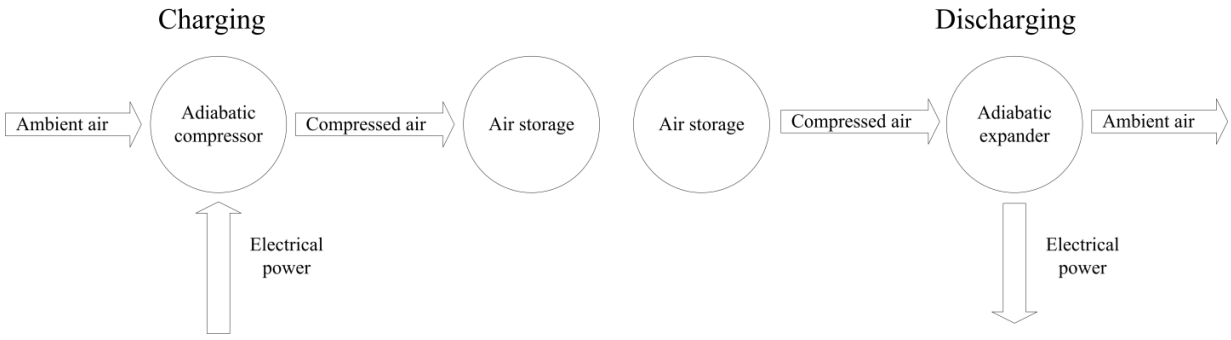

Fig. 7: Working principle of adiabatic compressed air storage. Figure adapted from [204].

To date, two large-scale dCAES are operational. The CAES power plant Huntdorf in Germany with a converter power of 321 MW and storage unit capacity of 642 MWh and the McIntosh CAES plant in the U.S. with a lower converter power (110 MW), but a significantly higher discharging duration (26 h) and hence bigger storage unit capacity (2,860 MWh) [73]. Adiabatic systems are currently in research and demonstration status.

Similar to PHS, CAES is suitable for mid to long-term storage applications with lower numbers of cycles. Moreover, fast response times enable applications for ancillary services (e.g. frequency and voltage control) [200]. For cost assessments of aCAES systems, somewhat discordant conclusions exist in the current research. Connolly [65] states high capital costs owing to the dependency on geographically suitable sites, whereas Fuchs et al. [200] or Aneke and Wang [66] name relatively low costs of the storage unit as one main advantage. Today, the cycle efficiency of dCAES is around 0.54 (Huntdorf plant), whereas for aCAES efficiencies of 0.7 are set as a goal for future developments [202, 204].

3.4 Lithium-ion batteries

The cathode material of lithium-ion batteries (Li-ion) typically consists of a lithium metal oxide (e.g. $LiCoO_2$, $LiMO_2$, $LiNiO_2$), whereas graphite carbon is used as anode material. Both cathode and anode are immerged into an electrolyte made of lithium salts (e.g. $LiPF_6$, $LiClO_4$) which again are dissolved in organic carbonates [198]. The fundamentals of operation are based on the electric potential difference of the electrodes to generate electricity. During charging, lithium ions of the cathode traverse through the electrolyte. At the carbon anode the lithium ions combine with external electrons and are placed between carbon layers as lithium atoms [198]. The reverse process occurs in discharging mode.

The high gravimetric energy (75–200 Wh/kg) and power density (150–315 W/kg) [198, 202] enables compact system sizes of lithium-ion batteries. Additionally, further benefits include round-trip efficiencies as high as 97%, storage cycles up to 10,000, short response times (milliseconds) [202], and low self-discharge rates (0.1–5%/day [67, 68, 198]).

To date, main drawbacks include the lifetime and depth of discharge (DOD) of Li-ion storage. Both parameters are temperature dependent and aging effects occur if not monitored sufficiently [75]. In this regard, a sophisticated battery management system is required [200], which, furthermore, ensures optimal operating [75]. In consequence, system costs of Li-ion storage are still high, primarily caused by special packaging and the battery management [198]. However, recently, substantial cost reductions have been achieved and current costs per cell (as of 2014) range from 225 to 800 USD/kWh for utility-scale applications [69]. Moreover, recent reviews of cost projections, such as the studies of Nykvist and Nilsson [70][16] or Cole et al. [71], show that

[16] Although the study only reviews current costs and cost projections for the application in battery electric vehicles (high capacity Li-ion batteries), the values are also transferable the stationary usage of Li-ion batteries.

the average costs are likely to fall below 300 USD/kWh by 2025 and even further cost degressions are possible.

For stationary applications, current Li-ion storage installations are usually used for frequency control. One of the largest systems in that regard is the KEPCO-owned (Korea Electric Power Corporation) EES in Gyeongsan, South Korea with a rated power of 48 MW and 12 MWh[17] storage capacity [73], or the WEMAG Li-ion storage in Germany (5 MW/5 MWh) [72]. As of today, Li-ion storage systems whose primary purpose is the large-scale integration of VRE generation technologies (i.e. *energy management*) on utility-scale outside of ancillary services are not common. However, some examples exist, such as the Tehachapi Wind Energy Storage Project in Southern California which consists of a 8 MW/32 MWh[17] system [73].

3.5 Redox-flow batteries

In redox-flow batteries two separate tanks store the electrolyte which is pumped through the cells of a reactor. An ion-permeable membrane divides the positive and negative electrolyte and the proton exchange between both electrodes generates the electric power output [75]. Currently, the most common types include Vanadium, Zinc-Bromine, and Iron-Chromium redox-flow batteries.

Opposed to other electrochemical storage options, the converter and storage unit of redox-flow batteries are detached from each other. Therefore, power and energy-related capacity can be scaled individually and unconstrained (*disjoint capacity* [97]). In this sense, the energy-to-power ratio (E2P) is only determined by the amount of electrolyte in relation to the power rating at the cell stack (active area) [198]. This enables a broad range of applications, including the use for ancillary services, load leveling, large-scale integration of VRE, or UPS for island grids [74]. Moreover, the lifetime of redox-flow batteries is independent from the DOD [75].

Main drawbacks of the technology are the low energy density (0.045–0.089 kWh/l) and their high investment costs [75], mainly driven by the system complexity of the cell (i.e. converter unit) [79] or maintenance of the tanks due to leakage [200].

[17] The Global Energy Storage Database of the U.S. department of energy provides installed converter capacity as well as the duration. The latter is defined as the amount of time the storage can discharge at the rated power capacity and used to conclude from the power-related to the energy-related capacity.

3.6 Hydrogen storage

Main advantages of H_2 are the high heating value of 141.9 MJ/kg[18] and its high gravimetric energy density of 33.3 kWh/kg. However, compared to other fuels, such as natural gas, the volumetric energy density of H_2 at atmospheric pressure is rather low (0.003 kWh/l). Therefore, H_2 is typically stored under pressure (up to 700 bar), improving its volumetric energy density to 1.9 kWh/l. Furthermore, H_2 allows the coupling of different energy sectors, such as transportation, heat, and the power sector.

The main idea of hydrogen storage (H_2) is to use surplus electricity for the electrolysis of water to hydrogen and oxygen.

The electrolysis process is comparable to a fuel cell, but with inverse current flow [203]. The most common technologies to convert water to H_2 are alkaline or polymer electrolyte membrane (PEM) electrolyzer[19]. Both options operate at cell temperatures around 50 to 80 °C and achieve efficiencies of 80% at atmospheric pressure [78]. Currently, alkaline electrolysis is the more mature technology of both options, allowing H_2 production up to 740 m³/h per stack and 30,000 m³/h for a complete system [76]. As of today, the most efficient alkaline electrolyzer require around 4.3 kWh of electricity to produce 1 m³ of H_2 [76]. Current systems are designed for an optimal operating point (maximum H_2 output at constant current), however, in principle, alkaline electrolyzer are able to operate in a flexible way, provided that the minimal load rate of 20–40% of its nominal capacity is ensured. Increasing module sizes are assumed to lower the specific energy demand for the electrolysis, thus improving its efficiency [76]. As of today, PEM electrolysis is mostly used for smaller systems (H_2 production < 30 m³/h, P_{el} < 50 kW); major drawbacks are the limited lifetime of the membranes [77]. However, PEM is assumed to be a valuable option in many applications as it benefits from the simple system design (e.g. no pumps for circulation of the electrolyte is required). By this means, improvements mainly with regard to the lifetimes as well as lower specific investment costs are required [78]. Further advantages include the flexible operation, as PEM are characterized by low minimum load rates (5% of the nominal capacity) and the possibility of overload operating up to 300% [203].

After electrolysis, H_2 can either be mixed into the natural gas grid infrastructure (1), stored in pressure tanks, underground salt caverns, pressure less in liquid form (-253°C) and in metal

[18] Higher heating value.

[19] Solid oxide electrolyzer cells (SOEC) are another technology which is currently only available in laboratory environments.

hybrids [79] (2), or converted to synthetic methane with the help of CO or CO_2 (3) (see Fig. 8). These concepts are also referred to as *power-to-X*.

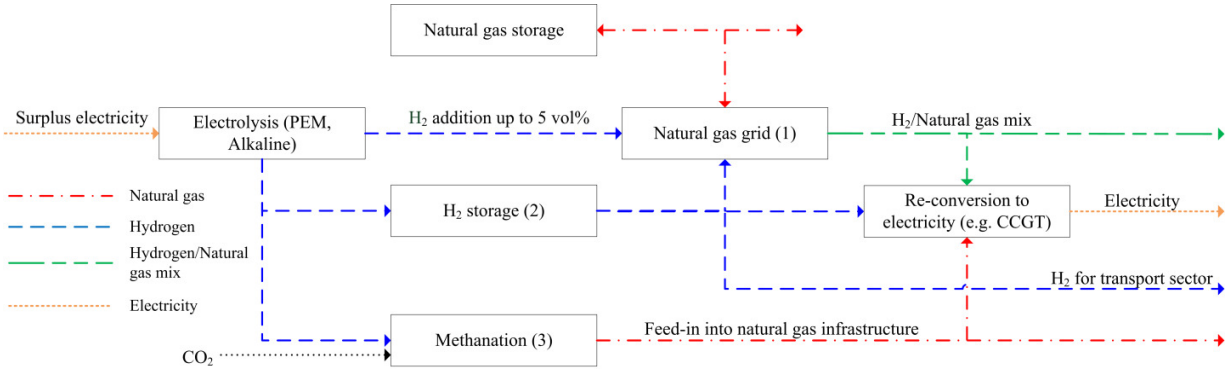

Fig. 8: Different options for hydrogen storage. Figure adapted from [80].

After the storage process, the stored medium can be re-converted to electricity in CCGTs (provided the input is a H_2/natural gas mix, natural gas, or possibly pure H_2), fuel cells (if H_2), or gas turbines (if H_2/natural gas mix or natural gas). Moreover, the H_2/natural gas mix can be fed into the natural gas infrastructure and used in the transport and heating sector. Similarly, pure H_2 can be utilized in hydrogen mobility (see e.g. [81]). In particular, the existing storage infrastructure (natural gas grid) and relatively low costs for additional storage options (natural gas storage or underground salt caverns) qualify H_2 storage for long-term applications. As of today, drawbacks mainly exist with regard to the high costs of the electrolyzer as well as the relatively low overall efficiency [200].

4 The REMix energy system modeling framework

This chapter provides an introduction to energy system models and the modeling framework REMix. The fundamental mathematical representation is included as well as a more in-depth discussion of the storage and thermal power plant modeling approach.

4.1 Introduction to energy system models

As questions of climate change and security of energy supply become more pressing, analyzing possible ways of integrating renewable energy technologies into the energy system has become a crucial issue. In this regard, "… coherent technical analyses of how renewable energy can be implemented, and what effects renewable energy has on other parts of the energy system" [85] are necessary. Energy system models can provide such insights and help to understand questions of future energy demand and supply structures.

A large variety of energy system models exists, each developed for different purposes and characterized by their very own advantages and drawbacks. Some of the differences with regard to the quantification of storage demand have already been discussed in Sec 2.1. An extensive review of energy system models that analyze the integration of renewable energies into the energy system is provided by Connolly et al. [85]. Hall and Buckley [82] discuss models with a focus on energy scenarios for the UK, whereas the review of Krishnan et al. [83] emphasizes models that rely on the co-optimization of the transmission grid, storage, and generation capacities.

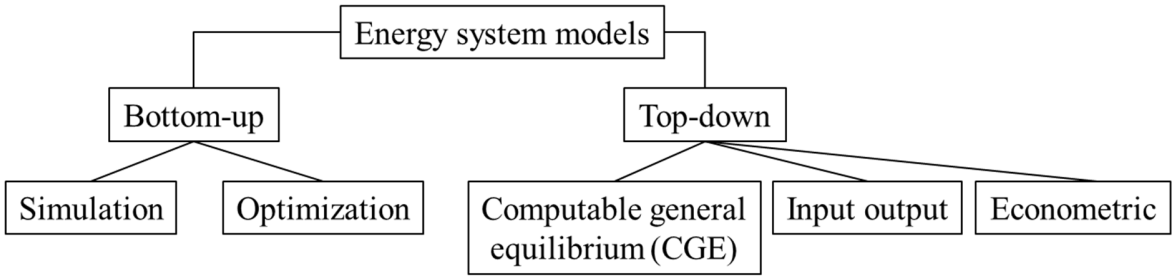

Fig. 9: Classification of energy system models. Figure adapted from [84].

Commonly, energy system models can be differentiated into top-down and bottom-up models (see Fig. 9).

Top-down models allow an aggregated, macroeconomic view of the economy and its energy sectors, identifying effects of energy or climate policies in monetary units [86]. In contrast, bottom-up models are characterized by a higher degree of technological detail, allowing the analysis of specific energy technologies [85]. The latter requires simplifications, such as temporal or spatial aggregations, to preserve traceability of the results [87]. Moreover, the ability of bottom-up models to consider technological progress as well as emerging technologies predestine these approaches for long-term analyses with time horizons of more than 20 years [86]. Bottom-up methods, such as used in the model presented in Sec. 4.2, are therefore an adequate remedy to answer the question of long-term storage demand.

Within bottom-up models, usually, a distinction between simulation and optimization can be found. Simulations typically incorporate a number of different methods, such as accounting frameworks or utility dispatch strategies. These methods aim to balance energy generation and demand over a given time period. Simulations focus on the development of an energy system, while optimizations, in contrary, derive possible future energy scenarios [87]. The most prominent methods in optimizations are linear programming (LP), mixed-integer linear programming (MILP), non-linear programming (NLP), or quadratic programming (QP). All approaches minimize or maximize an objective function subject to a number of constraints. A profound review of optimization approaches for renewable integration studies is provided by Baños et al. [88].

Advantages of LP approaches include efficient solution algorithms which allow the consideration of complex systems, good traceability of the model results, the ability to efficiently identify infeasibilities [89], and the guarantee of mathematical unique solutions [90]. However, some shortcomings of LP methods exist. First, these approaches cannot consider non-linear relations e.g. economies of scale or part load efficiencies of thermal power plants [90]. Yet, some effects, such as the latter, can be approximated via linearization. Second, LPs result in continuous values for decision variables. Some of these decision variables, however, might be of discrete nature, e.g. power plant starts and shutdowns. Third, LP is prone to penny switching solutions where results are extreme solutions which are not robust against parameter variations. In this sense, it is of great importance to validate the robustness of the model results against *parametric uncertainty* (see Sec. 2.3).

The subsequent equations show the standard formulation of LP problems. Eq. 4.1 defines the objective function which has to be minimized or maximized. Eq. 4.2 and Eq. 4.3 are constraints which restrict the solution space, where $x = (x_1,\ldots,x_n)$ is the vector of the decision variable,

c = $(c_1,\ldots,c_n)$ the coefficient of the objective function, and b = $(b_1,\ldots,b_m)$ the vector on the right-hand side. A is a $m \times n$ matrix, characterized by n variables and m constraints [91].

$$\begin{aligned} &\min/\max && c^T x, && 4.1 \\ &\text{s.t.} && Ax = b, && 4.2 \\ & && x \geq 0 && 4.3 \end{aligned}$$

4.2 REMix

The energy system model framework REMix consists of two sub-models: On the one hand, EnDAT (**En**ergy **D**ata **A**nalysis **T**ool) allows a global RE resource assessment, providing maximum installable RE capacities in a high spatial resolution and, furthermore, hourly potential generation time-series of VRE technologies. On the other hand, the optimization model OptiMo (**Opti**mization **Mo**del) enables least-cost capacity expansion and dispatch in energy scenarios. The model framework was initially developed by Scholz [213], and, in the context of several PhD-theses, enhanced by aspects of electric vehicles [191], global resource assessment [92], demand response, and thermal storage [146]. In the remainder of this work, REMix refers to the optimization sub-model OptiMo and is subsequently explained in more detail.

REMix allows a cost minimizing, integral optimization of utility dispatch and capacity expansion. The model minimizes the total system costs of an energy scenario, which are comprised of the annuities of the overnight investment costs of capacity expansion as well as the operating costs of the utility dispatch. The latter include fuel, emission certificates as well as operation and maintenance costs (O&M). The model's decision variables are hourly capacity dispatch and annual capacity expansion, which are optimized for each model interval. A cross-sectoral approach enables the consideration of the transport, heat, and power sector. In this thesis, however, only the latter is examined. The deterministic linear optimization considers techno-economic constraints, such as resource availability for renewable energy systems or cost and efficiency assumptions for generation technologies. The approach relies on an hourly resolution and perfect foresight over the optimization horizon. REMix is developed in the mathematical programming language GAMS (**G**eneral **A**lgebraic **M**odeling **S**ystem) [93] and solved with CPLEX [94]. An overview of the model functionality is provided by Fig. 10, whereas a detailed model description including the mathematical framework can be found in Gils et al. [112]. Additionally, Appendix D provides a concise model fact-sheet [95].

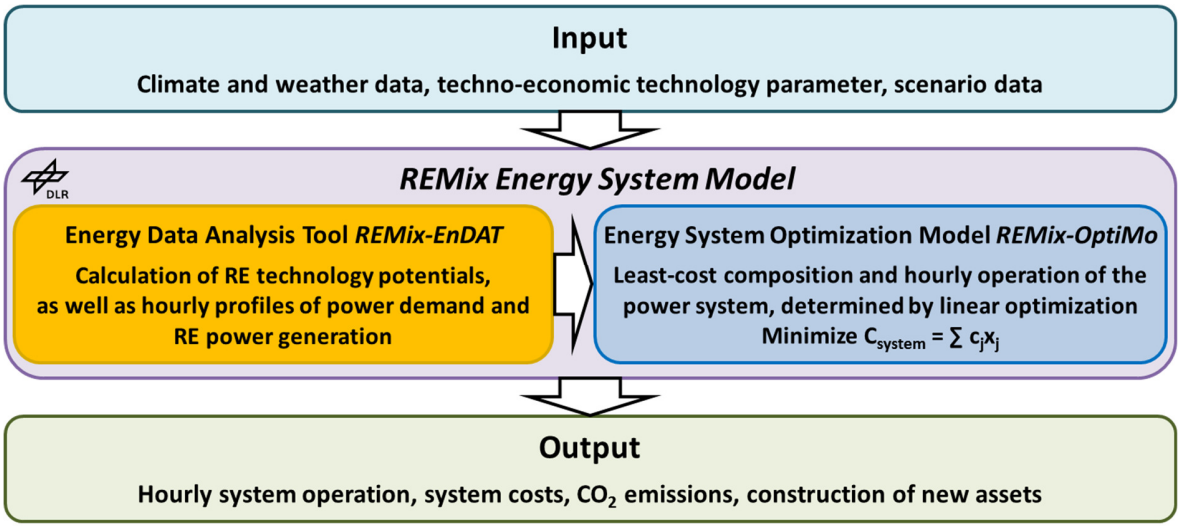

Fig. 10: Fundamental structure of the REMix modeling framework. Figure is based on [96].

Subsequently, the most relevant model equations are explained. This includes a detailed description of overarching equations and equations which describe the storage as well as thermal power plant modeling approach as they are of particular interest in this study. Variables are denoted in italic, whereas for parameters regular font is used. Specific parameters are written in small letters, indices in italic and subscript.

4.2.1 Objective function

The model minimizes the overall sum C^{Total} of the investment costs of capacity expansion C^{Inv} discounted through the annuity factor $f_x^{Annuity}$ as well as the operating costs for annual dispatch C^{Op} of all system components $x \in X$ and model regions $n \in N$. System components are defined as generation or flexibility technologies, such as power plants, VRE systems, storage, or grid infrastructure. The operating costs C^{Op} are derived over all time-steps $t \in T$ of the observed time period. Investments into new capacities C^{Inv}, in contrary, are only dependent on the additional required capacity $P_{x,n}^{Cap\_Added}$ to satisfy the electrical load. Moreover, the overall costs include a penalty term for the costs of artificial generation C^{Slack}, or, in other words, unsupplied power. The latter are, identical to the operating costs C^{Op}, derived over all time-steps $t \in T$ and dependent on the amount of unsupplied energy $P_{x,n}^{Slack}(t)$ over all time-steps. The specific costs of unsupplied power or artificial load c_x^{Slack} are typically assigned to very high costs to ensure that energy supply or load from other sources is used first, and, artificial generation or consumption is dispatched as last option to prevent the mathematical infeasibility of the model run.

$$C^{Total} = C^{Inv} + C^{Op} + C^{Slack} \tag{4.4}$$

s.t.

$$\begin{aligned} &= \min \sum_{x \in X} \sum_{n \in N} P_{x,n}^{Cap\_Added} * \mathrm{c}_x^{Inv} * \mathrm{f}_x^{Annuity} \\ &+ \sum_{x \in X} \sum_{n \in N} \sum_{t \in T} P_{x,n}^{Gen}(t) * \mathrm{c}_x^{Op} \\ &+ \sum_{n \in N} \sum_{t \in T} P_n^{Slack}(t) * \mathrm{c}^{Slack} \end{aligned} \tag{4.5}$$

$$C^{Total} \overset{!}{\geq} 0 \tag{4.6}$$

$$\forall\, x \in X, \forall\, n \in N, \forall\, t \in T$$

4.2.2 Operating costs

The operating costs consist of several cost components, namely variable as well as fixed operations and maintenance costs ($C^{O\&M\_Var}$, $C^{O\&M\_Fix}$), fuel costs C^{Op_Fuel}, and emission certificate costs C^{Op_CO2}. Fixed O&M costs are expressed relatively to the overall investment costs, variable O&M costs relatively to the output (e.g. power or heat generation) of a system component $x \in X$. The model region-specific capacity of a system component $P_{x,n}^{Cap\_Added}$ only includes investments into new capacities and excludes already existing capacities. The fuel costs C^{Op_Fuel} derive from the power generation $P_{x,n}^{Gen}(t)$ over all time-steps $t \in T$ divided by the net efficiency η_x^{Net} of the system component, multiplied with the technology-specific fuel costs c_x^{Fuel}. Costs that occur due to ramping processes in terms of wear and tear are incorporated in $C^{Op\_W\&T}$. The overall change of power due to ramping $P_{x,n}^{W\&T\_Total}$ is multiplied with the technology-specific ramping costs $\mathrm{c}_x^{W\&T}$.The CO_2 emission costs consist of the fuel consumption multiplied with the specific emission factor f_x^{CO2} for each technology (i.e. fuel type) and the specific CO_2 emission costs c_x^{CO2}. A mapping ensures the correct linkage of system components (i.e. technologies) to the fuel types and the specific CO_2 costs a therefore here shown as technology-specific. In this sense, open cycle gas turbines, for example, can only be natural gas fired.

$$C^{Op} = C^{Op\_Var} + C^{Op\_Fix} + C^{Op\_Fuel} + C^{Op\_W\&T} + C^{Op\_CO2} \quad 4.7$$

$$\begin{aligned}
&= \sum_{x\in X}\sum_{n\in N}\sum_{t\in T} P_{x,n}^{Gen}(t) * c_x^{O\&M_var} && \text{Variable operating and maintenance costs } C^{O\&M_Var}\\
&+ \sum_{x\in X}\sum_{n\in N} P_{x,n}^{Cap_Added} * c_x^{Inv} * c_x^{O\&M_Fix} && \text{Fixed operating and maintenance costs } C^{O\&M_fix}\\
&+ \sum_{x\in X}\sum_{n\in N}\sum_{t\in T} \frac{P_{x,n}^{Gen}(t)}{\eta_x^{Net}} * c_x^{Fuel} && \text{Fuel Costs } C^{Op_fuel}\text{[20]}\\
&+ \sum_{x\in X}\sum_{n\in N} P_{x,n}^{W\&T_Total} * c_x^{W\&T} && \text{Wear and tear costs } C^{Op_W\&T}\\
&+ \sum_{x\in X}\sum_{n\in N}\sum_{t\in T} \frac{P_{x,n}^{Gen}(t)}{\eta_x^{Net}} * f_x^{CO2} * c_x^{CO2} && \text{CO}_2\text{ emission costs } C^{Op_CO2}
\end{aligned} \quad 4.8$$

$$\forall\, x \in X, \forall\, n \in N, \forall\, t \in T$$

4.2.3 Investment costs

The investment costs C^{Inv}, sometimes referred to as capital expenditure costs (CAPEX), describe the discounted overnight investment costs of a system component x. Investment costs are calculated with regard to the model endogenously derived capacity expansion $P_{x,n}^{Cap\_Added}$ of system components at a specific model region n. They are expressed as annuities, i.e. equal payments over the technology-specific amortization period N_x^{AmorT}, for each observation year and dependent on the discount rate i. If a system component consists of several sub-components, such as for storage technologies which are comprised of the converter and storage unit, the annuity factor is derived for each sub-component individually.

$$C^{Inv} = \sum_{x\in X}\sum_{n\in N}\left(P_{x,n}^{Cap\_Added} * c_x^{Inv} * f_x^{Annuity}\right) \quad 4.9$$

$$f_x^{Annuity} = \frac{i * (1+i)^{N_x^{AmorT}}}{(1+i)^{N_x^{AmorT}} - 1} \quad 4.10$$

$$\forall\, x \in X, \forall\, n \in N$$

4.2.4 Power balance

The power balance equation is one of the most important model constraints. It ensures that the total generation of all system components equals the power demand in each time-step t of the

[20] This equation only applies for the simplified modeling approach for thermal power plants (see Sec. 4.2.10). Fuel costs in the more detailed mixed-integer unit commitment include fuel consumption due to start-up processes.

observation period as well as in all model regions n. Electricity demand consists of the power demand, storage charging, electricity export via the transmission grid, and grid losses at each time-step and model region. Moreover, the demand side includes artificial load $P_n^{Slack\_Neg}(t)$ in case surplus electricity exist that cannot be balanced through storage, grid, or curtailments. The generation can be provided by the dispatch $P_{x,n}^{Gen}(t)$ of thermal power plants, VRE systems, and discharging from EES $P_{x,n}^{Stor\_Dis}(t)$. If a power generation deficit exists in one model region, electricity can also be transferred via the transmission grid infrastructure from regions of power surplus $P_{x,n}^{Grid\_Imp}(t)$. Similar to the demand side, the slack variable $P_n^{Slack\_Pos}(t)$ ensures the feasibility of the model by providing artificial generation in case that the electrical demand cannot be satisfied by any other generation technologies, storage discharging, or electricity import.

$$\overbrace{P_n^{Load}(t) + P_n^{Slack\_Neg}(t) + \sum_{x \in X} P_{x,n}^{Stor\_Char}(t) + P_{x,n}^{Grid\_Exp}(t) + P_{x,n}^{Grid\_Loss}(t)}^{\text{Demand side}} \stackrel{!}{=} \underbrace{P_n^{Slack\_Pos}(t) + \sum_{x \in X} P_{x,n}^{Gen}(t) + P_{x,n}^{Stor\_Dis}(t) + P_{x,n}^{Grid\_Imp}(t)}_{\text{Supply side}} \quad 4.11$$

$$\forall\, x \in X, \forall\, n \in N, \forall\, t \in T$$

4.2.5 Capacity constraints

The model includes constraints that limit the capacity expansion for each model region n and system component x. These upper boundaries restrict the overall installable capacity, consisting of the already existing capacity $P_{x,n}^{Cap\_Installed}$ and the additional endogenously derived capacity $P_{x,n}^{Cap\_Added}$. Capacity constraints can be understood as technical potential for certain technologies. For VRE technologies for example, capacity limits are based on results of the REMix sub-model EnDAT and are subject to resource availability (e.g. wind speeds or solar irradiation) or site availability (e.g. exclusion of protected areas or water depth for offshore wind systems). However, capacity constraints may also include economic considerations, such as minimum wind speed for suitable locations of wind turbines.

$$P_{x,n}^{Cap\_Added} + \mathrm{P}_{x,n}^{Cap\_Installed} \overset{!}{\leq} \mathrm{P}_{x,n}^{Cap\_Total} \qquad 4.12$$

$$\forall\, x \in X, \forall\, n \in N$$

4.2.6 Generation constraints

Similar to the capacity constraints, generation constraints limit the possible generation (e.g. power or heat) from a certain system component x, at a certain time-step t, and model region n. Planned and unplanned outages of the generation technology are included by the availability factor τ.

$$P_{x,n}^{Gen}(t) \overset{!}{\leq} (P_{x,n}^{Cap\_Installed} + \mathrm{P}_{x,n}^{Cap\_Added}) * \tau_x \qquad 4.13$$

$$\forall\, x \in X, \forall\, n \in N, \forall\, t \in T$$

4.2.7 Curtailments of variable, renewable power generation

The subsequent equation defines the amount of energy that is curtailed, expressed in terms of surplus. $\mathrm{p}_{x,n}^{PotGen}(t)$ describes the normalized, potential, technology and region-specific power generation from VRE technologies. The overall installed VRE capacity is described by the sum of $P_{x,n}^{Cap\_Installed}$ and $\mathrm{P}_{x,n}^{Cap\_Added}$ (i.e. considering already existing and endogenously derived capacities). In this standard formulation, curtailments are unrestricted and not associated with any costs.

$$P_{x,n}^{Cur}(t) \overset{!}{=} \underbrace{(\mathrm{p}_{x,n}^{PotGen}(t) * \left(P_{x,n}^{Cap\_Installed} + \mathrm{P}_{x,n}^{Cap\_Added}\right) * \tau_x)}_{\text{Potential power generation from VRE}} - P_{x,n}^{Gen}(t) \qquad 4.14$$

$$\forall\, x \in X, \forall\, n \in N, \forall\, t \in T$$

4.2.8 Restricted curtailments of variable, renewable power generation

This formulation allows to restrict curtailments technology-specific over the whole observation area (e.g. Europe), expressed as a share of the potential power generation from VRE. The latter is included via the technology-specific curtailment share cur_x.

$$\sum_{t\in T} P_{x,n}^{Cur}(t) \overset{!}{\leq} \sum_{t\in T}\left[\mathrm{p}_{x,n}^{PotGen}(t) * \left(P_{x,n}^{Cap_{Installed}} + \mathrm{P}_{x,n}^{Cap_{Added}}\right) * \tau_x\right] * cur_x \qquad 4.15$$

$$\forall\, x \in X, \forall\, n \in N, \forall\, t \in T$$

4.2.9 Storage modeling

Subsequently, the most important equations for storage modeling are explained. Opposed to other generation technologies[21], each storage is comprised of two sub-components: a converter unit (power-related) and a storage unit (energy-related). In this sense, the converter unit of a pumped hydropower storage, for example, would refer to the pump and turbine, whereas the water reservoir can be defined as the storage unit. Similar to all other technologies, the model optimizes the hourly dispatch as well as the capacity expansion, i.e. investments into additional capacity.

Storage capacity constraints

Following the modeling approach of other technologies, investments into additional storage are limited by capacity constraints. More specifically, the capacity expansion is restricted for both converter $P_{x,n}^{Stor\_Added}$ and storage unit $E_{x,n}^{Stor\_Added}$ by the maximum installable converter capacity $\mathrm{P}_{x,n}^{Stor\_Total}$ and storage unit capacity $\mathrm{E}_{x,n}^{Stor\_Total}$ respectively. The ratio of installed power (converter) to energy (storage unit) capacity can either be dimensioned independently (*disjoint capacity* [97]) or via an E2P ratio (*integrated capacity* [97]). Again, the constraint is applied for the sum of already existing capacities (*Installed*) and capacity expansion (*Added*).

$$E_{x,n}^{Stor\_Added} + \mathrm{E}_{x,n}^{Stor\_Installed} \overset{!}{\leq} \mathrm{E}_{x,n}^{Stor\_Total} \qquad 4.16$$

$$P_{x,n}^{Stor\_Added} + \mathrm{P}_{x,n}^{Stor\_Installed} \overset{!}{\leq} \mathrm{P}_{x,n}^{Stor\_Total} \qquad 4.17$$

$$\forall\, x \in X, \forall\, n \in N$$

[21] Exceptions being concentrating solar power and conventional hydroelectricity (see Sec. 6.1 and Sec. 6.3 in Appendix C). The former consists of a solar field, a thermal energy storage, and a power block; the latter is comprised of a turbine/generator unit and optional retrofitted pumps.

Charge and discharge constraints

Similar to the generation constraints (see Sec. 4.2.6) storage charging $P_{x,n}^{Stor\_Char}$ and discharging $P_{x,n}^{Stor\_Dischar}$ for each storage technology x and model region n are limited by the overall storage converter power. The latter again includes already existing storage converter capacity $P_{x,n}^{Stor\_Installed}$ and endogenously derived capacity $P_{x,n}^{Stor\_Added}$.

$$P_{x,n}^{Stor\_Char}(t) + P_{x,n}^{Stor\_Dischar}(t) \overset{!}{\leq} P_{x,n}^{Stor\_Added} + P_{x,n}^{Stor\_Installed} \qquad 4.18$$

$$\forall\, x \in X, \forall\, n \in N, \forall\, t \in T$$

Storage balance

The storage balance equation assures that the storage fill level $E_{x,n}^{Stor\_Level}(t)$ in each time-step is equal to the fill level in the preceding time-step $E_{x,n}^{Stor\_Level}(t-1)$, considering the discharged and charged energy. Additionally, technology-specific charging $\eta_x^{Stor\_Char}$ and discharging efficiencies $\eta_x^{Stor\_Dischar}$ as well as the self-discharge rate $\mu_x^{Stor\_Selfdischar}$ are considered. Self-discharging is defined through the average difference in the fill level of two time-steps $\frac{E_{x,n}^{Stor\_Level}(t)+E_{x,n}^{Stor\_Level}(t-1)}{2}$.

$$\begin{aligned} & E_{x,n}^{Stor\_Level}(t) - E_{x,n}^{Stor\_Level}(t-1) \\ & \overset{!}{=} \\ & \left(P_{x,n}^{Stor\_Char}(t) * \eta_x^{Stor\_Char} - \frac{P_{x,n}^{Stor\_Dischar}(t)}{\eta_x^{Stor\_Dischar}}\right) * \Delta t \\ & - \\ & \frac{E_{x,n}^{Stor\_Level}(t) + E_{x,n}^{Stor\_Level}(t-1)}{2} * \mu_x^{Stor\_Selfdischar} \end{aligned} \qquad 4.19$$

$$\forall\, x \in X, \forall\, n \in N, \forall\, t \in T$$

The storage level variable $E_{x,n}^{Stor\_Level}(t)$ could be substituted through an alternative formulation, where the storage level is calculated via the sum of charging, discharging, and self-discharging. However, the calculation times of this approach were found to be significantly higher compared to the described method.

4.2.10 Power plant modeling: simplified merit order

Subsequently, the two different modeling approaches for thermal power plans—LP merit order method and MILP unit-commitment with economic dispatch—are explained. Both representations are required for the comparison of both approaches with regard to storage expansion in chapter 5.

As for all other system components x, the simplified merit order based thermal power plant approach includes equations for operating and investment costs as well as generation and capacity constraints. Some specific differences however exist, and are, additional to the power plant-specific equations, explained subsequently.

Generation constraint for thermal power plants

Similar to the generation constraint in Sec. 4.2.6, the available electrical power supply from thermal power plants for every hour is limited by the sum of existing capacities $\mathrm{P}_{x,n}^{Cap\_Installed}$ and the endogenously derived, additional capacities $P_{x,n}^{Cap\_Added}$. Furthermore, due to maintenance work and unexpected events, not all of the installed power is available at each time-step. This is taken into account through the availability factor τ_x. The internal consumption of thermal power plants, which is mainly caused by the pretreatment of fuels and pumps, is incorporated via the division of η_x^{Net} by η_x^{Gross}.

$$P_{x,n}^{Gen}(t) \overset{!}{\leq} \left(P_{x,n}^{Cap\_Added} + \mathrm{P}_{x,n}^{Cap\_Installed}\right) * \frac{\eta_x^{Net}}{\eta_x^{Gross}} * \tau_x \qquad 4.20$$

$$\forall\, x \in X, \forall\, n \in N, \forall\, t \in T$$

Fuel consumption

The fuel consumption of thermal power plants for each time-step t is obtained by the division of the electrical power generation $P_{x,n}^{Gen}(t)$ with the net efficiency η_x^{Net}.

$$E_{x,n}^{FuelCons}(t) = \frac{P_{x,n}^{Gen}(t)}{\eta_x^{Net}} \quad 4.21$$

$$\forall\, x \in X, \forall\, n \in N, \forall\, t \in T$$

Wear and tear costs

Wear and tear costs describe costs that arise due to positive and negative power changes of thermal power plants. First, all positive $P_{x,n}^{W\&T\_Pos}(t)$ and negative power changes $P_{x,n}^{W\&T\_Neg}(t)$ for each time-step t are derived. If the right-hand side of Eq. 4.22 becomes positive, ramping up of the power plant occurs. In turn, if the right-hand side in Eq. 4.22 becomes negative (i.e. down ramping), the equation becomes zero as $P_{x,n}^{W\&T\_Pos}(t)$ is declared as a positive variable. Eq. 4.23 for negative power changes works invers, as the right-hand side is multiplied by -1. Lastly, positive and negative power changes are summed over time to the amount of ramping energy and multiplied with the specific cost for ramping .

$$P_{x,n}^{W\&T\_Pos}(t) \overset{!}{\geq} P_{x,n}^{Gen}(t) - P_{x,n}^{Gen}(t-1) \quad 4.22$$

$$\forall\, x \in X, \forall\, n \in N, \forall\, t \in T$$

$$P_{x,n}^{W\&T\_Neg}(t) \overset{!}{\geq} -1 * \left(P_{x,n}^{Gen}(t) - P_{x,n}^{Gen}(t-1)\right) \quad 4.23$$

$$\forall\, x \in X, \forall\, n \in N, \forall\, t \in T$$

$$C_{x,n}^{W\&T\_Total} = \sum_{t \in T} \left(P_{x,n}^{W\&T\_Pos}(t) + P_{x,n}^{W\&T\_Neg}(t)\right) * \mathrm{c}^{W\&T} \quad 4.24$$

$$\forall\, x \in X, \forall\, n \in N, \forall\, t \in T$$

4.2.11 Power plant modeling: unit commitment with economic dispatch

The mixed-integer linear programming (MILP) modeling approach allows an optimized piecewise thermal power plant commitment. The method is based on the work of Carrión and Arroyo [108] and was initially implemented into the REMix framework by Fichter [150]. During this study, the method then was adapted into the sub-model OptiMo of the REMix framework. A

comparison of both power plant modeling approaches—simplified merit order and unit commitment with economic dispatch—is provided in chapter 5, emphasizing their impact on storage expansion planning.

The MILP methodology enables to model power plant dispatch on a unit or power block level and, moreover, incorporates a higher degree of technological detail than the LP approach (see Sec. 4.2.10). In this sense, MILP includes part load and temperature dependent efficiencies (via a piecewise linear production cost approach), minimum load rates, ramping processes and associated costs, minimum offline and online times, increased fuel usage and respectively increased costs owing to power plant start-ups as well as different cooling methods influencing the internal consumption (sometimes referred to as *parasitics*) of a power plant.

Maximal online units or power blocks

This equation restricts the number of online thermal power plant units, blocks, or power plant groups. $On_{x,n}(t)$ is an integer unit-commitment (UC) variable, or, in case of modeling each power plant individually, a binary variable [0/1]). The equation is essential for the clustering approach (grouped integer modeling) as it replaces the binary UC variable (on/off) from the single binary UC approach with the integer variable $On_{x,n}(t)$. The latter describes the number of operating units and is restricted by the number of power plants or power units within a cluster, which, again, is expressed as the installed capacity $\mathrm{P}_{x,n}^{Cap\_Installed}$ divided by a typical block or cluster size δ_x and rounded to the nearest integer. A cluster either refers to a power plant group (e.g. large coal-fired or midsize gas-fired power plants) or to power blocks within a power plant. Note that all blocks or units within a cluster are characterized by identical techno-economic parameters.

$$On_{x,n}(t) \overset{!}{\leq} \left\lfloor \left(\mathrm{P}_{x,n}^{Cap\_Installed} / \delta_x\right) \right\rceil \qquad 4.25$$

$$\forall\, x \in X, \forall\, n \in N, \forall\, t \in T$$

Initial commitment status

This equation determines the initial unit-commitment status κ_x, or, in other words, if a power plant is online or offline before the first time-step of the optimization.

$$On_{x,n}(t) = \kappa_x \tag{4.26}$$

$$\forall\, x \in X, \forall\, n \in N, t = 0$$

Power plant start

The power plant start equation determines if a start-up of a block or unit occurred, thus comparing the status of the power plant in the current time-step $On_{x,n}(t)$ with the previos time-step $On_{x,n}(t-1)$.

$$Start_{x,n}(t) \overset{!}{\geq} On_{x,n}(t) - On_{x,n}(t-1) \tag{4.27}$$

$$\forall\, x \in X, \forall\, n \in N, \forall\, t \in T$$

Possible load range

The possible load range is a generation constraint which restricts the upper and lower range of power generation of thermal units or power blocks.

Equation 4.28 describes the lower range of power generation dependent on the factor of minimum load of a power plant λ_x^{Min} with respect to its nominal capacity expressed by the multiplication of the typical block size δ_x with the number of operating units $On_{x,n}(t)$ and the availability τ_x.

$$\begin{aligned}
&\text{if } \theta_{n,t} \leq 10°C && f(\theta 1_{n,t}) * \lambda_x^{Min} * \delta_x * On_{x,n}(t) * \tau_x \overset{!}{\leq} P_{x,n}^{Gen}(t) \\
&\text{if } 10°C < \theta_{n,t} \leq 25°C && f(\theta 2_{n,t}) * \lambda_x^{Min} * \delta_x * On_{x,n}(t) * \tau_x \overset{!}{\leq} P_{x,n}^{Gen}(t) \\
&\text{if } \theta_{n,t} > 25°C && f(\theta 3_{n,t}) * \lambda_x^{Min} * \delta_x * On_{x,n}(t) * \tau_x \overset{!}{\leq} P_{x,n}^{Gen}(t)
\end{aligned} \tag{4.28}$$

$$\forall\, x \in X, \forall\, n \in N, \forall\, t \in T$$

Moreover, the ambient temperature has to be considered as the power output of some power plant technologies, such as gas turbines, is heavily dependent on the intake pressure (i.e. density of the air[22]). To incorporate the latter, the time-dependent temperature correction factor $f(\theta_{n,t})$ is introduced (see [174] and Eq. 4.29). $\theta_{n,t}$ describes the ambient temperature at the location n at the

[22] The air density is furthermore dependent on the geodesic height of the power plant. However, in this approach, only the influence of the ambient temperature is considered.

time-step t of the power plant. $f(\theta_{n,t})$ again is defined by the two coefficients A1 and A2 for temperature ranges ≤ 10°C (or A3 and A4 for 10–25°C or A5 and A6 for > 25°C).

$$\begin{aligned} f(\theta 1_{n,t}) &= \mathrm{A1} * \theta 1_{n,t} + \mathrm{A2} \\ f(\theta 2_{n,t}) &= \mathrm{A3} * \theta 2_{n,t} + \mathrm{A4} \\ f(\theta 3_{n,t}) &= \mathrm{A5} * \theta 3_{n,t} + \mathrm{A6} \end{aligned} \qquad 4.29$$

$$\forall\, n \in N, \forall\, t \in T$$

The upper limit of power generation is shown in Eq. 4.30. Similar to the lower limit of power generation, the temperature correction coefficients $f(\theta_{n,t})$ are considered.

$$\begin{aligned} &\text{if } \theta_{n,t} \leq 10°\mathrm{C} && f(\theta 1_{n,t}) * \delta_x * On_{x,n}(t) * \tau_x \overset{!}{\geq} P_{x,n}^{Gen}(t) \\ &\text{if } 10°\mathrm{C} < \theta_{n,t} \leq 25°\mathrm{C} && f(\theta 2_{n,t}) * \delta_x * On_{x,n}(t) * \tau_x \overset{!}{\geq} P_{x,n}^{Gen}(t) \\ &\text{if } \theta_{n,t} > 25°\mathrm{C} && f(\theta 3_{n,t}) * \delta_x * On_{x,n}(t) * \tau_x \overset{!}{\geq} P_{x,n}^{Gen}(t) \end{aligned} \qquad 4.30$$

$$\forall\, x \in X, \forall\, n \in N, \forall\, t \in T$$

Piecewise linear generation

These equations derive the overall power generation for each technology (power plant, power block) and each time-step t. The piecewise linear approach relies on the concept that the generation is divided into several generation ranges, here denoted $P_{x,n}^{Gen\_P1}(t)$ and $P_{x,n}^{Gen\_P2}(t)$. The lower bound of the power output in the first generation range ($P1$) is defined by the relative minimum load of a power plant λ_x^{Min} multiplied with the typical block size δ_x. The upper limit of the power generation in $P1$ is described by the relative maximum generation in the first range λ_x^{Part} multiplied with the typical block size δ_x. Consequently, the power generation in the first range $P_{x,n}^{Gen\_P1}(t)$ has to be lower than the power generation at the maximum generation in $P1$ subtracted by the power generation at the minimum generation point.

$$P_{x,n}^{Gen\_P1}(t) \overset{!}{\leq} On_{x,n}(t) * \tau_x * \left((\lambda_x^{Part} * \delta_x) - (\lambda_x^{Min} * \delta_x)\right) \qquad 4.31$$

$$\forall\, x \in X, \forall\, n \in N, \forall\, t \in T$$

The power output $P_{x,n}^{Gen\_P2}(t)$ of the second generation range ($P2$) is limited by the typical block size δ_x and the maximum generation from $P1$.

$$P_{x,n}^{Gen\_P2}(t) \overset{!}{\leq} On_{x,n}(t) * \tau_x * (\delta_x - \delta_x * \lambda_x^{Part}) \tag{4.32}$$

$$\forall\, x \in X, \forall\, n \in N, \forall\, t \in T$$

The overall generation than consists of the power output of the two generation ranges and the generation from start-up to the minimum generation. Again, each equation is defined by different ambient temperature ranges.

$$\begin{aligned}
&\text{if } \theta_{n,t} \leq 10°C && P_{x,n}^{Gen}(t) = f(\theta 1_{n,t}) * \left(On_{x,n}(t) * \delta_x * \lambda_x^{Min} * \tau_x + P_{x,n}^{Gen_P1}(t) + P_{x,n}^{Gen_P2}(t)\right) \\
&\text{if } 10°C < \theta_{n,t} \leq 25°C && P_{x,n}^{Gen}(t) = f(\theta 2_{n,t}) * \left(On_{x,n}(t) * \delta_x * \lambda_x^{Min} * \tau_x + P_{x,n}^{Gen_P1}(t) + P_{x,n}^{Gen_P2}(t)\right) \\
&\text{if } \theta_{n,t} > 25°C && P_{x,n}^{Gen}(t) = f(\theta 3_{n,t}) * \left(On_{x,n}(t) * \delta_x * \lambda_x^{Min} * \tau_x + P_{x,n}^{Gen_P1}(t) + P_{x,n}^{Gen_P2}(t)\right)
\end{aligned} \tag{4.33}$$

$$\forall\, x \in X, \forall\, n \in N, \forall\, t \in T$$

Minimum up time

The minimum up time determines how many hours a power plant must be online before it is able to shut down again. The parameter UT_x describes the technology-specific minimum up time in hours. Eq. 4.34–Eq. 4.36 also consider how many hours a power plant was online or offline before the actual time period of the power plant dispatch. This is implemented through the index g_x which represents the number of *initial* hours (before the actual time period of the power plant dispatch) during which the power plant is required to be online.

$$\sum_{t=1}^{g_x} \left(\left\lfloor \left(\mathrm{P}_{x,n}^{Cap\_Installed} / \delta_x\right) \right\rfloor\right) - On_{x,n}(t) \overset{!}{=} 0 \tag{4.34}$$

$$\forall\, x \in X, \forall\, n \in N, \forall\, t \in T$$

$$\sum_{j=t}^{t+\mathrm{UT}_x-1} On_{x,n}(j) \overset{!}{\geq} \mathrm{UT}_x \left[On_{x,n}(t) - On_{x,n}(t-1)\right] \tag{4.35}$$

$$\forall\, x \in X, \forall\, n \in N, \forall\, t = g_x + 1 \ldots T - \mathrm{UT}_x + 1$$

$$\sum_{j=t}^{T}\{On_{x,n}(j)-[On_{x,n}(t)-On_{x,n}(t-1)]\}\overset{!}{\geq}0 \tag{4.36}$$

$$\forall\, x\in X, \forall\, n\in N, \forall\, t=T-\mathrm{UT}_x+2\,\ldots T$$

Minimum down time

The minimum down time determines how many hours a power plant must be offline before it is able to ramp up again. The parameter DT_x describes the technology-specific minimum down time in hours. Eq. 4.37–Eq. 4.39 also consider how many hours a power plant was online or offline before the actual time period of the power plant dispatch. This is implemented through the index l_x which represents the number of *initial* hours (before the actual time period of the power plant dispatch) during which the power plant is required to be offline.

$$\sum_{t=1}^{l_x} On_{x,n}(t)\overset{!}{=}0 \tag{4.37}$$

$$\forall\, x\in X, \forall\, n\in N, \forall\, t\in T$$

$$\sum_{j=t}^{t+\mathrm{DT}_x-1}\left[1-On_{x,n}(j)\right]\overset{!}{\geq}\mathrm{DT}_x\left[On_{x,n}(t-1)-On_{x,n}(t)\right] \tag{4.38}$$

$$\forall\, x\in X, \forall\, n\in N, \forall\, t=l_x+1\,\ldots T-\mathrm{DT}_x+1$$

$$\sum_{j=t}^{T}\{1-On_{x,n}(j)-[On_{x,n}(t-1)-On_{x,n}(t)]\}\overset{!}{\geq}0 \tag{4.39}$$

$$\forall\, x\in X, \forall\, n\in N, \forall\, t=T-\mathrm{DT}_x+2\,\ldots T$$

5 Power plant modeling and its influence on storage demand

Merit order or unit-commitment dispatch: How does thermal power plant modeling affect storage demand in energy system models?[23]

As illustrated in Sec. 2.1, the influence of different modeling approaches on storage demand for the large-scale integration of power generation from VRE has not yet been analyzed. By this means, the following chapter sheds light on the question in how far different thermal power plant modeling approaches affect storage capacity expansion and utilization.

[23] This chapter is based on F. Cebulla and T. Fichter, "Merit order or unit-commitment: How does thermal power plant modeling affect storage demand in energy system models?," *Renewable Energy*, vol. 105, pp. 117–132, 2017.

Transparency checklist

Criterion	Page number
General Information	
1. Author, Institution	55
2. Aim and funding	55
3. Key term definitions	XII
Empirical Data	
4. Sources	Appendix B/C
5. Pre-processing	Appendix B/C
Assumptions	
6. Identification of uncertain factors	-
7. Uncertainty consideration	-
8. Storyline construction	-
9. Assumptions for data modification	60, Appendix C
Model exercise	
10. Model fact sheet	Appendix D
11. Model-specific properties	Appendix D
12. Model interaction	-
13. Model documentation	39
14. Output data access	66, Appendix B
15. Model validation	-
Results	
16. Post-processing	-
17. Sensitivity analyses	-
18. Robustness analyses	-
Conclusions and Recommendations	
19. Results-recommendation-relationship	77
20. Uncertainty communication	77

ABSTRACT

Flexibility requirements in prospective energy systems will increase to balance intermittent electricity generation from renewable energies. One option to tackle this problem is electricity storage. Its demand quantification often relies on optimization models for thermal and renewable dispatch as well as capacity expansion. Within these tools, power plant modeling is typically based on simplified linear programming merit order dispatch (LP) or mixed-integer unit-commitment with economic dispatch (MILP). While the latter is able to capture techno-economic characteristics to a large extent (e.g. ramping or start-up costs) and allows on/off decisions of generator units, LP is a simplified method, but superior in computational effort.

An assessment of how storage expansion is affected by the method of power plant modeling is presented and the cost minimizing optimization model REMix is applied, comparing LP with MILP. Moreover, the influence of wind and photovoltaic generation shares is evaluated, varying the granularity of the power plant mix within MILP.

The results show that LP underestimates storage demand, as it neglects technical restrictions which affect operating costs, leading to an unrealistically flexible thermal power plant dispatch. In contrast, storage expansion is higher in MILP. The deviation between both approaches, however, becomes less pronounced if the share of renewable generation increases.

5.1 Introduction

With growing shares of VRE generation in power systems, ensuring sufficient flexibility will play a crucial role as the temporal and spatial mismatch between demand and supply increases. Definitions of flexibility are broad (see [98, 99, 120]), however, the term is commonly understood as the ability to decouple electricity demand and supply to balance variations in the net load [122] (which, in turn, is defined as the electricity load minus the generation from VRE). It is likely that the temporal variability of VRE generation will go along with an increase in storage demand to prevent the aforementioned temporal mismatch [100, 132, 151, 164, 190]. Moreover, higher shares of VRE generation will require a more flexible operation of thermal power plants to meet steeper net load ramps [122].

5.1.1 Literature review

Model-based quantifications of future storage demand result in rather diverse ranges (see Sec. 2.2), depending on the observation area, spatial, temporal and technological resolution as well as the underlying modeling approach (e.g. for thermal power plant modeling in energy system models). Understanding such dependencies and quantifying the amount of storage demand is, therefore, essential for dimensioning future energy systems. Yet, the influence of assumptions in thermal power plant modeling on storage demand has not been considered so far.

Two main approaches of thermal power plant modeling in optimization models can be found in the literature: Detailed mixed-integer linear programming (MILP) approaches that optimize the unit-commitment and economic dispatch of the thermal power plant fleet and simplified linear programming (LP) where the dispatch of thermal power plants follows solely the merit order. Both approaches determine the optimal generation schedule, minimizing the operating costs of power plant dispatch, subject to device and operating constraints [101, 102], sometimes denoted as *operating*, *dynamic*, or *unit-commitment constraints*. MILP however, includes integer (or binary) decision variables, allowing on/off consideration of single power plant units or groups, which again enables greater technological detail (e.g. part load efficiencies, ramping behavior, or minimum offline times).

The influence of increasing shares of VRE generation and their effect in different modeling approaches for thermal power plants has been analyzed for example by Brouwer et al. [103] or Abujarad et al. [102]. The former provide a comprehensive overview of how much VRE generation impacts reserve requirements, curtailments of VRE generation, displacement of thermal generators, and resource adequacy. Abujarad et al. [102] review different approaches for

generation scheduling, such as heuristics (e.g. priority lists), mathematical methods (e.g. MILP or LP), or meta-heuristics (e.g. genetic algorithms), providing a qualitative assessment of their advantages and short-comings when considering increasing penetration levels of VRE and storage systems. The publication underscores the importance of storage as an additional flexibility option, which can enable improved power system reliability or smoothing of load patterns. As both studies [102, 103] review the current state of research, they cannot, by definition, provide a quantitative assessment how electricity storage demand is affected by the modeling approach for thermal power plants.

Other studies specifically compare linear programming with unit-commitment. Abrell et al. [104] for example, compare various LP and MILP formulations for power plant start-ups and ramping, assessing its influence with regard to power plant dispatch and marginal prices of electricity generation. The latter is also research focus of Langrene et al. [105], who investigate the role of technological detail (*dynamic constraints*) in a MILP approach on marginal prices. Raichur et al. [106] analyze the influence of technological detail (*operating constraints*) in power plant modeling with regard to electricity generation associated emissions for two real power systems (New York, Texas). The study mainly relies on scenario data from the year 2010. It is, therefore, difficult to transfer their conclusions to power systems with higher shares of VRE generation. Through the implementation of an integrated utility dispatch and capacity expansion optimization tool, Palmintier [168] shows that the importance of technological detail (*operating constraints*) in power plant modeling increases with greater requirements for flexibility owing to higher shares of VRE generation. Neglecting such technical constraints within capacity expansion optimization can lead to sub-optimal generation portfolios. Poncelet et al. [129] compare the utility dispatch through LP (*merit-order model*) with a MILP model, evaluating whether the influence of the temporal resolution or the influence of the technical detail in power plant modeling is more striking. The analysis is performed for different observation years which, in turn, are characterized by different shares of VRE generation up to 50%. Most recently, Stoll et al. [149] provide a broad comparison of a MILP power plant approach with LP for temporal resolutions of 1 h or 5 min and for differently sized energy systems (Colorado-based test system versus Western Interconnection model). Using PLEXOS [107], their analysis assesses the impact on production costs, VRE curtailment, CO_2 emissions as well as generator starts and ramps. Though comprehensive in terms of evaluated modeling assumptions on various metrics, the study only analyzes the dispatch of an exogenous capacity mix with a relatively low share of VRE penetration (up to 30%). Moreover, the two compared energy systems also show several

differences in the relative installed capacity of some technologies (e.g. coal-fired power plants, gas turbines). By reason of the latter, it can be argued that some effects, therefore, cannot be solely attributed to the power plant modeling approach.

5.1.2 Novelty and contributions

As energy system models become more diverse, their complexity grows, imposing new challenges with regard to computational effort and solution accuracy. As a result, the following questions arise: To which extent do simplifications affect the model's outcome? Under consideration of the model calculation times, which degree of detail is sufficient, without generating large errors? To the best knowledge of the author, the influence of the modeling approach for thermal power plants on storage demand (i.e. storage expansion) and utilization, especially in highly renewable energy scenarios, has not yet been analyzed. It is therefore assumed that dynamic behaviors and associated costs of thermal power plants—such as start-ups, ramping, and minimum down times—might have an effect on storage demand. Furthermore, a certain amount of resolution with regard to technical parameters of power plants and the number of represented units is probably needed since neglecting technical restrictions and aggregating too heavily might lead to a significant deviation from the optimal solution. By this means the future storage expansion in exemplary energy systems is quantified, emphasizing the influence of the modeling approach for thermal power plants, the degree of aggregation in a MILP unit-commitment clustering approach and the influence of different VRE and PV generation shares.

5.2 Methodology and data

5.2.1 Modeling approach

The methodology is based on the linear bottom-up optimization model REMix which minimizes the total system costs of an energy system under perfect foresight. An in-depth description of the basic functions and its mathematical representation is provided in Sec. 4.2.

5.2.2 Power plant modeling in REMix

REMix provides two different methods for thermal power plant modeling: a MILP unit-commitment approach with economic dispatch and a LP merit order method, both described subsequently.

The MILP method is based on a piecewise unit-commitment approach as described by Carróin and Arroyo [108]. At the highest level of detail it allows a generation-unit-specific consideration

of the following techno-economic parameters: part load and temperature dependent efficiencies (via a piecewise linear production cost approach), minimum load rates, ramping processes and associated costs, minimum offline and online times, increased fuel usage and respectively increased costs owing to power plant start-ups, different cooling methods influencing the internal consumption (parasitics) of a power plant. Moreover, each power plant (or power block) is characterized by its construction year which allows the consideration of power plant decommissioning based on the technical lifetime. This again allows to account for construction-year-based efficiencies. For all MILP model runs a relative MILP gap of 0.01% was used. A more detailed description of this modeling approach can be found in the work of Fichter et al. [183] and in Sec. 4.2.11.

The LP approach relies on the merit order and economic scheduling. As for MILP, the dispatch optimization is based on the operating costs (fuel and variable O&M costs, CO_2 allowance certificate costs), including the efficiencies of each technology. Ramping costs are incorporated via costs of power change in terms of wear and tear (€/kW_{el}), whereas the power plant's parasitics are implemented via the ratio of net to gross efficiency. Similar to the MILP approach, power plant technologies are described by their lifetime and construction year to include decommissioning and learning curves in terms of efficiencies.

MILP modeling is a suitable method to consider each power plant or power block of an energy system in detail. For complex power systems, however, the approach struggles with long calculation times. A self-evident solution to this problem is to reduce the number of binary variables by aggregating single power plants into groups with similar techno-economic parameters. Though computationally efficient, the approach fails to consider minimum load rates and start-up costs properly [168]. All power plants within one group are either on or off, due to the binary variable which describes the unit-commitment for each time-step (see [b] in Fig. 11). In consequence, the method systematically underestimates the flexibility of the power plant fleet.

Therefore, a clustering approach (grouped integer modeling) is applied as described by Palmintier [168], which replaces the binary decision variables with integer commitment variables. The value of the latter describes the number of power plants (or power blocks) within each cluster. Opposed to the classical MILP method (binary variable), the grouped integer modeling allows each power plant to start or ramp down individually (see [a] in Fig. 11).

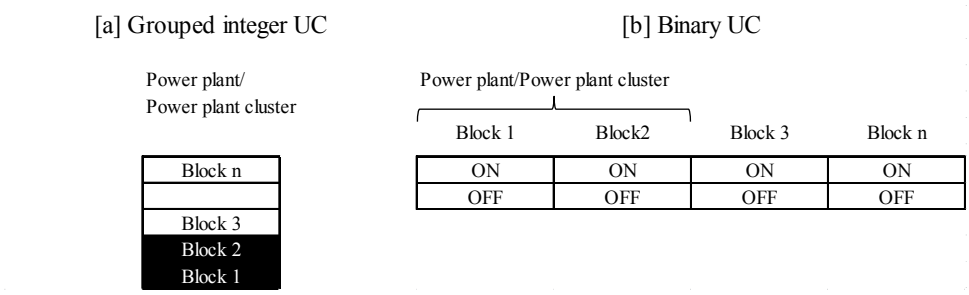

Fig. 11: Grouped integer modeling approach and binary unit-commitment. The figure is adapted from [168].

In this analysis, the power plant portfolio of Germany based on the Platts World Electric Power Plants Database (WEPP) of the year 2010 [210] is used. Furthermore, each power plant is aggregated into different groups (cluster) based on their technology type and plant size. Subsequently, 15 clusters are obtained (see Tab. 2) with an overall installed capacity of 96.18 GW. The clusters encompass fossil-fired (lignite, coal, natural gas) and nuclear power plants. Furthermore, a classification by technology and typical power plant size is applied (i.e. capacity ranges: large, midsize, and small). Within natural gas-fired power plants an additional distinction between gas turbines (GT) and combined cycle power plants (CCGT) is provided. All other techno-economic data for fossil and nuclear fired power plants as well as the assumptions regarding fuel prices and CO_2 emission costs can be found in Sec. 5.2.3.

Tab. 2: Cluster with regard to thermal power plant technology type and plant size.

Technology group	Capacity group	Capacity range [MW]	Number of blocks [-]	Installed capacity [MW]
Nuclear	Large	> 800	17	20,400
Nuclear	Midsize	-	-	-
Nuclear	Small	-	-	-
Lignite	Large	> 800	4	3,800
Lignite	Midsize	400 ≤ 800	18	9,900
Lignite	Small	< 400	74	7,400
Coal	Large	> 550	12	9,000
Coal	Midsize	350 ≤ 550	20	8,000
Coal	Small	< 350	116	11,600
CCGT	Large	> 350	15	6,750
CCGT	Midsize	150 ≤ 350	26	6,500
CCGT	Small	< 150	237	4,740
Gas turbine	Large	> 150	2	400
Gas turbine	Midsize	50 ≤ 150	57	3,990
Gas turbine	Small	< 50	370	3,700
Total			968	96,180

5.2.3 Scenario assumptions

As the main research focus lies in the analysis of the influence of different conceptual approaches in thermal power plant modeling on storage demand, not a real world energy scenario is modeled, but a simplified, hypothetical case study. All dispatch optimizations of the VRE technologies and the thermal power plants rely on exogenous capacity mixes, while the storage capacity is endogenously determined by capacity expansion. LP modeling is used for VRE and storage dispatch as well as storage capacity expansion. The thermal power plant modeling, in contrast, distinguishes between unit-commitment with economic dispatch (MILP) and simplified merit order dispatch (LP). A single node power system with no transmission to other regions or transmission constraints within the region ("copper plate") is assumed. The optimization period is divided into 8,760 hourly chronological time-steps of one observation year. Moreover, shares of VRE generation and the ratio of PV-to-VRE generation are pre-defined, subsequently denoted α and β, as described for example in [109, 110, 121, 122, 125, 190]. The VRE share α describes the ratio of theoretical annual electricity generation from VRE in relation to the annual electricity demand (see Eq. 5.40). The actual VRE share resulting from the optimization can be lower than the theoretical share owing to curtailments of VRE or storage losses. In this analysis, VRE curtailments are not restricted or associated with any costs. The theoretical PV-to-VRE ratio β is defined in Eq. 5.41.

$$\propto = \frac{\sum_{t=1}^{t=8760} \mathrm{P}_{Wind}(t) + \sum_{t=1}^{t=8760} \mathrm{P}_{PV}(t)}{\mathrm{D}} * \Delta\mathrm{t} \qquad 5.40$$

$$\beta = \frac{\sum_{t=1}^{t=8760} \mathrm{P}_{PV}(t)}{\sum_{t=1}^{t=8760} \mathrm{P}_{Wind}(t) + \sum_{t=1}^{t=8760} \mathrm{P}_{PV}(t)} \qquad 5.41$$

where

$\mathrm{P}_{Wind}(t)$	Theoretical electricity generation from wind power in each time-step *t* [GWh/h]
$\mathrm{P}_{PV}(t)$	Theoretical electricity generation from PV power in each time-step *t* [GWh/h]
$\Delta\mathrm{t}$	Length of one time-step [h]
D	Annual electrical demand [GWh]

Three main and two sub-scenarios for each main scenario are analyzed. The main scenarios distinguish between each other by the VRE share α (0.33, 0.66, 1.00), whereas the sub-scenarios are characterized by different PV-to-VRE ratios β (0.4, 0.6).

Exogenously pre-defined generation capacities include all thermal power plants (clustered as described in Sec. 5.2.2) as well as all PV and wind power capacities, subject to α and β. For the sake of comparing the influence of the power plant modeling approaches, the installed thermal

power plant capacity per cluster is identical in all scenarios, although higher VRE shares most likely would imply a change in the power plant portfolio. To derive the cost optimal dispatch of VRE, REMix requires the potential, technology-specific, hourly renewable electricity generation as input. These potential renewable generation time-series are a result of the REMix sub-model EnDAT (Energy Data Analysis Tool) and rely on solar irradiation and wind speeds of the weather year 2006, including technical constraints as well as the characteristic curves of wind power plants and PV systems (see [213]). These profiles are scaled with VRE capacities to reach the theoretical VRE share α and the PV-to-VRE ratio β (see Tab. 3). The optimized VRE input is derived from the potential generation less the curtailments.

Tab. 3: Exogenous installed PV and wind capacities for all considered scenarios.

Scenario	PV [GW]	Wind [GW]
$\alpha = 0.33\ \beta = 0.4$	51	63
$\alpha = 0.33\ \beta = 0.6$	76	42
$\alpha = 0.66\ \beta = 0.4$	101	126
$\alpha = 0.66\ \beta = 0.6$	152	83
$\alpha = 1.00\ \beta = 0.4$	153	191
$\alpha = 1.00\ \beta = 0.6$	230	127

Tab. 4: Fuel price scenarios for each fuel type.

Fuel type	Cost scenario[b]	Fuel costs [€/MWh$_{th}$]	CO_2 costs [€/t CO_2]	Source
Coal	low	77	27	[192][a]
Lignite	low	60	27	[192][a]
Natural gas	low	76	27	[192][a]
Uranium	low	3.3	27	[145]
Coal	medium	117	60	[192][a]
Lignite	medium	86	60	[192][a]
Natural gas	medium	113	60	[192][a]
Uranium	medium	3.3	60	[145]
Coal	high	136	75	[192][a]
Lignite	high	100	75	[192][a]
Natural gas	high	131	75	[192][a]
Uranium	high	3.3	75	[145]

[a] Price path A.
[b] *Low* cost scenario uses the values of the year 2020, *medium* of the year 2040 and *high* of the year 2050 of the cited sources.

For modeling thermal power plants, the analysis includes three fuel price and emission certificate cost variations (see Tab. 4). In the cited sources of Tab. 4, for fuel prices and CO_2 costs, the *low* cost scenarios are used in the scenarios with $\alpha = 0.33$, *medium* cost scenarios for $\alpha = 0.66$ and *high* cost scenarios for $\alpha = 1.00$.

High fuel prices might trigger a reduction in the number of CO_2 emissions certificates since they can lead to a decrease in the utilization of thermal power plants. As a result, decreased utilization of thermal power plants will increase the number of available emission certificates which lowers their costs. However, in this analysis, such inter-dependencies for the cost assumptions were not considered. The techno-economic parameters of thermal power plants for the LP and MILP modeling approach can be extracted from Tab. B 1 and Tab. B 2 in the Appendix. Note that the MILP modeling approach requires more parameters, as its degree of detail is much higher than in the LP approach.

The model uses an hourly load profile of Germany for the electricity demand, based on the load profiles from 2006 of the European Network of Transmission System Operators for Electricity (ENTSO-E) [111] which are scaled with an annual electricity demand of 500 TWh.

For storage expansion the model is only allowed to invest in one representative technology, whose techno-economical parameters are loosely orientated on the characteristics of stationary lithium-ion-batteries (Li-ion), assuming a significant decrease of power (converter) and energy (storage unit) related investment costs. The expansion of storage is based on a LP approach in all model runs. REMix optimizes the storage dispatch and furthermore allows for an individual and independent dimensioning of the storage converter size (kW_{el}) and the storage unit capacity (kWh_{el}), implying no pre-defined storage-unit-to-converter ratio (E2P). The E2P value describes the time in hours the storage needs for a complete cycle with its nominal power and allows an identification whether a storage technology is mainly used for short, mid, or long-term applications. A detailed description of the methodology for storage modeling is provided in Scholz et al. [112] as well as in Sec. 4.2.9, whereas the main techno-economic parameters are shown in Tab. 5. No constraints regarding the technical potential (both maximum installable converter power and storage capacity) for Li-ion were assumed.

Tab. 5: Techno-economic parameters for the representative storage technology. Parameters are loosely based on stationary Li-ion batteries [113, 193].

Parameter	Unit	Li-ion
$Invest_{converter}$	[€/kW_{el}]	50
$Invest_{storage}$	[€/kWh_{el}]	101
Amortization $time_{converter}$	[a]	25
Amortization $time_{storage}$	[a]	25
Interest-rate	[-]	0.07
$O\&M_{fix}$	[% Inv./a]	0.009
$O\&M_{var}$	[€/kWh_{el}]	0.00001
η_{charge}	[-]	0.93
$\eta_{discharge}$	[-]	0.93
Self-discharge rate	[1/h]	0.00007
Availability	[-]	0.98

5.3 Results and discussion

5.3.1 Storage expansion and utilization

Fig. 12 illustrates the amount of storage capacity expansion (in terms of converter power) and storage utilization (in terms of annually discharged electricity) comparing the MILP and LP power plant modeling approach over the scenarios with different VRE shares α, while the PV share is fixed (β = 0.40).

The following observations can be made:

i. Storage expansion and utilization increase with increasing VRE share α, as the growing temporal mismatch between generation and demand has to be balanced in some way. While one option is storage, VRE over-generation also can be balanced through curtailments.

ii. Storage expansion and utilization is always higher when using MILP modeling compared to LP. This observation also holds for the scenarios with a PV share β of 0.6 (see Fig. B 1 in Appendix B).

iii. With increasing VRE share α, the differences between LP and MILP in terms of storage expansion and utilization decrease.

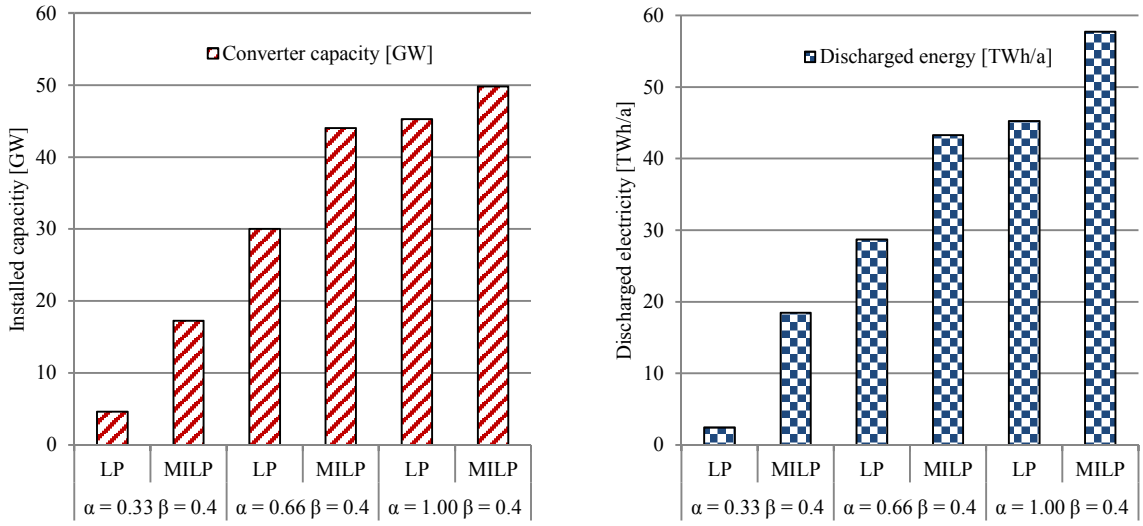

Fig. 12: Storage converter capacity expansion and storage utilization. Both metrics are compared with regard to the scenarios (β = 0.4) with increasing VRE share (α) and over the different modeling approaches (MILP, LP) for power plants.

While observation i is trivial and fostered by the high shares of VRE, observations ii and iii seem to be influenced by the modeling approach for thermal power plants as all others parameters are almost identical. Subsequently, the differences in system dispatch and annual utilization are analyzed.

5.3.2 Simulation of system dispatch

Fig. 13 compares the system dispatch between the LP and MILP approach in the scenarios with a VRE share of 0.33 and a PV share β of 0.4. Note that in the following analysis all capacity groups of a thermal power plant technology (cluster, see Tab. 2) are aggregated by technology type.

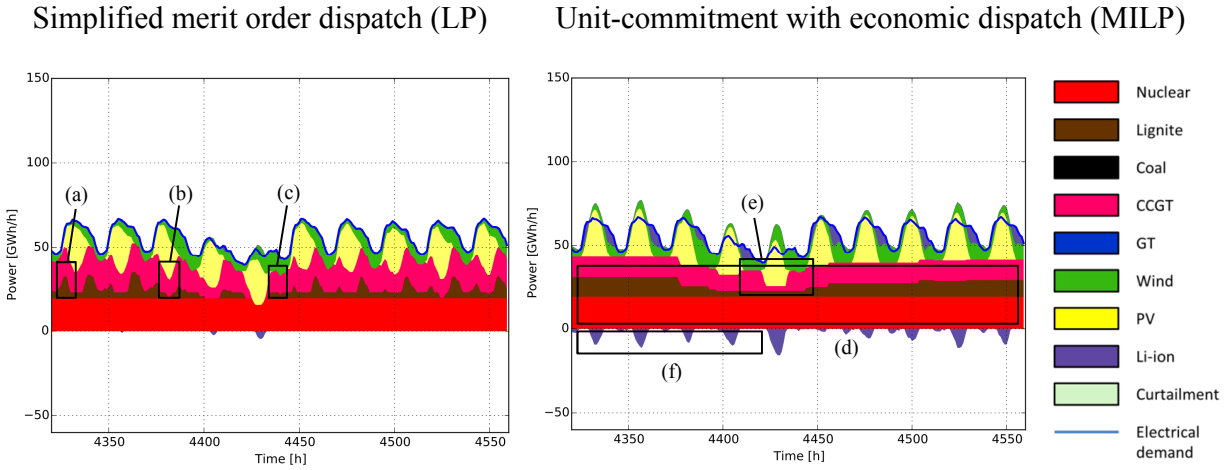

Fig. 13: Comparison of the simplified merit order and unit-commitment. Both approaches (LP, MILP) are compared for the hours 4320–4560 and for the scenario with a VRE share of 0.33 and a PV share β of 0.4. The letters in brackets refer to the observations described in the text below.

It can be observed that the LP modeling approach overestimates the flexibility of thermal power plants in comparison to the MILP methodology, mainly owing to neglecting technical restrictions, such as minimum load rates or ramping constraints. As shown in Fig. 13, especially the flexibility of lignite-fired power plants is overestimated in the LP approach, as they are able to ramp very rapidly (a), are not restricted by any minimum up or down times (b) and are not characterized with minimal load rates of the power plants (c). The specific operating expenditure costs (OPEX) result in the following merit order of power plant dispatch (sorted OPEX of power plant clusters): nuclear, lignite, CCGT, coal, and gas turbines. Slight changes in the merit order can occur depending on the scenario and its assumed CO_2 prices, fuel costs, and improvements in efficiency (see Tab. B 3 in Appendix B). Moreover, since power plants are categorized into different capacity groups (see Tab. 2), the merit becomes more diverse (see Tab. B 2 in Appendix B).

In contrast, the MILP approach shows a more realistic dispatch of the thermal power plants, where base-load power plants, such as nuclear systems, mainly provide electricity at a constant level with little to no power changes (d), while lignite-fired power plants and CCGT are more flexible in their dispatch (e), operating as mid and peak-load power plants. Additionally, Fig. 13 indicates a significantly higher utilization of storage capacities (f). In Fig. 13 and all following dispatch plots, storage charging is illustrated by negative y-values, while storage discharging is shown by positive y-values.

Fig. 14 illustrates the generation share σ similar as defined in [129] (see Eq. 5.42) for thermal power plants, renewable energy systems, and storage, comparing LP and MILP over the different renewable shares in the scenarios. Moreover, the figure illustrates the differences between MILP and LP with regard to the generation share (see Eq. 5.43), which is denoted by Δ σ and defined as the deviation of the technology-specific generation share σ between the MILP and LP approach in percent.

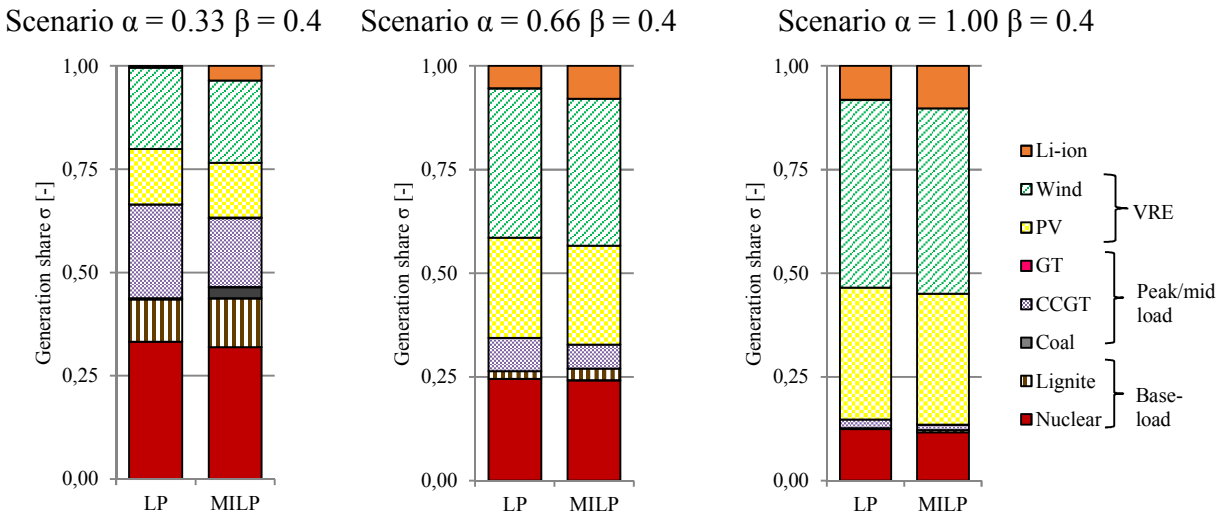

Technology	Δ σ [%]
Li-ion	3.1
VRE	0.2
Mid/peak-load	6.0
Base-load	2.7

Technology	Δ σ [%]
Li-ion	2.5
VRE	0.9
Mid/peak-load	2.2
Base-load	1.1

Technology	Δ σ [%]
Li-ion	2.0
VRE	0.8
Mid/peak-load	0.7
Base-load	0.5

Fig. 14: Comparison of technology-specific generation shares σ. The figure shows the scenarios with different VRE share α, comparing the simplified merit order dispatch (LP) to the unit-commitment with economic dispatch (MILP) modeling approach. Li-ion refers to the share of discharged electricity within the observation year. Moreover, the deviation of the generation share between LP and MILP is expressed as a percentage and denoted Δ σ.

$$\sigma_x = \frac{\sum_{t=1}^{t=8760} P'_x(t)}{\sum_x \sum_{t=1}^{t=8760} P'_x(t)}, \forall x \in X \qquad 5.42$$

where

x	Technology index
$P'_x(t)$	Actual electricity generation from technology x in each time-step t [GWh/h]

$$\Delta \sigma_x = |\sigma_x^{LP} - \sigma_x^{MILP}| * 100, \forall x \in X \qquad 5.43$$

where

x	Technology index
σ_x^{LP}	Generation share in LP approach of technology x
σ_x^{MILP}	Generation share in MILP approach of technology x

Within each scenario, the ratio of thermal to renewable generation does not differ significantly due to α. Furthermore, the PV share is similar in each scenario due to β. Distinct variations, however, can be observed in the composition of the generation share of thermal power plants and, as a result, the utilization of Li-ion storage:

(1) σ LP < σ MILP for base-load power plants (nuclear, lignite) in all scenarios.

(2) Δ σ for all thermal power plants and storage decreases with increasing VRE share α.

(1) In LP the stronger simplifications of operating constraints allows relatively inflexible base-load power plants to ramp up or down more frequently, and, for the scenario with low VRE share (α = 0.33), typically observed continuous operation of base-load power plants occurs only for the technology with the lowest operating costs (in this case electricity generation from nuclear power plants, see Fig. 13). Slightly higher operating costs, as for lignite-fired power plants, will result in a more discontinuous dispatch, following the characteristics of the hourly electrical demand. In scenarios with the highest VRE share (α = 1.00), even nuclear power plants are operating in a flexible way as a consequence of high VRE generation and a low or even negative net load as depicted in Fig. 15 (a).

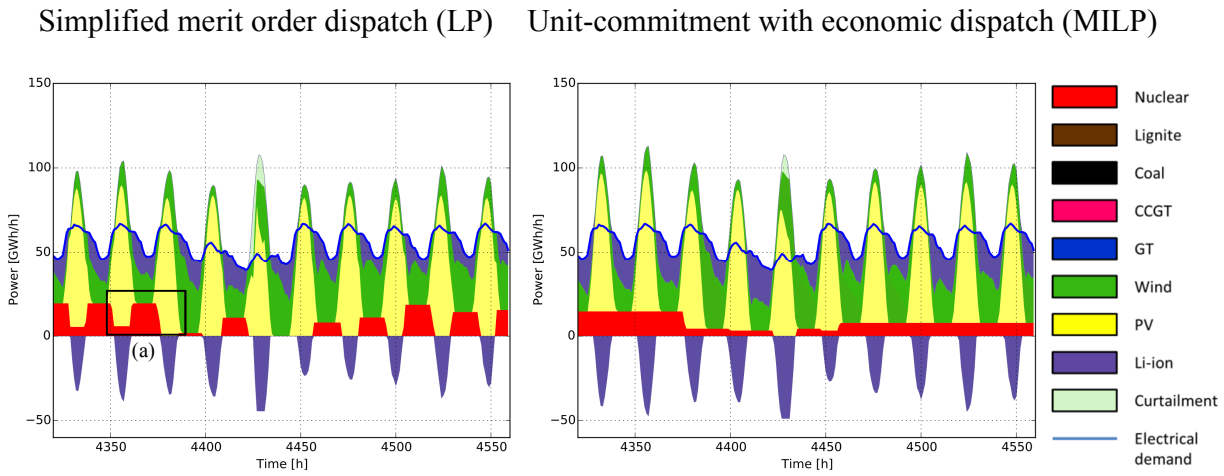

Fig. 15: Comparison of the simplified merit order and unit-commitment. Both approaches (LP, MILP) are compared for the hours 4320–4560 and for the scenario with a VRE share of 1.00 and a PV share β of 0.4. The letters in brackets refer to the observations described in the text below.

In contrast, the dispatch consideration in the MILP approach is characterized by a higher utilization of storage, facilitated by higher storage converter capacity expansion (see Sec. 5.3.1, enumeration ii). This enables more continuous operation of base-load power plants with less ramping events and results in higher generation shares of base-load power plants in MILP. The effect is illustrated in Fig. 16, which shows the dispatch of all utilities for the scenario α = 0.66, β = 0.4 and the hours 0–240. In the LP approach, for example, lignite and coal-fired power plants are able to follow the load in the hours 110–115 (a), whereas in MILP, it can be observed that

charging of storage ensures a continuous operation of lignite and coal-fired power plants as well as CCGT (b). In some hours (c), the generation from power plants (in this case CCGT) even exceeds the electrical load. In these situations, the model favors the continuous dispatch through storage utilization over a flexible operation of the power plant, which again leads to the higher storage utilization (and expansion, see Fig. 12) for the MILP approach.

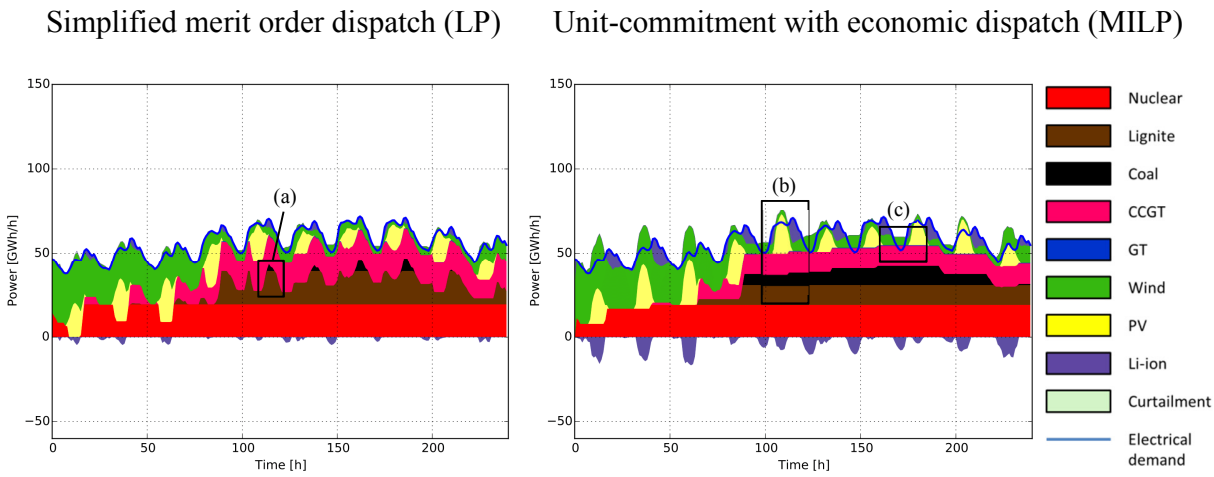

Fig. 16: Comparison of the simplified merit order and unit-commitment. Both approaches (LP, MILP) are compared for the hours 0–240 and for the scenario with a VRE share of 0.33 and a PV share β of 0.4. The letters in brackets refer to the observations described in the text below.

(2) It has been pointed out that, when comparing LP and MILP, the differences in storage capacity expansion and utilization decrease with increasing VRE share α (see Sec. 5.3.1, enumeration iii). This observation is in line with the results shown in Fig. 14, where $\Delta\sigma$ decreases with increasing VRE share α. In other words, the amount of discharged electricity of Li-ion storage converges between MILP and LP if the amount of renewable electricity generation increases. Similar observations can be made for base, mid, and peak-load power plants. On the one hand, thermal power plants become less important (i.e. their generation shares decrease) with higher VRE shares (i.e. increasing α). On the other hand, the dispatch patterns of thermal base and peak-load power plants also change with higher α. While scenarios with low shares of VRE are characterized by the continuous dispatch of power plants with low operating costs (i.e. base-load), enabled through storage utilization, in scenarios with higher VRE shares, mid and peak-load power plants almost completely disappear, as the renewable generation is sufficient to cover the electric load. More specifically, generation from coal disappears in scenarios with $\alpha = 0.66$, whereas the generation from almost all lignite capacities disappears in the scenario with $\alpha = 1.00$. In these high-share VRE scenarios, flexibility is mainly provided by storage utilization, whereas

nuclear power plants remain the only base-load technology, characterized by a more flexible dispatch (see Fig. 15, (a)).

5.3.3 Influence of power plant portfolio granularity

Next, it is tested whether the influence of the MILP approach on storage expansion and utilization is dependent on the flexibility of the power plant portfolio within the system (i.e. the number of power blocks). The analysis showed that—when incorporating endogenous storage expansion and dispatch into the optimization problem—the importance of a detailed MILP unit-commitment modeling approach decreases with increasing VRE shares. However, this might change if the assumed power plant portfolio only consists of a limited number of power blocks/units (as for example in small regions or countries). Consequently, the relative influence of technical constraints might increase as the system is less flexible. Likewise, the decreased flexibility might foster greater storage expansion and utilization.

Since in LP the number of blocks (Nb) can be considered unlimited, as the size of one block is infinitely small, LP is the most flexible system (see e.g. Fig. 13). Nevertheless, the reference power plant portfolio in the MILP approach (see Tab. 2) is already quite flexible, as it contains a rather high number of blocks (968) which enables numerous possible combinations of on and offline power blocks. To assess the influence of the power plant portfolio granularity, the number of power blocks is lowered from 968 of the reference case to 485, 20, and 5 blocks as shown in Fig. 17. The overall installed capacity remains identical in all scenarios (see Tab. B 4 in Appendix B).

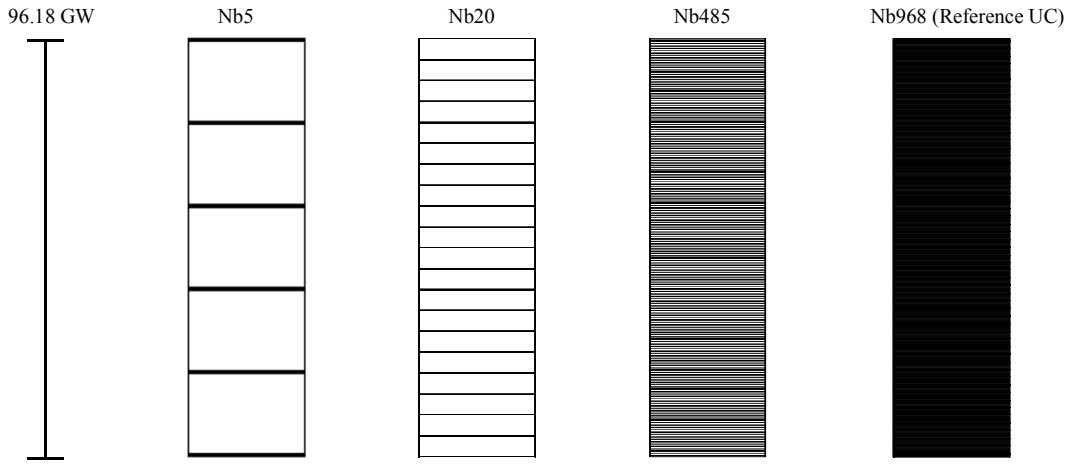

Fig. 17: Power plant granularity in terms of number of blocks. The exact number of blocks for each power plant cluster can be extracted from Tab. B 4.

To illustrate the effects of different granularities of the power plant portfolio, Fig. 18 shows the dispatch for two extreme cases: a capacity mix with 968 blocks (Nb968) and 5 blocks (Nb5). As expected, the inflexibility of Nb5 causes increased storage utilization at some hours (a), whereas in the system with 968 blocks, lignite power plants and CCGT provide flexibility during the same hours, preventing most of the storage charging (b). Again, CCGT operates as mid-load generation owing to the OPEX cost assumptions.

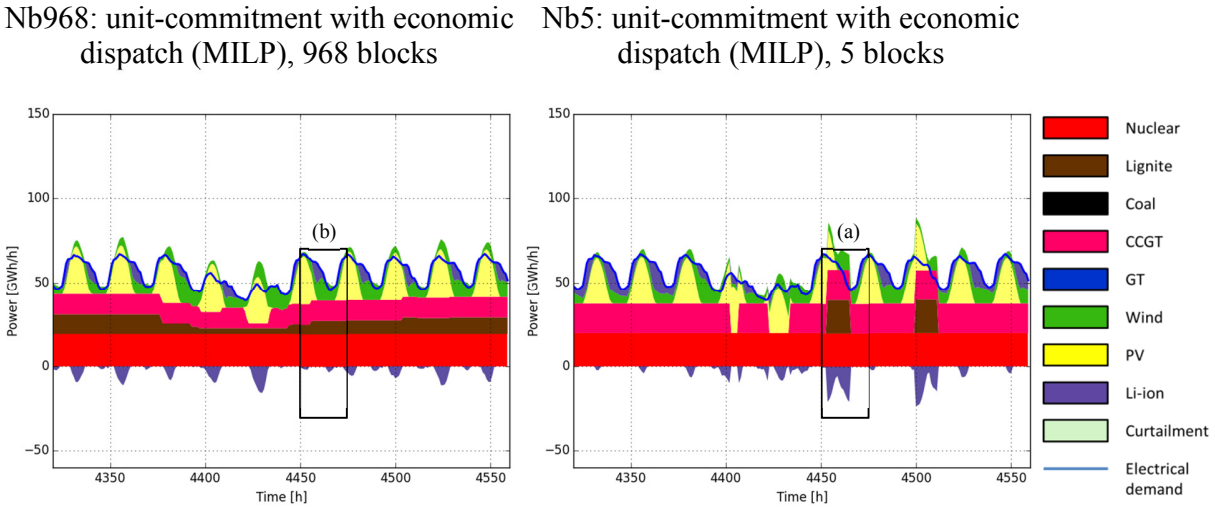

Fig. 18: Comparison of the simplified merit order and unit-commitment. The figure shows the hourly electricity generation of the unit-commitment with economic dispatch (MILP) power plant modeling approach consisting of 968 and 5 blocks. Moreover, the time period of hour 4320–4560 for the scenario with a VRE share of 0.33 and a PV share β of 0.4 is depicted. The letters in brackets refer to the observations described in the text above.

Fig. 19 depicts the annual, technology-specific generation shares σ dependent on the power plant portfolio granularity (Nb968–Nb5) over the scenarios of different VRE shares α and for the PV share $\beta = 0.4$. The most granular capacity mix (Nb968) is defined as benchmark and subsequently, the deviation of generation shares of less granular capacity mixes ($\Delta\sigma^{Nb485}$, $\Delta\sigma^{Nb20}$, $\Delta\sigma^{Nb5}$) are derived.

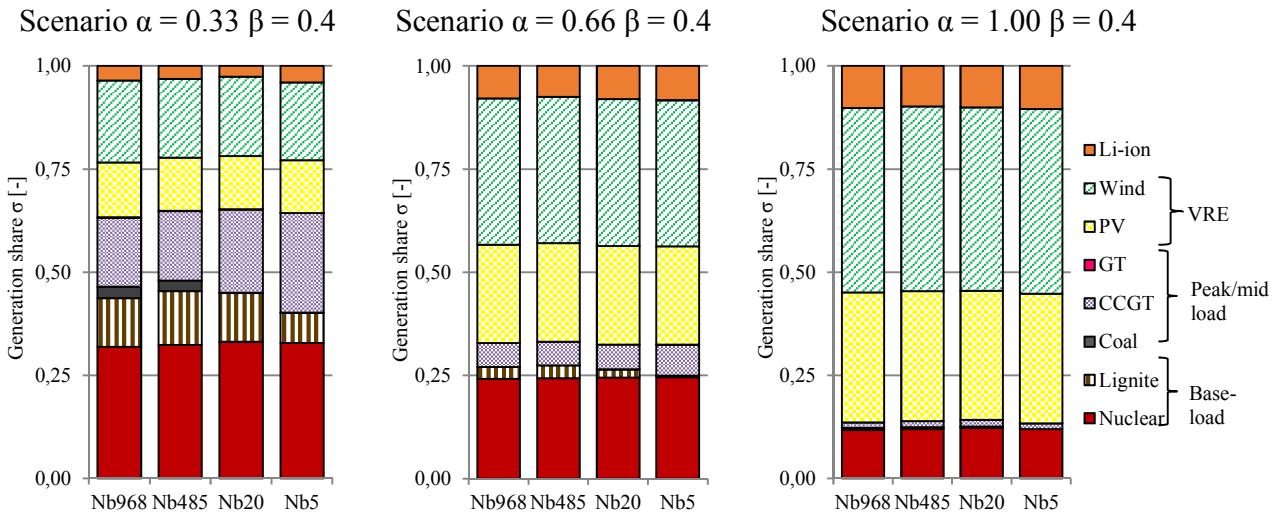

Technology	$\Delta\sigma^{Nb485}$	$\Delta\sigma^{Nb20}$	$\Delta\sigma^{Nb5}$	$\Delta\sigma^{Nb485}$	$\Delta\sigma^{Nb20}$	$\Delta\sigma^{Nb5}$	$\Delta\sigma^{Nb485}$	$\Delta\sigma^{Nb20}$	$\Delta\sigma^{Nb5}$
Li-ion	0.8	0.7	1.0	0.4	0.1	0.4	0.3	0.1	0.3
VRE	1.3	1.1	1.6	0.0	0.2	0.1	0.0	0.5	0.1
GT	-	-	-	-	-	-	-	-	-
CCGT	0.2	3.5	7.4	0.1	0.3	1.8	0.1	0.2	0.1
Coal	0.2	2.6	2.6	-	-	-	-	-	-
Lignite	1.2	0.1	4.6	0.3	0.9	2.5	0.0	0.2	0.5
Nuclear	0.5	1.2	4.6	0.1	0.3	0.4	0.3	0.6	0.3

Fig. 19: Comparison of technology-specific generation shares σ. The figure depicts the technology-specific generation shares σ in the scenarios with different VRE share α, comparing the unit-commitment with economic dispatch (MILP) modeling approach, containing different numbers of blocks. Li-ion refers to the share of discharged electricity within the observation year. Moreover, the deviation of the generation share between LP and MILP is expressed as a percentage and denoted Δ σ.

As shown on an hourly basis in the dispatch plots (Fig. 18), the effect of increasing storage utilization with decreasing number of blocks is also consistent on an annual basis to compensate the inflexibility of the power plant capacity mix. Additionally, instead of providing flexibility through the combinations of on and offline power blocks (as in NB968), Nb5 provides flexibility by the technical ability of mid and peak-load power plants to follow the net load. This is reflected by higher generation shares σ of CCGT in the less flexible scenarios (Nb5, Nb20). In contrast, the generation shares of lignite-fired power plants decreases over higher Nb, as their technical ability to provide flexibility is insufficient to follow the temporal variability of VRE generation. The described effects are visible for all scenarios but become less pronounced (decreasing Δ σ) with increasing VRE share α. In other words, under the premises of model endogenous storage expansion, MILP approaches are particularly important if the analysis focusses on smaller regions (i.e. a limited number of thermal blocks) in combination with low shares of VRE. This

also applies for larger energy systems, where the model user heavily aggregates the number of blocks. In turn, the aggregation of power blocks and the importance of MILP is less important in high share VRE scenarios.

5.3.4 Comparison to the state of research

The results corroborate some findings of the existing research. In terms of the deviation of the thermal power plant generation shares between the two modeling approaches (LP versus MILP), the results are in line with the work of Poncelet et al. [129], as $\Delta\sigma$ (*Generation mix error merit order dispatch* in [129]) is relatively low (max. 6.0%, see Fig. 14). The model results also indicate an increased utilization of storage in the MILP approach as shown by Stoll et al. [149]. This is especially the case in scenarios with low shares of VRE generation.

Differences exist, however, with regard to the importance of MILP depending on the VRE share α, and, more specifically, the trend of $\Delta\sigma$ over the different VRE shares α. Palmintier [168] finds that, in contrast to the results presented in this paper, the importance of operating detail in thermal power plant modeling increases with higher shares of VRE generation (and stricter CO_2 emission limits). The latter can be explained since Palmintier [168] performs an integrated optimization of dispatch and capacity expansion which leads to different initial power plant portfolios, whereas the analysis at hand uses identical generation portfolios, only optimizing their dispatch and storage expansion. Similar to Palmintier [168], the results of Poncelet et al. [129] show an increase of $\Delta\sigma$ with increasing α, i.e. detailed power plant modeling which considers operating constraints becomes more important with higher VRE shares. However, two important assumptions distinguish this work from Poncelet et al. [129]. First, the present analysis conducts optimization calculations up to a theoretical VRE share of 100%, whereas VRE shares in Poncelet et al. [129] reach 50% in the year 2050. Yet, the importance of power plant modeling might decrease as the share of thermal generation in highly renewable scenarios also decreases. Second, Poncelet et al. [129] do not include storage expansion as a flexibility option in their calculations. Consequently, all balancing of the intermittent VRE generation has to be provided by dispatchable power plants. As flexibility requirements increase with higher VRE shares (e.g. in terms of hourly or multi-hour ramp requirements, see e.g. [122]), technical constraints with regard to the dispatchability of power plants (as considered in the MILP approach) have a great influence and explain $\Delta\sigma$ between the LP and MILP approach in Poncelet et al. [129].

5.4 Conclusions

The influence of thermal power plant modeling (simplified merit order dispatch (LP) versus unit-commitment with economic dispatch (MILP)) on storage demand has been examined, using the cost minimizing capacity expansion and dispatch model REMix. The analysis was conducted for scenarios with different shares of PV and wind power generation, ranging from 33% up to 100% of theoretical generation share with regard to the annual power demand.

It was shown that LP systematically overestimates the flexibility of thermal power plants, thus leading to lower storage expansion and utilization compared to MILP in all scenarios. If endogenous storage expansion is considered in the capacity planning and dispatch optimization (and flexibility provision does not solely rely on the existing power plant portfolio), MILP modeling is superior in terms of realistic storage consideration. Power plants are restricted by minimum load rates or ramping constraints, consequently fostering an increase in storage utilization to ensure continuous operation of the thermal units. However, it was also found that—owing to the decreasing share of thermal power plants that are modeled either by LP or MILP—the differences of LP and MILP in storage expansion and utilization as well as the generation shares of thermal power plants merely decrease with increasing VRE shares. This leads to the conclusion that a high degree of detail in power plant modeling becomes less important in scenarios with high shares of VRE if network constraints are neglected.

Similar relations were observed for smaller energy systems with a lower number of available generation units. For low share VRE scenarios and in the case of very few units, significant deviations with the highly granular energy system become visible, especially for nuclear and lignite power plants as well as for combined cycle power plants. The differences in storage utilization are rather small. Again, the differences become less distinct with increasing shares of VRE.

There are limitations of the analysis and future work should carefully consider these. First, storage expansion and dispatch of a single technology was used as a proxy for flexibility demand. However, other options are possible and, for example, enable balancing of intermittent renewable generation through spatial balancing by the electricity grid or through changes in the electric load curve (i.e. demand response). As the fundamental functionalities of these alternative flexibility options vary quite heavily from the ones of storage, power plant modeling might have different effects as the results of this work show. Moreover, the hourly resolution of the REMix model does not capture sub-hourly flexibility requirements, such as frequency control.

Second, both in LP as well as in MILP, storage capacity expansion relies on linear programming. Similar to LP power plant modeling and as described in Sec. 4.2 the approach is not able to consider on/off behavior of single storage units or to capture some techno-economic characteristics as it would be possible with mixed-integer methods. For storage these constraints are heavily technology dependent, e.g. batteries include limitations in terms of depth of discharge or cycle stability, whereas pumped hydro storage is restricted by minimum storage levels or turbine power [114, 115]. Similar to the argumentation of power plant granularity in Sec. 5.3.3, the necessity of mixed-integer storage modeling depends on the granularity of the overall installed storage capacity and the typical capacity size of one storage unit. In this sense, mixed-integer approaches might be desirable for large-scale storage technologies and in smaller energy systems, whereas linear programming is likely to be sufficient in large energy systems in combination with smaller storage units.

Third, solely electricity was considered and no model interactions to other energy-related sectors—such as the transportation or heat sector—were modeled. Especially the latter might be affected by assumptions of power plant modeling, as some units operate as Combined Heat and Power Plants (CHP). In combination with heat storage, CHP units have the potential to operate in a more flexible way as shown in [146].

6 European storage demand

Storage demand, spatial distribution, and storage dispatch in a European power supply system with 80% variable renewable energies[24]

This chapter aims to shed light on the causes for the optimum spatial distribution of storage capacity expansion and storage dispatch in Europe for scenarios with high shares of non-dispatchable power generation from renewable energies. For this purpose, the linear, cost minimizing optimization model REMix is applied to a European energy scenario, endogenously determining all generation and storage capacities as well as their dispatch. With the help of correlation and extensive sensitivity analyses the research questions of robust storage demand and drivers for spatial storage capacity distribution are tackled (see Sec. 2.4).

[24] This chapter is based on F. Cebulla, T. Naegler, and M. Pohl, "Electrical energy storage in highly renewable European energy systems: Capacity requirements, spatial distribution, and storage dispatch," *Journal of Energy Storage*, vol. 14, pp. 211–223, 2017.

Transparency checklist

Criterion	Page number
General Information	
1. Author, Institution	79
2. Aim and funding	79
3. Key term definitions	XII
Empirical Data	
4. Sources	84, Appendix C
5. Pre-processing	Appendix C
Assumptions	
6. Identification of uncertain factors	103
7. Uncertainty consideration	103
8. Storyline construction	-
9. Assumptions for data modification	Appendix C
Model exercise	
10. Model fact sheet	Appendix D
11. Model-specific properties	Appendix D
12. Model interaction	-
13. Model documentation	39
14. Output data access	184
15. Model validation	103
Results	
16. Post-processing	-
17. Sensitivity analyses	103
18. Robustness analyses	103
Conclusions and Recommendations	
19. Results-recommendation-relationship	87
20. Uncertainty communication	124–125

ABSTRACT

One of the major challenges of renewable energy systems is the mismatch between electricity generation and load caused by the limited dispatchability of intermittent electricity generation. A promising option to increase system flexibility is electrical energy storage (EES).

In this chapter, the optimum spatial distribution of storage capacity is analyzed as well as its dispatch for five types of EES in a European energy system based on high shares of fluctuating renewable power production. The analysis applies the linear optimization model REMix, which endogenously determines both expansion and dispatch of all electricity generation and storage technologies.

The results indicate a high dependency of the spatial distribution of storage with the regionally predominant renewable technology and its temporal power generation characteristics. In this regard, significant correlations between the generation from offshore and onshore wind power with hydrogen storage charging can be observed. Onshore wind power production correlates with adiabatic compressed air storage, whereas the generation of photovoltaic systems is predominantly balanced by stationary lithium-ion batteries. Spatial storage capacity distribution in the model is furthermore influenced by assumptions on the ratio of energy and power-related storage investment costs (€/kW to €/kWh) as well as the region and technology-specific technical potential of storage and renewable electricity generation technologies.

6.1 Introduction

The reduction of greenhouse gas emissions is one of the main challenges of our society towards more sustainable energy supply. Electricity generation based on renewable resources represents a promising option to tackle this problem. However, the mismatch of electricity generation and load caused by the limited dispatchability of intermittent electricity generation such as PV or wind power (hereinafter referred to as variable renewable energies (VRE)) requires an increase of flexibility of future energy systems.

Flexibility might be provided, for example, by EES or the electricity grid [134, 145, 146, 148, 165, 190, 191]. While the former option provides flexibility on a temporal level, i.e. allows shifting of energy from one point in time to another, grid expansion can be considered as a spatial flexibility, as it enables large-scale balancing of generation and demand between different regions.

In this work, the focus is on flexibility demand provided by electricity storage which is characterized both in terms of necessary power (charge and discharge unit, e.g. pump and turbine of a pumped hydropower plant (PHS)) and energy-related capacity (storage unit, e.g. water reservoir of a PHS).

6.1.1 Literature review

Current research addresses the question of future storage demand typically via model-based analyses, often emphasizing the quantification of storage capacity for different energy scenarios (e.g. in [132, 134, 148, 164, 165, 190]).

Broad ranges of storage demand estimates in the literature exist (see Sec. 2.1 and Sec. 2.2), indicating the necessity of a thorough examination of the underlying assumptions in the original studies. For example, different RE shares [116, 120, 121, 125, 134, 145, 148, 151, 190], different wind-to-PV generation ratios [121, 125], weather years [121, 122, 125, 151], cost assumptions in cost optimizing approaches [164, 165] as well as the representation of the electric grid [119–121, 151, 164] might affect estimates of storage demand. Moreover, differences in storage demand quantifications exist with regard to the applied modeling approach (I), different temporal (II), technological (III), and spatial resolutions (IV). An in-depth discussion of these aspects is provided in Sec. 2.1.

(I) Concerning the modeling method, storage demand has been analyzed with the help of various modeling approaches; some of the most prominent ones are optimizations (see [117–119, 134, 145, 146, 148, 165, 190, 191]) and simulations (see [120–125]).

(II) The influence of the temporal resolution has been studied in an optimization model for ramp flexibility and system costs in Deane et al. [126], for day-ahead utility scheduling through unit-commitment in Pandzzic et al. [127] and in O'Dwyer and Flynn [128], and for utility dispatch in energy scenarios with high shares of RE generation in Poncelet et al. [129] as well as in Nahmmacher et al. [130].

(III) Technological resolution refers to the abstraction level in the modeling approach to characterize the technologies and to the considered energy sectors in the model-based analysis. With regard to the technological representation of storage, the literature shows numerous approaches, ranging from representations of a single generic storage (e.g. see [131]), to storage classes (e.g. short-, mid-, long-term, without further details on the assumed technologies, see [132]), or detailed representations of actual storage technologies, as in [133, 134, 148, 190]. Regarding the considered energy sectors for storage demand quantification, models typically analyze the power sector. If sector coupling is considered (e.g. with transportation, heating, or cooling), the approaches mostly rely on accounting frameworks on an annual basis (see [135, 136]) or optimizations which use a simplified temporal resolution in terms of representative time periods (see [137, 138]).

(IV) Storage demand has been analyzed for several observations areas with different spatial resolutions within the models, i.e. the number of model regions. The latter plays an important role, as it defines the distribution of capacities, generation, electricity load, and transmission grid topology within the observation area.

6.1.2 Novelty and contributions

As illustrated in the literature review, the question of storage demand has been tackled by a substantial amount of studies for various energy scenarios and under different assumptions, applying a broad spectrum of methods. Despite these manifold analyses, the number of studies which analyze storage demand for Europe with an adequate spatial resolution is limited. Furthermore, recent research rarely assesses the reasons for the “optimum” spatial distribution of storage expansion and its dispatch, but takes the model results as granted.

This chapter, therefore, aims to analyze the optimum spatial resolution and dispatch of different storage technologies in European energy systems with high shares of non-dispatchable renewable power production and sheds light on the underlying causes for both optimum spatial distribution of storage capacity and storage dispatch. For this purpose, the linear, cost minimizing optimization model REMix is applied, which endogenously determines all generation and storage

capacities as well as their dispatch. Furthermore, the consequences of different VRE scenarios as well as the sensitivity with respect to main input parameters and model assumptions are analyzed, in order to answer the aforementioned research questions.

6.2 Methodology and data

6.2.1 Modeling approach

The analysis relies on the cost minimizing energy system model REMix. A detailed model description can be found in Sec. 4.2.

6.2.2 Scenario assumptions

The main application of REMix is the dimensioning of a least cost supply system that can reliably cover the electric load at any time. For this analysis, a partial greenfield approach is incorporated, which optimizes the expansion and dispatch of all storage and most of the power generation capacities for the year 2050. Optimized power technologies comprise VRE technologies (PV, onshore and offshore wind, run-of-the-river hydroelectricity), dispatchable RE (biomass, conventional hydroelectricity, CSP), and fossil-fired power plants (lignite, hard coal, combined cycle gas turbine (CCGT), and gas turbine (GT) power plants). Additionally, the model encompasses geothermal and nuclear power plants, whose capacities are exogenously pre-defined (based on Trieb et al. [195]). Since the installed capacities of those technologies are relatively small (see Tab. C 3), their influence on the storage capacity distribution is expected to be small. Furthermore, this simplification reduces the solving time of the model. Curtailments of electricity generation from VRE technologies are not associated with any costs. In detail descriptions of the modeling approach and the underlying assumptions for each technology are provided in Appendix C.

The partial greenfield methodology is based on the assumption that almost no capacities are installed at the beginning of the observation year and investments are necessary to reliably cover the electric load at any time. The approach is valid since most of the existing capacities at the present will not last until the observation year 2050. However, due to their long lifetime, some technologies will prevail until 2050, including some fossil-fired and conventional hydropower plants (see Farfan and Breyer [139]). For this purpose, the decommissioning of generation capacity based on its technology-specific lifetime is considered (see Tab. C 4).

The analysis focusses on the electricity sector and excludes interactions with the transportation and heat sector. Therefore, heat extraction from combined heat and power plants is not

considered and the approach solely includes their electrical generation capacity. Moreover, the modeling approach for thermal power plants relies on a simplified linear programming methodology (no integer unit-commitment). This approach is sufficient as generation mix differences to the more detailed mixed-integer unit-commitment approach are rather small in energy scenarios with high shares of VRE generation, as shown in chapter 5.

As the objective of the analysis is to assess the role of electricity storage in scenarios with high shares of VRE, a model constraint which enforces at least 80% of electricity generation to come from VRE (averaged over the whole observation area) is included, hereinafter denoted by $80\%_{constr}$ (see Eq. 6.44).

$$\frac{\sum_{t=1}^{t=8760} P'_{Onshore\ wind}(t) + \sum_{t=1}^{t=8760} P'_{Offshore\ wind}(t) + \sum_{t=1}^{t=8760} P'_{PV}(t)}{D} * \Delta t \geq 0.8 \qquad 6.44$$

where

$P'_{Onshore\ wind}(t)$	Actual electricity generation from onshore wind in time-step t [GWh/h]
$P'_{Offshore\ wind}(t)$	Actual electricity generation from offshore wind in time-step t [GWh/h]
$P'_{PV}(t)$	Actual electricity generation from PV in time-step t [GWh/h]
Δt	Length of one time-step [h]
D	Annual electrical demand [GWh]

Although dispatchable RE (e.g. biomass or CSP with thermal storage) can also reduce CO_2 emissions, their availability in Europe is limited and $80\%_{constr}$ is, therefore, a valid assumption. For a detailed analysis of the influence of this model constraint see Sec. 6.3.5.

For the analyzed year 2050, the optimization period is divided into 8,760 hourly time-steps. The observation area comprises northern, western, and central Europe (see Fig. 20). While larger countries are generally represented by individual model regions, smaller European countries are aggregated (e.g. Poland, the Czech Republic, and Slovakia are grouped to the model region PL + CZ + SK). In contrast, Germany is split into 20 sub-regions, resulting in 29 overall model regions for this analysis (see Fig. C 1).

The model uses exogenous, hourly and model region-specific load profiles of the electricity demand. They are based on the load profiles from 2006 of the European Network of Transmission System Operators for Electricity (ENTSO-E) [140]. All profiles are scaled through estimates of the development of the total electricity demand for the year 2050 for each country, based on [192, 194, 195] (see Tab. C 14). This implies that the shape of the 2050 load profiles is identical with the 2006 ENTSO-E profiles. A change in form, for example through new consumers, such as an increased use of BEV or higher shares of heat pumps, is not considered.

A simplified representation of the transmission grid (exogenously specified in the standard analysis) allows electricity import and export between the model regions (see Sec. 2 in Appendix C). Within each region, a perfect grid without any transmission constraints is assumed ("copper plate"). In the sensitivity analysis, furthermore, an endogenously calculated transmission grid expansion between the model regions is allowed (see Sec. 6.3.5).

The model includes five storage technologies which are characterized by different possible charging and discharging efficiencies, investment costs for the converter and storage units, and O&M costs. These technologies are comprised of pumped hydropower (PHS), hydrogen storage (H_2), adiabatic compressed air (aCAES), stationary lithium-ion (Li-ion), and redox-flow batteries. For H_2 storage it is assumed that electricity is converted to H_2 via alkaline water electrolysis, stored in underground salt caverns and reconverted via a CCGT.

Although a large number of storage technologies is available, the aforementioned options have been selected as they are (a) representatives of different storage classifications (see Sec. 3.1), (b) considered to be suitable candidates for the large-scale integration of VRE power, and (c) characterized by distinct differences in their energy and power-related investment costs. Furthermore, high numbers of alternative expansion options, i.e. storage technologies, impose the risk of penny switching solutions (see Sec. 4.1). An overview of all relevant storage technology parameters can be found in Tab. C 15, whereas a more in-depth description of the modeling approach of storage is provided in Sec. 4.2.7.

Apart from storage expansion, REMix also optimizes the storage dispatch and furthermore allows an individual and independent dimensioning of the storage converter size (GW_{el}) and the storage unit capacity (GWh_{el}), implying no pre-defined storage unit to converter ratio (E2P). The E2P describes the time in hours the storage needs for a complete cycle with its nominal power and allows an identification whether a storage technology is mainly used for short, mid, or long-term applications. The main techno-economic parameters are shown in Tab. 6. The assumptions regarding the existing converter and storage capacity of PHS, aCAES, and H_2 as well as their technical expansion potentials are discussed in Sec. 8 in Appendix C. For Li-ion and redox-flow batteries it is assumed that there are no constraints regarding their technical potential (both maximal installable converter power and storage capacity).

Although the techno-economic input parameters are carefully chosen and based on a broad literature review as well as expert assessments, the author is aware that their exact values are highly uncertain for the observation year 2050. Therefore a broad sensitivity analysis is included

to validate the key results (see Sec. 6.3.5). The scenario setup as described above serves as the reference scenario for those sensitivity tests.

Tab. 6: Main techno-economic parameters for the storage technologies.

Technology	$Invest_{converter}$ [€/kW_{el}]	$Invest_{storage}$ [€/kWh_{el}]	η_{charge} [-]	$\eta_{discharge}$ [-]
H_2	1,200	1	0.75	0.62
Li-ion	50	150	0.97	0.97
aCAES	570	47	0.84	0.89
Redox-flow	630	100	0.92	0.92
PHS	450	10	0.91	0.91

6.3 Results and discussion

6.3.1 Generation capacity expansion

Fig. 20 illustrates model results of the generation capacities for renewable and fossil-fired technologies for the year 2050 in a power supply system with at least 80% VRE in the main model regions for the reference scenario. Moreover, the VRE share regarding the gross annual electricity generation for each model region is shown. Unless otherwise stated, the 20 German model regions are aggregated in the following sections. Moreover, the analysis concentrates on the technologies with the highest installed capacities and neglects technologies with smaller amounts of installed capacities, such as run-of-the-river hydroelectricity or biomass.

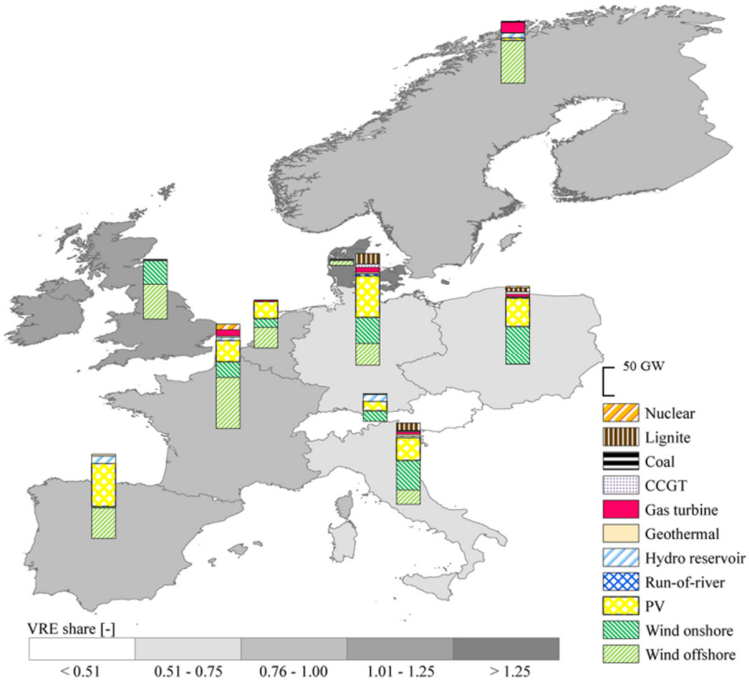

Fig. 20: Technology-specific installed generation capacities for Europe in 2050. Additionally, the VRE shares with regard to the annual gross electricity generation are depicted. All numerical values also can be found in Tab. C 18.

Within the examination area, the model derives a total VRE capacity of 1,185 GW. The largest share is provided by offshore wind with 465 GW, followed by PV and onshore wind with 392 GW and 328 GW, respectively. Installed capacities of fossil-fired technologies (lignite, CCGT, and GT power plants) sum up to 119 GW, mainly provided by gas turbines (58 GW). In terms of annual electricity generation, offshore wind systems provide 1,482 TWh, whereas onshore wind and PV result in 624 TWh and 419 TWh, which equals 47%, 20%, and 13% of the overall gross electricity generation.

Naturally, the optimization favors technologies which are (regionally) cost-effective with regard to capacity expansion and dispatch. In consequence, investments for VRE happen predominantly in regions with high technical potentials and high full load hours. In this sense, regions with high solar irradiation for example, such as Iberia, show comparatively high installations of PV systems, whereas high wind speeds, as in the UK + IE or the model region Northern Europe, will foster the installation of wind power plants. Furthermore, region-specific technical potentials restrict the capacity expansion of VRE, as this is, for instance, the case for onshore wind (in AT + CH, BeNeLux, PL + CZ + SK, Italy, UK + IE) and for PV (in BeNeLux, PL + CZ + SK, Iberia, Italy) (see Fig. 21).

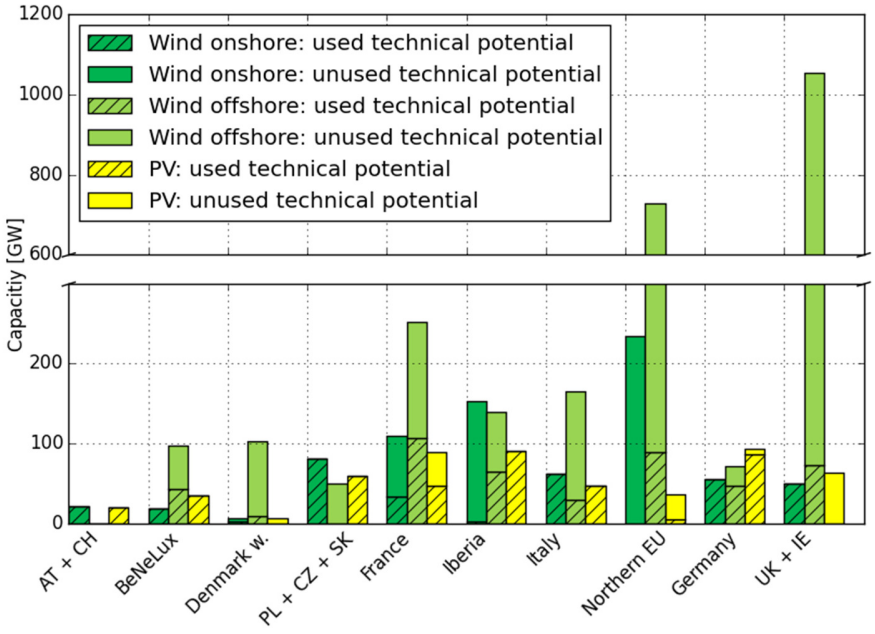

Fig. 21: Used and unused technical potential of VRE capacity. Results are shown for each model region. The sum of used and unused technical potential defines the total technical potential.

The high share of electricity generation from PV, onshore and offshore wind systems reflects the VRE constraint set for the reference scenario ($80\%_{constr}$, see Sec. 6.2.2). Excluding this constraint will result in significantly lower shares of power generation from VRE: assuming the same CO_2 certificate prices and fuel costs as well as identical investment and O&M costs, calculations without $80\%_{constr}$ derive a VRE share of 42% on the European average (see Sec. 6.3.5). However, if a very high CO_2 certificate price is chosen (130€/t CO_2 instead of 57€/t CO_2 in the standard case), optimum capacity expansion leads to a VRE share that is almost identical to the one of the reference scenario (75%).

Installed power generation capacities are on average approximately three times higher as the peak load in each model region (see Tab. 7), reflecting the strongly fluctuating character of power generation from wind and PV systems.

Tab. 7: Region-specific peak load (P_{peak}) and total generation capacity (Cap_{total}). Additionally, the Cap_{total}-to-P_{peak} ratio is shown as well as the shares of PV and wind power generation with regard to the total gross power demand in each region. Generation shares > 1, e.g. in Denmark west for offshore wind power, indicate net electricity export.

Model region	P_{peak} [GW]	Cap_{total} [GW]	Cap_{total}-to-P_{peak} [GW/GW]	PV share [kWh/kWh]	Offshore wind share [kWh/kWh]	Onshore wind share [kWh/kWh]
Germany	82	236	2.89	0.16	0.34	0.22
Austria + Switzerland	20	58	2.96	0.19	-	0.24
BeNeLux	31	101	3.26	0.16	0.59	0.23
Denmark w.	4	13	3.22	-	1.76	0.30
PL+CZ+SK	42	165	3.94	0.23	-	0.50
France	85	221	2.59	0.10	0.74	0.13
Iberia	57	177	3.10	0.34	0.45	0.01
Italy	55	171	3.09	0.17	0.16	0.25
Northern Europe	60	130	2.18	0.01	0.86	-
UK + IE	64	125	1.95	-	0.79	0.41

The highest capacity-to-peak load ratio can be observed in the model region PL + CZ + SK, in contrast to the region UK + IE, where the total capacity is only twice as high as the regional peak load. Slightly higher capacity-to-peak load ratios in regions with high PV share can be observed, due to the more volatile nature and lower full load hours of PV electricity generation. Moreover, Tab. 7 shows the wind and PV share of each region with regard to their annual gross electricity demand. In principal, no significant correlation between the wind shares and the capacity-to-peak load ratio can be observed.

6.3.2 Storage capacity expansion

Fig. 22 shows the total installed converter power of all storage options for the European model regions. For PHS this includes today's existing capacities (39 GW and 271 GWh, see Tab. C 12 and Tab. C 13) as it is assumed that these will not be retired until 2050 owing to the long lifetime of the water reservoir. Additionally, a simulation run with no existing capacities of PHS was performed as part of the sensitivity analysis. The scenario confirms that a stock of PHS capacities does not influence the installed PHS, as both model runs result in an identical expansion of PHS capacities (see Sec. 6.3.5, *Miscellaneous scenarios*). Apart from redox-flow batteries, the model derives investments into every storage technology and the endogenously determined storage converter power results in 166 GW. The largest share is provided by H_2 storage with 86 GW. Converter power expansion from Li-on batteries accounts for 58 GW.

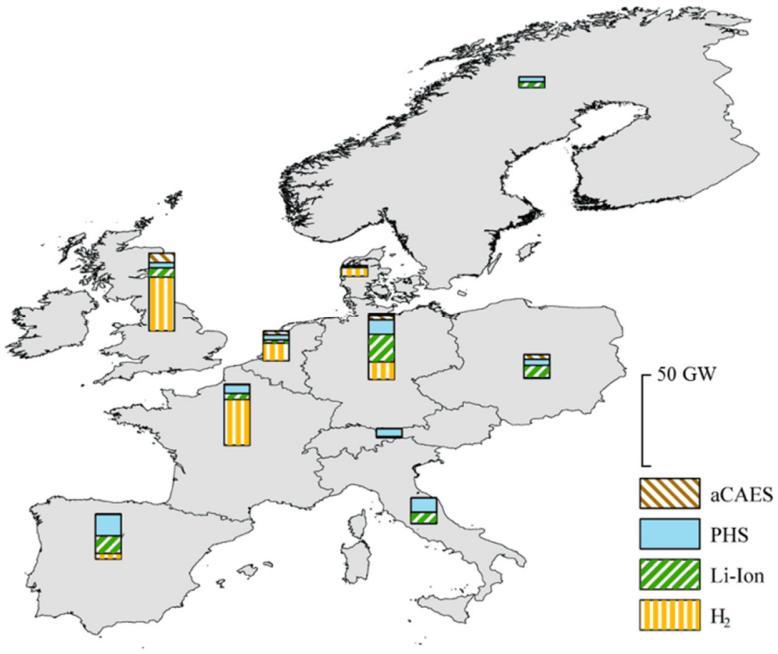

Fig. 22: Technology-specific storage converter power for Europe in 2050. All numerical values are shown in Tab. C 45.

The lack of redox-flow storage can be explained by the cost optimizing model logic. For mid-term applications, i.e. the balancing of surplus energy and deficits of time periods up to several days, redox-flow batteries compete with aCAES which have rather similar techno-economic characteristics (see Tab. 6). Despite the favorable efficiencies of redox-flow batteries, their higher storage capacity investment costs (at similar converter costs) prevent the expansion as long as aCAES expansion limits are not reached.

This hypothesis has been validated with model runs where storage investment costs for redox-flow batteries were set to the respective value of aCAES. The results confirm that mid-term storage applications of aCAES could be substituted by redox-flow batteries if their storage unit costs improve to the level of aCAES (see Sec. 6.3.5, *Miscellaneous scenarios*).

As a consequence of negligible installed capacities of redox flow batteries, this storage type has not been taken into account in the remainder of this work.

While the major amount of storage converter capacity is provided by H_2 storage and Li-lion batteries, aCAES and PHS also play an important role in certain regions. For PHS, one example is the model region Iberia. Here, the installed capacities in the model reach the technical potential of 137 GWh of storage capacity (see Tab. 8) and 12 GW of converter power. Another region where the capacity expansion of PHS reaches its technical potential is Italy (77 GWh).

Notable storage capacities of aCAES occur in UK + IE, resulting in 5 GW of converter power and a storage capacity of 72 GWh.

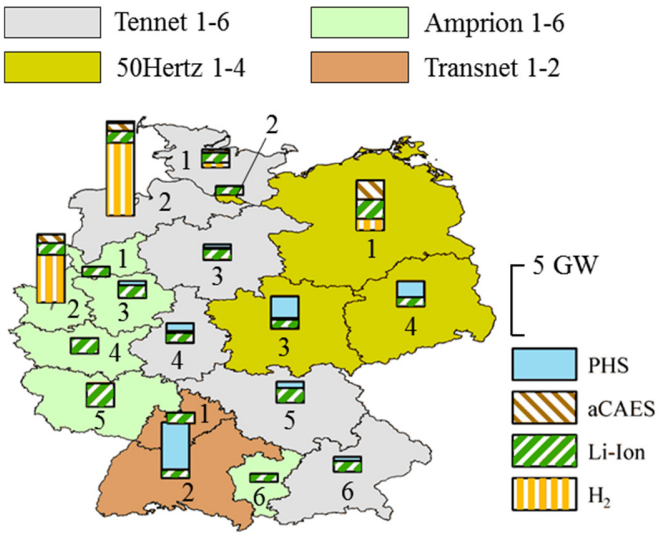

Fig. 23: Technology-specific storage converter power for Germany in 2050. All numerical values are shown in Tab. C 72.

For the German model regions (see Fig. 23) the optimization results in 30 GW of storage converter power. The largest share is provided by Li-ion batteries and H_2 storage with 16 GW and 10 GW respectively. The highest converter capacity can be observed in the model regions Tennet2, Amprion2, and 50Hertz1 (6.80 GW, 5.03 GW, 3.70 GW), mainly providing flexibility for the integration of offshore wind generation (Tennet2, 50Hertz1) and additionally high amounts of PV and onshore wind capacities (50Hertz1). In this regard, the favorable transmission grid infrastructure between Tennet2 and 50Hertz1 fosters the storage capacity expansion in these regions.

Particularly in regions with high shares of electricity from wind turbines, such as 50Hertz1 or Tennet2, the model results in higher amounts of aCAES expansion (1.38 GW, 0.59 GW). All model region and technology-specific converter power expansion is also shown in Tab. C 45.

Tab. 8 lists the model results for storage unit capacities (in GWh) for each model region.

Tab. 8: Installed storage capacity for all model regions in 2050.

	Storage unit capacity [GWh_{el}]			
	H_2	Li-ion	aCAES	PHS
AT + CH	36	-	1	40
BeNeLux	3,117	4	44	22
Denmark w.	2,264	1	4	-
PL + CZ + SK	86	30	48	25
France	6,927	6	5	37
Iberia	901	38	3	137
Italy	38	16	2	77
Northern Europe	-	13	-	27
Germany	3,671	32	58	54
UK + IE	12,578	10	72	22
Total	29,616	151	236	441

While the quantity, technology-specific composition and spatial distribution of the *converter power* is quite diverse over the observation area, *storage capacity* is, as expected, mainly provided by H_2 long-term storage (29,616 GWh). The highest storage unit capacities can be observed in the regions UK + IE, France, Germany, and BeNeLux, respectively (12,578 GWh, 6,927 GWh, 3,671 GWh, 3,117 GWh). With respect to storage capacity, aCAES, PHS, and Li-ion batteries play only a minor role (236 GWh, 168 GWh, 151 GWh, together less than 3% of the total storage capacity). These technologies mainly provide short and mid-term flexibility in order to compensate diurnal (1 h–1 d) and synoptic (2 d–10 d) fluctuations from VRE. H_2 in contrast serves as long-term storage (>10 d) for electricity from offshore wind turbines. Note that both storage converter power (GW) as well as the storage unit capacity (GWh) are endogenously derived by REMix for each storage technology. A more detailed analysis of storage dispatch and its spatial distribution is provided in Sec. 6.3.3.

6.3.3 Spatial distribution of storage capacity

For each model region the technology-specific storage expansion is determined by the temporal characteristics of the power generation from VRE and its regional mix (limited by the technical storage potentials) as well as the spatial balancing ability of the transmission grid between the regions.

Model regions with high shares of offshore wind generation, e.g. UK + IE, tend to require more long-term storage, while, in contrast, larger amounts of short-term storage (e.g. Li-ion batteries) seem to be characteristic for regions which are mainly supplied by electricity from PV systems. In the following analysis, a comparison of the hourly time-series of the net load

(electrical load minus VRE feed-in) with the hourly cumulative charging power of all storage technologies for the model regions France, PL + CZ + SK, and Iberia (Fig. 24) is provided. More specifically, the hourly values depicted in this figure are normalized with regard to the total VRE and storage converter capacity. These specific regions were chosen due to their different generation and storage portfolios (see Tab. 7, Tab. 8). A negative net load indicates a VRE surplus, while positive values require further generation from dispatchable technologies (e.g. fossil-fired power plants or biomass), storage discharging, or electricity import. Based on the main electricity generation technology with regard to the annual electricity demand, France can be described as a offshore wind region (74% electricity supply through offshore wind); PL + CZ + SK is an onshore wind region (50%). Although the power generation share of offshore wind (45%) in Iberia is higher than the generation share from PV (34%), this region shows the highest amount of PV generation in the whole examination area and is therefore defined as a PV region.

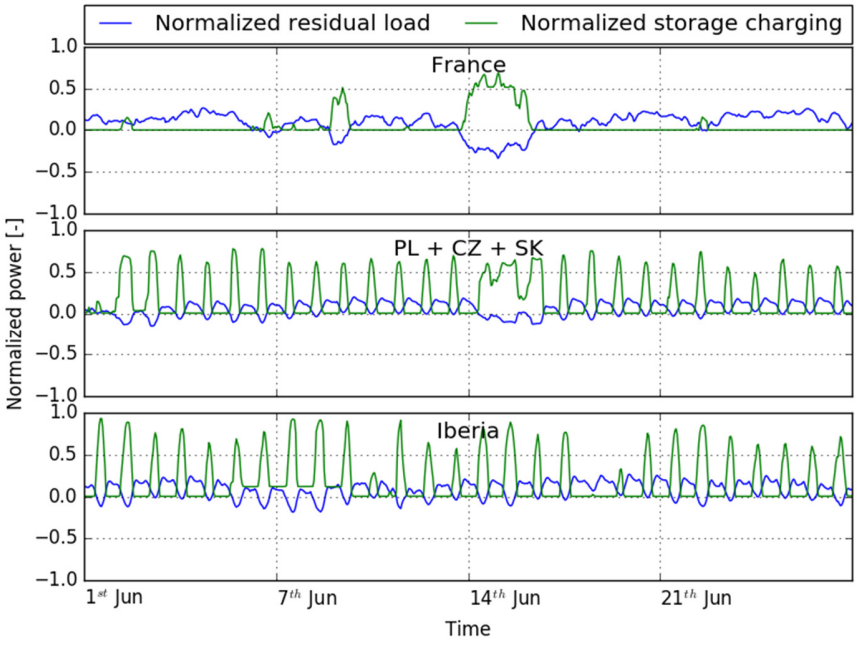

Fig. 24: Aggregated storage utilization. Model endogenously determined hourly net load and hourly cumulated charging capacity of all storage technologies for the model regions France, PL + CZ + SK, and Iberia. Storage charging is normalized to the total storage converter capacity; the net load to the region-specific, total VRE capacity.

The plots show a distinct correlation between the negative net load, i.e. VRE surplus generation, and storage charging. Within the regions PL + CZ + SK and Iberia, daily VRE peaks caused by PV generation occur, which, in contrast, fosters daily charging of storage. The PV-dominated pattern in PL + CZ + SK is superimposed by a short wind event of a few days. In the

offshore wind region France, in contrast, daily storage charging does not occur, but patterns that correlate on a more synoptic and seasonal basis.

To support these findings, the linear correlation coefficient ρ between the hourly net load and the hourly storage charging (cumulated over all storage technologies) for each model region (Pearson product-moment coefficient, Fig. 25) is analyzed. Moreover, the figure depicts the VRE share of each model region on the color axis.

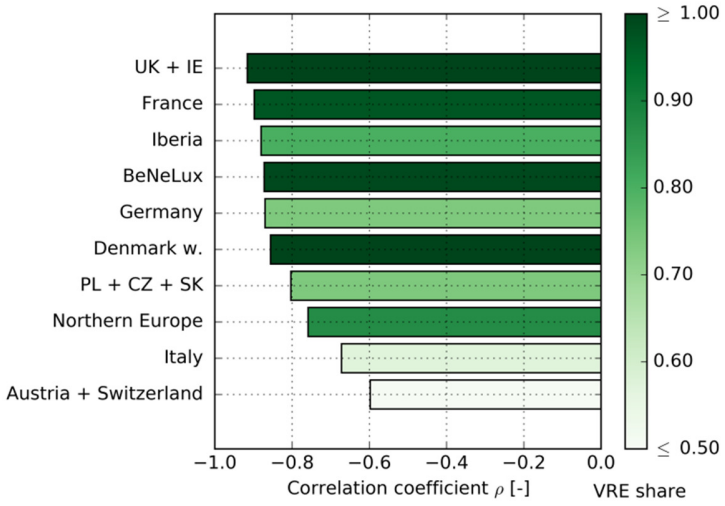

Fig. 25: Correlation of storage charging and net load. The correlation coefficients (ρ) (x-axis) of the model-endogenous, hourly times-series of the net load with the model-endogenous, hourly storage charging times-series for all model regions are shown. Moreover, the figure depicts the VRE shares (color axis).

A significant negative ρ between net load and storage charging can be observed in all regions, indicating that the regional VRE generation that exceeds the regional electrical load is predominantly used for storage charging. In this sense, storage is used to integrate power generation from VRE technologies, and does not, as for example shown for scenarios with lower shares of VRE penetration (see e.g. [141, 142]), ensure the continuous dispatch of thermal power plants and subsequently leads to higher CO_2 emissions. Alternatively, generation surplus can be curtailed or exported to other regions where an additional demand exists. Moreover, the results show that ρ tends to increase with higher VRE share, although, this observation does not hold for all model regions.

Still, both Fig. 24 and Fig. 25 cannot answer the question whether the generation from specific VRE technologies is complemented by certain storage technologies. For this purpose, the technology-specific correlation coefficients ρ of VRE feed-in and the storage charge time-series are analyzed for the model regions France, PL + CZ + SK, and Iberia. In all model regions, the

charging times-series of H_2 correlate significantly with the electricity generation from offshore wind. In general, also Li-ion storage charging is correlated with PV power production and aCAES charging with onshore wind. Particular in regions where an individual VRE generation technology dominates VRE power production, the correlation between this VRE technology and the corresponding storage technology is strong.

In France, high correlation coefficients for offshore wind and H_2 storage ($\rho = 0.85$) can be observed, illustrating the compensation of seasonal fluctuations of offshore wind by the storage. However, rather strong statistical links also exist between offshore wind with Li-Ion and PHS ($\rho = 0.60$). For the region PL + CZ + SK high correlations between onshore wind and H_2 as well as for aCAES storage can be observed ($\rho = 0.70, 0.57$), whereas the model region Iberia mainly shows correlations of PV with Li-ion batteries and PHS ($\rho = 0.73, 0.68$).

The described correlations are primarily driven by the assumptions of the investments costs of the storage, which are differentiated into storage power (€/kW_{el}) and energy-related costs (€/kWh_{el}). By this means, the ratio between converter power-specific and energy-specific investment costs (*energy-to-power-investment-ratio*) is crucial. On the one hand, storage technologies with low investment costs for the storage unit (energy-related costs) favor large amounts of stored energy and hence long-term applications. On the other hand, storage technologies which are characterized by a low storage-to-investment-ratio are preferred for the balancing of high power and short-term usage.

Although the storage modeling in REMix allows an individual sizing of the converter and storage unit (no pre-defined E2P of a storage technology, see Sec. 6.2.2), the energy-to-power-investment-ratio influences the dimensioning of the converter and storage unit to some extent. The temporal characteristics of the power generation from VRE in a model region (i.e. daily patterns versus more synoptic or seasonal generation), will lead to the expansion of a certain storage technology portfolio. The model endogenously determined E2P ratios, their mean values as well as the coefficient of variation (*cv*) are shown in Tab. 9. The *cv* describes a dimensionless measure of the spread of E2P among all regions and is defined as the standard deviation over all regions divided by the average E2P.

Tab. 9: Endogenously determined energy to power ratios (E2P). The latter are shown for all model regions, and, moreover, are averaged over all regions including the resulting coefficient of variation *cv* (standard deviation over all regions divided by average E2P).

	H_2	Li-ion	aCAES	PHS
AT + CH	-[a]	1	17	43
BeNeLux	311	2	19	13
Denmark west	454	1	20	-
PL + CZ + SK	179	4	18	-
France	267	2	19	13
Iberia	280	4	18	16
Italy	-[a]	3	16	16
Northern Europe	-	4	-	12
UK + IE	404	2	13	11
Mean	316	2	18	18
cv	0.53	0.49	0.33	0.66

[a] The model regions AT + CH and Italy result in a marginal capacity expansion of H_2. The E2P ratio, therefore, is not meaningful and neglected here.

The optimization approach favors the storage expansion of cost-effective technologies, such as PHS. Provided that further storage is required to meet $80\%_{constr}$, the model will pursue the expansion of such technologies as long as the technical potential is not reached (see Tab. 10).

Tab. 10: Used and unused technical potential of the storage unit capacity. Values are shown model region and technology-specific. Note that unlimited storage unit capacity potentials for Li-ion and redox-flow batteries are assumed.

	Used technical potential [GWh_{el}]			Unused technical potential [GWh_{el}]		
	PHS	aCAES	H_2	PHS	aCAES	H_2
Austria + Switzerland	40	1	36	22	137	13,155
BeNeLux	22	44	3,117	-	269	26,838
Denmark w.	-	4	2,264	-	183	15,709
PL + CZ + SK	25	48	86	-	1,577	155,691
France	37	5	6,927	-	620	52,982
Iberia	137	3	901	-	1,397	133,304
Italy	77	2	38	-	123	11,944
Northern Europe	27	-	-	-	-	-
Germany	54	58	3,671	-	1,192	116,161
UK + IE	22	72	12,578	-	403	32,959

Tab. 10 shows that nearly all model regions exploit their technical potential of PHS storage. An exception is the model region Austria + Switzerland, which, additionally to the existing PHS capacities, provides flexibility mainly through dispatchable conventional hydroelectricity (49 GWh, resp. 40% of the annual demand). In contrast, large amounts of unused technical

potential still remain for aCAES and H_2. The technical potentials for storage expansion are discussed in some more detail in Sec. 8 of Appendix C.

6.3.4 Storage dispatch

The following sections takes a closer look at storage utilization in terms of hourly charge and discharge. It addresses two main questions:

(1) Is the temporal storage dispatch pattern technology-specific?
(2) If so, are those patterns region-specific or do similar patterns occur in all regions?

(1) For the analysis of the hourly dispatch patterns, the total number of cycles (NC), the number of full cycles (NFC), the number of typical cycles (NC_{typ}) as well as the representative length (Φ) of one typical cycle are defined:

(I) NC describes each change from charging to discharging and is a measurement of the annual utilization of the storage.
(II) The NFC is defined as the ratio of the sum of annual storage energy (electrical output) and load (electrical input) to the storage capacity divided by two. The difference between NC and NFC helps to assess the intensity of the storage utilization.
(III) NC_{typ} is defined as the number of charge and discharge processes going through the following states of charge (SOC): $SOC \leq 0.2 \rightarrow SOC \geq 0.8 \rightarrow SOC \leq 0.2$. It is the precondition for defining Φ.
(IV) Φ denotes an average length (e.g. in hours or days) of a typical cycle NC_{typ}.

For the regions Iberia, PL + CZ + SK, and France, Fig. 26 displays the relative storage charge, discharge, and the fill level for Li-ion, aCAES, and H_2, respectively.

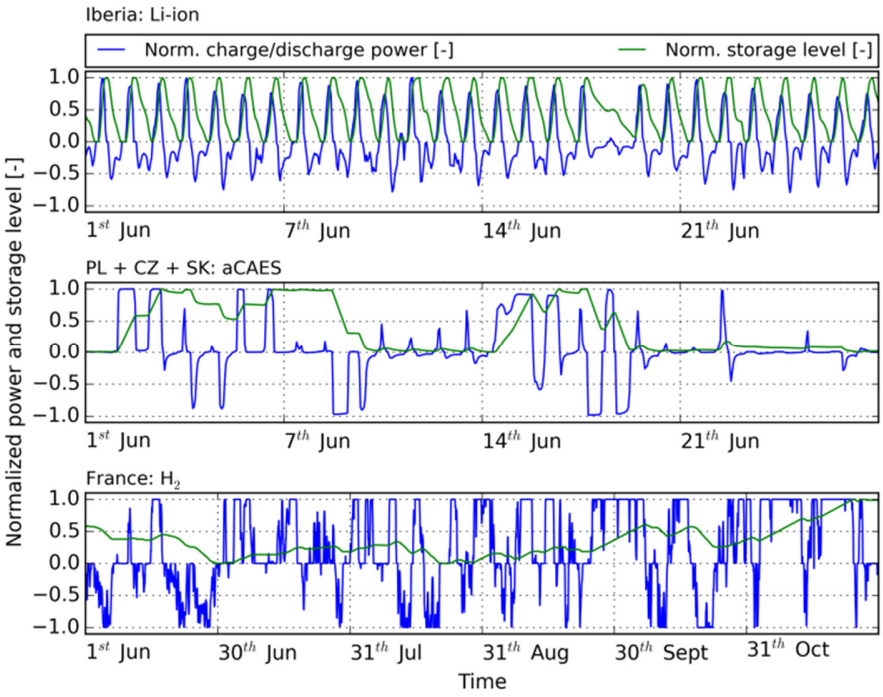

Fig. 26: Utilization of different storage technologies. Storage level, charge, and discharge power for the storage technologies Li-ion battery (Iberia), aCAES (PL + CZ + SK), and H_2 (France). The storage level is normalized to the total storage capacity; charge and discharge power are normalized to the total installed converter power. Note that the plots show different temporal intervals on the abscissa in order to illustrate the typical dispatch for each storage technology.

The expansion of short-term storage technologies, such as Li-ion batteries, is typical for regions with high shares of PV generation. The dispatch of these batteries in the model region Iberia (upper panel in Fig. 26) shows the most significant cyclicality of all storage technologies. Daily cycles can be observed, where charging mainly occurs in times of high PV power generation, as a single peak around noon. Furthermore, the high charging power is striking which usually reaches almost 100% (in absolute terms ≈ 10 GW, see Fig. 22). Discharging of Li-ion batteries in Iberia usually occurs during morning and evening hours. In contrast to the charging process, discharging of Li-ion batteries also occurs with partial converter power. This implies that the converter capacity is mainly optimized in the model in order to balance surplus PV production and less in order to balance nocturnal deficits. A complete discharge (SOC=0) is usually reached at night times; the typical cycle duration Φ is around one day.

The middle panel of Fig. 26 represents the dispatch pattern of aCAES in the model region PL + CZ + SK. Φ is around three to five days. Opposed to Li-ion batteries in Iberia, aCAES charging and discharging also occurs with partial converter power. Moreover, the cyclicality of

the storage dispatch is not as distinctive as for stationary Li-ion batteries, mainly since aCAES charging significantly correlates with the synoptic feed-in of onshore wind.

Regions with high shares of offshore wind penetration—namely the model regions Denmark west, Northern Europe, UK + IE, and France—require large amounts of H_2 long-term storage, provided that the technical potential of the storage unit is sufficient (see Tab. 10). The lower panel of Fig. 26 shows the dispatch behavior of H_2 storage in France. Since charging strongly correlates with offshore wind generation, seasonal changes of the storage fill level are characteristic. This is also indicated by a high E2P ratio (see Tab. 9). A typical cycle lasts ≈ 45 days and charging as well as discharging usually occurs with high converter power.

(2) Following, it is analyzed to what extent storage dispatch patterns for individual storage technologies are either model region-specific or similar in all model regions. For this purpose, a comparison of the NC to the NFC for all storage technologies (except for redox-flow batteries) is shown in Fig. 27.

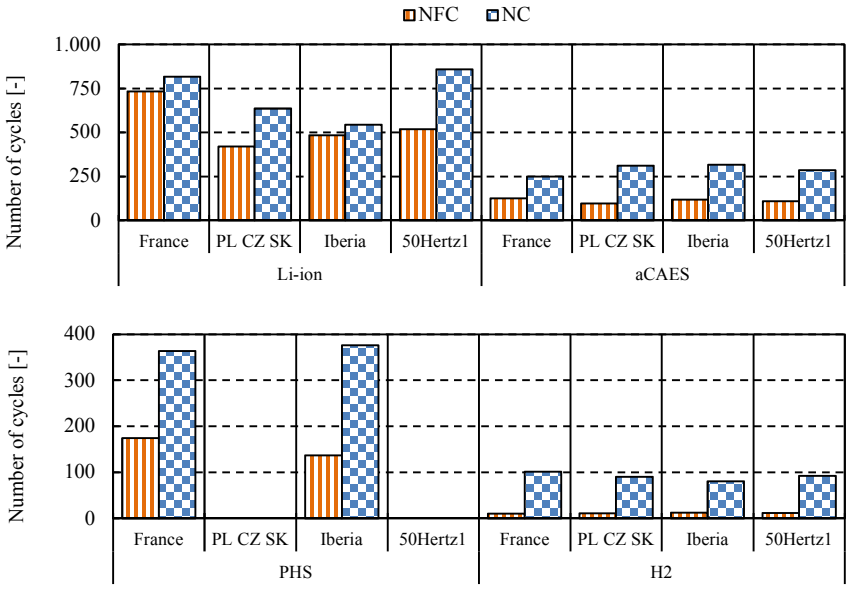

Fig. 27: Number of storage cycles (NC) and full cycles (NFC). The latter are depicted for each storage technology for the model regions France, PL + CZ + SK, Iberia, and 50Hertz1.

For the optimization year 2050, the NC of H_2 storage is between 80 and 100, for aCAES in the range of 250–320, for PHS 360–380, and for Li-ion batteries from 540 to 860. With regard to the NFC, model results range between 10 and 12 for H_2, 90–130 for aCAES, 140–170 for PHS, and 420–730 for Li-ion storage. For each storage technology, similar values for NC and NFC can be found in all model regions, however, with one exception: For Li-ion storage notable differences

occur between the regions with regard to the NC and the NFC. The model regions Iberia and PL + CZ + SK for example, exhibit rather low NC (≈ 500), whereas France and 50Hertz1 show relatively high NC (≈ 750). This also can be supported by the coefficient of variation (*cv*), which is shown in Tab. 11 for the NFC of each storage technology of all model regions with non-marginal installed storage capacities. Here, Li-ion batteries show the highest *cv* (0.67), indicating the regional differences in the utilization of this technology.

Tab. 11: Mean, standard deviation, and coefficient of variation of the number of full cycles. Values are derived over all model regions. Note that only model regions with a considerable amount of storage capacity were considered.

Number of full cycles (NFC)			
	Mean [-]	Std. deviation [-]	cv [-]
H_2	9	1.5	0.17
Li-ion	817	550	0.67
aCAES	119	19	0.16
PHS	117	56	0.18

This behavior could be explained by the fact that Li-ion batteries with low NC primarily balance electricity from PV. High NC, in contrast, indicate that Li-ion does not exclusively store electricity from PV (daily cycling), but additionally balances electricity from wind power. In order to validate this hypothesis, the region and technology-specific storage dispatch of Li-ion batteries are analyzed in detail using heat maps.

Fig. 28 shows the normalized charge (left panels) and discharge power (right panels) of Li-ion storage over the hours of a day on the abscissa and over the days of the year on the ordinate for the same model regions as in Fig. 27.

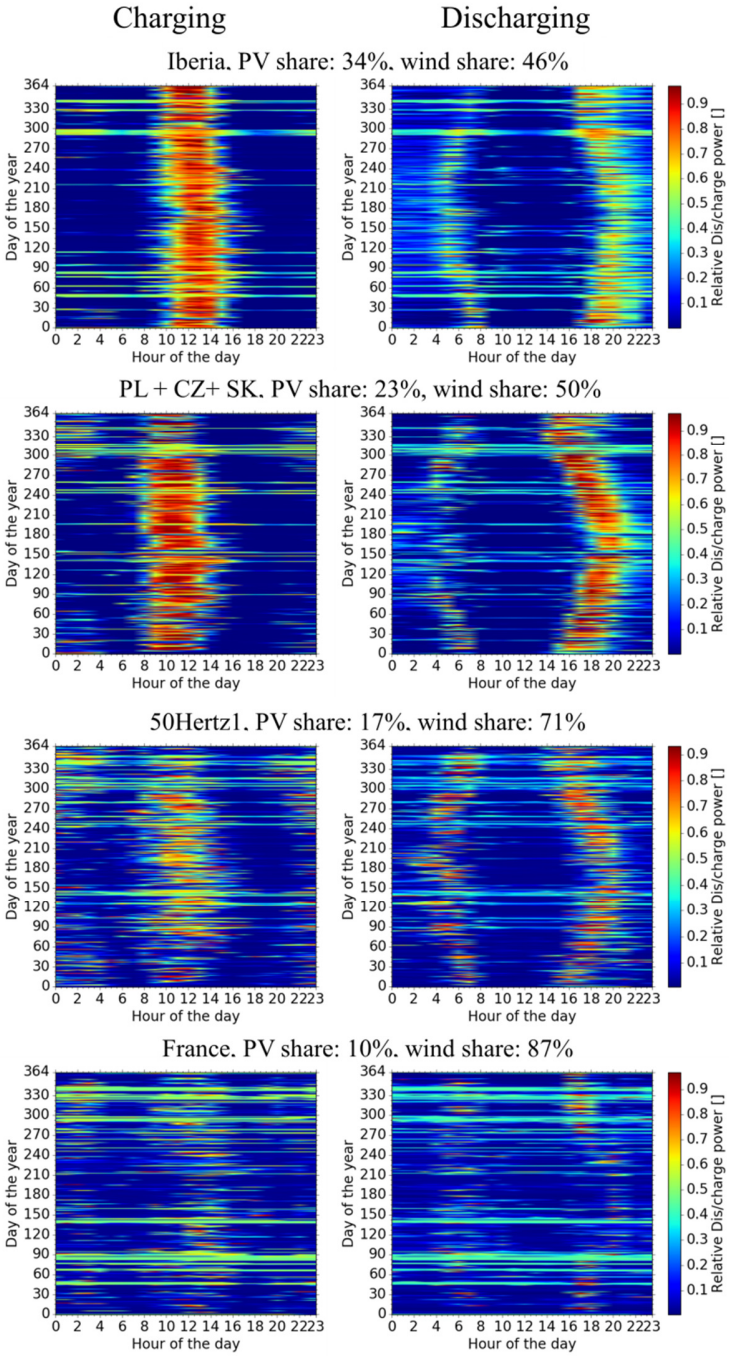

Fig. 28: Utilization of stationary Li-ion batteries. Normalized charge (left panels) and discharge power (right panels) over the hours of the day and over the days of the year in the model regions Iberia, PL + CZ + SK, 50Hertz1, and France.

In all regions shown in Fig. 28, storage loading processes generally occur daily and primarily in the hours of the highest PV power generation, while discharging mainly takes place during hours of high electricity demand and low PV power production. However, some differences exist. For the regions shown in Fig. 28, low PV shares, as in France or 50Hertz1, are associated with

high amounts of electricity generation from wind power due to the required high share of VRE ($80\%_{constr}$). In consequence, France and 50Hertz1 are characterized by a higher number of charging processes during the night times when compared to Iberia or PL + CZ + SK. This, in turn, leads to higher NC of Li-ion batteries in France and 50Hertz1 (see Fig. 27).

Furthermore, higher wind shares and hence increasing NC lead to lower relative charge powers. Consequently, PV regions which are characterized with higher Li-ion battery capacities and lower NC, the relative charge power is significantly higher than in wind-dominated regions.

In conclusion, Fig. 28 underlines the assumption that Li-ion batteries do not exclusively balance short-term diurnal fluctuations from PV generation, but also are charged in times of high wind penetration. Naturally, this effect is more distinctive with increasing wind shares. In these cases, Li-ion batteries complement mid and long-term storage with the balancing of synoptic and seasonal fluctuations from wind energy.

In contrast to Li-ion batteries, the dispatch of PHS, aCAES, and H_2 storage is largely region-independent (see Fig. 27).

6.3.5 Sensitivity analysis of generation and storage capacity

Following, the robustness of the endogenously determined generation and storage capacities is tested, using a sensitivity analysis. In this regard, several input parameters, as well as methodological approaches, are varied. Tab. 12 gives a summary of the sensitivity tests. The scenarios were chosen based on the findings of the literature review in Sec. 2.3.

Tab. 12: Scenario overview and respective main assumptions.

Scenario group	Sub-scenario	Specification
Reference scenario	Ref	Reference scenario (used for the analysis in the main text): unlimited curtailments, exogenous grid, mean price and cost paths
(1) Investment cost scenarios	a. Stor_Inv_low	Decreased investment costs for converter and storage unit by 50%
	b. Stor_Inv_high	Increased investment costs for converter and storage unit by 50%
	c.VRE_Inv_low	Decreased investment costs for VRE by 50%
	d. VRE_Inv_high	Increased investment costs for VRE by 50%
(2) Operating cost scenarios	a. FP_low	Fuel price path low (see Tab. 13)
	b. FP_high	Fuel price path high (see Tab. 13)
	c. CO_2_low	CO_2 certificate price path low (see Tab. 14)
	d. CO_2_high	CO_2 certificate price path high (see Tab. 14)
(3) Grid scenarios	a. G++	No transmission grid restrictions (“copper plate”)
	b. G+	Optimized grid in Europe, reference investment costs (see Tab. C 2)
	c. G+_Inv_high	Optimized grid in Europe, increased investment costs by 50%
	d. G+_Inv_veryhigh	Optimized grid in Europe, increased investment costs by 100%
(4) Curtailment scenarios	a. Cur.003	Technology and region-specific VRE curtailments restricted to 3%
	b. Cur.010	Technology and region-specific VRE curtailments restricted to 10%
(5) VRE constr. scenarios	a. VRE_exp_CO_2_med	No constraint which forces 80% VRE, medium CO_2 certificate price
	b. VRE_ exp_CO_2_high	No constraint which forces 80% VRE, high CO_2 certificate price
	c. VRE_ exp_CO_2_veryhigh	No constraint which forces 80% VRE, very high CO_2 certificate price
(6) Temp. resolution scenarios	a. TempRes_2h	Temporal resolution reduced to 2 hourly time-steps
	b. TempRes_6h	Temporal resolution reduced to 6 hourly time-steps
	c. TempRes_24h	Temporal resolution reduced to 24 hourly time-steps
(7) Weather scenarios	a. Weather 2007	Hourly, potential VRE power generation based on the weather year 2007
	b. Weather 2008	Hourly, potential VRE power generation based on the weather year 2008
	c. Weather 2009	Hourly, potential VRE power generation based on the weather year 2009
	d. Weather 2011	Hourly, potential VRE power generation based on the weather year 2011
	e. Weather 2012	Hourly, potential VRE power generation based on the weather year 2012
(8) Misc. scenarios	a. Redox-flow_Inv_low	Energy-related investment costs of redox-flow batteries decreased to the value of aCAES
	b. PHS_w/o_old_stock	No old stock capacities of PHS assumed

Storage demand is strongly affected by the model endogenously determined generation portfolio. Fig. 29 shows the overall installed generation capacities as well as the installed storage converter capacities for each scenario over all model regions. Furthermore, the figure depicts the shares of curtailed energy from VRE sources (percentage values in the middle plot). These values derive from curtailed energy divided by the potential annual VRE power generation.

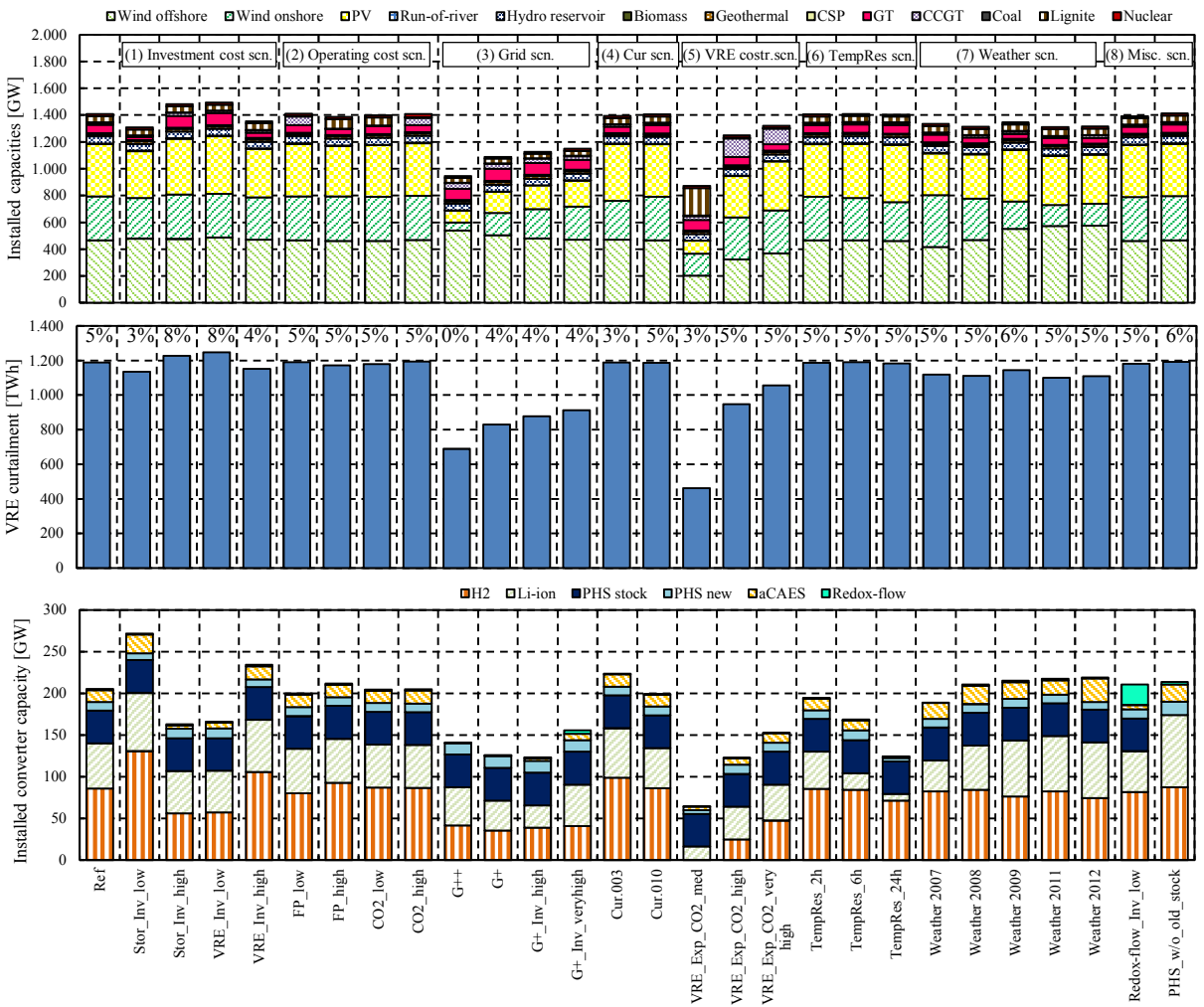

Fig. 29: Overview of the sensitivity cases. Installed generation capacities (upper plot), annual curtailments of VRE (middle plot), and installed storage converter capacities (lower plot) over all scenarios and all model regions. Note that for PHS a differentiation between existing (stock) and endogenously determined capacities (new) is shown (in the main text both capacities are shown aggregated). Additionally, the percentage values in the middle plot show the share of curtailed VRE electricity generation with regard to the potential annual electricity generation from VRE. All numerical values can be found in Sec. 9 of Appendix C.

In general, all scenarios are characterized by rather large shares of offshore wind, onshore wind, and PV, mainly fostered by the 80% VRE generation model constraint ($80\%_{constr}$). For the investment (1) and operating cost scenarios (2) as well as for the curtailment (4), temporal resolution (6), weather (7), and miscellaneous scenarios (8), the overall VRE capacities only differs in small amounts (≈ ±5%) compared to VRE capacities in the reference scenario (1,185 GW). In contrast, the grid and $80\%_{constr}$ scenarios heavily affect both the generation as well as the storage capacities structure. In the following sections, each scenario group will be analyzed separately, showing the differences in installed capacity compared to the reference scenario. Note that for both storage and generation technologies, only the most important (in terms of changes compared to the reference scenarios as well as the overall installed capacity) technologies are discussed.

Investment cost scenarios

Fig. 30 depicts the results of the investment cost scenarios with regard to the installed storage converter capacity compared to the reference scenario.

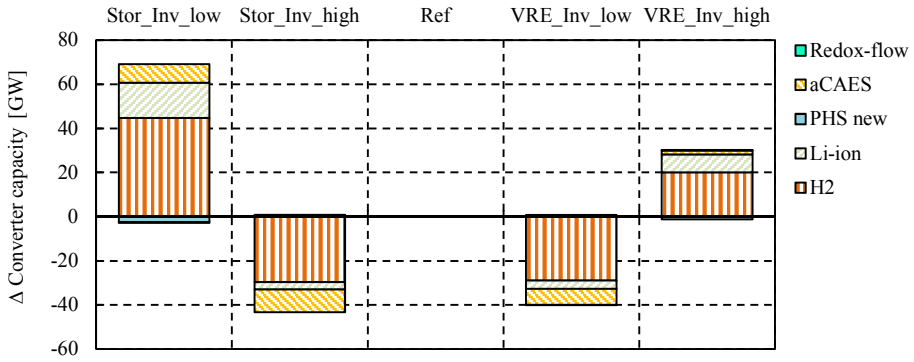

Fig. 30: Differences in installed capacity in the investment cost scenarios. The changes in converter power are compared to the reference scenario aggregated over all model regions.

The scenario Stor_Inv_low (reduced power and energy-related investment costs for storage technologies) results in an increase of H_2 converter power of 45 GW. In consequence, an increase of offshore wind integration is possible (+15 GW), where onshore wind (-27 GW), PV (-41 GW), and GTs (-33 GW) are substituted (see Fig. 30). A structurally similar effect (but less pronounced) can be observed for the scenario with increased investment costs for VRE technologies (VRE_Inv_high).

The scenarios Stor_Inv_high and VRE_Inv_low show roughly opposite effects compared with their counterparts Stor_Inv_low and VRE_Inv_high. Again, the analysis supports the finding that certain generation technologies complement certain storage technologies better than other (see Sec. 6.3.3). Especially offshore wind is often complemented by H_2 storage, whereas increased PV capacities most likely go along with a combination of Li-ion batteries and GTs. Due to the relatively low costs of the storage unit, H_2 storage primarily balances seasonal variations in terms of high amounts of energy. In contrast, the comparatively low power-related costs of Li-ion batteries (cheap storage converter unit) favor Li-ion batteries and GTs (low investment costs compared to other conventional power plants) for short-term power balancing.

Operating cost scenarios

Uncertainties for the cost projections of fossil-fired power plants mainly exist with regard to their fuel and emission certificate costs. From a cost minimizing optimization approach, low fuel prices (FP) and low CO_2 emission cost will increase the expansion of dispatchable, fossil-fired power plants (within the limitations set by $80\%_{constr}$, i.e. the remaining 20% of electricity generation from non-VRE capacities). In consequence, smaller capacities of storage might be required. In contrast, high price paths for fuels and CO_2 emissions most likely will favor an increase in storage demand through higher expansion rates of RE technologies. In order to quantify these effects, the analysis uses three different price paths as input parameter. The specific emissions are based on [143]. Tab. 13 shows the fuel price scenarios for each fuel type, whereas Tab. 14 illustrates the different cost scenarios for CO_2 emissions for the year 2050. Here, the high and medium costs scenarios are based on [192]. The low cost scenario, however, is assumed to be the arithmetic mean of the European emission allowance prices of the year 2013 from the European Energy Exchange (EEX).

Tab. 13: Fuel price scenarios for each fuel type.

Fuel type	Cost scenario	Fuel costs [€/MWh$_{th}$]	Source
Coal	low	14.04	[144]
Lignite	low	8.28	[184]
Natural gas	low	33.12	[144]
Uranium	low	4.03	[185]
Coal	medium	20.88	[189][a]
Lignite	medium	9.18	[184]
Natural gas	medium	47.52	[189][a]
Uranium	medium	5.24	[185]
Coal	high	35.28	[189][b]
Lignite	high	10.08	[184]
Natural gas	high	73.44	[189][b]
Uranium	high	6.45	[185]

[a] Scenario B, moderate price path.
[b] Scenario A, high price path.

Tab. 14: CO_2 emission costs scenarios.

Cost scenario	CO_2 costs [€/t CO_2]	Source
Very high	130.0	Own assumption
High	75.0	[192][a]
Med	57.0	[192][b]
Low	4.4	Own assumption[c]

[a] Scenario A in [81] ("high cost path").
[b] Scenario B in [81] ("moderate cost path").
[c] Arithmetic mean of European emission allowance prices in 2013.

Furthermore, one has to take into account that inter-dependencies between the fuel price and emission certificate costs might exist, where high fuel prices, for example, could foster low CO_2 emissions certificate costs and vice versa. This is due to the assumption that high fuel prices would decrease the dispatch of fossil-fired power plants and therefore increase the number of available emission certificates which again would lower their costs. To accommodate such effects, the cost projections are considered in a combined approach for consistent scenarios as shown in Tab. 15.

Tab. 15: Combinations of CO_2 costs and fuel price paths. These combinations are based on different fuel price and CO_2 emission cost scenarios.

	CO_2			Fuel price		
	High	Med	Low	High	Med	Low
Ref		x			x	
FP_high			x	x		
FP_low	x					x
CO_2_high	x				x	
CO_2_low			x		x	

Fig. 31 shows the differences in installed generation capacities for the operating cost scenarios compared to the reference scenario over all model regions.

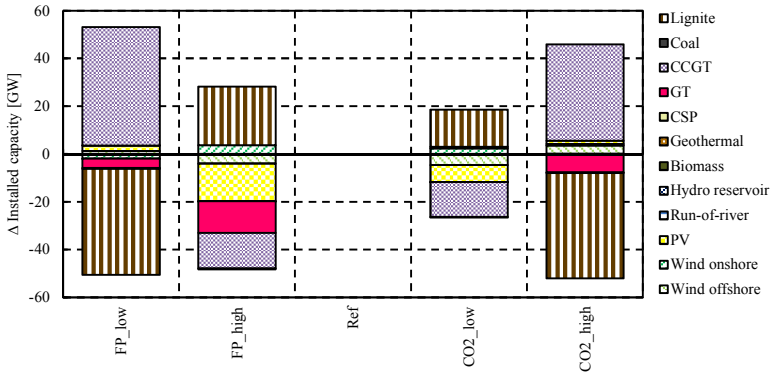

Fig. 31: Differences in installed capacities in the operating cost scenarios. Changes in converter power are compared to the reference scenario over all model regions.

Naturally, lower costs for CO_2 emission certificates will favor the expansion of CO_2 intensive generation technologies, such as lignite-fired power plants, whereas high CO_2 costs will foster the expansion of less CO_2 intensive technologies (e.g. CCGT power plants). The model results reflect this effect in the scenarios CO_2_high and CO_2_low. The scenario CO_2_high substitutes lignite power plants with CCGT when compared with the reference case, whereas the scenario CO_2_low, in contrast, is characterized by larger shares of lignite power plants. Similar observations can be made for the scenarios which vary the fuel price assumption (FP_low, FP_high). Here, higher fuel prices increase the capacity expansion of lignite power plants and decrease CCGT and gas turbines. In general, assumptions on fuel prices and costs CO_2 allowance certificates have only a minor influence on the capacity expansion of VRE technologies. This can be explained by the sheer amount of VRE technologies forced by the 80% VRE generation model constraint ($80\%_{constr}$). In consequence, also the differences in storage capacity expansion are negligible.

Grid scenarios

To evaluate the influence of transmission grid expansion as an additional option to allow large-scale spatial balancing of production and demand, particularly in highly renewable energy scenarios, several scenarios which endogenously determine the expansion of new grid lines were included, additionally to the exogenous alternating current (AC) and direct current (DC) grid infrastructure. The latter is based on the Ten Year Network Development Plan (TYNDP) of the European Network of Transmission System Operators for Electricity (ENTSO-E) (see Fig. C 2) and exogenously defined in the reference scenario. The different transmission grid scenarios vary in terms of their specific investment costs for grid expansion (see Tab. C 2) and include one scenario with no transmission grid restrictions (G++, "copper plate"). Fig. 32 depicts the AC and DC grid expansion for all model regions comparing the different scenarios. Only the existing grid topology (based on the TYNDP) can be extended; i.e. it is prohibited to establish new grid connections between two model regions.

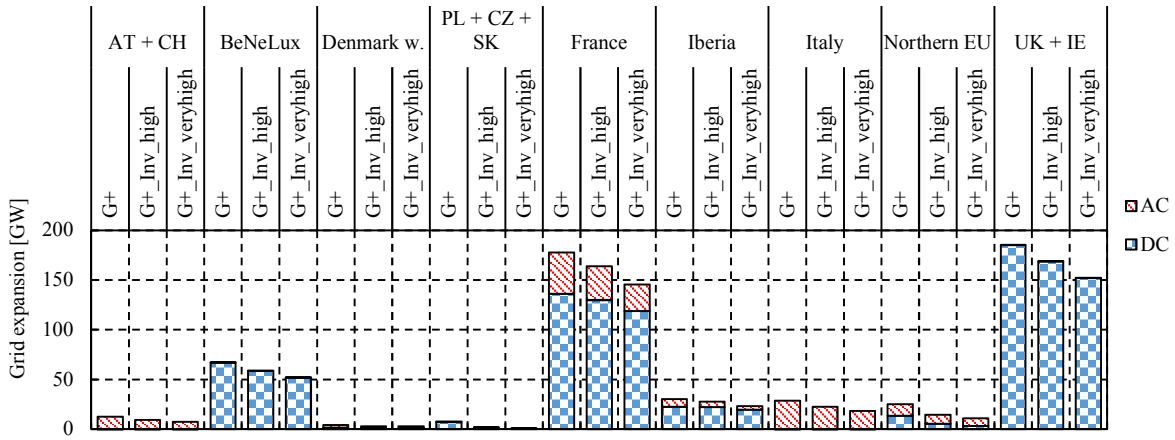

Fig. 32: Differences in grid expansion in the grid scenarios. Changes of the capacity are shown for each model region. Note that the figure depicts the capacity expansion of one model region to all surrounding regions. It is thereby applicable when observing each model region individually, but double accounts if aggregated over the whole observation area.

Fig. 32 highlights the important role of transmission grid expansion in highly renewable energy scenarios. Some regions, such as UK + IE or France, result in additional transmission grid capacities of more than 150 GW. For certain grid connections between two model regions, e.g. UK + IE to France, this translates into capacities of up to 113 GW per link. As expected due to the cost minimizing logic of model, the lowest investment costs lead to the highest grid

infrastructure expansion (scenario G+). Stepwise increasing these costs (scenario G+_Inv_high, G+_Inv_veryhigh) subsequently decreases grid expansion.

In consequence of changes in the transmission capacities, the electricity generation and storage infrastructure is strongly affected. Fig. 33 illustrates the generation capacity expansion and annual electricity generation for the most relevant technologies over all model regions for the different grid scenarios in comparison to the reference scenario.

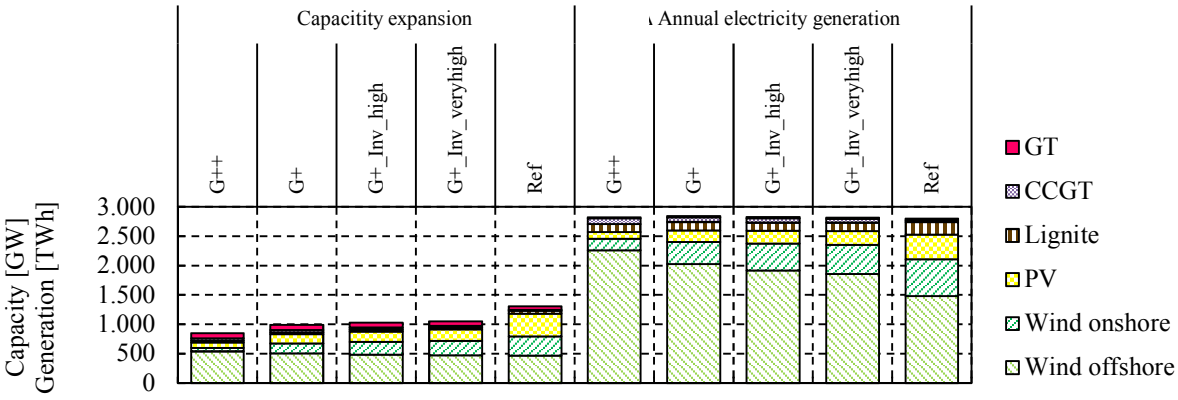

Fig. 33: Capacity expansion and annual electricity generation. Values are shown compared to the reference scenario and aggregated over all model regions.

In general, endogenous grid expansion allows a noticeable reduction of generation capacity expansion in the observation area. In the scenario with the lowest investment costs for grid expansion (G+), the net capacity expansion can be reduced by approximately 25% (312 GW) compared to total capacity in the reference scenario. Even increased investment costs in the scenarios G+_Inv_high and G+_Inv_veryhigh still result in around 20% less generation capacity expansion than in the reference scenario. In the hypothetical scenario of a “copper plate” grid infrastructure for all model regions (G++), capacity demand can be reduced by 35%.

For the annual electricity generation, the overall amount of electricity generation remains similar in all scenarios (in order to meet the demand), whereas the technological distribution changes significantly. Differences in the total electricity production compared with the reference scenario occur due to different amounts of curtailed power. Large shares of onshore wind and PV capacities (and smaller amounts of lignite capacities) are substitutes by comparatively lower amounts of capacity (GW) of offshore wind, gas turbines, and CCGT power plants. This can be explained by the increased transfer capacity of the transmission grid, which now allows a less

constrained transport of the electricity from offshore systems at the coast to the demand centers. As expected, improved transmission grid infrastructure generally allows a better utilization of VRE technologies in terms of full load hours (see Tab. 16).

Tab. 16: Comparison of full load hours of VRE technologies in the different grid scenarios.

	Full load hours [h]		
	Offshore wind	Onshore wind	PV
G++	4,198	3,253	1,305
G+	4,015	2,265	1,237
G+_Inv_high	3,990	2,118	1,211
G+_Inv_veryhigh	3,945	2,025	1,189
Ref	3,191	1,903	1,069

Considering each model region individually in the grid scenarios, the changes in capacity expansion are more diverse. Fig. 34 illustrates the differences in capacity expansion of generation technologies compared to the reference scenario for each model region.

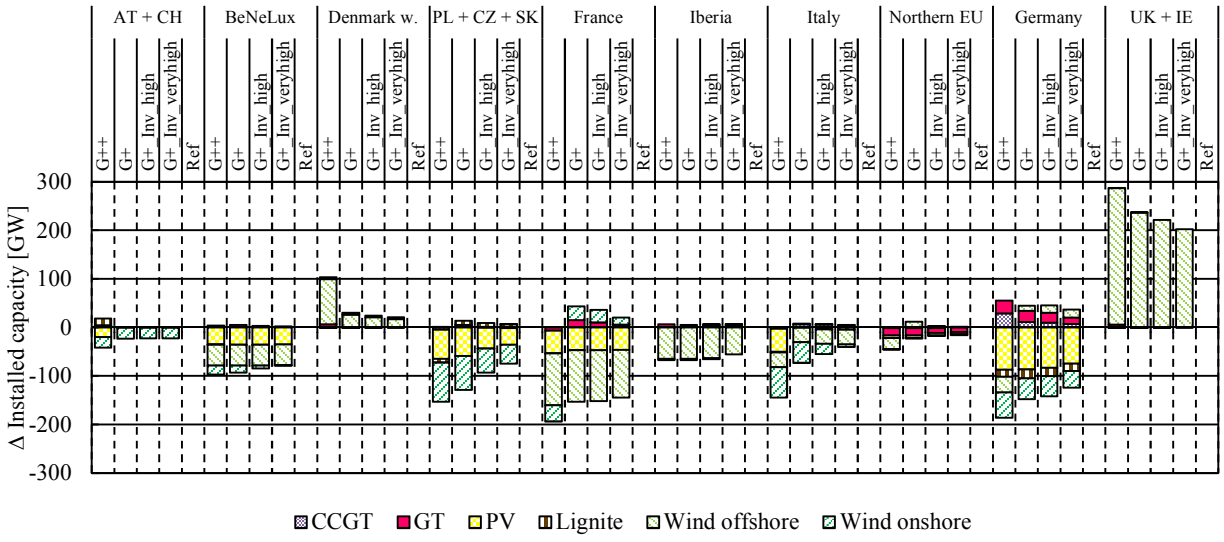

Fig. 34: Differences in capacity expansion of generation technologies. Differences are shown compared to the reference scenario and for each model region. The German model regions are aggregated.

For most of the model regions, a decrease of VRE capacity can be observed, compared with the reference scenario and if the grid expansion is endogenously calculated by the model. The shift to offshore wind generation which substitutes large amounts of PV and onshore wind can mainly be explained by an integration of large offshore wind potentials in the model region UK + IE (and to some extent Denmark west) through an enhanced grid between UK + IE and the

European mainland (including Scandinavia). Since $80\%_{constr}$ (see Sec. 6.2.2) still has to be met, reduced capacity expansion translates into improved utilization of the remaining generation assets, i.e. higher average full load hours (see Tab. 16) due to occupation of more favorable sites for wind and PV power production and less curtailment (see Tab. 17).

The scenario with the lowest investment costs for the grid infrastructure (G+)—which leads to the highest amount of AC and DC expansion (see Fig. 32)—results in the lowest overall curtailed energy, only outreached by scenario G++ where electricity transmission is unlimited and no curtailments are observed at all. Increasing the investment costs gradually (G+_Inv_high, G+_Inv_veryhigh) and in consequence reducing the grid extension, naturally, will lead to increasing curtailments. Curtailments are the highest in the reference scenarios since here grid capacity expansion is not allowed. Furthermore, Tab. 17 confirms the important role of offshore wind generation in the model region UK + IE for the whole energy system. Restricting grid expansion in this region will lead high curtailments of VRE. Moreover, when comparing the grid scenarios to the reference scenario, the differences in curtailment are the most distinct in UK + IE.

Tab. 17: Curtailments in the different grid scenarios. The values are deviations regarding the reference scenario and shown region-specific. The German model regions are aggregated. Furthermore, the table shows the share of annual curtailed energy of VRE with respect to the potential annual electricity generation of VRE (curtailment share).

Annual curtailments [TWh]					
	G++	G+	G+_Inv_high	G+_Inv_veryhigh	Ref
Austria + Switzerland	-	0.01	0.04	0.10	0.02
BeNeLux	-	0.15	0.43	1.23	1.98
Denmark west	-	13.81	12.05	9.56	3.92
PL + CZ + SK	-	0.03	0.07	0.34	8.52
France	-	0.21	0.53	1.62	23.19
Iberia	-	0.05	0.17	0.55	6.29
Italy	-	0.03	0.07	0.19	3.57
Northern Europe	-	15.23	17.20	17.96	34.66
Germany	-	3.28	6.83	12.66	26.45
UK + IE	-	63.27	65.94	64.47	27.84
Total	-	96.07	103.33	108.67	136.43
Total curtailment share of VRE[-]	-	0.04	0.04	0.04	0.05

Curtailment scenarios

Within the reference scenario, curtailments have no upper limit and, theoretically, all potential VRE power generation can be shed. The scenarios cur.010 and cur.003 restrict the curtailment

technology (wind onshore and offshore, PV) and model region-specific to 10% and 3% of the annual potential VRE electricity generation. Fig. 35 shows the annual curtailment share with regard to the theoretically annual VRE electricity generation, respectively. It can be observed that already in the reference scenario only a few technologies and model regions show higher curtailment shares than 10% (e.g. onshore wind in Northern EU or Denmark west, offshore wind in Germany) and, therefore, scenario Cur.010 will not influence generation and storage capacity expansion significantly. The latter, however, will be affected if the upper limit for curtailments is reduced to 3% (Cur.003).

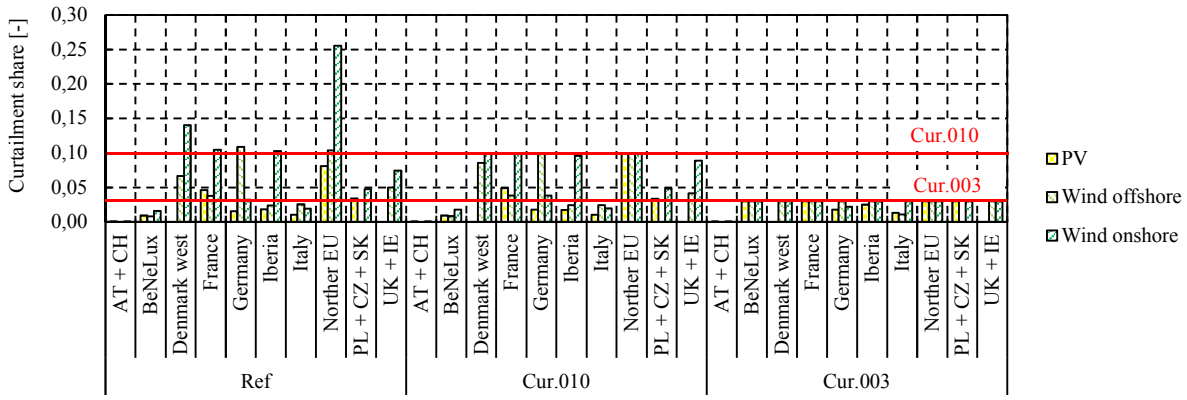

Fig. 35: Model region and technology-specific curtailment shares. The latter are shown with respect to the theoretical annual electricity generation from VRE.

More rigid curtailment requirements most likely will lead to an increase in storage expansion, since over-generation from VRE cannot be curtailed unlimitedly. Fig. 36 shows the differences in storage converter power in comparison to the reference scenario over all model regions.

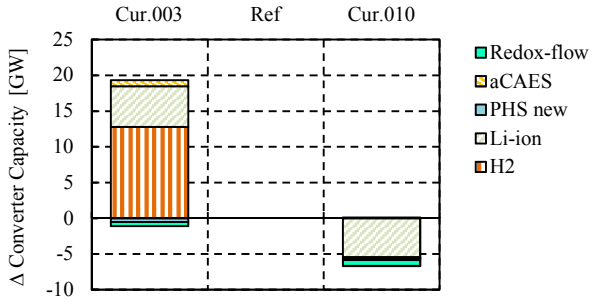

Fig. 36: Differences in the capacity of storage converter power. The changes are shown compared to the reference scenario and aggregated over all model regions.

For the most restrictive curtailment assumptions (scenario cur.003) the results show, as expected, an increase of storage converter power compared to the reference scenario. In line with the findings in Sec. 6.3.3 (certain storage utilization correlates with the generation of specific VRE technologies), the increased capacity expansion of PV and onshore wind correlate with more H_2 and stationary Li-ion storage. However, for less restrictive curtailment constraints in scenario cur.010 a decrease in storage converter capacity compared to the reference scenario can be observed, which contradicts the assumption that restricted curtailments increase storage demand. However, the deviation of storage converter capacity expansion in comparison to the reference scenario is only marginal and the affected regions and VRE technologies (e.g. onshore wind in Northern EU or Denmark west, offshore wind in Germany) compensate the restrictions in curtailment through an increased utilization (i.e. higher full load hours) of other VREs.

VRE constraint scenarios

Fig. 37 depicts the capacity expansion of the most important technologies in the scenarios where $80\%_{constr}$ is not active compared to the reference scenario. Furthermore, these scenarios differentiate in their costs of the CO_2 emission certificates, ranging from 57€/t CO_2 (*_med*) up to 130€/t CO_2 (*_veryhigh*, see Tab. 14).

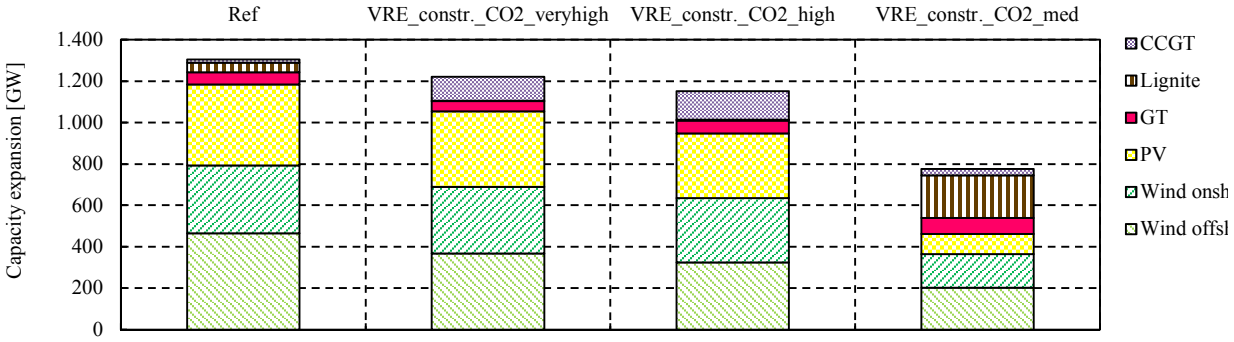

Fig. 37: Comparison of the capacity expansion. Changes are shown over all model regions of the scenarios without $80\%_{constr}$ and different assumptions regarding the CO_2 certificate price to the reference scenario.

The scenarios without $80\%_{constr}$ result in lower VRE shares than the reference scenario. While the reference scenario shows a VRE share of 86%, the rest of the scenarios, in the order from very high to medium CO_2 prices, range from 75% to 42%. A CO_2 certificate price of 130€/t CO_2 (VRE_constr._CO_2_veryhigh) however, is sufficient to almost reach the VRE share of the reference scenario. Furthermore, this scenario is characterized by noticeable larger amounts of CCGT generation which is less CO_2 intensive. As expected, higher CO_2 prices foster the replacement of CO_2 intensive technologies with less CO_2 intensive generation capacities. In the calculations at hand, this is the case for lignite power plants, which are substituted by capacities of CCGT. Moreover, higher CO_2 prices increase the diffusion of VRE technologies. These effects also can be observed when analyzing each model region individually (see Fig. 38).

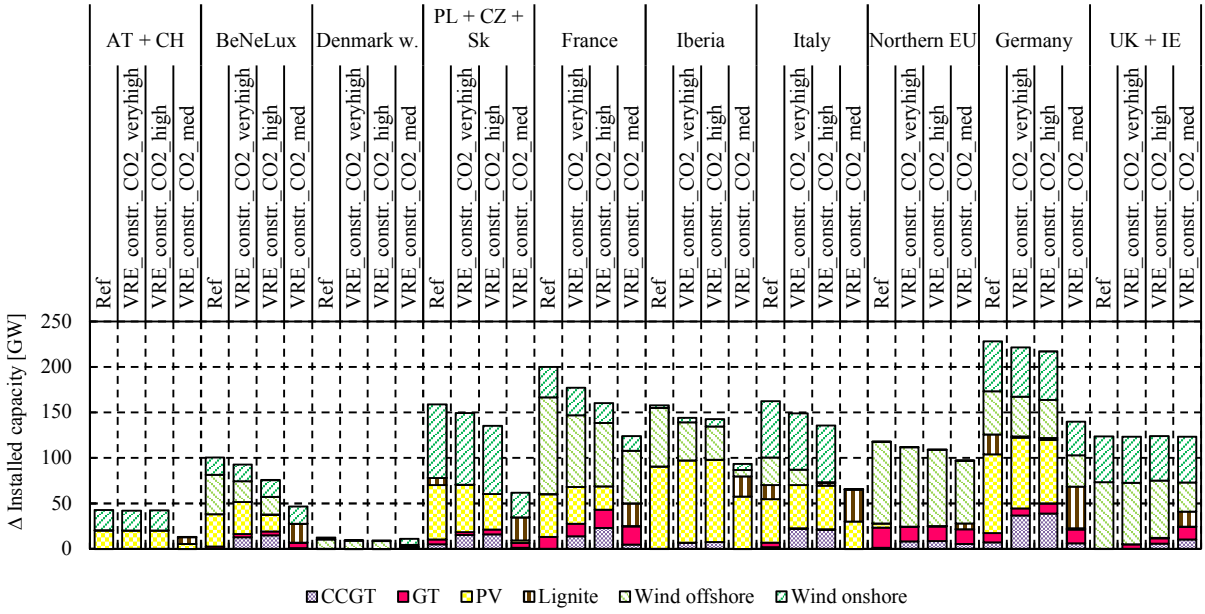

Fig. 38: Comparison of the capacity expansion. Differences are shown for each model region of the scenarios without 80%$_{constr}$ and different assumptions regarding the CO_2 certificate price to the reference scenario.

Fig. 39 shows the difference in annual electricity generation in the VRE constraint scenarios compared to the reference scenario for all VRE generation and storage technologies. More specifically, the annual electricity generation from storage refers to the discharged electricity over the observation year, and, opposed to the analyses in the main text, *not* to the storage unit capacity. The sensitivity analysis supports the findings from the main text, where generation from offshore wind correlates with the utilization H_2 storage, onshore wind with aCAES and partially Li-ion and PV mostly with Li-ion. Thereby, the distribution of annual electricity from storage follows the distribution of the annual electricity from VRE technologies.

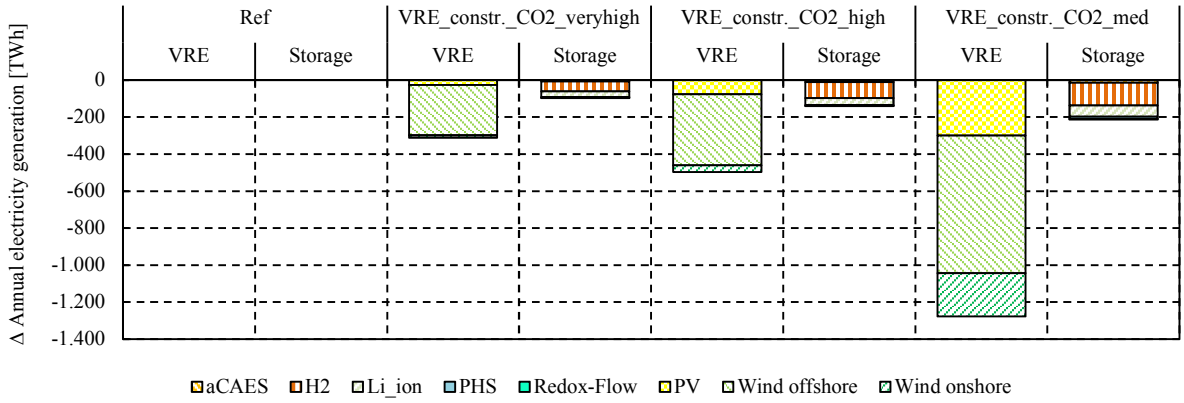

Fig. 39: Differences in annual power generation of VRE and storage. Deviations are shown compared to the reference scenario. Note that the annual electricity generation from storage refers the discharged electricity over the observation year.

Different temporal resolutions

In the course of this work, the influence of different temporal resolutions was analyzed. Therefore, the temporal resolution of the supply as well as the demand side was subsequently reduced from an hourly resolution in the reference scenario to a 2 h, 6 h, and 24 h resolution. Fig. 40 depicts the principal effects of aggregating in time on the dispatch of generation and storage technologies for one an exemplary day.

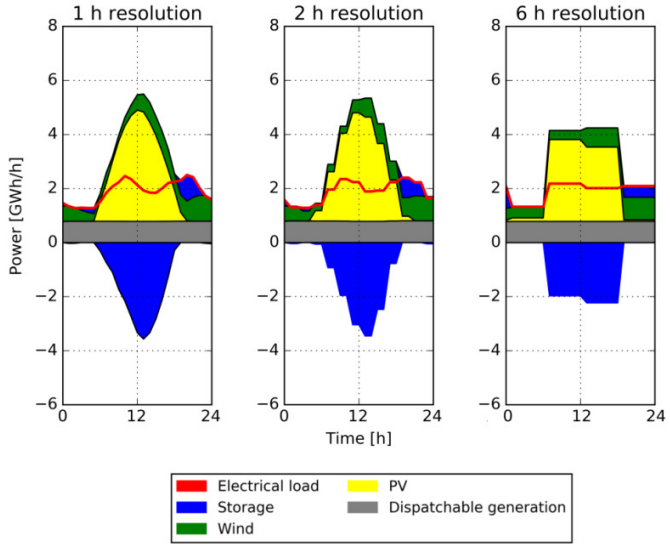

Fig. 40: Effects of lower temporal resolutions on the generation and storage dispatch. Storage charging is depicted negative, while storage discharging is shown positive.

The effects on the installed generation and storage capacities are shown in Fig. 41.

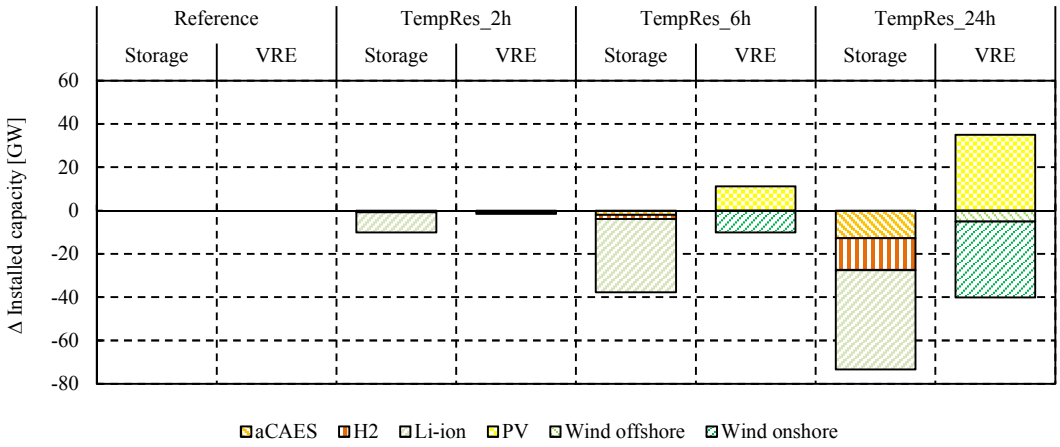

Fig. 41: Differences in installed capacity of VRE and storage technologies.

The results show that with decreasing temporal resolution the endogenously derived capacity of PV systems increases, substituting onshore and offshore systems, while the net capacity remains relatively stable over all scenarios. Naturally, a decrease in the temporal resolution leads to higher hourly power changes, i.e. discrete jumps in the generation. However, it also implies a more continuous dispatch of VRE technologies (see Fig. 40). As such power generation is, in practice, inherently volatile, the dispatch of these technologies is misrepresented. This is particularly the case for PV systems, which, in combination with their relatively low investment costs (compared to wind power), are then favored by the optimization.

Based on the findings from Sec. 6.3.3 (PV power correlates with Li-ion storage charging and hence its expansion) one would assume that the increase of PV capacities would go along with more expansion of Li-ion storage. However, this is not that case as the smoother generation profiles (i.e. continuous generation) of PV (but also for wind power systems) lowers the overall demand for storage. This effect is most pronounced for storage technologies with low power-related investment costs as the power gradients (i.e. ramps) decrease continuously with lower temporal resolutions.

In this regard—when analyzing aggregated results of large regions (e.g. Europe)—energy system models which rely on meteorological input data should at least use a temporal resolution below 6 h to appropriately represent the capacity expansion of VRE and storage technologies. However, if analyzing smaller model regions and emphasizing the dispatch of VRE systems and storage options, even 2 h resolutions can misrepresent the characteristic of the latter and, therefore, should rely on at least an hourly resolution (compare Haydt et al. [188]).

Weather year scenarios

The potential power generation of VRE is based on hourly values of wind speeds and solar irradiation of the year 2006 in the reference scenario. Within Sec. 6.3.3 of this study, it was shown that storage expansion and utilization is strongly dependent on the generation mix of a region as well as its temporal characteristics of power generation. As the latter again is influenced by the underlying weather year, the analysis tests to what extents other weather years influence VRE and storage capacity expansion. Fig. 42 shows the difference in installed capacity for the most relevant generation as well as storage technologies of the scenarios with different weather years compared to the reference scenario aggregated over all model regions. The results for the weather year 2010 are intentionally neglected, as it is characterized by unusual poor solar and wind potentials, resulting in unrealistically high storage expansion in some model regions in order to meet $80\%_{constr}$.

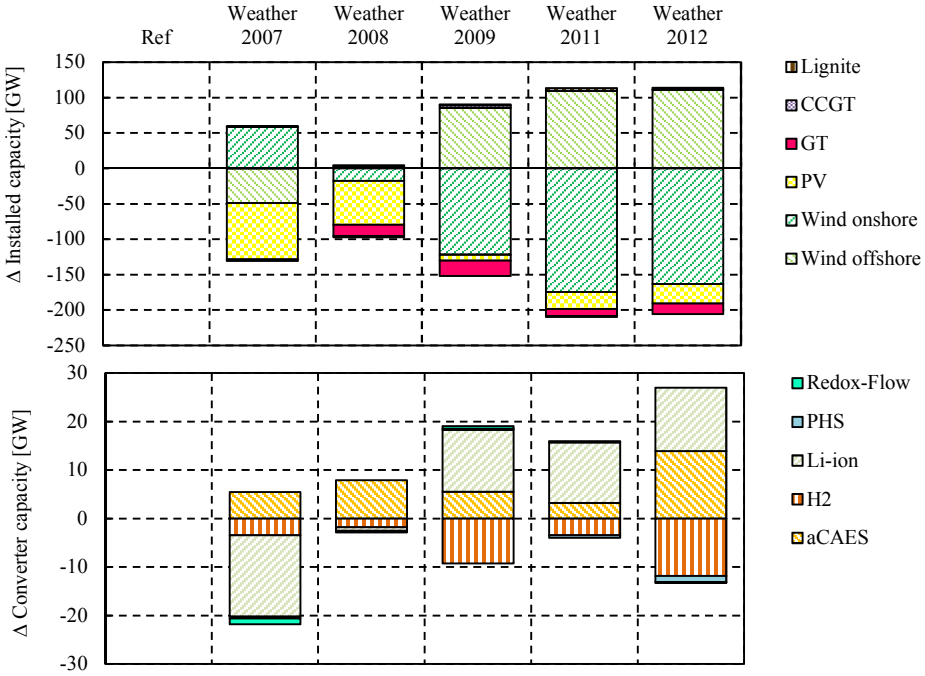

Fig. 42: Differences in installed generation and storage capacity. Deviations are shown compared to the reference scenario and aggregated over all model regions.

In relation to the overall installed capacities, the deviations of the installed capacities in the model runs with different weather years are rather small. However, the regional and technology-specific generation and storage portfolio is affected signifcantly. By this means, compared to the reference scenario, the installed PV capacity can differ by ±20% (±80 GW), onshore wind by +18% (+59 GW) or -53% (-175 GW), and offshore wind by +24% (+111 GW) or -11%

(-49 GW). Similar effects apply to the power generation. The most notable impact of the weather year on storage demand was observed for aCAES, resulting in an increased storage converter power up to 98% (+14 GW). For Li-ion storage converter power is affected as high as +24% (+13 GW) or -31% (-17 GW), and for H_2 storage up to ±14% (±12 GW).

Some of the sensitivity cases (e.g weather year 2007) support the findings of the main text, where, for example, the increase of onshore wind capacities goes along with higher capacities of aCAES storage. On the other hand, in the same year, PV capacities decrease which again fosters a decrease of Li-ion batteries. However, in the years 2009, 2011, and 2012 the increase of offshore wind capacities actually is complemented by more storage capacities of aCAES and Li-ion. As showed in Sec. 6.3.3, dual use of some storage technologies is common, where Li-ion not only balances daily fluctuations from PV power, but also stores surplus of wind electricity generation. This effect is particularly pronounced in regions with high shares of wind power generation.

Miscellaneous scenarios

Improved techno-economic input parameters for redox-flow batteries

Within the reference scenario, a lack of capacity expansion of redox-flow batteries is noticeable. As stated in Sec. 6.3.2, this presumably can be explained by the cost optimizing model logic, where redox-flow storage competes with aCAES for mid-term balancing. In comparison, both technologies show rather similar techno-economic parameters, differentiate however significantly in the energy-related investment costs (this includes the amortization time for the storage unit as well as the fixed operations and maintenance costs). On the one hand, these costs (€/kWh_{el}) are around twice as high for redox-flow batteries compared to aCAES, whereas the power-related costs (€/kW_{el}) are almost identical. On the other hand, charging and discharging efficiency slightly favors redox-flow batteries. Presumably large shares of aCAES can be substituted by redox-flow capacities if the energy-related investment costs decrease to the value of aCAES. To verify this hypothesis validation model runs with the aforementioned changes in the relevant parameters are performed. Fig. 43 shows the comparison of the storage converter capacity and generation expansion for each model region in the reference scenario (Ref) and scenario with changed techno-economic parameters for redox-flow batteries (Ref_VRF).

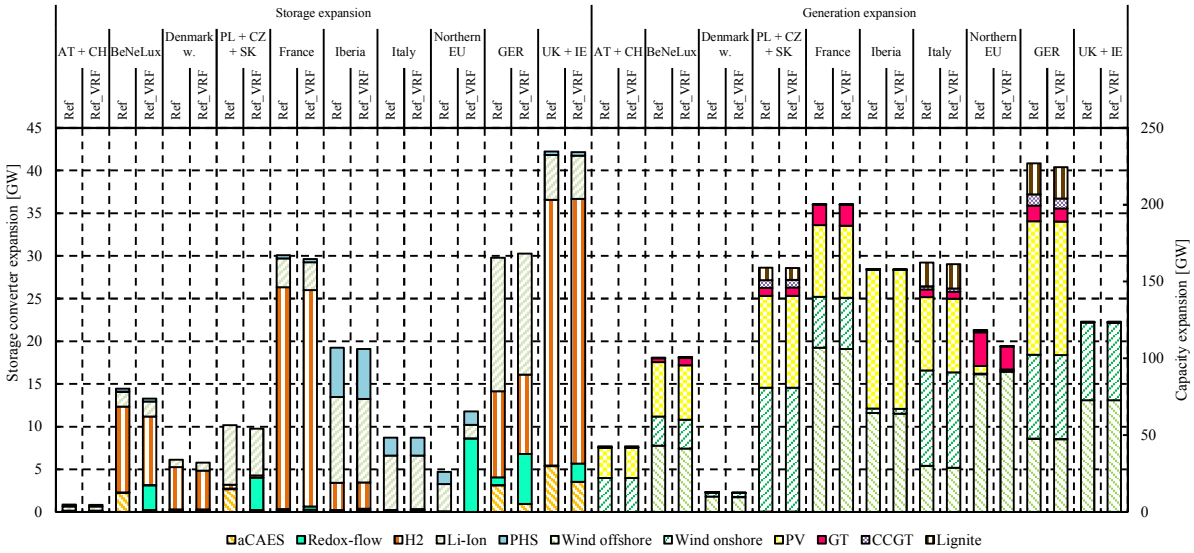

Fig. 43: Comparison of storage and generation capacity expansion. Scenario Ref_VRF is characterized by improved techno-economic parameters for the redox-flow batteries. The German model regions are aggregated to *GER*.

As expected, aCAES capacities are substituted in the relevant model regions (e.g. BeNeLux, Germany, or UK + IE), while the structure of the generation portfolio remains relatively unchanged in both scenarios. One exception can be found in the model region Northern Europe (Northern EU). As shown in Sec. 6.3.3, this region does not have any underground cavern storage available. In consequence, the balancing of the large shares of offshore wind electricity generation in the reference scenario is ensured via Li-ion batteries and GT capacities. In the scenario REF_VRF, the latter are partially substituted by redox-flow batteries. Furthermore, redox-flow storage allows an increase in offshore wind capacities, whereas capacities from PV systems disappear completely.

No existing stock capacities of PHS

In this scenario, no old capacities of PHS were assumed to exist in the observation year 2050. This sensitivity case aims to test whether the technical potentials of the storage unit are still reached. Sec. 6.3.2 showed that almost every model region (with an exception of AT + CH) completely uses the technical potential, as PHS is a very cost effective technology. Apart from the model region Austria + Switzerland, Tab. 18 shows that the storage unit capacity expansion for both scenarios is identical and the hypothesis is confirmed.

Tab. 18: Comparison of storage unit capacity expansion. The table shows the reference scenario and the scenario without old PHS capacities (PHS_w/o_old_stock).

Storage unit capacity expansion [GWh_{el}]		
	PHS_w/o_old_stock	Reference
Austria + Switzerland	32.00	9.51
BeNeLux	4.67	4.67
Denmark west	-	-
PL CZ SK	-	-
France	5.00	5.00
Iberia	93.00	93.00
Italy	35.00	35.00
Northern Europe	17.00	17.00
Germany	-	-
UK + IE	4.00	4.00

6.3.6 Discussion of sensitivity analysis results

The results of the sensitivity analysis show five major influence factors with regard to storage expansion. First, as expected, reduced storage investment costs (StorInv_low) lead to an increased storage expansion; similarly, higher storage costs reduce storage expansion compared to the reference run (StorInv_high).

Second, higher costs for VRE (VREInv_high) lead to reduced installed capacities of VRE and in consequence will foster higher storage capacities through reduced curtailments of VRE (in order to meet $80\%_{constr}$).

Third, more restrictive curtailment requirements (Cur.003) mainly lead to reduced curtailments of offshore wind generation. The wind power otherwise curtailed has to be stored in Cur.003. This results in increased H_2 storage capacities (as charging of these capacities correlates the most with offshore wind, see Sec. 6.3.3) in this scenario.

Forth, different weather years affect the regional and technology-specific generation and storage portfolio significantly. By this means, especially the capacities of onshore wind were affected by the choice of the weather year, resulting in variations by +18% (+59 GW) or -53% (-175 GW) and, thereby, also influencing the capacities of aCAES the most by up to 98% (+14 GW) of storage converter power.

Finally, it can be observed that the endogenously determined grid expansion (G+) is able to substitute large amounts of storage capacity. However, as also shown in other studies (see e.g. [152]), storage capacities are not completely interchangeable by transmission grid. In scenarios with high shares of VRE generation, grid expansion and storage are complementary flexibility

options. Furthermore, the sensitivity analysis shows that mostly H_2 storage capacities are substituted in the G+ scenarios. This effect can be attributed to the fact that in the reference case storage primarily integrates offshore wind power production which otherwise would have to be curtailed due to grid limitations.

The outcome of the sensitivity analysis supports the coherence of the optimization results and the underlying model assumptions. In comparison to the overall installed storage capacity in the reference scenario (166 GW, see Sec. 6.3.2) the variations shown in Fig. 29 are notable (for StorInv_low +32% and for G+ -39%). Other sensitivity cases, such as fuels or CO_2 emission certificate variations, only show minor effects. Moreover, the findings from Sec. 6.3 (spatial storage distribution and dispatch) remain robust over all scenarios.

6.3.7 Comparison to the state of research

It is difficult to compare results from this study with other estimates from the literature, as methodologies, as well as model and data assumptions, vary widely (see Sec. 2.1 and Sec. 2.2). The endogenously derived storage capacities aggregated over all model regions (166 GW, 30 TWh) are in line with some studies (I), while others result in significantly lower (II), or higher (III) storage capacities.

(I) Scholz et al. [190] assume similar model regions and quantify storage converter power expansion for various theoretical (before curtailment) VRE shares and PV-to-wind-ratios, including endogenously derived transmission grid capacities. Their results, therefore, were compared to scenario G+. The latter is characterized by a theoretical VRE share of 87% and a storage converter power (endogenously expansion, no stock capacities) of 87 GW. As expected—since the calculations are also based on the REMix model—the authors derive rather similar values for storage converter power; 93 GW in a 100% VRE share scenario and 58 GW in a 80% VRE share scenario, both assuming PV-to-wind-ratios of 0.25.

(II) Though analyzing a larger observation area (EU27), the cost minimizing model of Bertsch et al. [145] derives less storage converter power (68 GW, scenario B: high CO_2 prices), which mainly can be explained by the lower VRE share of 75%.

(III) The analysis of Bussar et al. [164] results in 1,060 GW of storage converter power, including PHS, battery systems, and the capacity of CCGT for the reconversion of H_2 (excluding the electrolyzer capacity). Again, it has to be stressed that comparability is limited, as this publication assumes a 100% VRE share and analyzes a larger observation area, which, compared to this study, additionally includes East and South-East Europe, Turkey, North Africa, and the

Middle East. Furthermore, the model assumes that at least 80% of each country's electricity demand is supplied by national resources. This assumption limits long-range load and generation balancing and thus increases the demand for required storage capacity.

6.3.8 Limitations and outlook

Subsequently, it is discussed whether some aspects of the chosen methodology and the assumptions might influence the derived storage demand.

First, the results of the sensitivity analysis already indicate that grid expansion limits the demand for storage (see Fig. 33). Including more flexibility options (e.g. demand side management) and incorporating the coupling to other energy-related sectors (e.g. heating, cooling, and transportation) is likely to decrease the demand for electricity storage (see e.g. [146]).

Second, the proposed method solely includes the high voltage transmission grid and in consequence neglects distribution grid restrictions within the defined model regions ("copper plates"). Thus, additional storage demand on distribution grid level is not taken into account in the model. This issue is somewhat compensated by using a high number of model regions which reduces the size of each "copper plate". However, the uneven disaggregation of countries into model regions (e.g. 20 German model regions compared to one model region for France) might lead to over or underestimation of grid restrictions and thereby affects storage demand. In the light of existing research, the influence of distribution grids and spatial resolution has not yet been analyzed for European long-term energy scenarios.

Third, it is likely that the modeling methodology for fossil-fired power plants leads to an underestimation of the required storage capacity as the power plants are modeled as unrealistically flexible. To at last partially take into account this problem, wear and tear costs for power change (€/kW_{el}, see Tab. C 4) of the cost calculations in the model are included. Nevertheless, the approach still neglects other flexibility related technical constraints, such as ramping rates, part-load behavior, or minimum idle times (opposed to mixed-integer (MIP) approaches). However, due to the model constraint of at least 80% VRE electricity generation, the relative impact of fossil-fired power plants is low. Storage demand and utilization in combination with detailed (MIP) fossil-fired power plant modeling has been addressed in Denholm et al. [147], Brouwer et al. [148], and Stoll et al. [149]. However, all three studies use exogenous scenario capacities as input. Therefore, the issue of over-estimating the flexibility of conventional power plants has been addressed in Sec. 5 showing that for energy scenarios with

high shares of VRE power generation and in large observation area (as for Europe), simplified LP modeling approaches are sufficient.

To answer the question of "optimal" spatial distribution of storage capacity, the simultaneous endogenous capacity expansion and dispatch optimization for generation technologies and flexibility options using a high level of temporal, spatial, and technological resolution is a novelty. Despite the aforementioned limitations, the analysis, therefore, is an adequate remedy to answer the research question.

6.4 Summary and conclusions

The linear cost minimizing optimization model REMix was applied, which endogenously determines the installed capacities and dispatch of all power generation and storage capacities in a system with at least 80% power production from variable renewable energies (VRE). The analysis region comprises of northern, western, south, southwest, and central Europe. Furthermore, the spatial distribution of those storage capacities and their dispatch was investigated in detail.

The model calculates a large expansion of offshore wind, followed by onshore wind, and PV capacities in the analysis area in order to meet the boundary condition. Moreover, distinctive generation portfolios for different model regions were observed. This allows categorizing the model regions into offshore/onshore wind and PV regions (e.g. France: offshore, PL + CZ + SK: onshore, and Iberia: PV, respectively).

Storage converter power is mainly provided H_2 and Li-ion batteries. While the expansion of these two technologies occurs in many model regions, aCAES and PHS can play a role for certain regions with higher shares of mid-term fluctuations through onshore wind (and the necessary storage potentials). In this regard, PHS expansion occurred in almost all model regions. In regions with limited technical potentials, PHS as mid-term balancing option is substituted by aCAES. In this analysis, redox-flow batteries only play an insignificant role for power balancing, mainly due to the more favorable techno-economic parameters of Li-ion batteries and aCAES.

From this analysis it can be concluded that the spatial distribution of storage capacity expansion is mainly influenced by two factors; model-based quantifications, therefore, should carefully consider these aspects in their assumptions:

First, the temporal characteristics of the VRE electricity generation heavily influence the expansion of H_2, Li-ion, aCAES, and PHS storage technologies. In general, surpluses from VRE generation, i.e. negative net loads, highly correlate with storage charging in all model regions.

Second, electricity generation from specific VRE technologies is complemented by the expansion of certain storage technologies. More precisely, high correlations between the generation of offshore wind and H_2 charging, onshore wind and H_2 as well as aCAES, and, finally, between PV generation and Li-ion charging were observed. These correlation coefficients can partly be explained by the energy-to-power-investment-ratio (€/kW_{el} to €/kWh_{el}) of each storage technology. Low energy-related investment costs favor capacity expansion of long-term storage, while low power-related investment costs will preferably result in power balancing storage technologies (e.g. Li-ion).

The results further show limited technical potentials (with respect to storage unit capacity in GWh_{el}) of one technology has an influence on the local, region-specific allocation of other storage technologies. In particular, limited technical potentials for PHS can be substituted by aCAES and stationary Li-ion batteries, if necessary.

For storage utilization, the results show typical dispatch patterns of different storage technologies: while Li-ion batteries in PV dominated regions (e.g. Iberia) generally cycle daily, onshore wind regions (e.g. PL + CZ + SK) are characterized by mid-term balancing of aCAES with typical cycle lengths of 3–5 days. In contrast, H_2 storage shows a more seasonal behavior with typical cycle lengths around 45 days. The results show that H_2, PHS, and aCAES have similar dispatch patterns in all model regions. The utilization of Li-ion storage, however, depends on the generation share of wind and PV generation. In regions with high shares of wind, a dual use of Li-ion batteries was observed, where this technology not only balances the daily fluctuation of PV feed-in but additionally was used to level the more diurnal and seasonal volatile generation from wind power.

7 Conclusions

7.1 Summary

This thesis assesses the required storage capacity in scenarios with high shares of renewable power generation in Europe. Naturally, such long-term energy scenarios are inherently associated with a wide range of uncertainties and this analysis, therefore, studies (I) the *robustness of calculated storage demand* against parametric as well as methodological assumptions and, moreover, discusses (II) *drivers of spatial storage capacity distribution* in a comprehensive model-based approach[25].

The analysis relies on the linear optimization energy system model REMix. In the course of this work, the model was parametrized for a European power system for the year 2050. Opposed to studies with a similar focus, this work is based on a high spatial (29 model regions) and temporal resolution (hourly), and, in particular, incorporates an integral optimization of capacity dispatch and expansion of generation technologies as well as flexibility options (*co-optimization*). This approach enables an in-depth analysis of drivers for the spatial distribution of storage capacity and, in addition, allows for a better understanding of the inter-dependencies of different flexibility options (*synergy* or *complementarity* of flexibility options).

(I) The robustness of the demand for electrical energy storage was tested against a wide range of parameter variations (*parametric uncertainty*) and the influence of methodological assumptions (*methodological uncertainty*). The former was tackled through different costs scenarios for investments into storage, renewable energy technologies, and transmission grid expansion, variations of fuel and CO_2 emissions certificate costs, and different weather years as the basis for the calculation of power generation from variable, renewable energy sources. Methodological uncertainty was included with regard to different temporal, spatial, and technological resolutions. The latter was discussed in more detail for two modeling approaches for thermal power plants and their effects on storage expansion and utilization. In this regard, REMix was enhanced by a mixed-integer modeling methodology for thermal power plants based

[25] At this point, the author stresses again that it is not intended to forecast future energy systems or transformation pathways, but to investigate inter-dependencies of model assumptions as well as to test the dynamics of energy systems by comparing a variety of scenarios.

on the work of Fichter [150]. Furthermore, REMix was extended by the ability to consider different ways of curtailments of renewable power generation (unlimited versus restricted).

(II) To analyze the drivers of the spatial distribution of storage capacity, an extensive scenarios analysis for the European observation area was performed, incorporating correlation analyses which compare the storage dispatch with the utilization of renewable generation technologies.

Several conclusions were derived and are subsequently summarized with regard to the two main research goals (I, II).

7.1.1 Robustness of storage demand

Parametric uncertainty

In the context of parametric uncertainty, particularly the assumptions for the overnight investments costs for renewable generation and storage technologies are striking. On the one hand, a cost reduction of the latter by 50% (energy and power-related costs) increases the overall storage converter power by 32% (+66 GW) and the storage unit capacity by 79% (+24 TWh, mainly caused by H_2 storage). On the other hand, increased costs lead to a reduction of 21% (-43 GW) for converter power and of 27% (-8 TWh) for the storage unit capacity. Similar effects occur in scenarios where the investment costs of variable renewable energy systems (VRE) were varied, since strong correlations between the VRE power generation and storage charging exists (see Sec. 6.3.3). In this sense, an increase of model endogenously derived storage capacities enables to compensate lower VRE capacities (caused by the higher costs) through an improved utilization in terms of full load hours and, hence, reduced curtailments. Lower VRE capacities cannot be substituted by a higher utilization of thermal power plants, as a model constraint forces a VRE generation share of at least 80% over Europe. Thereby, an increase of the VRE costs by 50% leads to an increase of converter power by 14% (+29 GW) and of storage unit capacity by 25% (+8 TWh), while a decrease of the VRE costs causes a reduction of storage power by 19% (-39 GW) and 27% (-8 TWh) for the storage unit.

In contrast, parameter variations of fuel costs and CO_2 certificate prices show little to no effect on the storage and generation capacity portfolio. The latter is affected by low fuel costs in terms of a substitution of lignite-fired power plants (-45 GW) by combined cycle gas turbines (+50 GW), which, in turn, only have a marginal influence on storage expansion. A structural similar effect, but less pronounced, can be observed for scenarios with increased CO_2 prices. The

relatively small influence of these sensitivity cases can be addressed to the relatively small generation share of thermal power plants, owing to the model constraint of 80% VRE generation. It is likely that energy scenario analyses which focus on transition pathways[25] are more sensitive to fuel cost and CO_2 price assumptions since they typically rely on methods of myopic or path optimization, which are able to capture technology lock-in's as they consider multiple years (opposed to this study, which relies on one static year[26])

Methodological uncertainty

Methodological uncertainty was studied with regard to various technological (a), temporal (b), and spatial resolutions (c) as well as more general assumptions like the influence of the choice of weather year (d).

(a) The influence of different technological resolutions was tackled by analyzing the dependencies of storage expansion and utilization reliant on the power plant modeling approach—i.e. a comparison between simplified merit order (LP) and detailed unit-commitment with economic dispatch (MILP)—and different methods to consider curtailments of VRE power generation (unlimited versus restricted).

In a nutshell: to appropriately model power plants for storage demand quantifications, one has to consider the VRE penetration level as well as the size of a power system (in terms of modeled thermal generator units). While larger observation areas (e.g. Europe) with high VRE shares do not necessarily require MILP modeling—in other word the derivation of storage expansion and utilization relative to the LP approach is marginal—smaller model region in combination with lower VRE penetration levels can greatly benefit from the higher detail of MILP methods. More specifically, MILP modeling in energy systems with a theoretical VRE share of 33% results in a 73% higher storage converter capacity expansion than its LP counterpart. In contrast, in scenarios with a high theoretical VRE share (100%), the difference between LP and MILP is only 9% for the storage converter power. By this means, for modeling storage demand for large observation areas and under the premises of high shares of VRE power generation, as presented in chapter 5, less detailed power plant modeling based on LP is sufficient.

Scenarios with restricted curtailments (10% and 3% in relation to the annual VRE power generation) were observed to have minor effects on the storage capacity mix on an overall

[26] For the purpose of this study (see footnote 25), the static single year analysis is a valid assumption as discussed in Sec. 2.3.2.

European perspective. If limited to 10%, changes of the storage capacity basically do not occur as the average curtailment share over all model regions in reference scenario is already below this value (5%, see Fig. 29). More restrictive curtailment limits (3%) increase the demand for storage converter power by 9% (+18 GW) and for the storage unit capacity by only 4% (+1 TWh) on the European average, as, especially curtailed wind power generation has to be compensated. When analyzing specific model regions, however, curtailment limits of 3% can have a notable influence on the local storage capacity as well as on the generation portfolio. In the case of the model region Northern Europe more rigid curtailments restrictions, for example, lead to a shift in the generation mix where offshore wind is replaced by PV systems (-16 GW offshore wind, +24 GW PV), thus increasing the demand for stationary lithium-ion batteries by 9 GW/22 GWh.

(b) A high temporal resolution was found to be of particular importance when emphasizing the utilization of storage and VRE technologies. If the focus lies on the installed capacities of a larger observation area, such as Europe, a temporal resolution of at least 2 h should be chosen. Otherwise, for example in case of a 6 h resolution, results show a 22% lower demand for storage converter power (-37 GW) and almost 50% lower (-81 GW) when modeling with a daily resolution. Moreover, a low temporal resolution especially misrepresents the demand for lithium-ion storage as high generation fluctuations are smoothened and lessen the demand for short-term storage which provides balancing of high powers at low costs.

(c) An adequate spatial resolution was found to be of special importance. The initial 29 region reference case with an exogenous transmission grid based on the Ten Year Network Development Plan [182] was compared to a scenario where all model regions were aggregated to a single model region. In such extreme case, no transmission grid restrictions are present (“copper plate”) and, thereby, allowing a quantification of the maximum potential of spatial balancing. Moreover, the scenario represents a lower bound for storage demand, as the potential for spatial balancing is fully exploited. More specifically, the copper plate scenario is characterized by 32% less storage converter power (-65 GW) and around half of the storage unit capacity (16 TWh) compared to the reference scenario. Reducing grid congestions mainly enables a better integration of offshore wind generation, connecting sites with good resource potentials (e.g. UK, France) with the demand centers (e.g. Germany), consequently reducing the demand for long-term storage (H_2).

This effect was further validated through more realistic grid expansion scenarios. More specifically, model endogenous grid expansion was possible in terms of increasing the AC and DC capacities of the reference grid. Even in scenarios where the line-specific investment costs

were further increased (doubled compared to the initial grid expansion scenario), endogenously derived grid expansion still substituted 24% of the storage converter power (-50 GW) and almost the identical amount of storage unit capacity as in the copper plate scenario (-16 TWh) compared to the reference scenario with pre-defined (exogenous) transmission grid.

Although it was found that reducing transmission grid congestions can lower the demand for storage capacity significantly, the analysis also showed that—even in the most optimistic grid scenario—around 120 GW of storage converter power and 13 TWh of storage unit capacity is still required for temporal balancing. In this sense, and, in the line with the findings from other studies (see [151, 152, 164]), grid expansion and storage are mostly not competing, but complementing flexibility options, both essential for future energy systems with high shares of VRE power generation.

(d) The weather year determines the power generation from PV, onshore, and offshore wind systems through the underlying wind speed and solar irradiation. Thereby, its choice can have a major impact on the derived full load hours of VRE systems, and, in consequence, influences their endogenous capacity expansion. Finally, this also determines storage expansion and utilization as a strong correlation between power generation from certain technologies and charging of certain storage options exists (see Sec. 7.1.2). Naturally—owing to the 80% VRE constraint—the overall installed VRE capacity, as well as its overall annual generation, is not affected significantly by the different weather years, in contrast to the technology-specific installed capacities and power generation of PV, onshore, and offshore wind, which differs considerably in each weather year scenario. By this means, compared to the reference scenario, the installed PV capacity can differ by ±20% (±80 GW), onshore wind by +18% (+59 GW) or -53% (-175 GW), and offshore wind by +24% (+111 GW) or -11% (-49 GW). Similar effects apply to the power generation. The most notable impact of the weather year on storage demand was observed for adiabatic compressed air storage (aCAES), resulting in an increased storage converter power up to 98% (+14 GW). For lithium-ion storage the converter power is affected as high as +24% (+13 GW) or -31% (-17 GW), and for hydrogen storage (H_2) up to ±14% (±12 GW). Storage capacities of redox-flow batteries and pumped hydro storage were only affected marginally.

7.1.2 Drivers of spatial storage capacity distribution

The spatial capacity distribution of storage is directly linked to the model-region-specific capacity expansion limits of the storage unit[27] (e.g. potentials for water reservoirs for PHS or underground salt caverns for H_2 and aCAES). Furthermore, limited technical potentials of one technology has an influence on the local, region-specific allocation of other storage technologies. Particularly, if potentials for PHS are restricted, this storage demand can be substituted by aCAES or stationary lithium-ion batteries, if necessary.

Moreover, the results show that charging of storage heavily correlates with negative net loads, or, in other word, electricity over-production from VRE sources. Thereby, the spatial storage capacity distribution is also implicitly influenced by the regional VRE resource potentials in terms of utilization and expansion limits.

Finally, electricity generation from specific VRE technologies is complemented by the expansion of certain storage technologies. By this means, high correlation coefficients between the generation of offshore wind and H_2 charging, onshore wind and H_2 as well as aCAES, and between PV generation and lithium-ion charging were obtained. These correlation coefficients can be explained by the energy-to-power-investment-ratio (€/kW_{el} to €/kWh_{el}) of each storage technology. Low energy-related investment costs favor capacity expansion of long-term storage, while low power-related investment costs will preferably result in short-term, power balancing storage technologies (e.g. lithium-ion).

7.2 Limitations and future research

Models and their assumptions have always been simplifications of the real world and abstractions at a certain level are required. Fostered by the bottleneck of calculation times, model reduction techniques have been essential since the beginning of computer-aided numerical simulations. Depending on the research question, a modeling approach might prioritize a high temporal resolution while neglecting other aspects, such as the technological degree of detail. Frew [153] describes such tradeoffs as the "high-level paradigm of power system modeling levers" which are subject to a conflict area of the research question, computing times, and the required solution accuracy. In this sense, limitations of the presented methodology are manifold[28]

[27] The storage converter power (e.g. pump or turbine capacity of a PHS) is not limited.

[28] The specific short-comings of each scenario analysis (see chapter 5 and chapter 6) have been discussed in the corresponding conclusions (see Sec. 5.4 and Sec. 6.3.8). This section provides a broader perspective on the general limitations of the chosen methodology.

and, for example, exist with respect to the uncertainties of the model input parameters and computing times. The former is addressed by an extensive scenario and sensitivity analysis (see Sec. 6.3.5); the latter through spatial aggregation, or simplifications in technology representations.

Furthermore, criticism on scenario techniques and the interpretation of their results, as well as the underlying modeling approaches (e.g. optimizations) has been raised, for example by Betz [154] or Trutnevyte [155]. The latter points out that quantitative scenarios—e.g. based on optimizations—particularly seem to miss disruptive events in the development of energy systems (compared qualitative methods), supposedly owing to constrained formulations of such models [156, 157]. This claim has been validated in a case study for the UK energy system by Trutnevyte [158], discussing the question whether cost minimizing approaches can approximate historic developments in energy systems. She concludes that cost optimization is likely to misrepresent historic developments and suggests to include near-optimal solutions as possible developments. With respect to this thesis, however, this criticism applies only partially as the main research goal was to highlight dependencies of assumptions on results, not to model energy transition pathways or policy scenarios[25].

Naturally, limitations also exist with regard to the technological (a), temporal (b), and spatial (c) resolution of a model and future research can always improve in this sense. Additionally, more general shortcomings (d) of the methodology are discussed subsequently.

(a) The flexibility options considered in this study are comprised of electrical energy storage, the transmission grid, curtailments, and dispatchable generation technologies. The analysis does not cover flexibility provided by demand response measures or options that arise from coupling the power system with other sectors (e.g. heat or transportation), thus possibly overestimating the demand for electrical energy storage.

Furthermore, storage was modeled in a simplified way, assuming the same fundamental principle for each technology, based on available expansion potentials, investment and operating cost assumptions, as well as charging and discharging efficiencies. Technology-specific characteristics—e.g. power limits or cycle stability—were neglected. However, such details might have an influence, as for example shown in cases of storage utilization for price arbitrage by Skati et al. [159] or Wankmüller et al.[160].

(b) Higher temporal resolutions might be desirable to capture sub-hourly ramps of VRE power generation which can be of particular interest in order to capture storage requirements and benefits for ancillary services.

(c) A higher spatial resolution is helpful to model region-specific effects of VRE power generation as well as grid congestions in more detail and their effects on flexibility demand.

Moreover, to consider PV self-generation in combination with distributed storage—which's penetration is likely to increase—a higher spatial resolution might be desirable for storage demand quantifications in order to consider distribution grids.

Future research should also emphasize on the influence of spatial aggregating of certain regions to model regions. In this study, only two extreme cases (29 model regions vs. one model region) were considered to illustrate the influence on the bandwidths of storage demand.

(d) Future model enhancements should focus on the implementation of further optimization criteria's (*multi-objective optimization*) to capture other relevant aspects (apart from the cost criterion) for sustainable energy usage, such as social acceptance, land-use, or resource demand [161]. The latter, for example, has been discussed by Berrill et al. [162]. However, the study relies on an ex-post analysis which does not consider dynamic feedback loops of resource demand on the cost and capacity mix of the power system.

For analyses which focus on transition pathways of energy scenarios, the methodology could be extended by path, myopic, or rolling horizon optimization approaches.

Finally, to this point, the deterministic nature of the modeling methods in REMix also prevents to capture the variability of PV and wind power. Here, stochastic approaches seem promising, where distinct data points are linked to a possibility space [163], illustrating their associated uncertainty.

Bibliography

Publications resulting from this work

F. Cebulla and T. Fichter, "Merit order or unit-commitment: How does thermal power plant modeling affect storage demand in energy system models?," *Renewable Energy*, vol. 105, pp. 117–132, 2017.

F. Cebulla, T. Naegler, and M. Pohl, "Electrical energy storage in highly renewable European energy systems: Capacity requirements, spatial distribution, and storage dispatch," *Journal of Energy Storage*, vol. 14, pp. 211–223, 2017.

F. Cebulla, J. Haas , J. Eichman, W. Nowak, and P. Mancarella, "How much electrical energy storage do we need? A synthesis for the U.S., Europe, and Germany," *Journal of Cleaner Production*, 2018, vol. 181, pp. 449–459, 2018.

F. Cebulla, "Stromspeicherbedarf in europäischen Langfristszenarien– Eine Analyse des Einflusses unterschiedlicher energiewirtschaftlicher Rahmenbedingungen," in *VDI Optimierung in der Energiewirtschaft*, 2015.

F. Cebulla, "Future storage demand under high uncertainties– a model-based sensitivity analysis," in *9th International Renewable Energy Storage Conference*, 2015.

J. Haas, F. Cebulla, K. Cao, W. Nowak, R. Palma-Behnke, C. Rahmann, and P. Mancarella, "Challenges and trends of energy storage expansion planning for flexibility provision in low-carbon power systems – a review," *Renewable and Sustainable Energy Reviews*, vol. 80, pp. 603–619, 2017.

K.-K. Cao, F. Cebulla, J. J. G. Vilchez, B. Mousavi, and S. Prehofer, "Raising awareness in model-based energy scenario studies—a transparency checklist," Energy, *Sustainability and Society*, vol. 6, 2016.

Literature

[1] IPCC, *Climate change 2013: The physical science basis: Working Group I contribution to the Fifth assessment report of the Intergovernmental Panel on Climate Change*. Cambridge University Press, 2014.

[2] IPCC, *Climate change 2014: Synthesis Report. Contribution of Working Groups I, II and III to the Fifth Assessment Report of the Intergovernmental Panel on Climate Change*. Cambridge University Press, 2014.

[3] N. H. Stern, *The economics of climate change: the Stern review*. Cambridge University Press, 2007.

[4] IPCC, *Climate change 2014: Mitigation of climate change*, vol. 3. Cambridge University Press, 2015.

[5] M. Lenzen, "Life cycle energy and greenhouse gas emissions of nuclear energy: A review," *Energy Conversion and Management*, vol. 49, no. 8, pp. 2178–2199, 2008.

[6] B. K. Sovacool, "Valuing the greenhouse gas emissions from nuclear power: A critical survey," *Energy Policy*, vol. 36, no. 8, pp. 2950–2963, 2008.

[7] M. Z. Jacobson, "Review of solutions to global warming, air pollution, and energy security," *Energy & Environmental Science*, vol. 2, no. 2, pp. 148–173, 2009.

[8] R. Turconi, A. Boldrin, and T. Astrup, "Life cycle assessment (LCA) of electricity generation technologies: Overview, comparability and limitations," *Renewable and Sustainable Energy Reviews*, vol. 28, pp. 555–565, 2013.

[9] S. Shafiee and E. Topal, "When will fossil fuel reserves be diminished?," *Energy Policy*, vol. 37, no. 1, pp. 181–189, 2009.

[10] H.-H. Rogner, R. F. Aguilera, C. Archer, R. Bertani, S. C. Bhattacharya, M. B. Dusseault, L. Gagnon, H. Haberl, M. Hoogwijk, A. Johnson, M. L. Rogner, H. Wagner, and V. Yakushev, "Global Energy Assessment - Toward a Sustainable Future," Cambridge, UK and New York, NY, USA and the International Institute for Applied Systems Analysis, Laxenburg, Austria: Cambridge University Press, 2012, pp. 423–512.

[11] C. Breyer and A. Gerlach, "Global overview on grid-parity," *Progress in Photovoltaics: Research and Applications*, vol. 21, no. 1, pp. 121–136, 2013.

[12] C. Candelise, M. Winskel, and R. J. K. Gross, "The dynamics of solar PV costs and prices as a challenge for technology forecasting," *Renewable and Sustainable Energy Reviews*, vol. 26, pp. 96–107, 2013.

[13] N. S. Lewis, “Research opportunities to advance solar energy utilization,” *Science*, vol. 351, no. 6271, 2016.

[14] M. A. Green, “Commercial progress and challenges for photovoltaics,” *Nature Energy*, vol. 1, no. 1, p. 15015, 2016.

[15] M. I. Blanco, “The economics of wind energy,” *Renewable and Sustainable Energy Reviews*, vol. 13, no. 6–7, pp. 1372–1382, 2009.

[16] M. Z. Jacobson and G. M. Masters, “Exploiting Wind Versus Coal,” *Science*, vol. 293, no. 5534, pp. 1438–1438, 2001.

[17] M. Taylor, K. Daniel, A. Ilas, and E. Y. So, “Renewable Power Generation Costs in 2014,” International Renewable Energy Agency (IRENA), 2015.

[18] A. Whiteman, T. Rinke, J. Esparrago, and S. Elsayed, “Renewable Capacity Statistics 2016,” International Renewable Energy Agency (IRENA), 2016.

[19] International Energy Agency (IEA), “World Energy Outlook 2015,” OECD Publishing, 2015.

[20] R. Ferroukhi, J. Sawin, F. Sverisson, H. Wuester, G. Kieffer, D. Nagpal, D. Hawila, A. Khalid, D. Saygin, and S. Vinci, “REthinking Energy 2017,” International Renewable Energy Agency (IRENA), 2017.

[21] J. Haas, F. Cebulla, K. Cao, W. Nowak, R. Palma-Behnke, C. Rahmann, and P. Mancarella, “Challenges and trends of energy storage expansion planning for flexibility provision in low-carbon power systems – a review,” *Renewable and Sustainable Energy Reviews*, vol. 80, pp. 603–619, 2017.

[22] F. Cebulla and T. Fichter, “Merit order or unit-commitment: How does thermal power plant modeling affect storage demand in energy system models?,” *Renewable Energy*, vol. 105, pp. 117–132, 2017.

[23] F. Cebulla, T. Naegler, and M. Pohl, “Electrical energy storage in highly renewable European energy systems: Capacity requirements, spatial distribution, and storage dispatch,” *Journal of Energy Storage*, vol. 14, pp. 211–223, 2017.

[24] D. Dallinger, G. Schubert, and M. Wietschel, “Integration of intermittent renewable power supply using grid-connected vehicles – A 2030 case study for California and Germany,” *Applied Energy*, vol. 104, pp. 666–682, 2013.

[25] D. Dallinger, “Plug-in electric vehicles Integrating fluctuating renewable electricity,” PhD dissertation, University of Kassel, 2012.

[26] R. Verzijlbergh, C. B. Martínez-Anido, Z. Lukszo, and L. de Vries, "Does controlled electric vehicle charging substitute cross-border transmission capacity?," *Applied Energy*, vol. 120, pp. 169–180, 2014.

[27] C. Krüger, M. Buddeke, F. Merten, and A. Nebel, "Modelling the interdependencies of storage, DSM and grid-extension for Europe," in *12th International Conference on the European Energy Market (EEM), 2015*, 2015, pp. 1–5.

[28] LEAP, *https://www.energycommunity.org*.

[29] S. Babrowski, T. Heffels, P. Jochem, and W. Fichtner, "Reducing computing time of energy system models by a myopic approach," *Energy Systems*, pp. 1–19, 2013.

[30] I. Keppo and M. Strubegger, "Short term decisions for long term problems - The effect of foresight on model based energy systems analysis," *Energy*, vol. 35, no. 5, pp. 2033–2042, 2010.

[31] S. Ludig, M. Haller, E. Schmid, and N. Bauer, "Fluctuating renewables in a long-term climate change mitigation strategy," *Energy*, vol. 36, no. 11, pp. 6674–6685, 2011.

[32] M. Nicolosi, A. Mills, and R. Wiser, "The importance of high temporal resolution in modeling renewable energy penetration scenarios," Lawrence Berkeley National Laboratory, 2011.

[33] D. Shi and D. J. Tylavsky, "A Novel Bus-Aggregation-Based Structure-Preserving Power System Equivalent," *IEEE Transactions on Power Systems*, vol. 30, no. 4, pp. 1977–1986, 2015.

[34] D. Shawhan, J. Taber, R. Zimmerman, J. Yan, C. Marquet, W. Schulze, R. Schuler, R. Thomas, D. Tylavsky, D. Shi, and others, "A Detailed Power System Planning Model: Estimating the Long-Run Impact of Carbon-Reducing Policies," in *System Sciences (HICSS), 2015 48th Hawaii International Conference on*, 2015, pp. 2497–2506.

[35] B. A. Corcoran, N. Jenkins, and M. Z. Jacobson, "Effects of aggregating electric load in the United States," *Energy Policy*, vol. 46, pp. 399–416, 2012.

[36] J. Metzdorf, "Development and implementation of a spatial clustering approach using a transmission grid energy system model," Master's thesis, University of Stuttgart, 2016.

[37] F. D. Munoz, E. E. Sauma, and B. F. Hobbs, "Approximations in power transmission planning: implications for the cost and performance of renewable portfolio standards," *Journal of Regulatory Economics*, vol. 43, no. 3, pp. 305–338, 2013.

[38] O. Koskinen and C. Breyer, "Energy Storage in Global and Transcontinental Energy Scenarios: A Critical Review," *Energy Procedia*, vol. 99, pp. 53–63, 2016.

[39] B. Droste-Franke, M. Carrier, M. Kaiser, M. Schreurs, C. Weber, and T. Ziesemer, *Improving Energy Decisions Towards Better Scientific Policy Advice for a Safe and Secure Future Energy System*. European Academy of Technology and Innovation Assessment, 2014.

[40] F. Cebulla, J. Haas, J. Eichman, W. Nowak, and P. Mancarella, "How much Electrical Energy Storage do we need? A synthesis for the U.S., Europe, and Germany," *Journal of Cleaner Production*, 2017, under review.

[41] E-mail communication with J. Bertsch by F. Cebulla, (11/20/2016).

[42] Y. Scholz, "Möglichkeiten und Grenzen der Integration verschiedener regenerativer Energiequellen zu einer 100% regenerativen Stromversorgung der Bundesrepublik Deutschland bis zum Jahr 2050," *Materialien zur Umweltforschung*, 2010.

[43] G. Pleßmann, M. Erdmann, M. Hlusiak, and C. Breyer, "Global Energy Storage Demand for a 100% Renewable Electricity Supply," *Energy Procedia*, vol. 46, no. 0, pp. 22–31, 2014.

[44] International Energy Agency (IEA), "Energy Technology Perspectives 2008," International Energy Agency (IEA), 2008.

[45] M. Fürsch, S. Hagspiel, C. Jägemann, S. Nagl, D. Lindenberger, L. Glotzbach, E. Tröster, and T. Ackermann, "Roadmap 2050- a closer look. Cost-efficient RES-E penetration and the role of grid extensions," Institute of Energy Economics (EWI), Energynautics, 2011.

[46] C. Budischak, D. Sewell, H. Thomson, L. Mach, D. E. Veron, and W. Kempton, "Cost-minimized combinations of wind power, solar power and electrochemical storage, powering the grid up to 99.9% of the time," *Journal of Power Sources*, vol. 225, pp. 60–74, 2013.

[47] N. Hartmann, "Rolle und Bedeutung der Stromspeicher bei hohen Anteilen erneuerbarer Energien in Deutschland: Speichersimulation und Betriebsoptimierung," PhD dissertation, University of Stuttgart, 2013.

[48] M. M. Hand, S. Baldwin, E. DeMeo, J. M. Reilly, T. Mai, D. Arent, G. Porro, M. Meshek, and D. Sandor, "Renewable Electricity Futures Study," National Renewable Energy Laboratory, Golden, CO, 2012.

[49] C. Pape, N. Gerhardt, P. Härtel, A. Scholz, R. Schwinn, T. Drees, A. Maaz, J. Sprey, C. Breuer, A. Moser, F. Sailer, S. Reuter, and T. Müller, "Roadmap Speicher - Speicherbedarf für erneuerbare Energien - Speicheralternativen - Speicheranreiz -

Überwindung rechtlicher Hemmnisse," Bundesministerium für Wirtschaft und Energie (BMWi), 2014.

[50] ENTSO-E, "10-Year Network Development Plan 2012," European Network of Transmission System Operators for Electricity (ENSTO-E), 2012.

[51] B. Steffen and C. Weber, "Efficient storage capacity in power systems with thermal and renewable generation," *Energy Economics*, vol. 36, pp. 556–567, 2013.

[52] F. Ueckerdt, R. Pietzcker, Y. Scholz, D. Stetter, A. Giannousakis, and G. Luderer, "Decarbonizing global power supply under region-specific consideration of challenges and options of integrating variable renewables in the REMIND model," *Energy Economics*, 2016.

[53] K.-K. Cao, F. Cebulla, J. J. G. Vilchez, B. Mousavi, and S. Prehofer, "Raising awareness in model-based energy scenario studies—a transparency checklist," *Energy, Sustainability and Society*, vol. 6, 2016.

[54] G. B. Dantzig, *Linear programming and extensions*. Princeton, N. J.: Princeton Univ. Pr., 1963.

[55] U. Remme, "Zukünftige Rolle erneuerbarer Energien in Deutschland : Sensitivitätsanalysen mit einem linearen Optimierungsmodell," PhD dissertation, University of Stuttgart, 2006.

[56] A. Kann and J. P. Weyant, "Approaches for performing uncertainty analysis in large-scale energy/economic policy models," *Environmental Modeling & Assessment*, vol. 5, no. 1, pp. 29–46, 2000.

[57] W.-P. Schill, "Residual load, renewable surplus generation and storage requirements in Germany," *Energy Policy*, vol. 73, pp. 65–79, 2014.

[58] J. Soares, M. A. F. Ghazvini, N. Borges, and Z. Vale, "A stochastic model for energy resources management considering demand response in smart grids," *Electric Power Systems Research*, vol. 143, pp. 599–610, 2017.

[59] P. D. Lund, J. Lindgren, J. Mikkola, and J. Salpakari, "Review of energy system flexibility measures to enable high levels of variable renewable electricity," *Renewable and Sustainable Energy Reviews*, vol. 45, no. 0, pp. 785–807, 2015.

[60] H. Kondziella and T. Bruckner, "Flexibility requirements of renewable energy based electricity systems - a review of research results and methodologies," *Renewable and Sustainable Energy Reviews*, vol. 53, pp. 10–22, 2016.

[61] U. Bossel, "Physics and Economy of Energy Storage," in *First International Renewable Energy Storage Conference*, 2006.

[62] B. Steffen, "Prospects for pumped-hydro storage in Germany," *Energy Policy*, vol. 45, pp. 420–429, 2012.

[63] H. van de Vegte and M. Huibers, "Overview of potential locations for new Pumped Storage Plants in EU 15, Switzerland and Norway," DNV GL, 2015.

[64] M. Gimeno-Gutiérrez and R. Lacal-Arántegui, "Assessment of the European potential for pumped hydropower energy storage: A GIS-based assessment of pumped hydropower storage potential," Joint Research Centre, 2013.

[65] D. Connolly, "A Review of Energy Storage Technologies," University of Limerick, 2009.

[66] M. Aneke and M. Wang, "Energy storage technologies and real life applications – A state of the art review," *Applied Energy*, vol. 179, pp. 350–377, 2016.

[67] I. Hadjipaschalis, A. Poullikkas, and V. Efthimiou, "Overview of current and future energy storage technologies for electric power applications," *Renewable and Sustainable Energy Reviews*, vol. 13, no. 6–7, pp. 1513–1522, 2009.

[68] W. F. Pickard, A. Q. Shen, and N. J. Hansing, "Parking the power: Strategies and physical limitations for bulk energy storage in supply–demand matching on a grid whose input power is provided by intermittent sources," *Renewable and Sustainable Energy Reviews*, vol. 13, no. 8, pp. 1934–1945, 2009.

[69] R. Kempener and E. Borden, "Battery Storage For Renewables: Market Status And Technology Outlook," International Renewable Energy Agency (IRENA), 2015.

[70] B. Nykvist and M. Nilsson, "Rapidly falling costs of battery packs for electric vehicles," *Nature Climate Change*, vol. 5, no. 4, pp. 329–332, 2015.

[71] W. J. Cole, C. Marcy, V. K. Krishnan, and R. Margolis, "Utility-scale lithium-ion storage cost projections for use in capacity expansion models," in *2016 North American Power Symposium (NAPS)*, 2016, pp. 1–6.

[72] F. Geth, T. Brijs, J. Kathan, J. Driesen, and R. Belmans, "An overview of large-scale stationary electricity storage plants in Europe: Current status and new developments," *Renewable and Sustainable Energy Reviews*, vol. 52, pp. 1212–1227, 2015.

[73] Department of Energy (DOE) Global Energy Storage Database, *http://www.energystorageexchange.org* (Accessed 01/29/2017).

[74] W. Leonhard, U. Bünger, F. Crotogino, C. Gatzen, W. Glaunsinger, S. Hübner, M. Kleimaier, M. Könemund, H. Landinger, T. Lebioda, D. U. Sauer, H. Weber, A. Wenzel,

E. Wolf, W. Woyke, and S. Zunft, "Energiespeicher in Stromversorgungssystemen mit hohem Anteil erneuerbarer Energieträger: Bedeutung, Stand der Technik, Handlungsbedarf," VDE, 2009.

[75] R. Amirante, E. Cassone, E. Distaso, and P. Tamburrano, "Overview on recent developments in energy storage: Mechanical, electrochemical and hydrogen technologies," *Energy Conversion and Management*, vol. 132, pp. 372–387, 2017.

[76] T. Smolinka, M. Günther, and J. Garche, "Stand und Entwicklungspotenzial der Wasserelektrolyse zur Herstellung von Wasserstoff aus regenerativen Energien," Nationale Organisation Wasserstoff- und Brennstoffzellentechnologie (NOW), 2011.

[77] M. Sterner, "Bioenergy and renewable power methane in integrated 100% renewable energy systems: Limiting global warming by transforming energy systems," PhD dissertation, University of Kassel, 2010.

[78] F. Graf, M. Götz, and S. Bajohr, "Injection of biogas, SNG and hydrogen into the gas grid," gwf-Gas Erdgas, 2011.

[79] M. Wietschel, M. Arens, C. Dötsch, S. Herkel, W. Krewitt, P. Markewitz, D. Möst, and M. Scheufen, "Energietechnologien 2050 - Schwerpunkte für Forschung und Entwicklung," 2009.

[80] J. Welsch and M. Blesl, "Modellierung von Energiespeichern und Power-to-X-Technologien mit dem europäischen Energiesystemmodell TIMES PanEU," in *11. VDI-Fachtagung Optimierung in der Energiewirtschaft*, 2015.

[81] J. Michalski, U. Bünger, F. Crotogino, S. Donadei, G.-S. Schneider, T. Pregger, K.-K. Cao, and D. Heide, "Hydrogen generation by electrolysis and storage in salt caverns: Potentials, economics and systems aspects with regard to the German energy transition," *International Journal of Hydrogen Energy*, vol. 42, no. 19, pp. 13427–13443, 2017.

[82] L. M. H. Hall and A. R. Buckley, "A review of energy systems models in the UK: Prevalent usage and categorisation," *Applied Energy*, vol. 169, pp. 607–628, 2016.

[83] V. Krishnan, J. Ho, B. F. Hobbs, A. L. Liu, J. D. McCalley, M. Shahidehpour, and Q. P. Zheng, "Co-optimization of electricity transmission and generation resources for planning and policy analysis: review of concepts and modeling approaches," *Energy Systems*, vol. 7, no. 2, pp. 297–332, 2015.

[84] U. Fahl, "Helmholtz Research School on Energy Scenarios (ESS): Seminar week on construction of energy scenarios," Institute of Energy Economics and Rational Energy Use (IER), 2012.

[85] D. Connolly, H. Lund, B. V. Mathiesen, and M. Leahy, "A review of computer tools for analysing the integration of renewable energy into various energy systems," *Applied Energy*, vol. 87, no. 4, pp. 1059–1082, 2010.

[86] A. Herbst, F. Toro, F. Reitze, and E. Jochem, "Introduction to energy systems modelling," *Swiss journal of economics and statistics*, vol. 148, no. 2, pp. 111–135, 2012.

[87] S. Pfenninger, A. Hawkes, and J. Keirstead, "Energy systems modeling for twenty-first century energy challenges," *Renewable and Sustainable Energy Reviews*, vol. 33, pp. 74–86, 2014.

[88] R. Baños, F. Manzano-Agugliaro, F. G. Montoya, C. Gil, A. Alcayde, and J. Gómez, "Optimization methods applied to renewable and sustainable energy: A review," *Renewable and Sustainable Energy Reviews*, vol. 15, no. 4, pp. 1753–1766, 2011.

[89] J. Zhu, *Optimization of power system operation*, 2. ed. Piscataway, NJ: IEEE Press, 2015.

[90] V. Krey, "Vergleich kurz- und langfristig ausgerichteter Optimierungsansätze mit einem multi-regionalen Energiesystemmodell unter Berücksichtigung stochastischer Parameter," PhD dissertation, Ruhr-Universität Bochum, 2006.

[91] R. E. Burkard and U. Zimmermann, *Einführung in die Mathematische Optimierung*. Berlin, Heidelberg: Springer, 2012.

[92] D. Stetter, "Enhancement of the REMix energy system model: Global renewable energy potentials, optimized power plant siting and scenario validation," PhD dissertation, University of Stuttgart, 2014.

[93] GAMS Development Corporation, "General Algebraic Modeling System (GAMS) Release 24.2.2." 2014.

[94] IBM, "IBM ILOG CPLEX Optimizer Release 12.4.0.1." 2014.

[95] Deutsches Zentrum für Luft- und Raumfahrt (DLR), Wuppertal Institut (WI), and Fraunhofer Institute for Solar Energy Systems (ISE), "Modellexperimente und -vergleiche zur Simulation von Wegen zu einer vollständig regenerativen Energieversorgung (RegMex)," 2017.

[96] H. C. Gils, "Economic potential for future demand response in Germany - Modeling approach and case study," *Applied Energy*, vol. 162, pp. 401–415, 2016.

[97] A. Belderbos, E. Delarue, and W. D'haeseleer, "Considerations on the need for electricity storage requirements: power versus energy," *Working paper*, 2016.

[98] North American Electric Reliability Corporation, "Flexibility requirements and metrics for variable generation," 2010.

[99] E. Lannoye, D. Flynn, and M. O'Malley, "Power system flexibility assessment - State of the art," in *Power and Energy Society General Meeting, 2012 IEEE*, 2012, pp. 1–6.

[100] V. T. Jensen and M. Greiner, "Emergence of a phase transition for the required amount of storage in highly renewable electricity systems," *The European Physical Journal Special Topics*, vol. 223, no. 12, pp. 2475–2481, 2014.

[101] G. B. Sheble and G. N. Fahd, "Unit commitment literature synopsis," *IEEE Transactions on Power Systems*, vol. 9, no. 1, pp. 128–135, 1994.

[102] S. Y. Abujarad, M. W. Mustafa, and J. J. Jamian, "Recent approaches of unit commitment in the presence of intermittent renewable energy resources: A review," *Renewable and Sustainable Energy Reviews*, vol. 70, pp. 215–223, 2017.

[103] A. S. Brouwer, M. van den Broek, A. Seebregts, and A. Faaij, "Impacts of large-scale Intermittent Renewable Energy Sources on electricity systems, and how these can be modeled," *Renewable and Sustainable Energy Reviews*, vol. 33, pp. 443–466, 2014.

[104] J. Abrell, F. Kunz, and H. Weigt, "Start Me Up: Modeling of Power Plant Start-Up Conditions and their Impact on Prices," *Working paper*, 2008.

[105] N. Langrene, W. van Ackooij, and F. Breant, "Dynamic Constraints for Aggregated Units: Formulation and Application," *IEEE Transactions on Power Systems*, vol. 26, no. 3, pp. 1349–1356, 2011.

[106] V. Raichur, D. S. Callaway, and S. J. Skerlos, "Estimating Emissions from Electricity Generation Using Electricity Dispatch Models: The Importance of System Operating Constraints," *Journal of Industrial Ecology*, vol. 20, no. 1, pp. 42–53, 2016.

[107] PLEXOS for Power systems, *http://www.energyexemplar.com* (Accessed 03/23/2016).

[108] M. Carróin and J. M. Arroyo, "A computationally efficient mixed-integer linear formulation for the thermal unit commitment problem," *IEEE Transactions on Power Systems*, vol. 21, no. 3, pp. 1371–1378, 2006.

[109] D. Heide, M. Greiner, L. von Bremen, and C. Hoffmann, "Reduced storage and balancing needs in a fully renewable European power system with excess wind and solar power generation," *Renewable Energy*, vol. 36, no. 9, pp. 2515–2523, 2011.

[110] D. Heide, L. von Bremen, M. Greiner, C. Hoffmann, M. Speckmann, and S. Bofinger, "Seasonal optimal mix of wind and solar power in a future, highly renewable Europe," *Renewable Energy*, vol. 35, no. 11, pp. 2483–2489, 2010.

[111] ENTSO-E Consumption Data, *https://www.entsoe.eu/db-query/consumption/mhlv-a-specific-country-for-a-specific-month* (Accessed 09/12/2015).

[112] H. C. Gils, Y. Scholz, T. Pregger, D. L. de Tena, and D. Heide, "Integrated modelling of variable renewable energy-based power supply in Europe," *Energy*, vol. 123, pp. 173–188 2017.

[113] C. Breyer, S. Afanasyeva, D. Brakemeier, M. Engelhard, S. Giuliano, M. Puppe, H. Schenk, T. Hirsch, and M. Moser, "Assessment of Mid-Term Growth Assumptions and Learning Rates for Comparative Studies of CSP and Hybrid PV-Battery Power Plants," in *22nd SolarPACES*, 2016.

[114] J. I. Pérez-Díaz and J. R. Wilhelmi, "Assessment of the economic impact of environmental constraints on short-term hydropower plant operation," *Energy Policy*, vol. 38, no. 12, pp. 7960–7970, 2010.

[115] J. I. Pérez-Díaz, R. Millán, D. García, I. Guisández, and J. R. Wilhelmi, "Contribution of re-regulation reservoirs considering pumping capability to environmentally friendly hydropower operation," *Energy*, vol. 48, no. 1, pp. 144–152, 2012.

[116] M. G. Rasmussen, G. B. Andresen, and M. Greiner, "Storage and balancing synergies in a fully or highly renewable pan-European power system," *Energy Policy*, vol. 51, no. 0, pp. 642–651, 2012.

[117] H.-M. Henning and A. Palzer, "A comprehensive model for the German electricity and heat sector in a future energy system with a dominant contribution from renewable energy technologies - Part I: Methodology," *Renewable and Sustainable Energy Reviews*, vol. 30, no. 0, pp. 1003–1018, 2014.

[118] A. Palzer and H.-M. Henning, "A comprehensive model for the German electricity and heat sector in a future energy system with a dominant contribution from renewable energy technologies - Part II: Results," *Renewable and Sustainable Energy Reviews*, vol. 30, no. 0, pp. 1019–1034, 2014.

[119] A. A. Solomon, D. M. Kammen, and D. Callaway, "The role of large-scale energy storage design and dispatch in the power grid: A study of very high grid penetration of variable renewable resources," *Applied Energy*, vol. 134, pp. 75–89, 2014.

[120] P. Denholm and M. Hand, "Grid flexibility and storage required to achieve very high penetration of variable renewable electricity," *Energy Policy*, vol. 39, no. 3, pp. 1817–1830, 2011.

[121] S. Weitemeyer, D. Kleinhans, L. Wienholt, T. Vogt, and C. Agert, "A European Perspective: Potential of Grid and Storage for Balancing Renewable Power Systems," *Energy Technology*, vol. 4, no. 1, pp. 114–122, 2015.

[122] M. Huber, D. Dimkova, and T. Hamacher, "Integration of wind and solar power in Europe: Assessment of flexibility requirements," *Energy*, vol. 69, no. 0, pp. 236–246, 2014.

[123] S.-I. Inage, "Prospects for large-scale energy storage in decarbonised power grids," International Energy Agency (IEA), 2009.

[124] P. Wrobel and D. Beyer, "Local Energy Balancing Demand for Germany," in *International Renewable Energy Storage Conference and Exhibition*, 2012.

[125] S. Weitemeyer, D. Kleinhans, T. Vogt, and C. Agert, "Integration of Renewable Energy Sources in future power systems: The role of storage," *Renewable Energy*, vol. 75, pp. 14–20, 2015.

[126] J. P. Deane, G. Drayton, and B. P. Ó. Gallachóir, "The impact of sub-hourly modelling in power systems with significant levels of renewable generation," *Applied Energy*, vol. 113, pp. 152–158, 2014.

[127] H. Pandzzic, Y. Dvorkin, Y. Wang, T. Qiu, and D. S. Kirschen, "Effect of time resolution on unit commitment decisions in systems with high wind penetration," in *PES General Meeting, Conference Exposition, 2014 IEEE*, 2014, pp. 1–5.

[128] C. O'Dwyer and D. Flynn, "Using Energy Storage to Manage High Net Load Variability at Sub-Hourly Time-Scales," *IEEE Transactions on Power Systems*, vol. 30, no. 4, pp. 2139–2148, 2015.

[129] K. Poncelet, E. Delarue, D. Six, J. Duerinck, and W. D'haeseleer, "Impact of the level of temporal and operational detail in energy-system planning models," *Applied Energy*, vol. 162, pp. 631–643, 2016.

[130] P. Nahmmacher, E. Schmid, L. Hirth, and B. Knopf, "Carpe diem: A novel approach to select representative days for long-term power system modeling," *Energy*, vol. 112, pp. 430–442, 2016.

[131] H. Oh, "Optimal Planning to Include Storage Devices in Power Systems," *IEEE Transactions on Power Systems*, vol. 26, no. 3, pp. 1118–1128, 2011.

[132] C. Bussar, P. Stöcker, Z. Cai, L. Moraes, R. Alvarez, H. Chen, C. Breuer, A. Moser, M. Leuthold, and D. U. Sauer, "Large-scale Integration of Renewable Energies and Impact on Storage Demand in a European Renewable Power System of 2050," *Energy Procedia*, vol. 73, pp. 145–153, 2015.

[133] S. Babrowski, P. Jochem, and W. Fichtner, "Electricity storage systems in the future German energy sector: An optimization of the German electricity generation system until

2040 considering grid restrictions," *Computers & Operations Research*, vol. 66, pp. 228–240, 2016.

[134] B. A. Frew, S. Becker, M. J. Dvorak, G. B. Andresen, and M. Z. Jacobson, "Flexibility mechanisms and pathways to a highly renewable US electricity future," *Energy*, vol. 101, pp. 65–78, 2016.

[135] M. Z. Jacobson, M. A. Delucchi, G. Bazouin, Z. A. F. Bauer, C. C. Heavey, E. Fisher, S. B. Morris, D. J. Y. Piekutowski, T. A. Vencill, and T. W. Yeskoo, "100% clean and renewable wind, water, and sunlight (WWS) all-sector energy roadmaps for the 50 United States," *Energy Environ. Sci.*, vol. 8, no. 7, pp. 2093–2117, 2015.

[136] M. Z. Jacobson, M. A. Delucchi, Z. A. F. Bauer, S. C. Goodman, W. E. Chapman, and M. A. Cameron, "100% Clean and Renewable Wind, Water, and Sunlight (WWS) All-Sector Energy Roadmaps for 139 Countries of the World," *Working paper*, 2016.

[137] R. Loulou, "ETSAP-TIAM: the TIMES integrated assessment model. part II: mathematical formulation," *Computational Management Science*, vol. 5, no. 1, pp. 41–66, 2007.

[138] R. Loulou and M. Labriet, "ETSAP-TIAM: the TIMES integrated assessment model Part I: Model structure," *Computational Management Science*, vol. 5, no. 1, pp. 7–40, 2007.

[139] J. Farfan and C. Breyer, "Aging of European power plant infrastructure as an opportunity to evolve towards sustainability," *International Journal of Hydrogen Energy*, 2017.

[140] ENTSO-E hourly load values of all countries for a specific month, *https://www.entsoe.eu/db-query/consumption/mhlv-all-countries-for-a-specific-month* (Accessed 03/20/2015).

[141] B. C. Ummels, E. Pelgrum, and W. L. Kling, "Integration of large-scale wind power and use of energy storage in the netherlands' electricity supply," *IET Renewable Power Generation*, vol. 2, no. 1, pp. 34–46, 2008.

[142] B. Nyamdash, E. Denny, and M. O'Malley, "The viability of balancing wind generation with large scale energy storage," *Energy Policy*, vol. 38, no. 11, pp. 7200–7208, 2010.

[143] J. Nitsch, T. Pregger, T. Naegler, D. Heide, F. Trieb, Y. Scholz, K. Niehaus, N. Gerhardt, M. Sterner, T. Trost, A. von Oehsen, R. Schwinn, C. Pape, H. Hahn, M. Wickert, and B. Wenzel, "Langfristszenarien und Strategien für den Ausbau der erneuerbaren Energien in Deutschland bei Berücksichtigung der Entwicklung in Europa und global," Bundesministerium für Umwelt, Naturschutz und Reaktorsicherheit (BMU), 2012.

[144] M. Schlesinger, D. Lindenberger, and C. Lutz, "Energieszenarien für ein Energiekonzept der Bundesregierung," Prognos [u.a.], 2010.

[145] J. Bertsch, C. Growitsch, S. Lorenczik, and S. Nagl, "Flexibility in Europe's power sector - An additional requirement or an automatic complement?," *Energy Economics*, vol. 53, pp. 118–131, 2016.

[146] H. C. Gils, "Balancing of Intermittent Renewable Power Generation by Demand Response and Thermal Energy Storage," PhD dissertation, University of Stuttgart, 2015.

[147] P. Denholm, J. Jorgenson, M. Hummon, T. Jenkin, D. Palchak, B. Kirby, O. Ma, and M. O'Malley, "The value of energy storage for grid applications," National Renewable Energy Laboratory (NREL), 2013.

[148] A. S. Brouwer, M. van den Broek, W. Zappa, W. C. Turkenburg, and A. Faaij, "Least-cost options for integrating intermittent renewables in low-carbon power systems," *Applied Energy*, vol. 161, pp. 48–74, 2016.

[149] B. Stoll, G. Brinkman, A. Townsend, and A. Bloom, "Analysis of Modeling Assumptions used in Production Cost Models for Renewable Integration Studies," National Renewable Energy Laboratory (NREL), 2016.

[150] T. Fichter, "Long-term capacity expansion planning with variable renewable energies-enhancement of the REMix energy system modelling framework," PhD dissertation, University of Stuttgart, 2017.

[151] F. Steinke, P. Wolfrum, and C. Hoffmann, "Grid vs. storage in a 100% renewable Europe," *Renewable Energy*, vol. 50, no. 0, pp. 826–832, 2013.

[152] C. B. Martínez-Anido, M.Vandenbergh, L.deVries, C.Alecu, A.Purvins, G. Fulli, and T.Huld, "Medium-term demand for European cross-border electricity transmission capacity," *Energy Policy*, vol. 61, pp. 207–222, 2013.

[153] B. A. Frew, "Optimizing the Integration of Renewable Energy in the United States," PhD dissertation, Stanford University, 2014.

[154] G. Betz, "What Range of Future Scenarios Should Climate Policy Be Based On? Modal Falsificationism and its Limitations," *Philosophia Naturalis*, vol. 46, no. 1, pp. 133–158, 2009.

[155] E. Trutnevyte, C. Guivarch, R. Lempert, and N. Strachan, "Reinvigorating the scenario technique to expand uncertainty consideration," *Climatic Change*, vol. 135, no. 3, pp. 373–379, 2016.

[156] P. W. Van Notten, A. Sleegers, and M. B. van Asselt, "The future shocks: on discontinuity and scenario development," *Technological forecasting and social change*, vol. 72, no. 2, pp. 175–194, 2005.

[157] T. J. Postma and F. Liebl, "How to improve scenario analysis as a strategic management tool?," *Technological Forecasting and Social Change*, vol. 72, no. 2, pp. 161–173, 2005.

[158] E. Trutnevyte, "Does cost optimization approximate the real-world energy transition?," *Energy*, vol. 106, pp. 182–193, 2016.

[159] A. Sakti, K. G. Gallagher, N. Sepulveda, C. Uckun, C. Vergara, F. J. de Sisternes, D. W. Dees, and A. Botterud, "Enhanced representations of lithium-ion batteries in power systems models and their effect on the valuation of energy arbitrage applications," *Journal of Power Sources*, vol. 342, pp. 279–291, 2017.

[160] F. Wankmüller, P. R. Thimmapuram, K. G. Gallagher, and A. Botterud, "Impact of battery degradation on energy arbitrage revenue of grid-level energy storage," *Journal of Energy Storage*, vol. 10, pp. 56–66, 2017.

[161] S. Pauliuk, A. Arvesen, K. Stadler, and E. G. Hertwich, "Industrial ecology in integrated assessment models," *Nature Climate Change*, vol. 7, no. 1, pp. 13–20, 2017.

[162] P. Berrill, A. Arvesen, Y. Scholz, H. C. Gils, and E. G. Hertwich, "Environmental impacts of high penetration renewable energy scenarios for Europe," *Environmental Research Letters*, vol. 11, no. 1, p. 014012, 2016.

[163] C. Dieckhoff, "Modellierte Zukunft," PhD dissertation, Karlsruhe Institute of Technology, 2015.

[164] C. Bussar, P. Stöcker, Z. Cai, L. Moraes, D. Magnor, P. Wiernes, N. van Bracht, A. Moser, and D. U. Sauer, "Large-scale integration of renewable energies and impact on storage demand in a European renewable power system of 2050—Sensitivity study," *Journal of Energy Storage*, vol. 6, pp. 1–10, 2016.

[165] A. Zerrahn and W. P. Schill, "A Greenfield Model to Evaluate Long-Run Power Storage Requirements for High Shares of Renewables," *DIW Discussion Paper*, no. 34, 2015.

[166] A. Mileva, J. Johnston, J. H. Nelson, and D. M. Kammen, "Power system balancing for deep decarbonization of the electricity sector," *Applied Energy*, vol. 162, pp. 1001–1009, 2016.

[167] M. R. Kühne, "Drivers of energy storage demand in the German power system: an analysis of the influence of methodology and parameters on modelling results," PhD dissertation, Technical University of Munich, 2016.

[168] B. S. Palmintier, "Incorporating operational flexibility into electric generation planning: impacts and methods for system design and policy analysis," PhD dissertation, Massachusetts Institute of Technology, 2013.

[169] T. S. Kim, "Comparative analysis on the part load performance of combined cycle plants considering design performance and power control strategy," *Energy*, vol. 29, no. 1, pp. 71–85, 2004.

[170] H. Chalmers, "Flexible operation of coal-fired power plants with post-combustion capture of carbon dioxide," PhD dissertation, University of Surrey, 2010.

[171] L. Balling, "Flexible future for combined cycle," *Modern power systems*, vol. 30, no. 12, pp. 61–65, 2010.

[172] EURELECTRIC, "Flexible generation: Backing up renewables," 2011.

[173] A. Vuorinen, *Planning of Optimal Power Systems*. Ekoenergo Oy, 2009.

[174] P. Konstantin, *Praxisbuch Energiewirtschaft: Energieumwandlung,-transport und -beschaffung im liberalisierten Markt*. Springer, 2009.

[175] J. S. Maulbetsch and M. N. DiFilippo, "Cost and value of water use at combined cycle power plants," *California Energy Commission*, 2006.

[176] H. Zhai and E. S. Rubin, "Performance and cost of wet and dry cooling systems for pulverized coal power plants with and without carbon capture and storage," *Energy Policy*, vol. 38, no. 10, pp. 5653–5660, 2010.

[177] U.S. EIA, "Updated Capital Cost Estimates for Utility Scale Electricity Generating Plants," *US Energy Information Administration,* 2013.

[178] N. Kumar, P. Besuner, S. Lefton, D. Agan, and D. Hilleman, "Power plant cycling costs," *Contract*, vol. 303, pp. 275–300, 2012.

[179] B. Stott, J. Jardim, and O. Alsac, "DC Power Flow Revisited," *IEEE Transactions on Power Systems*, vol. 24, no. 3, pp. 1290–1300, 2009.

[180] F. Trieb, C. Schillings, T. Pregger, and M. O'Sullivan, "Solar electricity imports from the Middle East and North Africa to Europe," *Energy Policy*, vol. 42, pp. 341–353, 2012.

[181] C. Noack, F. Burggraf, S. S. Hosseiny, P. Lettenmeier, S. Kolb, S. Belz, J. Kallo, K. A. Friedrich, T. Pregger, K. K. Cao, D. Heide, T. Naegler, F. Borggrefe, U. Bünger, J. Michalski, T. Raksha, C. Voglstätter, T. Smolinka, F. Crotogino, S. Donadei, P.-L. Horvath, and G.-S. Schneider, "Studie über die Planung einer Demonstrationsanlage zur Wasserstoff-Kraftstoffgewinnung durch Elektrolyse mit Zwischenspeicherung in

Salzkavernen unter Druck," Bundesministerium für Wirtschaft und Energie (BMWi), 2014.

[182] ENTSO-E, "10-Year Network Development Plan 2014," European Network of Transmission System Operators for Electricity (ENSTO-E), 2014.

[183] T. Fichter, F. Trieb, and M. Moser, "Optimized Integration of Renewable Energy Technologies Into Jordan's Power Plant Portfolio," *Heat Transfer Engineering*, vol. 35, no. 3, pp. 281–301, 2013.

[184] J. Nitsch and T. Pregger, "Kostenbilanz des Ausbaus erneuerbarer Energien in der Stromerzeugung bei unterschiedlichen Preisbildungen am Strommarkt," *Vierteljahrshefte zur Wirtschaftsforschung*, vol. 3, pp. 45–59, 2013.

[185] International Energy Agency (IEA), "World Energy Outlook 2014," OECD Publishing, 2014.

[186] S. Kühnel, "lnvestigation of the variability of solar and wind electricity generation potantials in Europe and North Africa," Master's thesis, Karl von Ossietzky Universität, Oldenburg, 2013.

[187] D. Treuherz, "The impact of various meteorological years on system reliability in a German energy scenario for 2025," Bachelor's thesis, University of Applied Sciences Mannheim, 2015.

[188] G. Haydt, V. Leal, A. Pina, and C. A. Silva, "The relevance of the energy resource dynamics in the mid/long-term energy planning models," *Renewable Energy*, vol. 36, no. 11, pp. 3068–3074, 2011.

[189] J. Nitsch, T. Pregger, Y. Scholz, T. Naegler, M. Sterner, N. Gerhardt, A. von Oehsen, C. Pape, Y.-M. Saint-Drenan, and B. Wenzel, "Leitstudie 2010 - Langfristszenarien und Strategien für den Ausbau der erneuerbaren Energien in Deutschland bei Berücksichtigung der Entwicklung in Europa und global," Deutsches Zentrum für Luft- und Raumfahrt (DLR), Fraunhofer Institut für Windenergie und Energiesystemtechnik (IWES), Ingenieurbüro für neue Energien (IFNE), 2010.

[190] Y. Scholz, H. C. Gils, and R. Pietzcker, "Application of a high-detail energy system model to derive power sector characteristics at high wind and solar shares," vol. 64, pp. 568–582, *Energy Economics*, 2016.

[191] D. Luca de Tena, "Large Scale Renewable Power Integration with Electric Vehicles," PhD dissertation, University of Stuttgart, 2014.

[192] T. Pregger, J. Nitsch, and T. Naegler, "Long-term scenarios and strategies for the deployment of renewable energies in Germany," *Energy Policy*, vol. 59, no. 0, pp. 350–360, 2013.

[193] Y. Scholz, H. C. Gils, T. Pregger, D. Heide, F. Cebulla, K.-K. Cao, D. Hess, and F. Borggrefe, "Möglichkeiten und Grenzen des Lastausgleichs durch Energiespeicher, verschiebbare Lasten und stromgeführte KWK bei hohem Anteil fluktuierender erneuerbarer Stromerzeugung," Deutsches Zentrum für Luft- und Raumfahrt (DLR), 2014.

[194] F. Trieb, C. Schillings, S. Kronshage, P. Viebahn, M. Kabariti, D. K.M., A. Bennouna, H. El Nokraschy, S. Hassan, L. G. Yussef, T. Hasni, N. El Bassam, and H. Satoguina, "Concentrating Solar Power for the Mediterranian Region: MED-CSP." German Aerospace Center, 2005.

[195] F. Trieb, C. Schillings, S. Kronshage, U. Klann, P. Viebahn, N. May, R. Wilde, C. Paul, M. Kabariti, A. Bennouna, H. El Nokraschy, S. Hassan, L. G. Yussef, T. Hasni, N. El Bassam, and H. Satoguina, "Trans-Mediterranean Interconnection for Concentrating Solar Power: TRANS-CSP." Deutsches Zentrum für Luft- und Raumfahrt (DLR), 2006.

[196] European Energy Agency (EEA), "CORINE Land Cover 2000," 2005.

[197] European Commission, Joint Research Center (JRC), "Global Land Cover 2000," 2003.

[198] H. Chen, T. N. Cong, W. Yang, C. Tan, Y. Li, and Y. Ding, "Progress in electrical energy storage system: A critical review," *Progress in Natural Science*, vol. 19, no. 3, pp. 291–312, 2009.

[199] F. Adamek, T. Aundrup, W. Glaunsinger, M. Kleimaier, H. Landinger, M. Leuthold, B. Lunz, A. Moser, C. P. amd Helge Pluntke, N. Rotering, D. U. Sauer, M. Sterner, and W. Wellßow, "Energiespeicher für die Energiewende: Speicherungsbedarf und Auswirkungen auf das Übertragungsnetz für Szenarien bis 2050," VDE-ETG, Frankfurt a.M., 2012.

[200] G. Fuchs, B. Lunz, M. Leuthold, and D. U. Sauer, "Technology Overview on Electricity Storage," RWTH Aachen- Institut für Stromrichtertechnik und elektrische Antriebe (ISEA), 2012.

[201] H. L. Ferreira, R. Garde, G. Fulli, W. Kling, and J. P. Lopes, "Characterisation of electrical energy storage technologies," *Energy*, vol. 53, no. 0, pp. 288–298, 2013.

[202] X. Luo, J. Wang, M. Dooner, and J. Clarke, "Overview of current development in electrical energy storage technologies and the application potential in power system operation," *Applied Energy*, vol. 137, pp. 511–536, 2015.

[203] F. Ausfelder, C. Beilmann, M. Bertau, S. Bräuninger, A. Heinzel, R. Hoer, W. Koch, F. Mahlendorf, A. Metzelthin, M. Peuckert, and others, "Energiespeicherung als Element einer sicheren Energieversorgung," *Chemie Ingenieur Technik*, vol. 87, no. 1–2, pp. 17–89, 2015.

[204] M. Budt, D. Wolf, R. Span, and J. Yan, "A review on compressed air energy storage: Basic principles, past milestones and recent developments," *Applied Energy*, vol. 170, pp. 250–268, 2016.

[205] M. Gimeno-Gutiérrez and R. Lacal-Arántegui, "Assessment of the European potential for pumped hydropower energy storage based on two existing reservoirs," *Renewable Energy*, vol. 75, pp. 856–868, 2015.

[206] P. Vennemann, K. Heinz Gruber, J. Ulrik Haaheim, A. Kunsch, H.-P. Sistenich, and H.-R. Thöni, "Pumped storage plants—status and perspectives," *VGB powertech*, vol. 91, no. 4, p. 32, 2011.

[207] J. P. Deane, B. P. Ó. Gallachóir, and E. J. McKeogh, "Techno-economic review of existing and new pumped hydro energy storage plant," *Renewable and Sustainable Energy Reviews*, vol. 14, no. 4, pp. 1293–1302, 2010.

[208] N. Hartmann, L. Eltrop, N. Bauer, J. Salzer, S. Schwarz, and M. Schmidt, "Stromspeicherpotenziale für Deutschland," Zentrum für Energieforschung Stuttgart (zfes), 2012.

[209] P. Vennemann, L. Thiel, and H.-C. Funke, "Pumped storage plants in the future power supply system," *VGB powertech*, vol. 90, no. 1, p. 44, 2010.

[210] P. M. H. Financial, "World Electric Power Plants Database." 2010.

[211] A. Gillhaus, "Natural Gas Storage in Salt Caverns: Present Status, Developments and Future Trends in Europe," 2007.

[212] U. I. Ehlers, "Windenergie und Druckluftspeicher- Netzentlastung und Reservestellung mit Druckluftspeicher im Rahmen einer deutschen Elektrizitätsversorgung mit hohem Windenergieanteil," Master's thesis, University of Flensburg, 2005.

[213] Y. Scholz, "Renewable energy based electricity supply at low costs: development of the REMix model and application for Europe," PhD dissertation, University of Stuttgart, 2012.

Appendix A

Tab. A 1: Storage converter power (discharge) and storage unit capacity of the scenarios in Bussar et al. [164]. Data is based on [164] and on personal communication with C. Bussar.

Scenario	Storage power [GW_{el}]				Storage unit capacity [TWh_{el}]			
	PHS	H_2	Battery	Total	PHS	H_2	Battery	Total
Base case	188	882	323	1,056	2.7	802	1.6	806
Grid max	251	550	139	939	4.1	844	0.7	849
Grid min	305	494	79	878	4.4	785	0.4	790
Hydrogen max	310	482	114	906	5.4	654	0.6	660
Hydrogen min	117	606	169	892	1.6	952	1.0	955
Battery max	253	526	52	830	3.9	751	0.3	755
Battery min	95	567	842	1,505	1.2	841	3.2	845
PHS max	24	568	289	880	0.5	753	1.9	755
PHS min	477	514	7	999	7.6	779	-	786
PV max	146	524	203	872	2.8	735	1.2	739
PV min	74	621	505	1,200	1.1	1,054	2.7	1,058
Wind max	426	595	307	1,329	5.5	1,157	0.9	1,163
Wind min	76	531	143	750	1.5	479	0.6	481
Grid 2.5 GW limit	338	731	365	1,434	4.6	1,409	1.4	1,415
Grid 5.0 GW limit	378	667	248	1,293	5.0	1,186	0.9	1,192
Grid 7.5 GW limit	330	652	143	1,125	4.5	1,011	0.9	1,017
Grid 10 GW limit	202	612	356	1,170	2.5	912	1.3	916
Grid 12.5 GW limit	300	573	213	1,087	3.8	882	1.1	887
Grid 15.0 GW limit	327	558	160	1,045	4.1	864	0.8	869
No PHS	-	570	381	952	-	773	2.1	775
No PHS or battery	-	758	-	758	-	738	-	738
No long-term storage	656	-	8	664	42.1	-	-[a]	42

[a] A small amount of 10 GWh of battery storage unit capacity results in this scenario.

Tab. A 2: Storage converter power and storage unit capacity of the scenarios in Zerrahn and Schill [165]. A constraint of the optimization enforces a renewable generation shares at least as high as listed in the scenario column. The data is based on [165] and on personal communication with A. Zerrahn.

Scenario	Storage power [GW_{el}]							Storage unit capacity [GWh_{el}]						
	Li-ion	PbA	NaS	Redox -flow	PHS	aCAES	PtG	Li-ion	PbA	NaS	Redox -flow	PHS	aCAES	PtG
60%	6.3	0.0	0.0	0.0	3.9	0.0	0.0	10.7	0.0	0.0	0.0	31.0	0.0	0.0
70%	6.3	0.0	0.0	0.0	3.9	0.0	0.0	10.7	0.0	0.0	0.0	31.0	0.0	0.0
80%	6.5	0.0	0.0	0.0	5.4	0.0	0.0	11.0	0.0	0.0	0.0	44.2	0.0	0.0
90%	4.8	0.0	0.0	0.0	16.9	0.0	0.0	8.5	0.0	0.0	0.0	150.1	0.0	0.0
100%	7.1	0.0	0.0	0.0	24.4	0.0	2.7	21.6	0.0	0.0	0.0	300.0	0.0	114.2

Tab. A 3: Storage converter power and storage unit capacity of the scenarios in Mileva et al. [166]. Data is based on [166] and on personal communication with A. Mileva.

Scenario	Storage power [GW_{el}]				Storage unit capacity [GWh_{el}]			
	Battery	CAES	PHS	Total	Battery	CAES	PHS	Total
Reference	5.9	13.9	4.0	23.8	9.4	142.8	32.0	184.2
SunShot	4.4	14.9	4.0	23.3	6.8	165.0	32.0	203.7
Low-Cost Batteries	68.1	10.2	4.0	82.3	403.8	113.6	32.0	549.5
SunShot/Low-Cost Batteries	105.5	19.4	4.0	128.9	622.5	228.8	32.0	883.2
High-Efficiency Batteries	5.9	13.9	4.0	23.7	14.9	141.4	32.0	188.3
Nuclear	1.8	21.5	4.0	27.3	2.2	167.4	32.0	201.6
High-Price Natural Gas	5.9	13.9	4.0	23.8	8.3	144.7	32.0	185.1
Methane Leakage	7.4	6.1	4.0	17.5	23.3	44.7	32.0	100.0
High-Cost Transmission	4.6	21.9	4.0	30.5	20.0	244.4	32.0	296.3
Limited Hydro	6.6	18.2	4.0	28.8	25.5	184.8	32.0	242.2
Limited-Flexibility Hydro	5.7	15.6	4.0	25.4	14.9	166.2	32.0	213.1
Limited Efficiency	10.0	22.9	4.0	37.0	37.1	291.9	32.0	361.0
Load-Shifting	6.6	9.5	4.0	20.1	6.5	85.0	32.0	123.4
Load-Shifting/Flexible EV Charging	9.9	4.0	4.0	17.8	9.7	38.6	32.0	80.2

Tab. A 4: Storage converter charge and discharge power of the scenarios in Kühne [167]. The data is based on [167] and on personal communication with M. Kühne.

Scenario	Storage charge power [GW_{el}]				Storage discharge power [GW_{el}]			
	PHS	aCAES	H_2	Total	PHS	aCAES	H_2	Total
Reference Scenario	3.0	18.4	14.9	36.3	2.4	9.8	3.7	15.9
Time Series 2003	2.4	14.3	20.6	37.4	2.0	8.1	3.5	13.6
Time Series 2004	2.6	15.3	20.3	38.2	2.0	9.6	5.2	16.9
Time Series 2005	2.7	13.8	14.5	31.0	2.2	8.1	3.3	13.6
Time Series 2006	2.5	11.3	18.7	32.5	2.0	7.8	3.8	13.5
Time Series 2007	2.2	-	5.4	7.6	2.6	-	5.3	7.9
Time Series 2008	2.6	4.8	14.0	21.4	2.1	3.5	6.7	12.2
Time Series 2009	2.4	20.5	11.1	34.1	2.0	12.3	2.2	16.4
Time Series 2010	2.5	22.1	8.5	33.1	2.0	11.0	1.7	14.6
Time Series 2011	2.3	1.4	13.5	17.3	2.5	1.3	8.6	12.4
RE share 40 %	-	-	-	-	-	-	-	-
RE share 50 %	2.2	-	-	2.2	1.7	-	-	1.7
RE share 60 %	2.6	5.4	0.6	8.6	2.1	2.1	-	4.2
RE share 70 %	2.9	14.2	9.3	26.4	2.3	6.7	1.2	10.2
RE share 90 %	2.2	1.6	3.0	6.8	2.7	2.2	3.9	8.7
RE share 100 %	2.2	1.1	3.7	7.0	2.6	1.6	5.7	9.9
RE structure: Var 1	2.4	17.5	24.8	44.7	2.0	8.7	4.6	15.2
RE structure: Var 2	3.8	23.7	15.5	42.9	3.0	11.3	3.1	17.4
RE structure: Var 3	6.2	48.1	11.6	66.0	5.0	19.6	2.7	27.3
RE structure: Var 4	7.0	68.4	8.8	84.1	5.6	30.4	2.0	38.0
RE structure: Var 5	7.0	87.7	12.5	107.3	5.6	39.8	2.5	47.9
RE structure: Var 6	2.5	16.2	24.3	43.0	2.0	9.3	4.8	16.2
RE structure: Var 7	3.7	22.2	14.0	39.8	2.9	11.4	3.3	17.6
RE structure: Var 8	6.2	44.0	9.4	59.5	4.9	19.2	2.5	26.6
RE structure: Var 9	7.0	65.0	9.9	81.9	5.6	29.0	1.8	36.4
RE structure: Var 10	2.2	15.3	24.3	41.8	2.0	10.0	5.5	17.4
RE structure: Var 11	3.5	14.9	10.1	28.5	2.8	9.5	3.4	15.7
RE structure: Var 12	6.1	37.7	7.8	51.6	4.9	18.3	2.1	25.3
RE structure: Var 13	2.4	16.1	23.8	42.2	2.2	10.9	5.9	19.1
RE structure: Var 14	2.4	6.2	4.0	12.6	2.7	6.0	3.4	12.1
RE structure: Var 15	2.4	13.6	18.8	34.8	2.3	10.0	7.5	19.8
Fuel Costs Level minus 10 %	2.9	15.3	12.3	30.5	2.3	8.9	3.1	14.4
Fuel Cost Level plus 10 %	3.1	20.1	16.5	39.6	2.5	10.7	4.0	17.2
Expensive Gas & Oil I	3.3	21.7	20.4	45.3	2.6	11.0	5.0	18.6
Expensive Gas & Oil II	3.4	28.5	29.3	61.3	2.7	13.2	4.0	20.0
Discount 0 %	2.8	1.9	0.7	5.4	2.3	1.4	0.2	3.9
Discount 10 %	2.8	4.2	3.7	10.7	2.2	2.9	1.0	6.1
Discount 20 %	2.8	6.9	6.5	16.2	2.2	4.4	1.7	8.3
Discount 30 %	2.9	10.5	8.0	21.3	2.3	6.2	2.3	10.8
Discount 40 %	3.0	13.5	11.7	28.2	2.4	8.0	3.1	13.5
Lower storage costs I	4.2	10.0	20.3	34.5	3.4	5.9	5.6	14.8
Lower storage costs II	4.5	5.8	36.6	46.8	3.6	4.0	9.4	16.9

Tab. A 5: Storage unit capacity of the scenarios in Kühne [167]. The data is based on [167] and on personal communication with M. Kühne.

Scenario	Storage unit capacity [GWh_{el}]			
	PHS	aCAES	H_2	Total
Reference Scenario	40	490	4,655	5,184
Time Series 2003	40	371	5,572	5,982
Time Series 2004	40	462	6,364	6,866
Time Series 2005	40	414	7,326	7,780
Time Series 2006	40	305	7,148	7,493
Time Series 2007	40	-	3,947	3,987
Time Series 2008	40	118	6,397	6,555
Time Series 2009	40	708	2,107	2,855
Time Series 2010	40	689	3,289	4,018
Time Series 2011	40	47	5,701	5,788
RE share 40 %	-	-	-	-
RE share 50 %	40	-	-	40
RE share 60 %	40	106	179	325
RE share 70 %	40	313	3,247	3,600
RE share 90 %	40	52	1,339	1,431
RE share 100 %	40	36	1,785	1,861
RE structure: Var 1	40	417	11,784	12,241
RE structure: Var 2	40	524	5,210	5,774
RE structure: Var 3	40	604	5,897	6,540
RE structure: Var 4	40	486	8,318	8,844
RE structure: Var 5	40	551	12,115	12,706
RE structure: Var 6	40	434	12,011	12,485
RE structure: Var 7	40	501	4,366	4,906
RE structure: Var 8	40	506	4,686	5,232
RE structure: Var 9	40	497	8,079	8,617
RE structure: Var 10	40	443	12,313	12,796
RE structure: Var 11	40	377	2,790	3,207
RE structure: Var 12	40	495	5,755	6,290
RE structure: Var 13	40	468	12,438	12,947
RE structure: Var 14	40	179	1,918	2,138
RE structure: Var 15	40	391	9,269	9,700
Fuel Costs Level minus 10 %	40	412	3,820	4,272
Fuel Cost Level plus 10 %	40	550	5,158	5,748
Expensive Gas & Oil I	40	595	6,343	6,978
Expensive Gas & Oil II	40	871	10,319	11,230
Discount 0 %	40	47	202	288
Discount 10 %	40	103	1,129	1,272
Discount 20 %	40	174	2,008	2,222
Discount 30 %	40	258	2,273	2,571
Discount 40 %	40	363	3,473	3,875
Lower storage costs I	40	205	5,113	5,358
Lower storage costs II	40	98	8,379	8,517

Appendix B

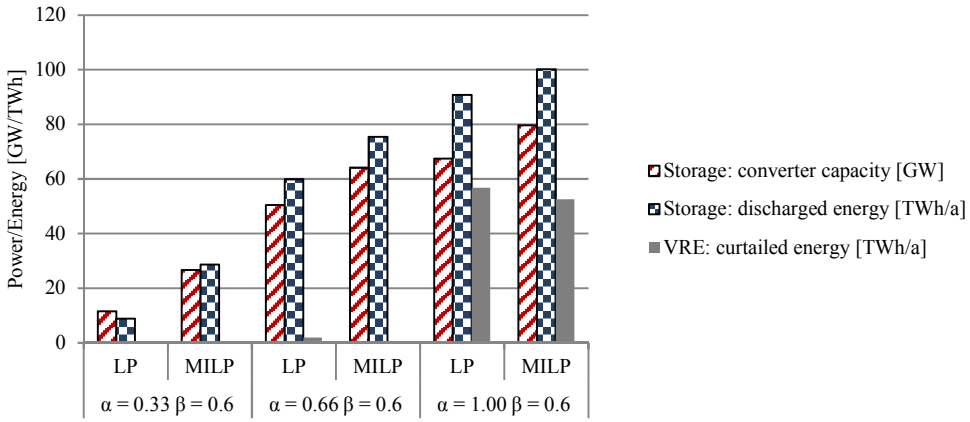

Fig. B 1: Storage converter capacity expansion (GW) and storage utilization in terms of annually discharged energy (TWh/a) compared over the scenarios (PV share β of 0.6) with increasing VRE share (α) and over the different modeling approaches (MILP, LP) for power plants.

Tab. B 1: Techno-economic parameters of thermal power plant clusters for the LP modeling approach.

Power plant cluster	η_{gross} [-][a]	η_{net} [-][b]	$O\&M_{var}$ [€/kWh]	Wear & tear costs [€/kW][c]
Nuclear large	0.324	0.309	0.00171	0.0015
Nuclear midsize	0.324	0.309	0.00171	0.0015
Nuclear small	0.324	0.309	0.00171	0.0015
Lignite large	0.433	0.406	0.00358	0.0015
Lignite midsize	0.395	0.370	0.00358	0.0015
Lignite small	0.373	0.350	0.00358	0.0015
Coal large	0.414	0.379	0.00358	0.0015
Coal midsize	0.415	0.380	0.00358	0.0015
Coal small	0.405	0.371	0.00358	0.0015
CCGT large	0.461	0.453	0.00288	0.0005
CCGT midsize	0.517	0.508	0.00288	0.0005
CCGT small	0.493	0.484	0.00288	0.0005
Gas turbine large	0.400	0.395	0.01236	0.0005
Gas turbine midsize	0.289	0.285	0.01236	0.0005
Gas turbine small	0.358	0.354	0.01236	0.0005

[a] η_{gross} is based on [168].

[b] As reference [168] does not provide data for η_{net}, the ratio of η_{gross} to η_{net} provided by Scholz et al. [193] is used. Note that this publication does not differentiate between capacity groups and includes only technology-specific efficiencies. In consequence, the ratio of η_{gross} to η_{net} in this table is identical within each technology group.

[c] Based on [177]. For nuclear power plants, the values of *Advanced Nuclear* were used, for lignite and coal power plants the values of *Advanced Pulverized Coal Facility*, for gas turbines *Conventional Combustion Turbine* and for CCGT *Conventional Natural Gas Combined Cycle*. To conclude to €, an exchange rate of 1.3US $/€ and an inflation rate of 2% p.a. is assumed.

Tab. B 2: Techno-economic parameters of thermal power plant clusters for the MILP modeling approach. $\eta@P_{max}$ describes the efficiency at maximal power; $\eta@P_{min}$ the efficiency at minimum load of the unit. Load $rate_{min}$ is defined as the minimal load rate of the unit relative to the gross capacity.

Power plant cluster	$\eta@P_{max}$ [a]	$\eta@P_{min}$ [b]	Load $rate_{min}$ [-] [c]	Fuel cons. start [MWh_{th}/MW_{el}] [d]	Auxiliary power $cooling_{min}$ [e] [MW]	Auxiliary power $others_{min}$ [e] [MW]	Minimum on-line time [h]	Minimum off-line time [h]	$O\&M_{var}$ [k€/GWh_{el}] [f]	Startup costs [k€/GW] [g]	Ramping costs [k€/GW] [g]
Nuclear large	0.3240	0.2786	0.50	2.27	6.10	32.00	48	48	1.71	6.6	2.53
Nuclear midsize	0.3240	0.2786	0.50	2.27	104.10	32.00	48	48	1.71	6.6	2.53
Nuclear small	0.3240	0.2786	0.50	2.27	104.10	32.00	48	48	1.71	6.6	2.53
Lignite large	0.4325	0.3720	0.40	3.08	3.20	57.00	12	12	3.58	6.52	2.53
Lignite midsize	0.3950	0.3397	0.40	2.05	2.00	60.76	12	12	3.58	5.01	2.83
Lignite small	0.3725	0.3204	0.40	2.05	0.50	91.20	12	12	3.58	5.01	3.13
Coal large	0.4137	0.3558	0.40	3.08	2.50	57.00	12	8	3.58	6.52	2.53
Coal midsize	0.4150	0.3569	0.40	2.05	1.40	60.76	12	8	3.58	5.01	2.83
Coal small	0.4052	0.3484	0.40	2.05	0.50	91.20	12	8	3.58	5.01	3.13
CCGT large	0.4612	0.2652	0.30	0.14	0.30	16.50	8	4	2.88	1.56	0.60
CCGT midsize	0.5171	0.2973	0.30	0.14	0.20	21.95	8	4	2.88	1.56	0.60
CCGT small	0.4928	0.2834	0.30	0.14	0.00	27.51	8	4	2.88	1.56	0.60
Gas turbine large	0.4000	0.1520	0.20	0.062	0.00	16.50	0	1	12.36	0.78	2.80
Gas turbine midsize	0.2895	0.1100	0.20	0.062	0.00	21.95	0	1	12.36	0.78	2.10
Gas turbine small	0.3585	0.1362	0.20	0.062	0.00	27.51	0	1	12.36	0.78	1.40

[a] Based on [168].

[b] Based on [169–171, 173].

[c] Based on [171–173].

[d] Based on [178]. Assumed to be warm start.

[e] All other parasitics, excluding cooling. Based on [173–176].

[f] Based on [177]. For nuclear power plants, the values of *Advanced Nuclear* were used, for lignite and coal power plants the values of *Advanced Pulverized Coal Facility*, for gas turbines *Conventional Combustion Turbine* and for CCGT *Conventional Natural Gas Combined Cycle*. To conclude to €, an exchange rate of 1.3US $/€ and an inflation rate of 2% p.a was assumed.

[g] Based on [178]. For nuclear power plants, internal assumptions were used.

Tab. B 3: Total specific operating expenditures (OPEX) disaggregated into the cost components CO_2 and fuel costs as well as variable operations and maintenance costs ($O\&M_{var}$) over the scenarios with different VRE shares for the LP approach. Note that the total OPEX in this table do not include wear & tear costs as they are a result of the optimization.

VRE share α [-]	Technology	CO_2 costs [€/t CO_2]	Fuel costs [€/MWh_{th}]	η_{net} [-]	CO_2 costs [€/MWh_{el}][a]	Fuel costs [€/MWh_{el}]	$O\&M_{var}$ [€/MWh_{el}]	Total OPEX [€/MWh_{el}]
0.33	Nuclear large	27	3.3	0.309	0.00	10.68	1.71	12.39
0.33	Nuclear midsize	27	3.3	0.309	0.00	10.68	1.71	12.39
0.33	Nuclear small	27	3.3	0.309	0.00	10.68	1.71	12.39
0.33	Lignite large	27	60.0	0.406	26.57	147.78	3.58	177.94
0.33	Lignite midsize	27	60.0	0.370	29.16	162.16	3.58	194.90
0.33	Lignite small	27	60.0	0.350	30.83	171.43	3.58	205.83
0.33	Coal large	27	77.0	0.379	23.85	203.17	3.58	230.60
0.33	Coal midsize	27	77.0	0.380	23.79	202.63	3.58	230.00
0.33	Coal small	27	77.0	0.371	24.37	207.55	3.58	235.49
0.33	CCGT large	27	76.0	0.453	12.02	167.77	2.88	182.67
0.33	CCGT midsize	27	76.0	0.508	10.71	149.61	2.88	163.20
0.33	CCGT small	27	76.0	0.484	11.25	157.02	2.88	171.15
0.33	GT large	27	76.0	0.395	13.78	192.41	12.36	218.55
0.33	GT midsize	27	76.0	0.285	19.10	266.67	12.36	298.13
0.33	GT small	27	76.0	0.354	15.38	214.69	12.36	242.43
0.66	Nuclear large	60	3.3	0.309	0.00	10.68	1.71	12.39
0.66	Nuclear midsize	60	3.3	0.309	0.00	10.68	1.71	12.39
0.66	Nuclear small	60	3.3	0.309	0.00	10.68	1.71	12.39
0.66	Lignite large	60	86.0	0.406	59.05	211.82	3.58	274.46
0.66	Lignite midsize	60	86.0	0.370	64.80	232.43	3.58	300.81
0.66	Lignite small	60	86.0	0.350	68.50	245.71	3.58	317.80
0.66	Coal large	60	117.0	0.379	53.00	308.71	3.58	365.29
0.66	Coal midsize	60	117.0	0.380	52.86	307.89	3.58	364.34
0.66	Coal small	60	117.0	0.371	54.15	315.36	3.58	373.09
0.66	CCGT large	60	113.0	0.453	26.70	249.45	2.88	279.03
0.66	CCGT midsize	60	113.0	0.508	23.81	222.44	2.88	249.13
0.66	CCGT small	60	113.0	0.484	24.99	233.47	2.88	261.34
0.66	GT large	60	113.0	0.395	30.62	286.08	12.36	329.06
0.66	GT midsize	60	113.0	0.285	42.44	396.49	12.36	451.29
0.66	GT small	60	113.0	0.354	34.17	319.21	12.36	365.74
1.00	Nuclear large	75	3.3	0.309	0.00	10.68	1.71	12.39
1.00	Nuclear midsize	75	3.3	0.309	0.00	10.68	1.71	12.39
1.00	Nuclear small	75	3.3	0.309	0.00	10.68	1.71	12.39
1.00	Lignite large	75	100.0	0.406	73.82	246.31	3.58	323.70
1.00	Lignite midsize	75	100.0	0.370	81.00	270.27	3.58	354.85
1.00	Lignite small	75	100.0	0.350	85.63	285.71	3.58	374.92
1.00	Coal large	75	136.0	0.379	66.25	358.84	3.58	428.67
1.00	Coal midsize	75	136.0	0.380	66.08	357.89	3.58	427.55
1.00	Coal small	75	136.0	0.371	67.68	366.58	3.58	437.84
1.00	CCGT large	75	131.0	0.453	33.38	289.18	2.88	325.44
1.00	CCGT midsize	75	131.0	0.508	29.76	257.87	2.88	290.52
1.00	CCGT small	75	131.0	0.484	31.24	270.66	2.88	304.78
1.00	GT large	75	131.0	0.395	38.28	331.65	12.36	382.28
1.00	GT midsize	75	131.0	0.285	53.05	459.65	12.36	525.06
1.00	GT small	75	131.0	0.354	42.71	370.06	12.36	425.13

[a] The following specific emission factors were assumed [t CO_2/MWh_{th}]: uranium = 0.00, lignite = 0.40, coal = 0.33, natural gas = 0.20.

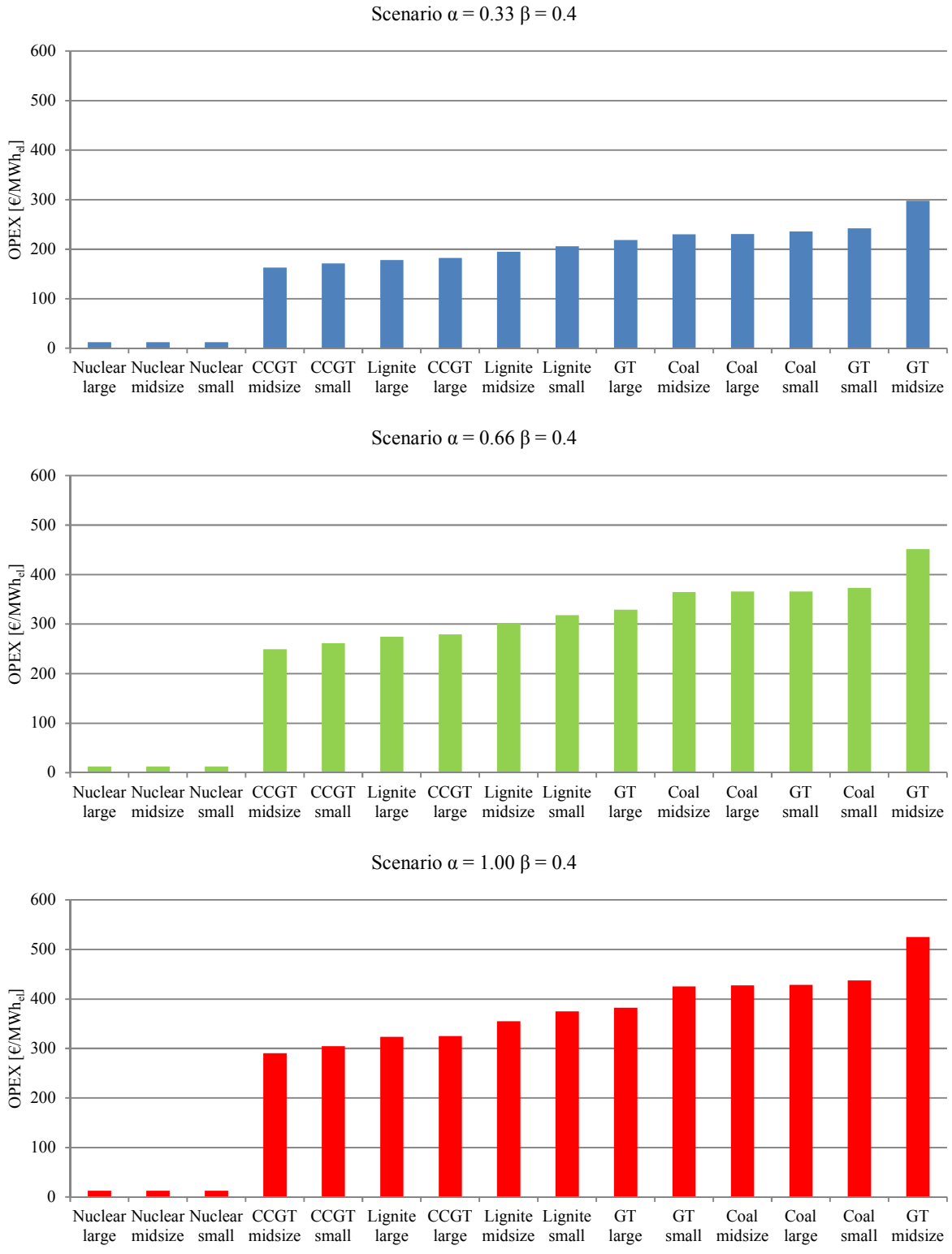

Fig. B 2: Merit order for the scenarios differing in their VRE share α for all power plant groups in the LP approach.

Tab. B 4: Cluster with regard to power plant technology type and plant size for the scenario with reduced number of blocks (485, 20, 5).

Technology group	Capacity group	Capacity range [MW]	Number of blocks [-]			Installed capacity [MW]
			485	20	5	
Nuclear	Large	> 800	8	1	1	20,400
Nuclear	Midsize	-	-	-	-	-
Nuclear	Small	-	-	-	-	-
Lignite	Large	> 800	2	1	-	3,800
Lignite	Midsize	400 ≤ 800	9	1	1	9,900
Lignite	Small	< 400	37	1	-	7,40
Coal	Large	> 550	6	1	-	9,000
Coal	Midsize	350 ≤ 550	10	1	1	8,000
Coal	Small	< 350	58	2	-	11,600
CCGT	Large	> 350	8	1		6,750
CCGT	Midsize	150 ≤ 350	13	1	1	6,500
CCGT	Small	< 150	119	3	-	4,740
Gas turbine	Large	> 150	1	1	-	400
Gas turbine	Midsize	50 ≤ 150	29	1	1	3,990
Gas turbine	Small	< 50	185	5	-	3,700
Total			485	20	5	96,180

Appendix C

1. Spatial examination area and resolution

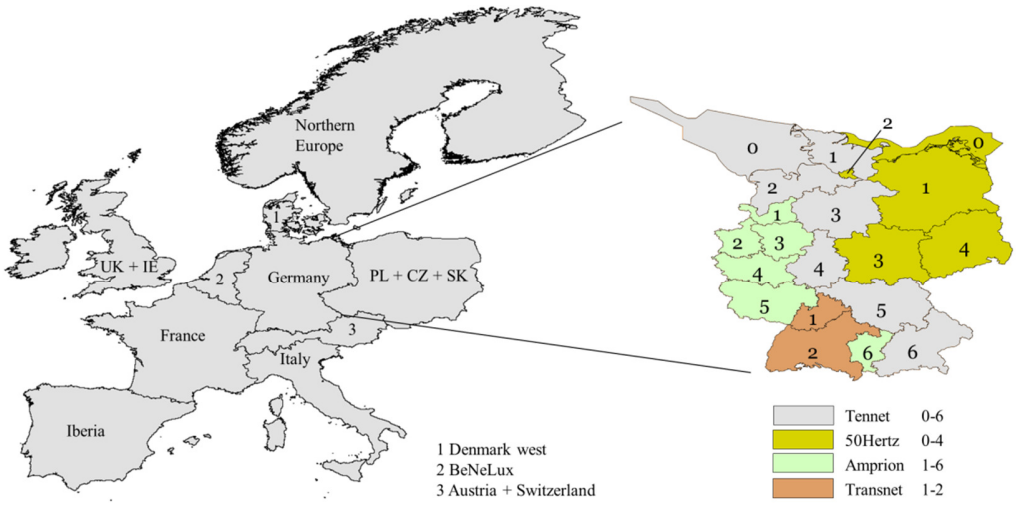

Fig. C 1: European and German observation area.

2. Electricity transmission grid

Storage systems allow a temporal decoupling of electricity demand and supply. The transmission and distribution grid, on the other hand, is able to shift energy on a spatial level. In this analysis both—the three-phase transmission system (AC) as well as the direct current (DC) grid—are considered. Both grid modeling approaches do not include each individual grid line but aggregate all lines of one model region to a link between two regions. The AC transmission system is modeled as a DC approximation (see [179]). It is characterized by its net transfer capacity (NTC) between two neighboring regions, length (approximate air-line distance between geographic centers of the regions), the associated losses, and the lifetime. In addition, investment cost assumptions for land- and sea-lines, necessary converter stations as well as fix and variable operations and maintenance costs are part of the optimization problem. The AC transmission line technology is considered to be a 380 kV four bundle Al/St, whereas DC differentiates between underground cables and overhead high voltage direct current lines as well as between various rated powers from 500 MW up to 3,200 MW for each line. This modeling approach neglects lower voltage levels (distribution grid) and assumes perfect electricity distribution without any losses or limitations within each model region (“copper plate”). The technical and economic

parameters for the AC and DC transmission grid can be found in Tab. C 1 and Tab. C 2. The values are based on [180, 181].

Tab. C 1: Technical parameter of AC and DC transmission grid.

	Rated power [MW]	Losses land [1/100Km][a]	Losses sea [1/100Km]	Losses converter [-][b]
HVDC_2200_UC	2,200	0.0035	0.0027	0.007
HVDC_3200	3,200	0.0045	0.0027	0.007
HVDC_1400	1,400	0.0045	0.0027	0.007
HVDC_1000	1,000	0.0045	0.0027	0.007
HVDC_0950	950	0.0045	0.0027	0.007
HVDC_0750	750	0.0045	0.0027	0.007
HVDC_0700	700	0.0045	0.0027	0.007
HVDC_0600	600	0.0045	0.0027	0.007
HVDC_0500	500	0.0045	0.0027	0.007
AC 380kV	1,500	0.0002[c]	0.0002	-

[a] Land losses for AC transmission grid given in 1/km.
[b] Losses factor for each converter station. Only modeled for DC transmission grid.
[c] The AC modeling approach does not differentiate between land and sea losses. The values here are therefore identical and should not be understood additively.

Tab. C 2: Length-specific overnight investment costs for AC and DC transmission grid lines based on [180, 181].

Scenario	Technology	Invest land [k€/km]	Invest sea [k€/km][a]	Interest rate [-]	Amor. time [a]	$O\&M_{fix}$
G+	AC 380kV	1,000	1,000	0.06	40	0.003
G+	HVDC_2200_UC	913	1,815	0.06	40	0.010
G+	HVDC_3200	384	2,640	0.06	40	0.010

[a] For the modeling of the AC transmission grid no differentiation between land and sea investment costs is considered. The values of invest land and invest sea are therefore identical and should not be understood additively.

The topology of the AC and DC transmission grid is based on the Ten Year Network Development Plan (TYNDP) of the European Network of Transmission System Operators for Electricity (ENTSO-E) [182]. However, the grid infrastructure used in this work was developed for the time horizon 2022 and therefore does not match the high amounts of RE capacities fostered by $80\%_{constr}$. In consequence, an initial model run with the grid topology of the TYNDP was performed and the NTCs of overloaded lines were increased subsequently. More specifically, the NTCs of the German offshore grid connection (Tennet0-Tennet1, 50Hertz0-50Hertz2) were increased by 5 GW. The resulting AC and DC transmission grids with their associated NTCs are illustrated in Fig. C 2.

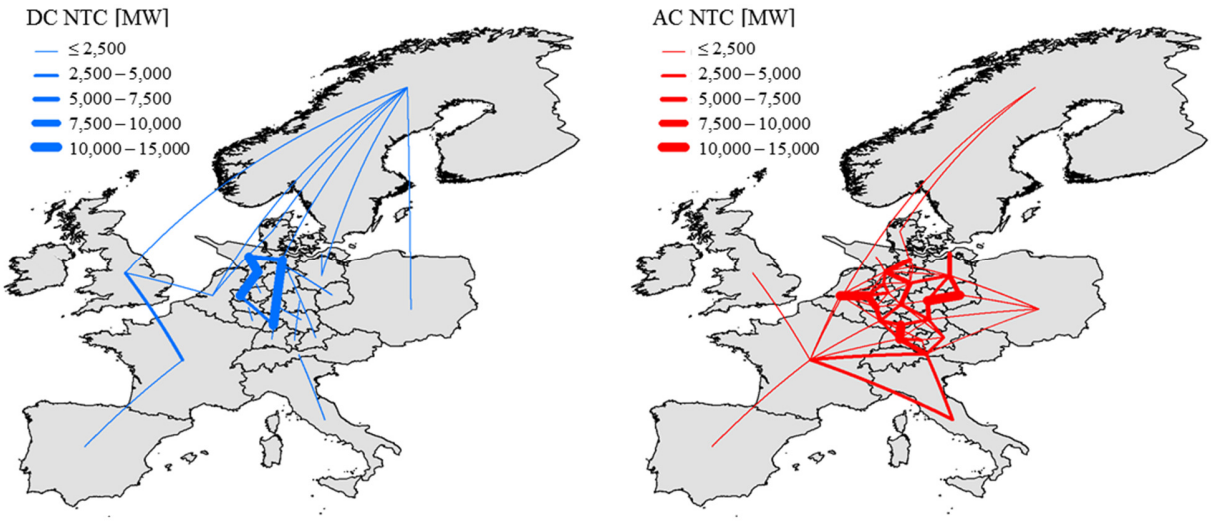

Fig. C 2: Exogenous AC and DC infrastructure for the European examination area based on a modification of the Ten Year Network Development Plan (TYNDP).

3. Stock of generation capacities

Although the capacity expansion of most of the generation technologies is endogenously optimized (partial greenfield approach), some technologies are exogenously pre-defined and illustrated in Tab. C 3. This either refers to capacities which were built before 2050 and still exist in the observation year (e.g. some fossil-fired technologies) or to technologies which capacities were defined based on an exogenous scenario.

Tab. C 3: Stock of generation capacities which were exogenously pre-defined for the year 2050.

	Existing generation capacities [GW]						
	Nuclear	Lignite	Coal	CSP	Geothermal power	Conventional hydro	PHS
Austria + Switzerland	-	-	-	-	0.90	14.45	4.32
BeNeLux	-	-	-	-	0.30	-	2.51
Denmark west	-	-	-	-	0.10	-	-
PL + CZ + SK	2.94	0.16	-	-	1.95	0.98	3.50
France	11.71	-	-	0.70	2.70	6.52	4.52
Iberia	-	-	-	7.88	3.50	15.54	6.30
Italy	-	-	1.00	1.00	3.74	3.35	5.94
Northern Europe	-	-	1.00	-	0.90	10.11	1.45
Germany	-	1.07	-	-	2.95	0.35	8.23
UK + IE	1.32	-	-	-	0.17	0.15	2.54
Total	15.97	1.23	2.00	9.58	17.21	51.44	39.31

4. Electricity generation from fossil-fired and nuclear power plants

REMix provides two modeling approaches for the representation of fossil-fired power plants: a linear programming- (LP, see [191]) and a mixed-integer, clustered unit-commitment approach (MIP, see [183]). For this analysis, the LP methodology was chosen, mainly due to its favorable computational performance. However, this approach neglects certain technological aspects of the power plant representation, such as part-load behavior or ramping constraints. Furthermore, LP modeling does not allow discrete dispatch and expansion decision variables (e.g. on/off decision of a specific power plant). The approach, however, seems sufficient, since the importance of the degree of detail in conventional power plant modeling decreases with increasing share of RE generation. Moreover, as shown in chapter 5, in highly renewable energy scenario for large observations areas (e.g. Europe) LP modeling for thermal power plants is sufficient when analyzing storage expansion. Conventional power plant technologies considered here comprise lignite and coal-fired power plants, gas turbines (GT), combined cycle gas turbines (CCGT), and nuclear power plants. Within the scenarios, capacity expansion of nuclear power plants is not allowed. The techno-economic parameters can be found in Tab. C 4, whereas the existing capacity stock is shown in Tab. C 3.

Tab. C 4: Techno-economic parameters for fossil-fired thermal power-plants which are relevant for the observation year 2050 due to their lifetime. Each technology is further separated into different cohorts' with regard to their construction year. These groups differentiate from each other only by their net and gross efficiencies η net and η gross. Furthermore, the table shows the availability, the amortization and lifetime, interest rate and specific investment costs. The wear and tear costs describe a cost factor that occurs due to power plant ramping. The variable operations and maintenance costs $O\&M_{var}$ are specific to the power output, while the fixed operations and maintenance costs $O\&M_{Fix}$ are related relatively to the total investment.

	Construc. year [-]	η gross [-]	η net [-]	Avail-ability [-]	Amor. time [a]	Life time [a]	Interest rate [-]	Investment costs [€/kW$_{el}$]	$O\&M_{Fix}$ [-]	$O\&M_{Var}$ [€/kWh$_{el}$]	Wear & tear costs [€/kW$_{el}$]
CCGT	2020	0.61	0.60	0.96	25	30	0.06	700	0.04	0.0003	0.0005
CCGT	2030	0.63	0.62	0.96	25	30	0.06	700	0.04	0.0003	0.0005
CCGT	2040	0.63	0.62	0.96	25	30	0.06	700	0.04	0.0003	0.0005
CCGT	2050	0.63	0.62	0.96	25	30	0.06	700	0.04	0.0003	0.0005
GT	2020	0.44	0.44	0.95	25	30	0.06	400	0.04	0.0003	0.0005
GT	2030	0.46	0.46	0.95	25	30	0.06	400	0.04	0.0003	0.0005
GT	2040	0.47	0.47	0.95	25	30	0.06	400	0.04	0.0003	0.0005
GT	2050	0.47	0.47	0.95	25	30	0.06	400	0.04	0.0003	0.0005
Lignite	2010	0.46	0.43	0.90	25	40	0.06	1,500	0.04	0.0001	0.0015
Lignite	2020	0.50	0.47	0.90	25	40	0.06	1,500	0.04	0.0001	0.0015
Lignite	2030	0.52	0.49	0.90	25	40	0.06	1,500	0.04	0.0001	0.0015
Lignite	2040	0.52	0.49	0.90	25	40	0.06	1,500	0.04	0.0001	0.0015
Lignite	2050	0.52	0.49	0.90	25	40	0.06	1,500	0.04	0.0001	0.0015
Nuclear	2000	0.32	0.31	0.90	25	50	0.06	5,000[a]	0.04[a]	0.0001	0.0015
Nuclear	2010	0.32	0.31	0.90	25	50	0.06	5,000[a]	0.04[a]	0.0001	0.0015
Nuclear	2020	0.32	0.31	0.90	25	50	0.06	5,000[a]	0.04[a]	0.0001	0.0015
Nuclear	2030	0.32	0.31	0.90	25	50	0.06	5,000[a]	0.04[a]	0.0001	0.0015
Nuclear	2040	0.32	0.31	0.90	25	50	0.06	5,000[a]	0.04[a]	0.0001	0.0015
Nuclear	2050	0.32	0.31	0.90	25	50	0.06	5,000[a]	0.04[a]	0.0001	0.0015

[a] Not used since the capacity expansion of nuclear power plants is restricted.

4.1. Fuel price and CO_2 emission certificate assumptions

Tab. C 5: Prices for each fuel type and CO_2 emission costs scenarios for the sensitivity analysis (see Sec. 6.3.5).

Fuel type	Fuel price [€$_{2010}$/MWh$_{therm}$]	Source
Coal	20.88	[189]
Lignite	9.18	[184]
Natural gas	47.52	[189]
Uranium	5.24	[185]

[a] Scenario B, moderate price path.

Cost scenario	CO_2 costs [€/tCO_2]	Source
Reference	57	[192][a]
High	150	Own assumption

[a] Price path B.

5. Electricity generation from variable renewable energies (VRE)

The model includes representations of photovoltaic, on- and offshore wind as well as run-of-the-river hydroelectricity. Conventional hydroelectricity, sometimes referred to as impoundment facilities ('dams'), are accounted as dispatchable renewable energy and therefore covered in Sec 6. In order to derive the cost optimal dispatch of VRE, REMix requires the potential, technology and region-specific, hourly renewable electricity generation on the one hand (solar irradiation, wind speeds, water runoff) as input (see Fig. C 3). On the other hand, for the capacity expansion, an upper threshold for the maximal installable capacity based on the renewable resource potential of the region is necessary (e.g. maximum installable PV capacity in one region, see Fig. 21).

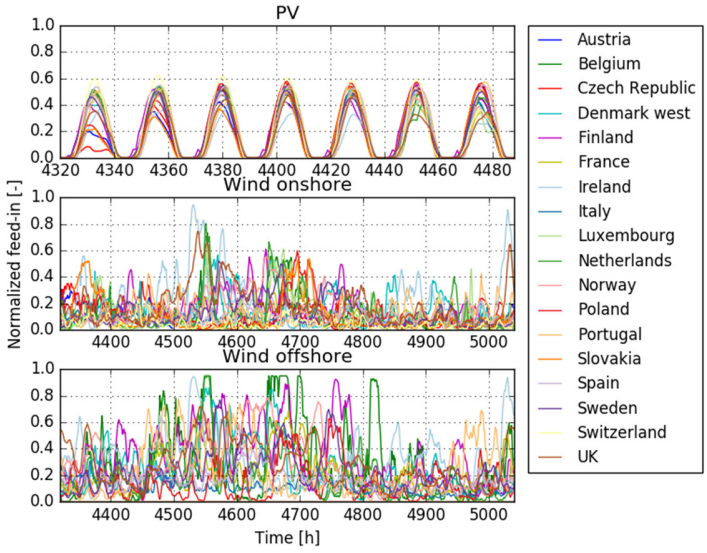

Fig. C 3: Potential technology and region-specific, hourly renewable electricity generation of PV, wind on, and offshore based on the Energy Data Analysis Tool (EnDAT).

Both, the potential renewable generation time-series as well as the maximal installable capacities are a result of the REMix sub-model EnDAT (Energy Data Analysis Tool) and based on the weather year 2006. In terms of annual electricity generation potential for the VRE technologies, this year shows rather small variations from the mean annual electricity generation over the time period of 2006–2012 (see [186, 187]). It, therefore, can be considered as a 'typical' weather year and is suitable as a base year. Moreover, in the sensitivity analysis, the effect of different weather years has been analyzed (see Sec. 6.3.5). The results show that their influence with regard to storage and capacity expansion is negligible. The optimized VRE feed-in derives from the potential generation less the curtailments. The techno-economic parameters of all VRE technologies are shown in Tab. C 6.

Tab. C 6: Technology and cost parameter for electricity generation from variable renewable energies. Values are based on [189]. The fixed operations and maintenance costs $O\&M_{Fix}$ are related relatively to the total investment.

Technology	Invest [€/kW_{el}]	Amor. time [a]	Interest rate [-]	$O\&M_{fix}$ [-]
PV	903	20	0.06	0.010
Offshore wind	1,300	18	0.06	0.055
Onshore wind	900	18	0.06	0.040
Hydro run-of-the-river	5,030	60	0.06	0.050

6. Electricity generation from dispatchable renewable energies

Within the REMix model, dispatchable renewable energies include electricity generation from concentrating solar power (CSP), geothermal and solid biomass systems, and conventional hydroelectricity (reservoir hydroelectricity). Although the electricity generation from conventional hydroelectricity and CSP is dependent on a fluctuating resource, i.e. water inflow and solar irradiation, their ability to store energy over several hours makes these technologies dispatchable to some extent.

6.1. Concentrating solar power (CSP)

The modeling of CSP power plants includes a solar field (SF), a thermal energy storage (TES), a power block (PB), and a natural gas-fired backup system. Additionally to the dispatch optimization, the dimensioning of these components can be endogenously and individually determined by the model. As another option, the model allows using a pre-defined TES to PB ratio and a solar multiple. The latter describes the ratio of the SF to the PB. For the analysis at hand, the expansion of each individual component is not treated model endogenously but fixed via a solar multiple of three and a TES to PB ratio of 12. Based on the hourly solar irradiation, the thermal output of the SF is calculated by the sub-model EnDAT. The TES is characterized by

the hourly charging and discharging as well as the associated efficiencies, the storage level, and a self-discharge rate. The techno-economic parameters are shown in Tab. C 7.

Tab. C 7: Technology and cost parameter for electricity generation from concentrating solar power plants. Values are based on [189]. The variable operations and maintenance costs $O\&M_{var}$ are specific to the power output of the power block, while the fixed operations and maintenance costs $O\&M_{Fix}$ are related relatively to the total investment.

CSP		
Invest SF	[€/kW_{therm}]	252
Invest TES	[€/kWh_{therm}]	25
Invest PB	[€/kW_{el}]	971
η TES	[-]	0.95
η PB	[-]	0.37
TES to PB ratio	[-]	12
TES self-discharge rate	[-]	0.0005
SM	[-]	3
Availability	[-]	0.95
Amortization time	[a]	25
Interest rate	[-]	0.06
$O\&M_{fix}$	[-]	0.025
$O\&M_{var}$	[€/kWh_{el}]	0.0000001

6.2. Solid biomass and geothermal systems

For solid biomass systems, REMix endogenously determines the capacities. In this analysis, no upper capacity expansion limits (technical potential) are assumed. The techno-economic parameters of biomass and geothermal systems are shown in Tab. C 8.

Tab. C 8: Technology and cost parameter for electricity generation from biomass and geothermal systems. Values are based on [190]. The variable operations and maintenance costs $O\&M_{var}$ are specific to the power output, while the fixed operations and maintenance costs $O\&M_{Fix}$ are related relatively to the total investment.

Technology	η [-]	Availability [-]	Invest [€/kW_{el}]	Amortization time [a]	Interest rate [-]	$O\&M_{fix}$ [-]	$O\&M_{var}$ [€/kWh_{el}]
Solid biomass	0.28	0.95	2,500	20	0.06	0.05	0.0000001
Geothermal	0.11	0.95	7,600[a]	20	0.06	0.045	0.0000001

[a] Not used for optimization since only dispatch optimization is applied for geothermal technologies.

Geothermal electricity generation is modeled via pre-defined scenario capacities. In consequence, only the dispatch is optimized, but no capacity expansion. The values are based on [193] and shown subsequently.

Tab. C 9: European exogenous scenario capacities for electricity generation from geothermal systems based on [193]. The German regions are aggregated and a model region-specific illustration is shown in Tab. C 10.

Country	Model region	Capacity [MW]
Austria	Austria + Switzerland	200
Switzerland	Austria + Switzerland	700
Belgium	BeNeLux	150
Netherlands	BeNeLux	135
Luxembourg	BeNeLux	15
Denmark west	Denmark west	100
Czech Republic	PL + CZ + SK	1,300
Poland	PL + CZ + SK	500
Slovakia	PL + CZ + SK	150
France	France	2,700
Portugal	Iberia	1,300
Spain	Iberia	2,200
Italy	Italy	3,738
Finland	Northern Europe	200
Norway	Northern Europe	200
Sweden	Northern Europe	400
Denmark east	Northern Europe	100
Germany	Germany	2,950
Ireland	UK + IE	70
UK	UK + IE	100

Tab. C 10: German exogenous scenario capacities for electricity generation from geothermal systems based on [193].

Country	Model region	Capacity [MW]
Germany	Amprion1	103
Germany	Amprion2	98
Germany	Amprion3	105
Germany	Amprion4	40
Germany	Amprion5	184
Germany	Amprion6	92
Germany	Transnet1	95
Germany	Transnet2	325
Germany	Tennet0	-
Germany	Tennet1	108
Germany	Tennet2	174
Germany	Tennet3	264
Germany	Tennet4	73
Germany	Tennet5	267
Germany	Tennet6	186
Germany	50Hertz0	-
Germany	50Hertz1	604
Germany	50Hertz2	13
Germany	50Hertz3	98
Germany	50Hertz4	121

6.3. Conventional hydroelectricity

For conventional hydroelectricity, the model uses a daily, model region-specific, normalized (with regard to the turbine power) water inflow to the upper reservoir, based on a GIS analysis in [213] of the sub-model EnDAT (see Fig. C 4). In order to use the daily resolution in the hourly REMix model, all 24 hours of one day are characterized by the same inflow value. This approximation is valid assumption as the temporal variability of conventional hydroelectricity typically is based on seasonal cycles, influenced by water runoff due to the melting of snow and precipitation. Moreover, in this analysis, conventional hydroelectricity modeling relies on systems with a water reservoir as storage, and, as shown in Haydt et al. [188], hourly variations of the water inflow are negligible in such approaches.

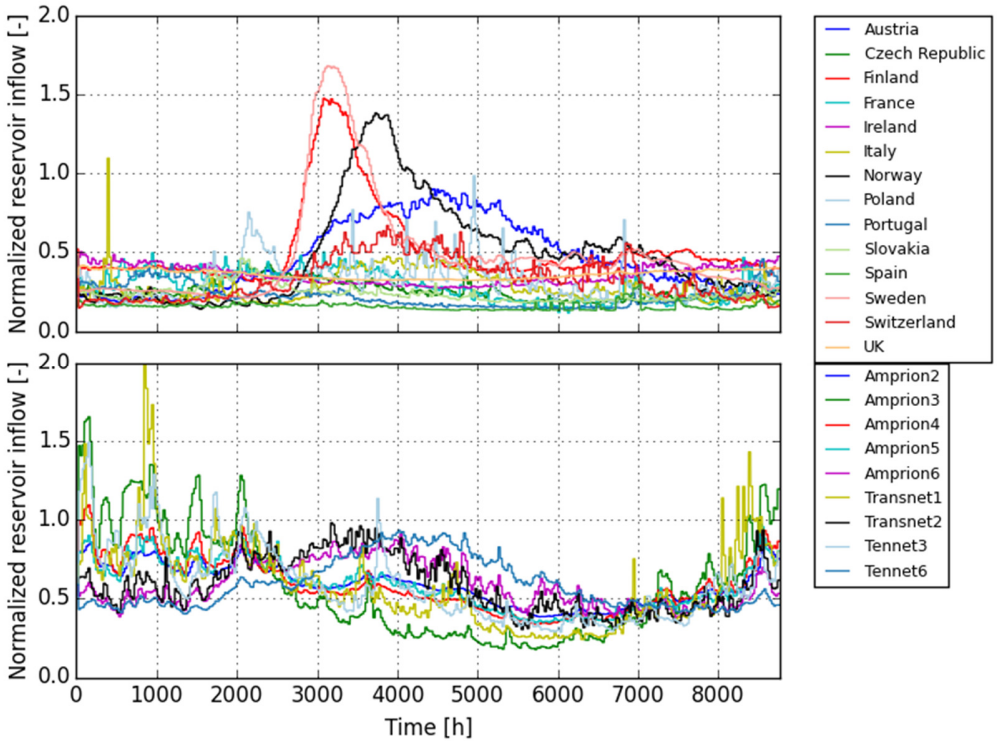

Fig. C 4: Normalized, hourly water inflow based on calculations of the REMix sub-model EnDAT. The upper plot shows all considered European model regions excluding the German regions. The lower plot depicts all relevant German model regions. The normalized values can be > 1 since the normalization of the water inflow is calculated with regard to the turbine power.

Furthermore, REMix is able to calculate new capacities for the turbine, also including the option to retrofit existing systems with a pump if a suitable lower reservoir is existent. In this analysis, however, the dispatch of pre-defined, exogenous pump and turbine capacities is optimized, based on data from [191, 213] (see Tab. C 12, Tab. C 13). The techno-economic parameters of conventional hydroelectricity are shown in Tab. C 11. Purely PHS systems are covered in Sec. 8.

Tab. C 11: Technology and cost parameter for electricity generation from conventional, reservoir hydropower plants. Values are based on [189, 190]. The variable operations and maintenance costs $O\&M_{var}$ are specific to the power output, while the fixed operations and maintenance costs $O\&M_{Fix}$ are related relatively to the total investment.

Technology	η turbine [-]	η pump[a] [-]	Availability [-]	Invest system [€/kW$_{el}$]	Invest retrofit pump [€/kW$_{el}$]	Amor. time system [a]	Amor. time pump [a]	Interest rate [-]	$O\&M_{fix}$ [-]	$O\&M_{var}$ [€/kWh$_{el}$]
Reservoir hydro	0.90	0.89	0.98	1,565	640	60	20	0.06	0.05	0.0000001

[a] Only used if the reservoir hydro system is retrofitted with a pump.

Tab. C 12: European turbine and pump power (if retrofitted) as well as the reservoir capacity of conventional hydroelectricity based on [191, 213]. The German regions are here shown aggregated and a model region-specific illustration is shown in Tab. C 13.

Country	Model region	Turbine power [MW]	Pump power [MW]	Reservoir capacity [MWh_{el}]
Austria	Austria + Switzerland	5,500	3,006	3,259,259
Switzerland	Austria + Switzerland	10,000	3,219	8,842,105
Belgium	BeNeLux	-	-	-
Netherlands	BeNeLux	-	-	-
Luxembourg	BeNeLux	-	-	-
Denmark west	Denmark west	-	-	-
Czech Republic	PL + CZ + SK	660	-	737,975
Poland	PL + CZ + SK	156	-	174,430
Slovakia	PL + CZ + SK	167	-	186,730
France	France	12,317	-	10,405,741
Portugal	Iberia	2,426	-	3,003,619
Spain	Iberia	13,113	-	31,334,961
Italy	Italy	3,350	-	3,576,351
Finland	Northern Europe	593	-	663,059
Norway	Northern Europe	8,960	846	102,057,707
Sweden	Northern Europe	832	-	930,295
Denmark east	Northern Europe	-	-	-
Germany	Germany	350	-	391,361
UK	UK + IE	25	-	27,954
Ireland	UK + IE	122	-	136,414

Tab. C 13: German turbine and pump power (if retrofitted) as well as the reservoir capacity of conventional hydroelectricity based on [191, 213].

Country	Model region	Turbine power [MW]	Pump power [MW]	Reservoir capacity [MWh_{el}]
Germany	Amprion1	-	-	-
Germany	Amprion2	11	-	11,785
Germany	Amprion3	19	-	21,144
Germany	Amprion4	8	-	9,415
Germany	Amprion5	30	-	32,985
Germany	Amprion6	134	-	149,798
Germany	Transnet1	17	-	18,841
Germany	Transnet2	116	-	129,693
Germany	Tennet1	-	-	-
Germany	Tennet2	-	-	-
Germany	Tennet3	2	-	2,359
Germany	Tennet4	-	-	-
Germany	Tennet5	-	-	-
Germany	Tennet6	14	-	15,341
Germany	50Hertz1	-	-	-
Germany	50Hertz2	-	-	-
Germany	50Hertz3	-	-	-
Germany	50Hertz4	-	-	-

7. Electricity demand

Tab. C 14: Annual electricity demand for all model regions of the observation area for the year 2050.

Country	Model region	El. demand [TWh][a]
Austria	Austria + Switzerland	60.43
Switzerland	Austria + Switzerland	60.38
Belgium	BeNeLux	82.47
Netherlands	BeNeLux	109.93
Luxembourg	BeNeLux	6.63
Denmark west	Denmark west	22.4
Czech Republic	PL + CZ + SK	72.03
Poland	PL + CZ + SK	162.83
Slovakia	PL + CZ + SK	22.87
France	France	473.88
Portugal	Iberia	55.86
Spain	Iberia	284.95
Italy	Italy	331.7
Finland	Northern Europe	77.75
Norway	Northern Europe	119.71
Sweden	Northern Europe	132.53
Denmark east	Northern Europe	13.32
Germany	Germany[b]	514
UK	UK + IE	343.85
Ireland	UK + IE	29.78

[a] The annual electricity demand for Germany is based on a modified version of scenario A of [192]. Opposed to [192], the electricity demand for this analysis excludes the demand for electric vehicles (44 TWh/a) and heat pumps (16 TWh/a). These values again are based on [193]. For the European countries values from [194, 195] were used. In order to disaggregate Germany's electricity demand to the 20 sub-regions, artificial surfaces and associated areas from [213] were applied, which again are based on [196] and [197].

[b] In this table the German model regions are aggregated to Germany. The actual model region resolution within Germany is shown in Fig. C 1.

8. Storage technologies

8.1. Techno-economic parameters

Tab. C 15: Technology and cost parameter for all considered storage technologies. Values are based on [198–204, 208]. The variable operations and maintenance costs $O\&M_{var}$ are specific to storage charging, while the fixed operations and maintenance costs $O\&M_{Fix}$ are related relatively to the total investment.

	aCAES	H_2	Li-ion	PHS	Redox-flow
Invest storage [€/kWh$_{el}$]	47	1	150	10	100
Invest converter [€/kW$_{el}$]	570	1,200	50	450	630
Amortization time$_{storage}$ [a]	40	30	25	60	20
Amortization time$_{converter}$ [a]	20	15	25	20	20
Interest-rate [-]	0.06	0.06	0.06	0.06	0.06
$O\&M_{fix}$ [-]	0.010	0.020	0.005	0.010	0.032
$O\&M_{var}$ [€/kWh]	0.00001	0.00001	0.00001	0.00001	0.00001
η charge [-]	0.84	0.75	0.97	0.91	0.92
η discharge [-]	0.89	0.62	0.97	0.91	0.92
Self-discharge rate [-]	0.000833	0.000000	0.000011	0.000005	0.000054
Availability [-]	0.95	0.95	0.98	0.98	0.98

8.2. Potentials for pumped hydropower

Due to the long lifetime of the storage unit, i.e. the water reservoir, existing PHS also play a role for the observation year 2050. For Germany, the existing pump and turbine power are based on a literature review. The data is shown in Tab. C 16.

For converter power in the other European countries, the Platts World Electric Power Plants Database (WEPP) of 2010 is used [210]. This database, however, does not provide information for the storage capacity. To conclude from converter power to the storage capacity, an energy-to-power ratio (E2P) of 7h for all PHS is assumed.

Within the analysis, PHS expansion is limited by the potential storage capacity of the reservoirs (technical potential), whereas the power for the turbine and the pump has no upper limit. For the installable storage capacity, Gimeno-Guitiérrz and Arantegui [205] provide a GIS-based assessment of PHS potentials. Here, a conservative scenario (“Topology 1, realisable potential”) of this study is used, where for example no further capacity expansion of PHS in Germany is assumed. The calculation of the PHS potentials in this scenario requires two existing reservoirs with an adequate difference in elevation and a sufficient proximity to connect both with a new penstock and electrical equipment. Furthermore, a number of constraints, such as centers of population, protected natural areas or transport infrastructure, reduce the potential for the storage capacity. The technical potential for the PHS storage capacity for each region can be found in Tab. 10 in the main text. To conclude from the German potential storage capacity of

[205] to the German model regions as used in this analysis (see Fig. C 1), it is assumed that the storage potentials within Germany are equally distributed as the already existing PHS systems.

Tab. C 16: Existing German PHS capacities mapped to the model regions based on [206–209].

Location[b]	Model region	Turbine power [MW]	Storage capacity [MWh_{el}]
Atdorf[a]	Transnet2	1,400	13,000
Blautal[a]	Transnet2	46	370
Bleiloch	50Hertz3	80	753
Einoden[a]	Tennet6	200	1,600
Einsiedel	Transnet2	1	23
Erzhausen	Tennet3	220	940
Geesthacht	Tennet2	120	600
Glems	Transnet2	90	560
Goldisthal	50Hertz3	1,060	8,480
Happburg	Tennet5	160	900
Häusern	Transnet2	144	514
Hohenwarte I	50Hertz3	63	795
Hohenwarte II	50Hertz3	320	2,087
Koepchenwerk Herdecke	Amprion3	153	590
Langenprozelten	Tennet5	168	950
Leitzachwerk 1	Tennet6	49	225[c]
Leitzachwerk 2	Tennet6	49	225[c]
Markersbach	50Hertz4	1,050	4,018
Maxhofen-Oberberg	Tennet6	10	547
Niederwartha	50Hertz4	120	591
Reisach Rabenleite	Tennet5	105	630
Rönkhausen	Amprion3	140	690
Säckingen	Transnet2	353	2,064
Schwarzenbachwerk	Transnet2	45	198
Sorpetalsperre	Amprion3	10	44
Tanzmühle Rabenleite	Tennet5	35	404
Waldeck 1	Tennet4	140	478
Waldeck 2	Tennet4	440	3,428
Waldshut	Transnet2	176	476
Wehr	Transnet2	980	6,073
Wendefurth	50Hertz3	80	523
Witznau	Transnet2	220	642
Total		8,227	53,418

[a] Planned and therefore included (at the time of the model parametrization).
[b] PHS capacities that are connected to the German transmission grid infrastructure but not located in Germany are not accounted to the German model regions. This applies for the PHS Vianden (Luxembourg) and the Austrian units Robund I/II, Kopswerk II, Kühtai/Sellrain-Silz, and Lünersee.
[c] Leitzachwerk 1 and 2 share the same reservoir but have 2 power blocks (each consisting of a pump and a turbine). To account for that in the modeling approach, the storage capacity of 550 MWh_{el} is divided by 2.

Tab. C 17: Existing European PHS capacities based on [210].

Model region	Turbine power [GW]	Storage capacity [GWh_{el}]
Austria + Switzerland	4.32	30.25
BeNeLux	2.51	17.56
Denmark west	0.00	0.00
PL + CZ + SK	3.50	24.50
France	4.52	31.64
Iberia	6.30	44.12
Italy	5.94	41.55
Northern Europe	1.45	10.16
UK + IE	2.54	17.79
Total	39.31	271.08

8.3. Potentials for adiabatic compressed air and hydrogen storage

As for PHS, the capacity expansion of aCAES is only constrained by an upper limit of the storage unit (technical potential) and hence the volume of an underground salt cavern. The converter power for aCAES is not limited. As for all storage technologies in this analysis, the charging and discharging converter unit are not modeled individually. In this regard, the converter power of an aCAES consists of the compression unit and the generator. The potentials for the underground salt cavern are based on [213], which, in turn, relies on data from [211]. These volumina are converted into storable electric energy via an energy density of 2.73 kWh_{therm}/m^3 (lower heating value). This value again is based on an aCAES pressure difference from 30 to 70 bar [212].

Using the specific energy density of gaseous H_2 at a pressure of 120bar and a temperature of 300 K in the cavern, the cavern volumina potentials from [213] are converted into storable electricity. For H_2 storage the charging converter unit is an alkaline water electrolyzer; the discharging converter a CCGT. Again, the converter power for the electricity reconversion is not constrained by an upper expansion limit. Since both, aCAES and H_2 storage, require an underground salt cavern as a storage unit, it is assumed that these technologies both use 50% of the resource potential.

9. Detailed results

9.1. Overall generation capacities in Europe

The following tables show the overall generation capacities for all European model regions. The values of the German model regions (see Fig. C 1) are aggregated (*Germany*).

Tab. C 18: Overall generation capacities in GW for the *reference scenario*, including the model endogenously derived capacities as well as the exogenous stock. The table refers to Fig. 22.

	Austria + Switzerland	BeNeLux	Denmark west	PL + CZ+ SK	France	Iberia	Italy	Northern Europe	Germany	UK + IE
Offshore wind	-	43.20	9.97	0.05	106.74	64.44	29.95	89.66	47.51	72.81
Onshore wind	22.00	18.72	2.59	80.89	33.35	2.88	62.14	0.37	54.86	50.41
PV	19.91	35.51	0.06	59.78	46.74	90.45	47.73	5.03	86.90	0.06
Run-of-river	0.02	0.01	-	0.01	0.01	0.01	0.01	0.02	4.24	0.01
Hydro res.	14.45	-	-	0.98	6.52	15.54	3.35	10.11	0.35	0.15
CSP	-	-	-	-	0.70	7.88	1.00	-	-	-
Lignite	0.65	0.08	0.02	8.09	0.02	0.07	15.62	0.04	21.42	0.02
CCGT	0.04	0.24	0.02	5.13	0.12	0.10	2.05	1.23	7.20	0.04
Coal	0.03	0.03	0.02	0.05	0.02	0.03	1.05	1.03	0.63	0.02
GT	0.05	2.52	0.04	5.11	13.19	0.05	4.89	21.84	10.1	0.26
Geothermal	0.90	0.30	0.10	1.95	2.70	3.50	3.74	0.90	2.95	0.17
Nuclear	0.01	0.01	0.01	2.95	11.72	0.01	0.01	0.01	0.17	1.33

Tab. C 19: Overall generation capacities in GW for the scenario *Stor_Inv_low*, including the model endogenously derived capacities as well as the exogenous stock. The table refers to Fig. 29.

	Austria + Switzerland	BeNeLux	Denmark west	PL + CZ + SK	France	Iberia	Italy	Northern Europe	Germany	UK + IE
Offshore wind	-	53.87	8.03	0.01	133.73	60.79	16.78	89.12	45.35	71.69
Onshore wind	22.00	18.72	6.38	80.89	4.41	0.73	62.14	0.13	55.42	50.41
PV	19.91	35.51	0.02	59.78	11.16	90.45	47.73	0.12	86.00	0.02
Run-of-river	0.01	0.00	0.00	0.00	0.00	0.00	0.00	0.00	3.14	0.00
Hydro res.	14.45	-	-	0.98	6.52	15.54	3.35	10.11	0.35	0.15
CSP	-	-	-	-	0.70	7.88	1.00	-	-	-
Lignite	0.86	0.01	0.01	7.51	0.01	0.01	18.20	0.01	19.01	0.01
CCGT	0.01	0.01	0.01	3.18	0.01	0.01	0.85	0.14	2.96	0.01
Coal	0.01	0.01	0.01	0.02	0.01	0.01	1.02	1.01	0.25	0.01
GT	0.02	0.02	0.01	0.05	0.02	0.02	4.16	18.27	2.11	0.01
Geothermal	0.90	0.30	0.10	1.95	2.70	3.50	3.74	0.90	2.95	0.17
Nuclear	0.01	0.00	0.00	2.94	11.71	0.00	0.01	0.00	0.07	1.32

Tab. C 20: Overall generation capacities in GW for the scenario *Stor_Inv_high*, including the model endogenously derived capacities as well as the exogenous stock. The table refers to Fig. 29.

	Austria + Switzerland	BeNeLux	Denmark west	PL + CZ + SK	France	Iberia	Italy	Northern Europe	Germany	UK + IE
Offshore wind	-	35.99	10.31	0.07	92.10	63.81	40.47	91.83	50.33	92.18
Onshore wind	22.00	18.72	1.20	80.89	54.28	9.17	62.14	0.59	54.90	25.83
PV	19.91	35.51	0.11	59.78	62.98	90.45	47.73	8.12	90.62	0.13
Run-of-river	0.05	0.02	0.01	0.02	0.01	0.01	0.02	0.02	4.24	0.01
Hydro res.	14.45	-	-	0.98	6.52	15.54	3.35	10.11	0.35	0.15
CSP	-	-	-	-	0.70	7.88	1.00	-	-	-
Lignite	0.45	0.36	0.02	8.61	0.04	0.12	13.86	0.05	21.58	0.03
CCGT	0.05	3.86	0.04	5.11	0.19	0.99	2.56	1.58	9.30	0.07
Coal	0.04	0.06	0.02	0.07	0.03	0.05	1.08	1.04	0.88	0.03
GT	0.07	6.61	0.06	7.17	22.33	0.11	5.60	21.74	13.48	10.52
Geothermal	0.90	0.30	0.10	1.95	2.70	3.50	3.74	0.90	2.95	0.17
Nuclear	0.02	0.01	0.01	2.95	11.72	0.01	0.02	0.01	0.22	1.33

Tab. C 21: Overall generation capacities in GW for the scenario *VRE_Inv_low*, including the model endogenously derived capacities as well as the exogenous stock. The table refers to Fig. 29.

	Austria + Switzerland	BeNeLux	Denmark west	PL + CZ + SK	France	Iberia	Italy	Northern Europe	Germany	UK + IE
Offshore wind	-	44.36	9.42	0.09	83.06	58.00	43.58	89.30	53.13	107.78
Onshore wind	22.00	18.72	0.83	80.89	62.06	17.84	62.14	1.10	55.42	0.84
PV	19.91	35.51	0.22	59.78	63.88	90.45	47.73	17.09	93.13	2.27
Run-of-river	1.89	0.02	0.01	0.02	0.02	0.01	0.02	0.02	4.24	0.01
Hydro res.	14.45	-	-	0.98	6.52	15.54	3.35	10.11	0.35	0.15
CSP	-	-	-	-	0.70	7.88	1.00	-	-	-
Lignite	0.05	0.06	0.02	8.33	0.02	0.03	12.89	0.03	19.67	0.02
CCGT	0.03	0.26	0.03	5.21	0.14	0.04	2.82	1.36	7.99	0.06
Coal	0.02	0.03	0.02	0.04	0.02	0.02	1.04	1.03	0.54	0.02
GT	0.04	5.35	0.04	6.09	23.81	0.05	5.58	21.31	14.27	13.31
Geothermal	0.90	0.30	0.10	1.95	2.70	3.50	3.74	0.90	2.95	0.17
Nuclear	0.01	0.01	0.01	2.95	11.72	0.01	0.01	0.01	0.15	1.33

Tab. C 22: Overall generation capacities in GW for the scenario *VRE_Inv_high*, including the model endogenously derived capacities as well as the exogenous stock. The table refers to Fig. 29.

	Austria + Switzerland	BeNeLux	Denmark west	PL + CZ + SK	France	Iberia	Italy	Northern Europe	Germany	UK + IE
Offshore wind	-	43.59	8.36	0.03	129.24	62.26	20.34	88.17	45.39	72.30
Onshore wind	22.00	18.72	6.36	80.89	18.30	0.95	62.14	0.28	55.34	50.41
PV	19.91	35.51	0.04	59.78	23.78	90.45	47.73	0.24	86.10	0.04
Run-of-river	0.01	0.01	0.00	0.01	0.01	0.01	0.01	0.01	2.67	0.01
Hydro res.	14.45	-	-	0.98	6.52	15.54	3.35	10.11	0.35	0.15
CSP	-	-	-	-	0.70	7.88	1.00	-	-	-
Lignite	1.00	0.08	0.02	7.75	0.02	0.60	17.44	0.05	22.22	0.02
CCGT	0.05	0.32	0.03	5.36	0.08	0.73	1.54	1.67	7.73	0.03
Coal	0.03	0.04	0.02	0.06	0.02	0.05	1.06	1.04	0.76	0.02
GT	0.06	0.62	0.04	3.99	0.19	0.05	4.62	20.10	8.48	0.06
Geothermal	0.90	0.30	0.10	1.95	2.70	3.50	3.74	0.90	2.95	0.17
Nuclear	0.01	0.01	0.01	2.95	11.72	0.01	0.01	0.01	0.19	1.33

Tab. C 23: Overall generation capacities in GW for the scenario *FP_low*, including the model endogenously derived capacities as well as the exogenous stock. The table refers to Fig. 29.

	Austria + Switzerland	BeNeLux	Denmark west	PL + CZ + SK	France	Iberia	Italy	Northern Europe	Germany	UK + IE
Offshore wind	-	40.00	10.16	0.04	104.38	63.06	37.25	89.23	48.18	73.34
Onshore wind	22.00	18.72	2.45	80.89	32.55	2.07	62.14	0.39	54.68	50.41
PV	19.91	35.51	0.07	59.78	49.50	90.45	47.73	4.26	87.19	0.06
Run-of-river	0.03	0.01	0.00	0.01	0.01	0.01	0.01	0.01	4.23	0.01
Hydro res.	14.45	-	-	0.98	6.52	15.54	3.35	10.11	0.35	0.15
CSP	-	-	-	-	0.70	7.88	1.00	-	-	-
Lignite	0.02	0.02	0.01	0.18	0.02	0.02	0.02	0.02	1.38	0.01
CCGT	0.08	2.90	0.03	13.21	0.11	1.04	17.02	2.20	29.06	0.04
Coal	0.02	0.02	0.01	0.03	0.02	0.02	1.03	1.02	0.39	0.02
GT	0.05	2.66	0.04	4.29	14.47	0.06	3.50	21.15	7.64	0.21
Geothermal	0.90	0.30	0.10	1.95	2.70	3.50	3.74	0.90	2.95	0.17
Nuclear	0.02	0.01	0.01	2.95	11.72	0.01	0.02	0.01	0.25	1.33

Tab. C 24: Overall generation capacities in GW for the scenario *FP_high*, including the model endogenously derived capacities as well as the exogenous stock. The table refers to Fig. 29.

	Austria + Switzerland	BeNeLux	Denmark west	PL + CZ + SK	France	Iberia	Italy	Northern Europe	Germany	UK + IE
Offshore wind	-	42.47	8.56	0.04	117.38	62.91	19.24	92.52	45.87	71.36
Onshore wind	22.00	18.72	3.47	80.89	36.32	2.81	62.14	0.37	54.75	50.41
PV	19.91	35.51	0.05	59.78	36.76	90.45	47.73	1.60	84.58	0.05
Run-of-river	0.02	0.01	0.00	0.01	0.01	0.01	0.01	0.01	4.22	0.01
Hydro res.	14.45	-	-	0.98	6.52	15.54	3.35	10.11	0.35	0.15
CSP	-	-	-	-	0.70	7.88	1.00	-	-	-
Lignite	1.13	0.30	0.02	13.95	0.03	1.83	20.49	2.69	30.05	0.02
CCGT	0.03	0.04	0.02	0.08	0.04	0.02	0.07	0.18	0.74	0.03
Coal	0.02	0.02	0.01	0.03	0.02	0.02	1.02	1.03	0.37	0.02
GT	0.05	1.96	0.04	3.81	6.02	0.04	3.45	20.21	9.06	0.27
Geothermal	0.90	0.30	0.10	1.95	2.70	3.50	3.74	0.90	2.95	0.17
Nuclear	0.01	0.01	0.00	2.95	11.72	0.01	0.01	0.01	0.11	1.32

Tab. C 25: Overall generation capacities in GW for the scenario *CO_2_low*, including the model endogenously derived capacities as well as the exogenous stock. The table refers to Fig. 29.

	Austria + Switzerland	BeNeLux	Denmark west	PL + CZ + SK	France	Iberia	Italy	Northern Europe	Germany	UK + IE
Offshore wind	-	40.02	9.44	0.04	114.23	65.07	21.28	91.66	46.25	71.66
Onshore wind	22.00	18.72	3.12	80.89	36.02	2.37	62.14	0.33	54.64	50.41
PV	19.91	35.51	0.05	59.78	41.41	90.45	47.73	4.18	86.11	0.05
Run-of-river	0.01	0.01	0.00	0.01	0.01	0.01	0.01	0.01	4.21	0.01
Hydro res.	14.45	-	-	0.98	6.52	15.54	3.35	10.11	0.35	0.15
CSP	-	-	-	-	0.70	7.88	1.00	-	-	-
Lignite	1.09	0.83	0.01	11.51	0.02	1.07	18.67	0.07	28.22	0.02
CCGT	0.02	0.06	0.02	0.24	0.07	0.03	0.09	0.13	0.93	0.03
Coal	0.02	0.03	0.01	0.04	0.02	0.03	1.04	1.03	0.49	0.01
GT	0.04	3.60	0.03	7.20	8.14	0.04	4.86	22.74	11.62	0.35
Geothermal	0.90	0.30	0.10	1.95	2.70	3.50	3.74	0.90	2.95	0.17
Nuclear	0.01	0.01	0.00	2.95	11.72	0.01	0.01	0.00	0.10	1.32

Tab. C 26: Overall generation capacities in GW for the scenario *CO_2_high*, including the model endogenously derived capacities as well as the exogenous stock. The table refers to Fig. 29.

	Austria + Switzerland	BeNeLux	Denmark west	PL + CZ + SK	France	Iberia	Italy	Northern Europe	Germany	UK + IE
Offshore wind	-	43.97	9.93	0.04	104.28	62.92	36.09	89.33	48.59	72.74
Onshore wind	22.00	18.72	2.42	80.89	33.59	3.52	62.14	0.36	54.77	50.41
PV	19.91	35.51	0.07	59.78	45.62	90.45	47.73	5.55	88.81	0.06
Run-of-river	0.03	0.01	0.00	0.01	0.01	0.01	0.01	0.01	4.24	0.01
Hydro res.	14.45	-	-	0.98	6.52	15.54	3.35	10.11	0.35	0.15
CSP	-	-	-	-	0.70	7.88	1.00	-	-	-
Lignite	0.02	0.02	0.01	0.20	0.02	0.02	0.06	0.02	1.58	0.01
CCGT	0.04	0.79	0.02	13.84	0.22	0.16	15.06	2.90	23.58	0.04
Coal	0.02	0.02	0.01	0.03	0.02	0.02	1.04	1.02	0.45	0.02
GT	0.05	2.01	0.04	2.84	13.94	0.04	3.61	20.18	7.35	0.28
Geothermal	0.90	0.30	0.10	1.95	2.70	3.50	3.74	0.90	2.95	0.17
Nuclear	0.73	0.01	0.01	2.97	11.72	0.01	1.97	0.01	4.00	1.33

Tab. C 27: Overall generation capacities in GW for the scenario *G++*, including the model endogenously derived capacities as well as the exogenous stock. The table refers to Fig. 29.

	Austria + Switzerland	BeNeLux	Denmark west	PL + CZ + SK	France	Iberia	Italy	Northern Europe	Germany	UK + IE
Offshore wind	-	-	103.02	-	-	-	-	66.62	15.54	353.56
Onshore wind	-	-	6.38	-	-	-	-	-	2.51	50.41
PV	-	-	-	-	-	90.45	-	-	0.01	-
Run-of-river	-	-	-	-	-	-	-	-	-	-
Hydro res.	14.45	-	-	0.98	6.52	15.54	3.35	10.11	0.35	0.15
CSP	-	-	-	-	0.70	7.88	1.00	-	-	-
Lignite	14.32	-	-	0.16	-	-	14.32	-	6.43	-
CCGT	2.63	0.25	0.25	0.25	0.25	0.25	2.63	0.25	35.93	0.25
Coal	-	-	-	-	-	-	1.00	1.00	0.01	-
GT	1.76	6.18	6.18	6.18	6.18	6.18	1.76	6.18	36.87	6.18
Geothermal	0.90	0.30	0.10	1.95	2.70	3.50	3.74	0.90	2.95	0.17
Nuclear	-	-	-	2.94	11.71	-	-	-	-	1.32

Tab. C 28: Overall generation capacities in GW for the scenario *G+*, including the model endogenously derived capacities as well as the exogenous stock. The table refers to Fig. 29.

	Austria + Switzerland	BeNeLux	Denmark west	PL + CZ + SK	France	Iberia	Italy	Northern Europe	Germany	UK + IE
Offshore wind	-	0.01	36.28	-	0.55	0.06	0.02	101.31	57.88	308.96
Onshore wind	0.02	5.00	6.38	10.84	61.80	0.11	19.29	0.09	12.04	50.41
PV	19.84	0.01	0.01	0.73	0.02	90.43	47.73	0.02	0.50	0.01
Run-of-river	-	-	-	-	-	-	-	-	0.04	-
Hydro res.	14.45	-	-	0.98	6.52	15.54	3.35	10.11	0.35	0.15
CSP	-	-	-	-	0.70	7.88	1.00	-	-	-
Lignite	0.01	0.01	0.01	16.10	0.01	0.05	15.10	0.01	2.60	0.01
CCGT	0.02	0.03	0.01	6.99	0.05	3.01	8.25	0.04	18.35	0.02
Coal	0.01	0.01	0.01	0.01	0.01	0.01	1.01	1.01	0.16	0.01
GT	0.07	7.51	0.06	8.59	27.95	2.10	6.54	6.26	32.87	0.12
Geothermal	0.90	0.30	0.10	1.95	2.70	3.50	3.74	0.90	2.95	0.17
Nuclear	-	-	-	2.94	11.71	-	-	-	0.04	1.32

Tab. C 29: Overall generation capacities in GW for the scenario *G+_Inv_high*, including the model endogenously derived capacities as well as the exogenous stock. The table refers to Fig. 29.

	Austria + Switzerland	BeNeLux	Denmark west	PL + CZ + SK	France	Iberia	Italy	Northern Europe	Germany	UK + IE
Offshore wind	-	0.04	30.55	0.02	1.41	0.71	0.05	91.47	62.08	294.04
Onshore wind	0.06	13.08	6.38	31.29	59.08	1.38	41.24	0.40	13.59	50.41
PV	19.91	0.06	0.03	16.71	0.09	90.44	47.73	0.06	3.78	0.04
Run-of-river	0.01	0.01	0.00	0.01	0.01	0.00	0.01	0.01	0.12	0.01
Hydro res.	14.45	-	-	0.98	6.52	15.54	3.35	10.11	0.35	0.15
CSP	-	-	-	-	0.70	7.88	1.00	-	-	-
Lignite	0.04	0.04	0.02	15.97	0.04	0.82	11.48	0.04	4.09	0.03
CCGT	0.06	0.09	0.04	4.57	0.13	3.49	8.01	0.31	17.07	0.05
Coal	0.02	0.02	0.02	0.04	0.02	0.03	1.04	1.02	0.47	0.02
GT	0.19	6.07	0.13	6.52	23.45	2.58	5.90	11.15	30.67	0.29
Geothermal	0.90	0.30	0.10	1.95	2.70	3.50	3.74	0.90	2.95	0.17
Nuclear	0.01	0.01	0.01	2.95	11.72	0.01	0.01	0.01	0.11	1.33

Tab. C 30: Overall generation capacities in GW for the scenario *G+_In_veryhigh*, including the model endogenously derived capacities as well as the exogenous stock. The table refers to Fig. 29.

	Austria + Switzerland	BeNeLux	Denmark west	PL + CZ + SK	France	Iberia	Italy	Northern Europe	Germany	UK + IE
Offshore wind	-	0.14	26.35	0.07	8.68	8.80	0.20	87.58	64.19	274.18
Onshore wind	0.23	18.72	6.38	41.97	47.40	3.78	56.70	1.01	20.36	50.41
PV	19.91	0.20	0.13	24.64	0.33	90.41	47.73	0.23	12.22	0.13
Run-of-river	0.03	0.02	0.01	0.02	0.03	0.02	0.02	0.02	0.40	0.02
Hydro res.	14.45	-	-	0.98	6.52	15.54	3.35	10.11	0.35	0.15
CSP	-	-	-	-	0.70	7.88	1.00	-	-	-
Lignite	0.12	0.12	0.07	14.29	0.12	2.20	10.27	0.12	6.08	0.08
CCGT	0.17	0.24	0.13	4.17	0.35	1.65	6.53	1.73	14.36	0.15
Coal	0.07	0.08	0.06	0.11	0.08	0.10	1.12	1.08	1.49	0.07
GT	0.41	3.70	0.33	5.37	19.02	2.31	5.47	12.61	22.64	0.75
Geothermal	0.90	0.30	0.10	1.95	2.70	3.50	3.74	0.90	2.95	0.17
Nuclear	0.02	0.02	0.02	2.97	11.73	0.02	0.03	0.02	0.40	1.34

Tab. C 31: Overall generation capacities in GW for the scenario *Cur.003*, including the model endogenously derived capacities as well as the exogenous stock. The table refers to Fig. 29.

	Austria + Switzerland	BeNeLux	Denmark west	PL + CZ + SK	France	Iberia	Italy	Northern Europe	Germany	UK + IE
Offshore wind	-	49.51	11.74	0.03	110.15	65.19	31.09	74.15	40.19	87.56
Onshore wind	22.00	18.72	0.16	80.89	22.15	3.14	62.14	0.14	55.42	25.93
PV	19.91	35.51	0.05	59.78	51.81	90.45	47.73	28.68	90.42	0.06
Run-of-river	0.01	0.01	0.00	0.01	0.00	0.00	0.01	0.01	4.24	0.00
Hydro res.	14.45	-	-	0.98	6.52	15.54	3.35	10.11	0.35	0.15
CSP	-	-	-	-	0.70	7.88	1.00	-	-	-
Lignite	0.83	0.04	0.01	7.72	0.01	0.04	15.37	0.03	22.42	0.01
CCGT	0.03	0.07	0.01	5.20	0.08	0.06	2.14	1.59	5.95	0.02
Coal	0.02	0.02	0.01	0.03	0.01	0.02	1.03	1.02	0.40	0.01
GT	0.03	0.61	0.02	2.59	8.09	0.03	4.98	19.78	10.15	0.03
Geothermal	0.90	0.30	0.10	1.95	2.70	3.50	3.74	0.90	2.95	0.17
Nuclear	0.01	0.00	0.00	2.95	11.72	0.00	0.01	0.00	0.10	1.32

Tab. C 32: Overall generation capacities in GW for the scenario *Cur.010*, including the model endogenously derived capacities as well as the exogenous stock. The table refers to Fig. 29.

	Austria + Switzerland	BeNeLux	Denmark west	PL + CZ + SK	France	Iberia	Italy	Northern Europe	Germany	UK + IE
Offshore wind	-	43.42	10.14	0.02	106.28	65.22	29.71	89.61	47.36	72.79
Onshore wind	22.00	18.72	2.38	80.89	33.79	1.78	62.14	0.17	54.58	50.41
PV	19.91	35.51	0.03	59.78	46.48	90.45	47.73	4.91	86.40	0.03
Run-of-river	0.01	0.00	0.00	0.00	0.00	0.00	0.00	0.00	4.19	0.00
Hydro res.	14.45	-	-	0.98	6.52	15.54	3.35	10.11	0.35	0.15
CSP	-	-	-	-	0.70	7.88	1.00	-	-	-
Lignite	0.68	0.04	0.01	8.07	0.01	0.04	15.70	0.02	21.68	0.01
CCGT	0.02	0.15	0.01	5.14	0.06	0.05	1.99	1.20	7.14	0.02
Coal	0.01	0.02	0.01	0.02	0.01	0.02	1.02	1.01	0.30	0.01
GT	0.02	2.99	0.02	5.29	13.32	0.02	4.97	21.97	10.07	0.14
Geothermal	0.90	0.30	0.10	1.95	2.70	3.50	3.74	0.90	2.95	0.17
Nuclear	0.01	0.00	0.00	2.94	11.71	0.00	0.01	0.00	0.07	1.32

Tab. C 33: Overall generation capacities in GW for the scenario *VRE_exp_CO_2_med*, including the model endogenously derived capacities as well as the exogenous stock. The table refers to Fig. 29.

	Austria + Switzerland	BeNeLux	Denmark west	PL + CZ + SK	France	Iberia	Italy	Northern Europe	Germany	UK + IE
Offshore wind	-	0.03	2.18	0.01	57.83	6.59	0.01	68.99	34.52	32.00
Onshore wind	0.03	18.72	6.38	26.88	16.21	7.10	0.06	0.09	36.56	50.41
PV	5.30	0.03	0.01	2.75	0.04	57.53	30.13	0.02	1.34	0.01
Run-of-river	-	-	-	-	-	-	-	-	0.04	-
Hydro res.	14.45	-	-	0.98	6.52	15.54	3.35	10.11	0.35	0.15
CSP	-	-	-	-	0.70	7.88	1.00	-	-	-
Lignite	7.55	20.77	0.12	25.45	25.03	22.36	35.27	6.49	46.04	16.62
CCGT	0.01	0.97	0.92	1.18	4.83	0.01	0.02	5.25	6.23	10.11
Coal	0.01	0.01	0.01	0.01	0.01	0.01	1.01	1.01	0.17	0.01
GT	0.01	5.88	1.23	5.17	20.07	0.01	0.05	16.20	14.91	14.26
Geothermal	0.90	0.30	0.10	1.95	2.70	3.50	3.74	0.90	2.95	0.17
Nuclear	-	-	-	2.94	11.71	-	-	-	-	1.32

Tab. C 34: Overall generation capacities in GW for the scenario *VRE_exp_CO₂_high*, including the model endogenously derived capacities as well as the exogenous stock. The table refers to Fig. 29.

	Austria + Switzerland	BeNeLux	Denmark west	PL + CZ + SK	France	Iberia	Italy	Northern Europe	Germany	UK + IE
Offshore wind	-	19.46	8.32	0.01	69.51	36.80	1.03	84.12	41.68	63.04
Onshore wind	22.00	18.72	0.68	74.89	21.99	8.17	62.14	0.12	53.64	48.84
PV	19.91	18.42	0.02	39.05	25.74	90.35	47.73	0.06	70.17	0.02
Run-of-river	-	-	-	-	-	-	-	-	0.29	-
Hydro res.	14.45	-	-	0.98	6.52	15.54	3.35	10.11	0.35	0.15
CSP	-	-	-	-	0.70	7.88	1.00	-	-	-
Lignite	0.05	0.02	0.01	0.19	0.02	0.02	2.99	0.01	1.90	0.01
CCGT	0.33	14.97	0.03	16.12	23.04	7.55	20.92	8.39	39.12	5.90
Coal	0.01	0.01	0.01	0.01	0.01	0.01	1.02	1.01	0.22	0.01
GT	0.02	4.15	0.02	4.93	19.94	0.01	0.71	16.41	10.68	6.09
Geothermal	0.90	0.30	0.10	1.95	2.70	3.50	3.74	0.90	2.95	0.17
Nuclear	-	-	-	2.94	11.71	-	-	-	-	1.32

Tab. C 35: Overall generation capacities in GW for the scenario *VRE_exp_CO₂_veryhigh*, including the model endogenously derived capacities as well as the exogenous stock. The table refers to Fig. 29.

	Austria + Switzerland	BeNeLux	Denmark west	PL + CZ + SK	France	Iberia	Italy	Northern Europe	Germany	UK + IE
Offshore wind	-	22.33	8.76	0.01	78.75	41.91	16.66	87.14	43.87	67.62
Onshore wind	22.00	18.72	0.53	78.58	30.16	5.20	62.14	0.13	54.32	50.41
PV	19.91	35.35	0.02	51.93	40.53	90.45	47.73	0.12	77.75	0.02
Run-of-river	0.01	-	-	-	-	-	-	-	2.59	-
Hydro res.	14.45	-	-	0.98	6.52	15.54	3.35	10.11	0.35	0.15
CSP	-	-	-	-	0.70	7.88	1.00	-	-	-
Lignite	0.01	0.01	0.01	0.17	0.01	0.01	0.01	0.01	1.20	0.01
CCGT	0.11	12.86	0.02	15.49	14.05	6.74	21.74	8.29	36.56	0.15
Coal	0.01	0.01	0.01	0.01	0.01	0.01	1.01	1.01	0.15	0.01
GT	0.02	3.59	0.02	3.06	13.47	0.02	0.67	15.99	7.97	4.92
Geothermal	0.90	0.30	0.10	1.95	2.70	3.50	3.74	0.90	2.95	0.17
Nuclear	-	-	-	2.94	11.71	-	-	-	-	1.32

Tab. C 36: Overall generation capacities in GW for the scenario *TempRes_2h*, including the model endogenously derived capacities as well as the exogenous stock. The table refers to Fig. 29.

	Austria + Switzerland	BeNeLux	Denmark west	PL + CZ + SK	France	Iberia	Italy	Northern Europe	Germany	UK + IE
Offshore wind	-	42.99	10.11	0.02	106.20	65.03	29.78	89.69	47.60	72.76
Onshore wind	22.00	18.72	2.39	80.89	33.91	1.94	62.14	0.22	54.66	50.41
PV	19.91	35.51	0.04	59.78	46.81	90.45	47.73	4.81	86.66	0.04
Run-of-river	0.01	0.01	0.00	0.01	0.00	0.00	0.01	0.01	4.21	0.00
Hydro res.	14.45	-	-	0.98	6.52	15.54	3.35	10.11	0.35	0.15
CSP	-	-	-	-	0.70	7.88	1.00	-	-	-
Lignite	0.65	0.06	0.01	8.10	0.01	0.05	15.72	0.02	21.63	0.01
CCGT	0.02	0.19	0.01	5.04	0.08	0.07	1.99	1.19	7.17	0.02
Coal	0.02	0.02	0.01	0.03	0.01	0.02	1.03	1.02	0.39	0.01
GT	0.03	3.41	0.02	5.32	13.41	0.03	4.99	21.73	9.83	0.18
Geothermal	0.90	0.30	0.10	1.95	2.70	3.50	3.74	0.90	2.95	0.17
Nuclear	-	-	-	2.94	11.71	-	-	-	-	1.32

Tab. C 37: Overall generation capacities in GW for the scenario *TempRes_6h*, including the model endogenously derived capacities as well as the exogenous stock. The table refers to Fig. 29.

	Austria + Switzerland	BeNeLux	Denmark west	PL + CZ + SK	France	Iberia	Italy	Northern Europe	Germany	UK + IE
Offshore wind	-	41.81	10.20	0.03	106.33	65.07	29.95	89.79	48.27	72.73
Onshore wind	22.00	18.72	2.31	80.89	25.96	1.06	62.14	0.27	54.64	50.41
PV	19.91	35.51	0.07	59.78	57.43	90.45	47.73	4.00	88.50	0.07
Run-of-river	0.01	0.01	0.00	0.01	0.01	0.01	0.01	0.01	4.23	0.01
Hydro res.	14.45	-	-	0.98	6.52	15.54	3.35	10.11	0.35	0.15
CSP	-	-	-	-	0.70	7.88	1.00	-	-	-
Lignite	0.71	0.07	0.01	8.05	0.02	0.06	15.68	0.03	21.33	0.01
CCGT	0.03	0.23	0.02	5.10	0.10	0.12	1.56	1.30	7.13	0.03
Coal	0.02	0.03	0.01	0.04	0.02	0.03	1.04	1.02	0.51	0.01
GT	0.04	4.38	0.03	5.05	13.58	0.04	5.47	21.43	9.29	0.24
Geothermal	0.90	0.30	0.10	1.95	2.70	3.50	3.74	0.90	2.95	0.17
Nuclear	-	-	-	2.94	11.71	-	-	-	-	1.32

Tab. C 38: Overall generation capacities in GW for the scenario *Weather 2007*, including the model endogenously derived capacities as well as the exogenous stock. The table refers to Fig. 29.

	Austria + Switzerland	BeNeLux	Denmark west	PL + CZ + SK	France	Iberia	Italy	Northern Europe	Germany	UK + IE
Offshore wind	-	48.16	5.58	0.01	93.74	37.18	29.29	84.30	45.07	72.16
Onshore wind	22.00	18.72	6.38	80.89	61.65	28.56	62.14	0.61	55.42	50.41
PV	19.91	21.91	0.01	42.28	22.39	90.45	47.73	0.01	67.95	0.02
Run-of-river	-	-	-	-	-	-	-	-	3.18	-
Hydro res.	14.45	-	-	0.98	6.52	15.54	3.35	10.11	0.35	0.15
CSP	-	-	-	-	0.70	7.88	1.00	-	-	-
Lignite	0.21	0.03	-	8.29	-	0.82	14.37	0.01	22.74	-
CCGT	0.01	0.07	0.01	3.33	0.01	1.06	1.33	0.28	7.49	0.01
Coal	0.01	0.01	-	0.01	-	0.01	1.01	1.01	0.14	-
GT	0.01	1.05	0.01	9.62	6.11	0.56	7.95	21.40	11.71	0.02
Geothermal	0.90	0.30	0.10	1.95	2.70	3.50	3.74	0.90	2.95	0.17
Nuclear	-	-	-	2.94	11.71	-	-	-	0.03	1.32

Tab. C 39: Overall generation capacities in GW for the scenario *Weather 2008*, including the model endogenously derived capacities as well as the exogenous stock. The table refers to Fig. 29.

	Austria + Switzerland	BeNeLux	Denmark west	PL + CZ + SK	France	Iberia	Italy	Northern Europe	Germany	UK + IE
Offshore wind	-	52.37	6.02	0.04	134.34	50.11	27.38	86.38	48.12	62.57
Onshore wind	22.00	18.72	6.38	80.89	1.35	13.86	62.14	0.29	54.47	50.41
PV	19.91	22.24	0.18	53.66	18.94	90.45	47.73	0.14	77.11	0.05
Run-of-river	0.03	0.01	-	0.01	0.01	0.01	0.01	0.01	3.85	0.01
Hydro res.	14.45	-	-	0.98	6.52	15.54	3.35	10.11	0.35	0.15
CSP	-	-	-	-	0.70	7.88	1.00	-	-	-
Lignite	0.87	0.04	0.02	8.16	0.02	0.03	17.23	0.04	20.86	0.02
CCGT	0.03	0.06	0.03	3.25	0.06	0.06	1.67	1.84	7.76	0.04
Coal	0.03	0.03	0.02	0.05	0.02	0.03	1.05	1.03	0.62	0.02
GT	0.04	0.12	0.04	7.62	4.13	0.47	7.07	14.70	7.47	0.20
Geothermal	0.90	0.30	0.10	1.95	2.70	3.50	3.74	0.90	2.95	0.17
Nuclear	0.01	0.01	0.01	2.95	11.72	0.01	0.01	0.01	0.17	1.33

Tab. C 40: Overall generation capacities in GW for the scenario *Weather 2009*, including the model endogenously derived capacities as well as the exogenous stock. The table refers to Fig. 29.

	Austria + Switzerland	BeNeLux	Denmark west	PL + CZ + SK	France	Iberia	Italy	Northern Europe	Germany	UK + IE
Offshore wind	-	54.57	8.33	0.07	124.07	56.44	80.66	96.60	52.04	76.97
Onshore wind	0.62	18.72	5.50	80.89	0.27	0.17	0.13	0.15	53.54	46.30
PV	19.91	35.51	0.07	59.78	50.82	90.45	47.73	0.09	79.61	0.06
Run-of-river	0.05	0.01	0.01	0.01	0.01	0.01	0.02	0.01	4.24	0.01
Hydro res.	14.45	-	-	0.98	6.52	15.54	3.35	10.11	0.35	0.15
CSP	-	-	-	-	0.70	7.88	1.00	-	-	-
Lignite	4.78	0.03	0.02	10.42	0.02	0.02	12.58	0.04	19.34	0.02
CCGT	0.06	0.05	0.03	6.10	0.07	0.04	3.74	0.89	8.89	0.04
Coal	0.04	0.03	0.02	0.07	0.03	0.02	1.07	1.04	0.78	0.02
GT	0.05	0.07	0.05	6.57	6.20	0.56	3.31	14.17	5.20	0.10
Geothermal	0.90	0.30	0.10	1.95	2.70	3.50	3.74	0.90	2.95	0.17
Nuclear	0.02	0.01	0.01	2.95	11.72	0.01	0.01	0.01	0.22	1.33

Tab. C 41: Overall generation capacities in GW for the scenario *Weather 2011*, including the model endogenously derived capacities as well as the exogenous stock. The table refers to Fig. 29.

	Austria + Switzerland	BeNeLux	Denmark west	PL + CZ + SK	France	Iberia	Italy	Northern Europe	Germany	UK + IE
Offshore wind	-	53.72	6.38	0.10	140.01	61.64	73.86	86.76	49.14	102.26
Onshore wind	0.16	18.72	6.38	80.89	0.11	0.11	0.10	0.14	46.34	0.70
PV	19.91	35.51	0.05	59.78	28.72	90.45	47.73	0.07	86.13	0.06
Run-of-river	0.06	0.01	-	0.01	0.01	0.01	0.01	0.01	4.24	0.01
Hydro res.	14.45	-	-	0.98	6.52	15.54	3.35	10.11	0.35	0.15
CSP	-	-	-	-	0.70	7.88	1.00	-	-	-
Lignite	4.97	0.03	0.02	10.25	0.02	0.02	16.15	0.03	18.40	0.02
CCGT	0.05	0.04	0.03	5.77	0.05	0.03	2.31	0.17	6.56	0.04
Coal	0.04	0.02	0.02	0.06	0.02	0.02	1.06	1.03	0.67	0.02
GT	0.05	0.12	0.04	6.86	1.02	0.05	7.94	19.77	10.05	1.65
Geothermal	0.90	0.30	0.10	1.95	2.70	3.50	3.74	0.90	2.95	0.17
Nuclear	0.02	0.01	0.01	2.95	11.72	0.01	0.01	0.01	0.19	1.33

Tab. C 42: Overall generation capacities in GW for the scenario *Weather 2012*, including the model endogenously derived capacities as well as the exogenous stock. The table refers to Fig. 29.

	Austria + Switzerland	BeNeLux	Denmark west	PL + CZ + SK	France	Iberia	Italy	Northern Europe	Germany	UK + IE
Offshore wind	-	56.55	8.42	0.04	132.78	62.63	73.18	88.51	50.09	103.23
Onshore wind	10.76	18.72	3.31	80.89	0.20	0.08	0.09	0.10	50.48	0.20
PV	19.91	31.00	0.04	59.78	35.94	90.45	47.73	0.05	79.61	0.04
Run-of-river	0.02	0.01	-	0.01	0.01	0.01	0.01	0.01	4.23	0.01
Hydro res.	14.45	-	-	0.98	6.52	15.54	3.35	10.11	0.35	0.15
CSP	-	-	-	-	0.70	7.88	1.00	-	-	-
Lignite	3.77	0.02	0.01	10.25	0.02	0.07	15.08	0.03	19.13	0.01
CCGT	0.04	0.05	0.02	4.97	0.23	0.77	2.29	0.40	7.84	0.04
Coal	0.03	0.02	0.01	0.05	0.02	0.03	1.05	1.02	0.54	0.01
GT	0.04	0.07	0.03	6.94	3.91	0.05	4.36	17.07	8.41	2.10
Geothermal	0.90	0.30	0.10	1.95	2.70	3.50	3.74	0.90	2.95	0.17
Nuclear	-	-	-	2.94	11.71	-	-	-	-	1.32

Tab. C 43: Overall generation capacities in GW for the scenario *Redox-flow_Inv_low*, including the model endogenously derived capacities as well as the exogenous stock. The table refers to Fig. 29.

	Austria + Switzerland	BeNeLux	Denmark west	PL + CZ + SK	France	Iberia	Italy	Northern Europe	Germany	UK + IE
Offshore wind	-	41.23	9.75	0.04	106.06	64.10	28.74	91.18	47.34	72.73
Onshore wind	22.00	18.72	2.47	80.89	33.15	3.00	62.14	0.37	54.81	50.41
PV	19.91	35.51	0.06	59.78	47.17	90.45	47.73	1.12	86.78	0.06
Run-of-river	0.02	0.01	-	0.01	0.01	0.01	0.01	0.01	4.24	0.01
Hydro res.	14.45	-	-	0.98	6.52	15.54	3.35	10.11	0.35	0.15
CSP	-	-	-	-	0.70	7.88	1.00	-	-	-
Lignite	0.69	0.09	0.02	7.91	0.02	0.10	15.94	0.03	21.62	0.02
CCGT	0.04	0.30	0.03	4.98	0.13	0.13	1.87	0.18	6.47	0.04
Coal	0.03	0.04	0.02	0.05	0.02	0.03	1.05	1.03	0.63	0.02
GT	0.05	4.79	0.04	5.31	13.66	0.05	4.83	14.89	8.54	0.26
Geothermal	0.90	0.30	0.10	1.95	2.70	3.50	3.74	0.90	2.95	0.17
Nuclear	-	-	-	2.94	11.71	-	-	-	-	1.32

Tab. C 44: Overall generation capacities in GW for the scenario *PHS_w/o_old_stock*, including the model endogenously derived capacities as well as the exogenous stock. The table refers to Fig. 29.

	Austria + Switzerland	BeNeLux	Denmark west	PL + CZ + SK	France	Iberia	Italy	Northern Europe	Germany	UK + IE
Offshore wind	-	43.01	9.67	0.11	108.60	63.03	29.83	89.46	47.36	72.86
Onshore wind	22.00	18.72	3.07	80.89	33.51	5.64	62.14	0.72	55.24	50.41
PV	19.91	35.51	0.13	59.78	44.17	90.45	47.73	5.17	87.60	0.12
Run-of-river	0.06	0.02	0.01	0.02	0.02	0.01	0.02	0.02	4.24	0.01
Hydro res.	14.45	-	-	0.98	6.52	15.54	3.35	10.11	0.35	0.15
CSP	-	-	-	-	0.70	7.88	1.00	-	-	-
Lignite	0.70	0.13	0.03	7.88	0.04	0.11	15.61	0.07	21.42	0.03
CCGT	0.07	0.31	0.05	5.20	0.22	0.18	2.19	1.41	7.50	0.07
Coal	0.05	0.06	0.03	0.10	0.04	0.06	1.11	1.06	1.17	0.03
GT	0.10	2.21	0.08	4.85	12.27	0.09	5.88	21.74	10.66	0.38
Geothermal	0.90	0.30	0.10	1.95	2.70	3.50	3.74	0.90	2.95	0.17
Nuclear	-	-	-	2.94	11.71	-	-	-	-	1.32

9.2. Storage converter capacity in Europe

The following tables show the overall generation capacities for all European model regions. The values of the German model regions (see Fig. C 1) are aggregated (*Germany*); their model region-specific values are described in Sec. 9.3.

Tab. C 45: Region-specific installed storage converter capacity in GW (including old existing PHS capacities) for the *reference scenario*. The table refers to Fig. 29. The 20 German model regions are aggregated in this table.

	H_2	Li-ion	aCAES	PHS	Redox-flow
Austria + Switzerland	0.02	0.51	0.05	4.54	0.04
BeNeLux	10.02	1.76	2.24	2.86	0.06
Denmark west	4.99	0.87	0.21	-	0.06
PL + CZ + SK	0.48	6.97	2.66	3.50	0.06
France	25.99	3.42	0.25	4.89	0.06
Iberia	3.22	10.02	0.15	12.09	0.07
Italy	0.05	6.36	0.11	8.08	0.06
Northern Europe	-	3.21	-	2.86	0.07
Germany	10.10	15.65	3.11	8.23	0.93
UK + IE	31.14	5.28	5.36	2.92	0.07

Tab. C 46: Region-specific installed storage converter capacity in GW (including old existing PHS capacities) for the scenario *Stor_Inv_low*. The table refers to Fig. 29. The 20 German model regions are aggregated in this table.

	H_2	Li-ion	aCAES	PHS	Redox-flow
Austria + Switzerland	0.01	0.39	0.04	5.11	0.03
BeNeLux	18.42	1.36	4.64	2.78	0.04
Denmark west	7.59	0.64	0.69	-	0.04
PL + CZ + SK	7.83	11.57	2.19	3.50	0.04
France	39.37	1.63	6.00	4.89	0.05
Iberia	5.16	15.39	0.12	9.81	0.05
Italy	0.15	7.21	0.16	8.30	0.04
Northern Europe	-	11.96	-	2.12	0.06
Germany	15.33	18.47	4.40	8.23	0.67
UK + IE	36.91	1.45	4.23	2.87	0.05

Tab. C 47: Region-specific installed storage converter capacity in GW (including old existing PHS capacities) for the scenario *Stor_Inv_high*. The table refers to Fig. 29. The 20 German model regions are aggregated in this table.

	H_2	Li-ion	aCAES	PHS[a]	Redox-flow
Austria + Switzerland	0.02	0.51	0.05	4.47	0.05
BeNeLux	3.50	2.09	0.67	2.87	0.06
Denmark west	3.47	1.02	0.15	-	0.06
PL + CZ + SK	0.07	5.94	0.51	3.50	0.06
France	15.87	4.43	0.20	4.95	0.07
Iberia	1.46	8.26	0.15	12.91	0.07
Italy	0.05	6.27	0.11	7.92	0.06
Northern Europe	-	2.22	-	2.94	0.07
Germany	7.20	14.94	1.56	8.23	0.96
UK + IE	24.66	5.02	0.42	2.95	0.07

Tab. C 48: Region-specific installed storage converter capacity in GW (including old existing PHS capacities) for the scenario *VRE_Inv_low*. The table refers to Fig. 29. The 20 German model regions are aggregated in this table.

	H_2	Li-ion	aCAES	PHS	Redox-flow
Austria + Switzerland	0.02	0.46	0.05	4.42	0.04
BeNeLux	8.32	2.39	1.06	2.87	0.05
Denmark west	2.50	0.78	0.14	-	0.05
PL + CZ + SK	0.15	5.75	1.84	3.50	0.05
France	14.29	4.82	0.18	4.95	0.06
Iberia	3.97	6.81	0.13	12.81	0.06
Italy	0.10	6.79	0.12	7.83	0.05
Northern Europe	-	2.84	-	3.13	0.06
Germany	7.69	14.72	2.14	8.23	0.86
UK + IE	20.01	4.83	1.28	2.97	0.06

Tab. C 49: Region-specific installed storage converter capacity in GW (including old existing PHS capacities) for the scenario *VRE_Inv_high*. The table refers to Fig. 29. The 20 German model regions are aggregated in this table.

	H_2	Li-ion	aCAES	PHS	Redox-flow
Austria + Switzerland	0.02	0.59	0.06	4.61	0.05
BeNeLux	10.78	1.68	3.22	2.84	0.07
Denmark west	6.83	1.20	0.49	-	0.07
PL + CZ + SK	1.40	9.02	2.87	3.50	0.07
France	39.50	2.29	1.49	4.88	0.07
Iberia	2.18	13.29	0.18	10.80	0.08
Italy	0.05	6.03	0.12	8.31	0.06
Northern Europe	-	6.58	-	2.61	0.09
Germany	10.93	17.37	3.75	8.23	1.06
UK + IE	34.38	4.20	3.67	2.90	0.08

Tab. C 50: Region-specific installed storage converter capacity in GW (including old existing PHS capacities) for the scenario *FP_low*. The table refers to Fig. 29. The 20 German model regions are aggregated in this table.

	H_2	Li-ion	aCAES	PHS	Redox-flow
Austria + Switzerland	0.02	0.52	0.05	4.51	0.05
BeNeLux	7.43	1.62	2.38	2.87	0.06
Denmark west	4.76	0.94	0.23	-	0.06
PL + CZ + SK	0.29	5.99	3.29	3.50	0.06
France	24.43	3.94	0.27	4.91	0.07
Iberia	2.39	10.27	0.16	11.97	0.07
Italy	0.07	6.51	0.12	7.98	0.06
Northern Europe	-	2.94	-	2.88	0.07
Germany	9.72	15.12	3.21	8.23	0.96
UK + IE	31.34	5.41	5.15	2.93	0.07

Tab. C 51: Region-specific installed storage converter capacity in GW (including old existing PHS capacities) for the scenario *FP_high*. The table refers to Fig. 29. The 20 German model regions are aggregated in this table.

	H_2	Li-ion	aCAES	PHS	Redox-flow
Austria + Switzerland	0.02	0.50	0.05	4.50	0.04
BeNeLux	11.07	1.81	1.81	2.86	0.06
Denmark west	5.03	0.95	0.21	-	0.06
PL + CZ + SK	1.34	5.83	3.27	3.50	0.06
France	32.92	2.90	0.24	4.86	0.06
Iberia	1.62	10.15	0.15	11.77	0.06
Italy	0.05	5.99	0.12	8.33	0.05
Northern Europe	-	4.01	-	2.79	0.07
Germany	10.13	15.20	3.18	8.23	0.92
UK + IE	30.78	5.49	5.91	2.93	0.07

Tab. C 52: Region-specific installed storage converter capacity in GW (including old existing PHS capacities) for the scenario *CO_2_low*. The table refers to Fig. 29. The 20 German model regions are aggregated in this table.

	H_2	Li-ion	aCAES	PHS	Redox-flow
Austria + Switzerland	0.02	0.45	0.05	4.46	0.04
BeNeLux	8.55	2.02	2.16	2.86	0.05
Denmark west	5.13	0.93	0.20	-	0.05
PL + CZ + SK	0.24	6.08	2.99	3.50	0.05
France	30.47	3.34	0.21	4.85	0.05
Iberia	2.20	10.10	0.14	11.85	0.06
Italy	0.04	6.01	0.10	8.33	0.05
Northern Europe	-	3.38	-	2.85	0.06
Germany	9.57	14.08	3.11	8.23	0.83
UK + IE	30.82	5.36	5.76	2.92	0.06

Tab. C 53: Region-specific installed storage converter capacity in GW (including old existing PHS capacities) for the scenario *CO_2_high*. The table refers to Fig. 29. The 20 German model regions are aggregated in this table.

	H_2	Li-ion	aCAES	PHS	Redox-flow
Austria + Switzerland	0.02	0.48	0.05	4.51	0.04
BeNeLux	10.11	1.62	2.50	2.86	0.06
Denmark west	4.81	0.77	0.21	-	0.06
PL + CZ + SK	0.94	5.90	3.47	3.50	0.06
France	25.37	3.20	0.28	4.89	0.06
Iberia	3.94	9.46	0.13	12.21	0.06
Italy	0.09	6.62	0.14	7.88	0.05
Northern Europe	-	3.01	-	2.86	0.07
Germany	10.54	15.13	3.30	8.23	0.91
UK + IE	30.90	5.27	5.61	2.92	0.07

Tab. C 54: Region-specific installed storage converter capacity in GW (including old existing PHS capacities) for the scenario *G++*. The table refers to Fig. 29. The 20 German model regions are aggregated in this table.

	H_2	Li-ion	aCAES	PHS	Redox-flow
Austria + Switzerland	0.50	1.38	-	6.65	-
BeNeLux	4.31	3.23	-	2.85	-
Denmark west	4.34	3.23	-	-	-
PL + CZ + SK	4.31	3.23	-	3.50	-
France	4.33	3.24	-	4.88	-
Iberia	4.34	3.24	-	13.08	-
Italy	0.50	1.38	-	8.49	-
Northern Europe	-	3.23	-	2.69	-
Germany	14.65	20.36	0.02	8.23	0.01
UK + IE	4.34	3.24	-	2.83	-

Tab. C 55: Region-specific installed storage converter capacity in GW (including old existing PHS capacities) for the scenario *G+*. The table refers to Fig. 29. The 20 German model regions are aggregated in this table.

	H_2	Li-ion	aCAES	PHS	Redox-flow
Austria + Switzerland	0.02	0.26	0.04	6.65	0.01
BeNeLux	0.07	0.69	0.08	2.85	0.01
Denmark west	0.12	1.81	0.08	-	0.01
PL + CZ + SK	0.02	1.45	0.06	3.50	0.01
France	0.09	4.09	0.09	4.89	0.01
Iberia	0.03	7.03	0.05	13.08	0.01
Italy	0.02	3.55	0.05	8.49	0.01
Northern Europe	-	4.86	-	2.72	0.01
Germany	0.46	11.32	0.54	8.23	0.24
UK + IE	34.86	0.69	0.12	2.84	0.01

Tab. C 56: Region-specific installed storage converter capacity in GW (including old existing PHS capacities) for the scenario *G+_Inv_high*. The table refers to Fig. 29. The 20 German model regions are aggregated in this table.

	H_2	Li-ion	aCAES	PHS	Redox-flow
Austria + Switzerland	0.04	0.58	0.10	6.63	0.04
BeNeLux	0.16	0.84	0.22	2.86	0.04
Denmark west	0.49	1.00	0.26	-	0.04
PL + CZ + SK	0.05	0.81	0.13	3.50	0.04
France	0.21	1.28	0.27	4.89	0.04
Iberia	0.07	3.68	0.15	13.07	0.04
Italy	0.04	2.05	0.12	8.49	0.04
Northern Europe	-	1.61	-	2.69	0.04
Germany	0.94	14.32	1.47	8.23	0.71
UK + IE	36.86	0.94	0.41	2.85	0.04

Tab. C 57: Region-specific installed storage converter capacity in GW (including old existing PHS capacities) for the scenario *G+_Inv_veryhigh*. The table refers to Fig. 29. The 20 German model regions are aggregated in this table.

	H_2	Li-ion	aCAES	PHS	Redox-flow
Austria + Switzerland	0.12	1.61	0.28	6.50	0.14
BeNeLux	0.40	1.76	0.67	2.89	0.15
Denmark west	1.09	1.87	0.63	-	0.15
PL + CZ + SK	0.15	1.77	0.38	3.50	0.14
France	0.53	2.00	0.67	4.93	0.15
Iberia	0.20	3.29	0.43	13.04	0.15
Italy	0.12	2.52	0.33	8.46	0.14
Northern Europe	-	2.16	-	2.71	0.16
Germany	2.21	30.90	3.06	8.23	2.58
UK + IE	36.12	2.04	1.27	2.90	0.16

Tab. C 58: Region-specific installed storage converter capacity in GW (including old existing PHS capacities) for the scenario *Cur.003*. The table refers to Fig. 29. The 20 German model regions are aggregated in this table.

	H_2	Li-ion	aCAES	PHS	Redox-flow
Austria + Switzerland	0.01	0.30	0.03	4.46	0.03
BeNeLux	11.85	1.16	2.42	2.85	0.03
Denmark west	6.90	0.81	0.73	-	0.04
PL + CZ + SK	2.75	8.55	3.52	3.50	0.04
France	30.81	4.22	0.32	4.88	0.04
Iberia	3.27	9.81	0.09	12.08	0.04
Italy	0.04	6.39	0.07	8.04	0.03
Northern Europe	-	11.70	-	2.52	0.05
Germany	10.79	12.60	3.33	8.23	0.56
UK + IE	32.35	4.21	4.47	2.89	0.04

Tab. C 59: Region-specific installed storage converter capacity in GW (including old existing PHS capacities) for the scenario *Cur.010*. The table refers to Fig. 29. The 20 German model regions are aggregated in this table.

	H_2	Li-ion	aCAES	PHS	Redox-flow
Austria + Switzerland	0.01	0.22	0.02	4.45	0.02
BeNeLux	10.13	1.79	2.38	2.85	0.03
Denmark west	5.06	0.39	0.11	-	0.03
PL + CZ + SK	0.33	6.85	2.78	3.50	0.03
France	25.89	3.64	0.13	4.86	0.03
Iberia	3.32	10.04	0.07	12.05	0.03
Italy	0.02	6.43	0.05	8.10	0.02
Northern Europe	-	2.92	-	2.86	0.03
Germany	10.12	11.14	2.89	8.23	0.42
UK + IE	31.23	5.15	5.47	2.90	0.03

Tab. C 60: Region-specific installed storage converter capacity in GW (including old existing PHS capacities) for the scenario *VRE_exp_CO_2_med*. The table refers to Fig. 29. The 20 German model regions are aggregated in this table.

	H_2	Li-ion	aCAES	PHS	Redox-flow
Austria + Switzerland	-	0.12	0.01	4.34	0.01
BeNeLux	0.01	0.17	0.03	2.88	0.01
Denmark west	0.03	0.30	0.69	-	0.01
PL + CZ + SK	0.01	0.13	0.02	3.50	0.01
France	0.01	1.10	0.04	4.89	0.01
Iberia	-	1.91	0.02	6.39	0.01
Italy	0.01	2.56	0.02	7.64	0.01
Northern Europe	-	0.28	-	2.79	0.01
Germany	0.05	3.97	0.41	8.23	0.21
UK + IE	0.41	5.13	3.41	2.88	0.01

Tab. C 61: Region-specific installed storage converter capacity in GW (including old existing PHS capacities) for the scenario *VRE_exp_CO_2_high*. The table refers to Fig. 29. The 20 German model regions are aggregated in this table.

	H_2	Li-ion	aCAES	PHS	Redox-flow
Austria + Switzerland	0.01	0.17	0.02	4.36	0.02
BeNeLux	0.02	0.62	0.05	2.83	0.02
Denmark west	1.72	0.42	0.22	-	0.02
PL + CZ + SK	0.02	5.15	0.31	3.50	0.02
France	0.31	4.13	0.06	4.80	0.02
Iberia	0.02	6.86	0.04	12.54	0.02
Italy	0.01	5.61	0.03	8.37	0.02
Northern Europe	-	1.42	-	2.93	0.02
Germany	1.74	10.11	1.31	8.23	0.34
UK + IE	21.10	4.67	5.72	2.95	0.02

Tab. C 62: Region-specific installed storage converter capacity in GW (including old existing PHS capacities) for the scenario *VRE_exp_CO₂_veryhigh*. The table refers to Fig. 29. The 20 German model regions are aggregated.

	H_2	Li-ion	aCAES	PHS	Redox-flow
Austria + Switzerland	0.01	0.19	0.02	4.36	0.02
BeNeLux	0.05	1.80	0.11	2.85	0.02
Denmark west	2.04	0.32	0.10	-	0.02
PL + CZ + SK	0.09	5.01	3.07	3.50	0.02
France	13.33	4.38	0.09	4.82	0.02
Iberia	0.05	7.75	0.05	12.31	0.03
Italy	0.01	5.89	0.04	8.37	0.02
Northern Europe	-	1.71	-	2.88	0.03
Germany	4.90	11.17	2.27	8.23	0.37
UK + IE	27.06	4.85	5.75	2.93	0.03

Tab. C 63: Region-specific installed storage converter capacity in GW (including old existing PHS capacities) for the scenario *TempRes_2h*. The table refers to Fig. 29. The 20 German model regions are aggregated in this table.

	H_2	Li-ion	aCAES	PHS	Redox-flow
Austria + Switzerland	0.01	0.29	0.03	4.46	0.03
BeNeLux	9.75	1.67	2.59	2.86	0.03
Denmark west	5.02	0.48	0.13		0.03
PL + CZ + SK	0.41	6.51	2.61	3.50	0.04
France	25.71	3.26	0.15	4.87	0.04
Iberia	3.21	9.72	0.09	12.00	0.04
Italy	0.03	5.21	0.07	8.13	0.03
Northern Europe		3.19		2.74	0.04
Germany	10.11	11.12	2.93	8.23	0.55
UK + IE	31.32	3.17	5.35	2.89	0.04

Tab. C 64: Region-specific installed storage converter capacity in GW (including old existing PHS capacities) for the scenario *TempRes_6h*. The table refers to Fig. 29. The 20 German model regions are aggregated in this table.

	H_2	Li-ion	aCAES	PHS	Redox-flow
Austria + Switzerland	0.02	0.37	0.04	4.48	0.03
BeNeLux	9.19	0.51	1.94	2.85	0.04
Denmark west	4.90	0.62	0.16		0.04
PL + CZ + SK	0.57	2.93	2.11	3.50	0.04
France	24.75	0.58	0.17	4.82	0.04
Iberia	3.22	2.24	0.11	13.55	0.05
Italy	0.04	0.83	0.09	8.35	0.05
Northern Europe		2.35		2.45	0.05
Germany	10.21	8.44	2.71	8.23	0.70
UK + IE	31.29	1.34	4.85	2.93	0.06

Tab. C 65: Region-specific installed storage converter capacity in GW (including old existing PHS capacities) for the scenario *Weather 2007*. The table refers to Fig. 29. The 20 German model regions are aggregated in this table.

	H_2	Li-ion	aCAES	PHS	Redox-flow
Austria + Switzerland	-	0.10	0.01	4.39	0.01
BeNeLux	10.99	0.67	2.76	2.86	0.01
Denmark west	5.61	0.18	0.83	-	0.01
PL + CZ + SK	1.80	2.76	3.83	3.50	0.01
France	28.36	2.50	0.11	4.83	0.01
Iberia	1.42	13.26	0.04	11.77	0.01
Italy	0.01	4.15	0.04	8.31	0.01
Northern Europe	-	3.36	-	2.79	0.02
Germany	9.54	7.16	4.83	8.23	0.18
UK + IE	24.83	3.14	7.14	2.88	0.01

Tab. C 66: Region-specific installed storage converter capacity in GW (including old existing PHS capacities) for the scenario *Weather 2008*. The table refers to Fig. 29. The 20 German model regions are aggregated in this table.

	H_2	Li-ion	aCAES	PHS	Redox-flow
Austria + Switzerland	0.02	0.49	0.05	4.47	0.04
BeNeLux	11.91	0.80	2.91	2.84	0.06
Denmark west	4.42	0.86	0.25	-	0.06
PL + CZ + SK	1.80	4.52	2.67	3.50	0.06
France	25.66	1.98	4.29	4.90	0.06
Iberia	2.82	13.15	0.19	11.74	0.07
Italy	0.06	5.12	0.14	8.20	0.05
Northern Europe	-	3.65	-	2.91	0.07
Germany	10.06	14.25	3.57	8.23	0.92
UK + IE	27.46	8.50	7.94	2.92	0.07

Tab. C 67: Region-specific installed storage converter capacity in GW (including old existing PHS capacities) for the scenario *Weather 2009*. The table refers to Fig. 29. The 20 German model regions are aggregated in this table.

	H_2	Li-ion	aCAES	PHS	Redox-flow
Austria + Switzerland	0.02	0.65	0.06	4.41	0.06
BeNeLux	10.90	1.38	4.21	2.86	0.08
Denmark west	5.36	1.15	0.55	-	0.08
PL + CZ + SK	0.15	7.34	1.64	3.50	0.08
France	23.17	6.77	3.33	4.96	0.09
Iberia	0.97	15.08	0.26	12.73	0.09
Italy	0.26	7.51	0.48	7.95	0.07
Northern Europe	-	4.37	-	2.71	0.10
Germany	7.79	18.57	5.31	8.23	1.22
UK + IE	28.10	4.00	3.81	2.92	0.10

Tab. C 68: Region-specific installed storage converter capacity in GW (including old existing PHS capacities) for the scenario *Weather 2011*. The table refers to Fig. 29. The 20 German model regions are aggregated in this table.

	H_2	Li-ion	aCAES	PHS	Redox-flow
Austria + Switzerland	0.02	0.56	0.06	4.41	0.05
BeNeLux	14.85	1.56	1.74	2.86	0.07
Denmark west	5.56	1.15	0.31	-	0.07
PL + CZ + SK	0.17	6.95	2.38	3.50	0.07
France	22.52	2.93	6.52	4.87	0.07
Iberia	1.14	14.71	0.28	11.94	0.08
Italy	0.08	5.78	0.14	7.48	0.06
Northern Europe	-	5.96	-	2.95	0.10
Germany	11.38	17.46	4.06	8.23	1.08
UK + IE	26.85	9.52	1.86	3.17	0.09

Tab. C 69: Region-specific installed storage converter capacity in GW (including old existing PHS capacities) for the scenario *Weather 2012*. The table refers to Fig. 29. The 20 German model regions are aggregated in this table.

	H_2	Li-ion	aCAES	PHS	Redox-flow
Austria + Switzerland	0.02	0.44	0.04	4.39	0.04
BeNeLux	12.24	0.85	5.95	2.84	0.05
Denmark west	4.99	0.92	0.56	-	0.05
PL + CZ + SK	0.41	7.59	1.47	3.50	0.05
France	24.38	2.37	4.28	4.94	0.06
Iberia	1.49	17.19	0.22	11.30	0.06
Italy	0.08	8.25	0.19	7.83	0.05
Northern Europe	-	5.95	-	2.69	0.07
Germany	8.79	14.39	5.26	8.23	0.83
UK + IE	21.77	9.15	10.11	2.98	0.07

Tab. C 70: Region-specific installed storage converter capacity in GW (including old existing PHS capacities) for the scenario *Redox-flow_Inv_low*. The table refers to Fig. 29. The 20 German model regions are aggregated in this table.

	H_2	Li-ion	aCAES	PHS	Redox-flow
Austria + Switzerland	0.02	0.51	0.05	4.52	0.06
BeNeLux	8.02	1.79	0.21	2.85	2.92
Denmark west	4.57	0.93	0.13	-	0.14
PL + CZ + SK	0.28	5.46	0.22	3.50	3.77
France	25.37	3.29	0.22	4.89	0.42
Iberia	3.10	9.82	0.14	12.12	0.20
Italy	0.05	6.30	0.11	8.06	0.15
Northern Europe	-	1.61	-	3.01	8.62
Germany	9.30	14.16	0.93	8.23	5.86
UK + IE	31.06	5.08	3.52	2.94	2.11

Tab. C 71: Region-specific installed storage converter capacity in GW (excluding old existing PHS capacities) for the scenario *PHS_w/o_old_stock*. The table refers to Fig. 29. The 20 German model regions are aggregated in this table.

	H_2	Li-ion	aCAES	PHS	Redox-flow
Austria + Switzerland	0.04	1.15	0.13	1.38	0.10
BeNeLux	9.50	3.65	3.79	0.44	0.12
Denmark west	4.98	1.64	0.37	-	0.12
PL + CZ + SK	0.69	10.15	3.28	-	0.12
France	27.10	7.10	1.14	0.58	0.14
Iberia	3.56	13.96	0.37	8.06	0.14
Italy	0.12	9.70	0.42	3.63	0.13
Northern Europe	-	4.78	-	1.45	0.15
Germany	10.19	28.08	4.23	-	1.92
UK + IE	31.07	6.87	6.57	0.44	0.14

9.3. Storage converter capacity in Germany

Tab. C 72: Overall model endogenously derived storage converter power (in GW) for all German model regions (including existing PHS capacities) and the scenarios *reference, Stor_Inv_low*, and *Stor_Inv_high*.

Reference scenario																		
	Amp.1	Amp.2	Amp.3	Amp.4	Amp.5	Amp.6	Transn.1	Transn.2	Tennet1	Tennet2	Tennet3	Tennet4	Tennet5	Tennet6	50Hertz1	50Hertz2	50Hertz3	50Hertz4
H_2	-	3.50	-	-	-	-	-	-	0.37	5.31	0.03	0.04	-	-	0.83	-	0.03	-
Li-ion	0.71	0.86	0.92	1.14	1.72	0.60	0.79	0.62	0.73	0.85	0.79	0.72	1.06	0.78	1.42	0.64	0.64	0.66
aCAES	-	0.62	-	-	-	-	-	-	0.22	0.59	0.10	0.10	-	-	1.38	-	0.10	-
PHS	-	-	0.30	-	-	-	-	3.45	-	0.12	0.22	0.58	0.47	0.31	-	-	1.60	1.17
Redox-fl.	0.05	0.06	0.05	0.05	0.06	0.05	0.05	0.05	0.05	0.06	0.05	0.05	0.05	0.05	0.05	0.05	0.05	0.05
Total	0.76	5.03	1.28	1.20	1.77	0.64	0.84	4.12	1.38	6.92	1.18	1.49	1.58	1.14	3.70	0.68	2.41	1.88

Stor_Inv_low																		
H_2	-	4.03	-	-	-	-	-	-	0.96	7.54	0.03	0.18	-	-	2.56	-	0.03	-
Li-ion	0.56	0.90	1.00	1.69	2.00	0.57	0.75	0.51	0.57	0.69	1.10	0.89	1.36	1.22	2.47	0.76	0.57	0.85
aCAES	-	0.55	-	-	-	-	-	-	0.17	1.69	0.07	0.08	-	-	1.76	-	0.07	-
PHS	-	-	0.30	-	-	-	-	3.45	-	0.12	0.22	0.58	0.47	0.31	-	-	1.60	1.17
Redox-fl.	0.04	0.04	0.04	0.04	0.04	0.03	0.04	0.03	0.04	0.04	0.03	0.03	0.04	0.04	0.04	0.03	0.03	0.03
Total	0.60	5.53	1.34	1.73	2.04	0.60	0.79	4.00	1.74	10.08	1.46	1.77	1.87	1.57	6.82	0.79	2.31	2.06

Stor_Inv_high																		
H_2	-	2.54	-	-	-	-	-	-	0.30	4.18	0.02	0.03	-	-	0.10	-	0.03	-
Li-ion	0.74	0.89	0.89	0.92	1.51	0.58	0.82	0.62	0.78	0.90	0.73	0.70	0.92	0.69	1.41	0.59	0.63	0.62
aCAES	-	0.30	-	-	-	-	-	-	0.24	0.32	0.10	0.10	-	-	0.42	-	0.09	-
PHS	-	-	0.30	-	-	-	-	3.45	-	0.12	0.22	0.58	0.47	0.31	-	-	1.60	1.17
Redox-fl.	0.05	0.06	0.06	0.05	0.06	0.05	0.06	0.05	0.06	0.06	0.05	0.05	0.05	0.05	0.06	0.05	0.05	0.05
Total	0.79	3.79	1.24	0.97	1.57	0.63	0.87	4.13	1.38	5.58	1.12	1.45	1.44	1.05	1.99	0.64	2.40	1.84

Tab. C 73: Overall model endogenously derived storage converter power (in GW) for all German model regions (including existing PHS capacities) and the scenarios *VRE_Inv_low*, *VRE_Inv_high*, and *FP_low*.

VRE_Inv_low																		
	Amp.1	Amp.2	Amp.3	Amp.4	Amp.5	Amp.6	Transnet1	Transnet2	Tennet1	Tennet2	Tennet3	Tennet4	Tennet5	Tennet6	50Hertz1	50Hertz2	50Hertz3	50Hertz4
H_2	-	3.33	-	-	-	-	-	-	0.29	3.60	0.03	0.04	-	-	0.38	-	0.03	-
Li-ion	0.70	0.81	0.81	0.87	1.73	0.58	0.74	0.59	0.69	0.80	0.72	0.70	1.10	0.73	1.33	0.57	0.62	0.62
aCAES	-	0.28	-	-	-	-	-	-	0.22	0.27	0.11	0.13	-	-	1.04	-	0.10	-
PHS	-	-	0.30	-	-	-	-	3.45	-	0.12	0.22	0.58	0.47	0.31	-	-	1.60	1.17
Redox-fl.	0.05	0.05	0.05	0.05	0.05	0.04	0.05	0.05	0.05	0.05	0.05	0.05	0.05	0.05	0.05	0.04	0.05	0.05
Total	0.75	4.47	1.16	0.92	1.79	0.62	0.79	4.09	1.25	4.84	1.12	1.50	1.62	1.09	2.80	0.61	2.40	1.83

VRE_Inv_high																		
H_2	-	3.82	-	-	-	-	-	-	0.59	5.48	0.03	0.04	-	-	0.94	-	0.04	-
Li-ion	0.77	0.95	0.95	1.21	1.58	0.66	0.86	0.67	0.80	0.95	0.85	0.77	1.25	0.97	1.89	0.69	0.73	0.81
aCAES	-	0.64	-	-	-	-	-	-	0.21	1.17	0.09	0.10	-	-	1.43	-	0.10	-
PHS	-	-	0.30	-	-	-	-	3.45	-	0.12	0.22	0.58	0.47	0.31	-	-	1.60	1.17
Redox-fl.	0.06	0.06	0.06	0.06	0.06	0.05	0.06	0.05	0.06	0.07	0.06	0.06	0.06	0.06	0.06	0.05	0.05	0.06
Total	0.83	5.48	1.32	1.27	1.65	0.71	0.92	4.18	1.67	7.79	1.24	1.55	1.78	1.34	4.32	0.75	2.53	2.03

FP_low																		
H_2	-	3.40	-	-	-	-	-	-	0.42	5.21	0.03	0.03	-	-	0.61	-	0.03	-
Li-ion	0.69	0.88	0.96	1.04	1.68	0.57	0.83	0.62	0.77	0.88	0.64	0.68	0.89	0.74	1.44	0.55	0.61	0.63
aCAES	-	0.72	-	-	-	-	-	-	0.24	0.70	0.09	0.09	-	-	1.29	-	0.09	-
PHS	-	-	0.30	-	-	-	-	3.45	-	0.12	0.22	0.58	0.47	0.31	-	-	1.60	1.17
Redox-fl.	0.05	0.06	0.06	0.05	0.06	0.05	0.06	0.05	0.06	0.06	0.05	0.05	0.05	0.05	0.06	0.05	0.05	0.05
Total	0.75	5.06	1.32	1.10	1.74	0.62	0.89	4.13	1.48	6.97	1.02	1.43	1.41	1.10	3.39	0.60	2.38	1.84

Tab. C 74: Overall model endogenously derived storage converter power (in GW) for all German model regions (including existing PHS capacities) and the scenarios *FP_high*, *CO_2_low*, and *CO_2_high*.

FP_high																		
	Amp.1	Amp.2	Amp.3	Amp.4	Amp.5	Amp.6	Transnet1	Transnet2	Tennet1	Tennet2	Tennet3	Tennet4	Tennet5	Tennet6	50Hertz1	50Hertz2	50Hertz3	50Hertz4
H_2	-	3.43	-	-	-	-	-	-	0.32	5.31	0.03	0.06	-	-	0.94	-	0.04	-
Li-ion	0.70	0.83	0.99	1.08	1.71	0.59	0.76	0.61	0.73	0.83	0.77	0.73	0.92	0.75	1.31	0.65	0.62	0.63
aCAES	-	0.43	-	-	-	-	-	-	0.23	0.48	0.09	0.11	-	-	1.73	-	0.10	-
PHS	-	-	0.30	-	-	-	-	3.45	-	0.12	0.22	0.58	0.47	0.31	-	-	1.60	1.17
Redox-fl.	0.05	0.05	0.05	0.05	0.05	0.05	0.05	0.05	0.05	0.06	0.05	0.05	0.05	0.05	0.05	0.05	0.05	0.05
Total	0.76	4.74	1.34	1.13	1.76	0.64	0.82	4.11	1.33	6.80	1.16	1.53	1.45	1.10	4.03	0.70	2.41	1.85

CO_2_low																		
H_2	-	3.39	-	-	-	-	-	-	0.29	5.16	0.02	0.04	-	-	0.64	-	0.03	-
Li-ion	0.65	0.78	0.90	0.99	1.61	0.53	0.71	0.55	0.67	0.76	0.73	0.67	0.91	0.68	1.23	0.61	0.56	0.56
aCAES	-	0.44	-	-	-	-	-	-	0.23	0.51	0.09	0.10	-	-	1.66	-	0.08	-
PHS	-	-	0.30	-	-	-	-	3.45	-	0.12	0.22	0.58	0.47	0.31	-	-	1.60	1.17
Redox-fl.	0.05	0.05	0.05	0.05	0.05	0.04	0.05	0.04	0.05	0.05	0.04	0.04	0.05	0.04	0.05	0.04	0.04	0.04
Total	0.69	4.66	1.25	1.04	1.66	0.58	0.76	4.05	1.23	6.61	1.11	1.43	1.42	1.03	3.57	0.65	2.32	1.77

CO_2_high																		
H_2	-	3.64	-	-	-	-	-	-	0.46	5.42	0.03	0.04	-	-	0.92	-	0.03	-
Li-ion	0.69	0.79	1.00	1.11	1.57	0.58	0.76	0.61	0.71	0.78	0.78	0.69	1.09	0.80	1.18	0.81	0.59	0.60
aCAES	-	0.69	-	-	-	-	-	-	0.22	0.60	0.14	0.12	-	-	1.42	-	0.10	-
PHS	-	-	0.30	-	-	-	-	3.45	-	0.12	0.22	0.58	0.47	0.31	-	-	1.60	1.17
Redox-fl.	0.05	0.05	0.05	0.05	0.05	0.05	0.05	0.05	0.05	0.05	0.05	0.05	0.05	0.05	0.05	0.05	0.05	0.05
Total	0.74	5.17	1.36	1.16	1.62	0.63	0.81	4.11	1.44	6.98	1.22	1.48	1.61	1.15	3.57	0.86	2.38	1.82

Tab. C 75: Overall model endogenously derived storage converter power (in GW) for all German model regions (including existing PHS capacities) and the scenarios *G++*, *G+*, and *G+_Inv_high*.

G++																		
	Amp.1	Amp.2	Amp.3	Amp.4	Amp.5	Amp.6	Transnet1	Transnet2	Tennet1	Tennet2	Tennet3	Tennet4	Tennet5	Tennet6	50Hertz1	50Hertz2	50Hertz3	50Hertz4
H_2	-	3.84	-	-	-	-	-	-	1.16	4.32	0.27	0.41	-	-	4.32	-	0.32	-
Li-ion	0.24	3.23	0.24	1.12	1.12	0.14	3.23	0.12	3.23	3.23	0.12	0.25	0.25	0.16	3.23	0.16	0.14	0.16
aCAES	-	-	-	-	-	-	-	-	-	-	-	-	-	-	-	-	-	-
PHS	-	-	0.30	-	-	-	-	3.45	-	0.12	0.22	0.58	0.47	0.31	-	-	1.60	1.17
Redox-fl.	-	-	-	-	-	-	-	-	-	-	-	-	-	-	-	-	-	-
Total	0.24	7.08	0.54	1.12	1.12	0.14	3.23	3.57	4.40	7.68	0.61	1.24	0.72	0.47	7.55	0.16	2.07	1.33

G+																		
H_2	-	0.07	-	-	-	-	-	-	0.09	0.09	0.08	0.05	-	-	0.05	-	0.03	-
Li-ion	0.75	0.57	0.58	0.76	0.74	0.37	0.52	0.35	0.74	0.64	0.76	0.47	0.49	0.39	1.40	0.92	0.39	0.49
aCAES	-	0.07	-	-	-	-	-	-	0.08	0.08	0.09	0.07	-	-	0.09	-	0.06	-
PHS	-	-	0.30	-	-	-	-	3.45	-	0.12	0.22	0.58	0.47	0.31	-	-	1.60	1.17
Redox-fl.	0.01	0.01	0.01	0.01	0.01	0.01	0.01	0.01	0.01	0.01	0.01	0.01	0.01	0.01	0.01	0.01	0.01	0.01
Total	0.77	0.73	0.90	0.77	0.76	0.38	0.54	3.81	0.92	0.94	1.16	1.18	0.97	0.71	1.56	0.93	2.10	1.67

G+_Inv_high																		
H_2	-	0.14	-	-	-	-	-	-	0.18	0.20	0.14	0.10	-	-	0.11	-	0.07	-
Li-ion	0.86	0.79	0.86	0.92	0.87	0.66	0.74	0.65	0.79	0.82	0.88	0.81	0.79	0.71	0.88	0.86	0.71	0.72
aCAES	-	0.21	-	-	-	-	-	-	0.28	0.25	0.20	0.16	-	-	0.23	-	0.14	-
PHS	-	-	0.30	-	-	-	-	3.45	-	0.12	0.22	0.58	0.47	0.31	-	-	1.60	1.17
Redox-fl.	0.04	0.04	0.04	0.04	0.04	0.04	0.04	0.04	0.04	0.04	0.04	0.04	0.04	0.04	0.04	0.04	0.04	0.04
Total	0.90	1.19	1.20	0.96	0.91	0.70	0.77	4.15	1.28	1.42	1.48	1.69	1.30	1.06	1.25	0.90	2.57	1.93

Tab. C 76: Overall model endogenously derived storage converter power (in GW) for all German model regions (including existing PHS capacities) and the scenarios *G+_Inv_veryhigh, Cur003*, and *Cur010*.

G+_Inv_veryhigh																		
	Amp.1	Amp.2	Amp.3	Amp.4	Amp.5	Amp.6	Transnet1	Transnet2	Tennet1	Tennet2	Tennet3	Tennet4	Tennet5	Tennet6	50Hertz1	50Hertz2	50Hertz3	50Hertz4
H_2	-	0.34	-	-	-	-	-	-	0.43	0.46	0.31	0.23	-	-	0.25	-	0.19	-
Li-ion	1.78	1.72	1.77	1.80	1.74	1.63	1.69	1.66	1.74	1.75	1.79	1.69	1.66	1.65	1.80	1.73	1.63	1.65
aCAES	-	0.49	-	-	-	-	-	-	0.33	0.51	0.44	0.41	-	-	0.51	-	0.37	-
PHS	-	-	0.30	-	-	-	-	3.45	-	0.12	0.22	0.58	0.47	0.31	-	-	1.60	1.17
Redox-fl.	0.15	0.14	0.14	0.15	0.14	0.14	0.14	0.14	0.15	0.15	0.14	0.14	0.14	0.14	0.14	0.15	0.14	0.14
Total	1.93	2.70	2.22	1.95	1.88	1.77	1.84	5.26	2.64	2.98	2.90	3.06	2.27	2.10	2.71	1.88	3.94	2.96
Cur003																		
H_2	-	3.58	-	-	-	-	-	-	0.23	5.88	0.02	0.02	-	-	1.05	-	0.02	-
Li-ion	0.49	0.69	0.74	1.01	1.79	0.38	0.57	0.39	0.51	0.71	0.63	0.52	0.87	0.61	1.47	0.44	0.40	0.39
aCAES	-	0.47	-	-	-	-	-	-	0.17	0.78	0.05	0.06	-	-	1.74	-	0.05	-
PHS	-	-	0.30	-	-	-	-	3.45	-	0.12	0.22	0.58	0.47	0.31	-	-	1.60	1.17
Redox-fl.	0.03	0.03	0.03	0.03	0.03	0.03	0.03	0.03	0.03	0.03	0.03	0.03	0.03	0.03	0.03	0.03	0.03	0.03
Total	0.52	4.77	1.08	1.04	1.82	0.41	0.61	3.87	0.94	7.52	0.95	1.21	1.37	0.95	4.30	0.47	2.10	1.58
Cur010																		
H_2	-	3.65	-	-	-	-	-	-	0.20	5.39	0.01	0.02	-	-	0.83	-	0.01	-
Li-ion	0.40	0.54	0.69	0.89	1.70	0.34	0.48	0.29	0.39	0.50	0.64	0.50	0.93	0.53	1.20	0.41	0.34	0.37
aCAES	-	0.54	-	-	-	-	-	-	0.15	0.62	0.04	0.05	-	-	1.46	-	0.04	-
PHS	-	-	0.30	-	-	-	-	3.45	-	0.12	0.22	0.58	0.47	0.31	-	-	1.60	1.17
Redox-fl.	0.02	0.02	0.02	0.02	0.03	0.02	0.02	0.02	0.02	0.03	0.02	0.02	0.02	0.02	0.02	0.02	0.02	0.02
Total	0.42	4.76	1.02	0.91	1.73	0.36	0.50	3.77	0.76	6.66	0.94	1.17	1.42	0.86	3.51	0.43	2.03	1.57

Tab. C 77: Overall model endogenously derived storage converter power (in GW) for all German model regions (including existing PHS capacities) and the scenarios *VRE_exp_CO₂_med*, *VRE_exp_CO₂_high,* and *VRE_exp_CO₂_veryhigh*.

VRE_exp_CO2_med																		
	Amp.1	Amp.2	Amp.3	Amp.4	Amp.5	Amp.6	Transnet1	Transnet2	Tennet1	Tennet2	Tennet3	Tennet4	Tennet5	Tennet6	50Hertz1	50Hertz2	50Hertz3	50Hertz4
H_2	-	0.01	-	-	-	-	-	-	0.01	0.01	0.01	0.01	-	-	0.01	-	0.01	-
Li-ion	0.19	0.38	0.19	0.17	0.24	0.13	0.23	0.14	0.26	0.79	0.18	0.14	0.13	0.15	0.20	0.20	0.13	0.13
aCAES	-	0.05	-	-	-	-	-	-	0.04	0.19	0.04	0.03	-	-	0.05	-	0.03	-
PHS	-	-	0.30	-	-	-	-	3.45	-	0.12	0.22	0.58	0.47	0.31	-	-	1.60	1.17
Redox-fl.	0.01	0.01	0.01	0.01	0.01	0.01	0.01	0.01	0.01	0.01	0.01	0.01	0.01	0.01	0.01	0.01	0.01	0.01
Total	0.20	0.44	0.50	0.18	0.25	0.14	0.25	3.60	0.32	1.13	0.45	0.76	0.61	0.47	0.26	0.21	1.77	1.31

VRE_exp_CO2_high																		
H_2	-	0.13	-	-	-	-	-	-	0.06	1.50	0.01	0.01	-	-	0.02	-	0.01	-
Li-ion	0.33	0.72	0.38	0.75	0.77	0.28	0.49	0.22	0.39	0.66	0.49	0.36	1.49	0.43	1.40	0.24	0.33	0.38
aCAES	-	0.17	-	-	-	-	-	-	0.09	0.68	0.04	0.04	-	-	0.24	-	0.04	-
PHS	-	-	0.30	-	-	-	-	3.45	-	0.12	0.22	0.58	0.47	0.31	-	-	1.60	1.17
Redox-fl.	0.02	0.02	0.02	0.02	0.02	0.02	0.02	0.02	0.02	0.02	0.02	0.02	0.02	0.02	0.02	0.02	0.02	0.02
Total	0.34	1.04	0.70	0.77	0.79	0.30	0.51	3.69	0.56	2.97	0.78	1.01	1.98	0.76	1.69	0.26	2.00	1.57

VRE_exp_CO2_veryhigh																		
H_2	-	1.30	-	-	-	-	-	-	0.12	3.37	0.01	0.01	-	-	0.06	-	0.01	-
Li-ion	0.35	0.62	0.54	0.82	1.18	0.33	0.50	0.25	0.40	0.58	0.39	0.39	1.78	0.46	1.61	0.24	0.34	0.38
aCAES	-	0.29	-	-	-	-	-	-	0.12	0.81	0.05	0.05	-	-	0.92	-	0.05	-
PHS	-	-	0.30	-	-	-	-	3.45	-	0.12	0.22	0.58	0.47	0.31	-	-	1.60	1.17
Redox-fl.	0.02	0.02	0.02	0.02	0.02	0.02	0.02	0.02	0.02	0.02	0.02	0.02	0.02	0.02	0.02	0.02	0.02	0.02
Total	0.37	2.23	0.87	0.84	1.20	0.35	0.52	3.72	0.66	4.91	0.68	1.04	2.27	0.79	2.62	0.26	2.03	1.57

Tab. C 78: Overall model endogenously derived storage converter power (in GW) for all German model regions (including existing PHS capacities) and the scenarios *TempRes_2h* and *TempRes_6h*.

TempRes_2h																		
	Amp.1	Amp.2	Amp.3	Amp.4	Amp.5	Amp.6	Transnet1	Transnet2	Tennet1	Tennet2	Tennet3	Tennet4	Tennet5	Tennet6	50Hertz1	50Hertz2	50Hertz3	50Hertz4
H_2	-	3.60	-	-	-	-	-	-	0.26	5.37	0.02	0.02	-	-	0.83	-	0.02	-
Li-ion	0.45	0.55	0.66	0.82	1.43	0.39	0.51	0.34	0.45	0.53	0.61	0.51	0.92	0.54	1.18	0.43	0.40	0.42
aCAES	-	0.58	-	-	-	-	-	-	0.20	0.60	0.06	0.07	-	-	1.37	-	0.06	-
PHS	-	-	0.30	-	-	-	-	3.45	-	0.12	0.22	0.58	0.47	0.31	-	-	1.60	1.17
Redox-fl.	0.03	0.03	0.03	0.03	0.03	0.03	0.03	0.03	0.03	0.03	0.03	0.03	0.03	0.03	0.03	0.03	0.03	0.03
Total	0.48	4.76	1.00	0.85	1.46	0.42	0.54	3.82	0.93	6.65	0.93	1.21	1.42	0.88	3.41	0.46	2.11	1.62

TempRes_6h																		
H_2	-	3.54	-	-	-	-	-	-	0.33	5.49	0.02	0.03	-	-	0.78	-	0.03	-
Li-ion	0.44	0.49	0.48	0.57	0.72	0.39	0.48	0.43	0.48	0.50	0.40	0.41	0.47	0.42	0.59	0.38	0.40	0.40
aCAES	-	0.58	-	-	-	-	-	-	0.20	0.63	0.07	0.08	-	-	1.08	-	0.07	-
PHS	-		0.30	-	-	-	-	3.45	-	0.12	0.22	0.58	0.47	0.31	-	-	1.60	1.17
Redox-fl.	0.04	0.04	0.04	0.04	0.04	0.04	0.04	0.04	0.04	0.04	0.04	0.04	0.04	0.04	0.04	0.04	0.04	0.04
Total	0.48	4.64	0.83	0.61	0.76	0.43	0.52	3.92	1.05	6.79	0.75	1.14	0.98	0.76	2.49	0.42	2.13	1.60

Tab. C 79: Overall model endogenously derived storage converter power (in GW) for all German model regions (including existing PHS capacities) and the scenarios *weather 2007*, *weather 2008*, and *weather 2009*.

Weather 2007																		
	Amp.1	Amp.2	Amp.3	Amp.4	Amp.5	Amp.6	Transnet1	Transnet2	Tennet1	Tennet2	Tennet3	Tennet4	Tennet5	Tennet6	50Hertz1	50Hertz2	50Hertz3	50Hertz4
H_2	-	3.45	-	-	-	-	-	-	0.09	4.70	0.01	0.01	-	-	1.27	-	0.01	-
Li-ion	0.15	0.19	0.33	0.76	1.20	0.30	0.18	0.13	0.17	0.18	0.42	0.23	0.80	0.62	0.77	0.41	0.15	0.18
aCAES	-	0.74	-	-	-	-	-	-	0.20	2.17	0.02	0.02	-	-	1.66	-	0.02	-
PHS	-		0.30	-	-	-	-	3.45	-	0.12	0.22	0.58	0.47	0.31	-	-	1.60	1.17
Redox-fl.	0.01	0.01	0.01	0.01	0.01	0.01	0.01	0.01	0.01	0.01	0.01	0.01	0.01	0.01	0.01	0.01	0.01	0.01
Total	0.16	4.39	0.64	0.77	1.21	0.30	0.19	3.59	0.47	7.19	0.68	0.85	1.28	0.94	3.71	0.42	1.79	1.36

Weather 2008																		
H_2	-	3.27	-	-	-	-	-	-	0.35	5.05	0.03	0.04	-	-	1.29	-	0.03	-
Li-ion	0.61	0.69	0.85	0.99	1.41	0.58	0.68	0.57	0.66	0.71	0.77	0.67	0.95	0.84	1.34	0.67	0.61	0.64
aCAES	-	0.70	-	-	-	-	-	-	0.23	1.08	0.09	0.11	-	-	1.28	-	0.08	-
PHS	-		0.30	-	-	-	-	3.45	-	0.12	0.22	0.58	0.47	0.31	-	-	1.60	1.17
Redox-fl.	0.05	0.05	0.05	0.05	0.06	0.05	0.05	0.05	0.05	0.06	0.05	0.05	0.05	0.05	0.05	0.05	0.05	0.05
Total	0.67	4.72	1.21	1.05	1.46	0.62	0.73	4.07	1.29	7.02	1.16	1.45	1.47	1.20	3.97	0.72	2.37	1.86

Weather 2009																		
H_2	-	2.87	-	-	-	-	-	-	0.44	3.90	0.03	0.04	-	-	0.48	-	0.03	-
Li-ion	0.82	0.96	1.06	1.47	1.93	0.75	0.92	0.76	0.89	0.96	0.95	0.84	1.08	1.02	1.79	0.81	0.77	0.79
aCAES	-	0.66	-	-	-	-	-	-	0.23	2.60	0.11	0.12	-	-	1.48	-	0.10	-
PHS	-		0.30	-	-	-	-	3.45	-	0.12	0.22	0.58	0.47	0.31	-	-	1.60	1.17
Redox-fl.	0.07	0.07	0.07	0.07	0.08	0.06	0.07	0.06	0.07	0.07	0.06	0.06	0.06	0.07	0.07	0.06	0.06	0.06
Total	0.89	4.56	1.44	1.54	2.01	0.81	0.99	4.28	1.63	7.65	1.38	1.63	1.62	1.39	3.83	0.87	2.58	2.02

Tab. C 80: Overall model endogenously derived storage converter power (in GW) for all German model regions (including existing PHS capacities) and the scenarios *weather 2011 and weather 2012*.

Weather 2011																		
	Amp.1	Amp.2	Amp.3	Amp.4	Amp.5	Amp.6	Transnet1	Transnet2	Tennet1	Tennet2	Tennet3	Tennet4	Tennet5	Tennet6	50Hertz1	50Hertz2	50Hertz3	50Hertz4
H_2	-	4.13	-	-	-	-	-	-	0.42	5.17	0.03	0.04	-	-	1.54	-	0.04	-
Li-ion	0.77	0.92	1.04	1.34	1.93	0.66	0.87	0.66	0.81	0.93	0.91	0.77	1.26	0.85	1.55	0.71	0.73	0.75
aCAES	-	0.61	-	-	-	-	-	-	0.21	1.24	0.09	0.11	-	-	1.70	-	0.10	-
PHS	-	-	0.30	-	-	-	-	3.45	-	0.12	0.22	0.58	0.47	0.31	-	-	1.60	1.17
Redox-fl.	0.06	0.06	0.06	0.06	0.07	0.05	0.06	0.06	0.06	0.07	0.06	0.06	0.06	0.06	0.06	0.05	0.06	0.06
Total	0.83	5.72	1.40	1.41	1.99	0.71	0.93	4.17	1.51	7.53	1.31	1.55	1.79	1.22	4.86	0.76	2.53	1.97

Weather 2012																		
H_2	-	2.94	-	-	-	-	-	-	0.31	4.43	0.02	0.03	-	-	1.02	-	0.03	-
Li-ion	0.56	0.65	0.80	1.16	1.66	0.52	0.64	0.51	0.61	0.63	0.76	0.65	0.91	0.66	1.93	0.63	0.55	0.56
aCAES	-	0.75	-	-	-	-	-	-	0.23	2.78	0.09	0.10	-	-	1.24	-	0.07	-
PHS	-		0.30	-	-	-	-	3.45	-	0.12	0.22	0.58	0.47	0.31	-	-	1.60	1.17
Redox-fl.	0.05	0.05	0.05	0.05	0.05	0.04	0.05	0.04	0.05	0.05	0.04	0.04	0.04	0.04	0.05	0.04	0.04	0.04
Total	0.60	4.39	1.16	1.21	1.71	0.57	0.69	4.01	1.20	8.02	1.13	1.40	1.43	1.01	4.24	0.68	2.29	1.77

Tab. C 81: Overall model endogenously derived storage converter power (in GW) for all German model regions and the scenarios *Redox-flow_Inv_low* and *PHS_w/o_old_stock*. Scenario *Redox-flow_Inv_low* includes the existing PHS capacities; scenario *PHS_w/o_old_stock* assumes no existing PHS capacities.

Redox-flow_Inv_low																		
	Amp.1	Amp.2	Amp.3	Amp.4	Amp.5	Amp.6	Transnet1	Transnet2	Tennet1	Tennet2	Tennet3	Tennet4	Tennet5	Tennet6	50Hertz1	50Hertz2	50Hertz3	50Hertz4
H_2	-	3.25	-	-	-	-	-	-	0.35	5.04	0.03	0.04	-	-	0.57	-	0.03	
Li-ion	0.68	0.78	0.80	0.92	1.11	0.58	0.73	0.59	0.70	0.79	0.81	0.72	1.09	0.71	1.15	0.65	0.65	0.67
aCAES	-	0.17	-	-	-	-	-	-	0.14	0.18	0.08	0.09	-	-	0.19	-	0.08	-
PHS	-	-	0.30	-	-	-	-	3.45	-	0.12	0.22	0.58	0.47	0.31	-	-	1.60	1.17
Redox-fl.	0.17	0.52	0.27	0.25	0.72	0.08	0.27	0.09	0.20	0.73	0.12	0.12	0.17	0.11	1.72	0.08	0.11	0.11
Total	0.86	4.73	1.37	1.17	1.84	0.66	1.00	4.14	1.40	6.87	1.26	1.55	1.73	1.13	3.64	0.73	2.46	1.96

PHS_w/o_old_stock																		
H_2	-	3.44	-	-	-	-	-	-	0.66	5.02	0.05	0.07	-	-	0.89	-	0.06	-
Li-ion	1.34	1.49	1.66	1.50	2.26	1.17	1.44	1.98	1.37	1.50	1.38	1.48	1.58	1.53	2.19	1.21	1.35	1.66
aCAES	-	0.76	-	-	-	-	-	-	0.28	1.08	0.17	0.25	-	-	1.50	-	0.19	-
PHS	-	-	-	-	-	-	-	-	-	-	-	-	-	-	-	-	-	-
Redox-fl.	0.11	0.11	0.11	0.11	0.11	0.10	0.11	0.11	0.11	0.12	0.10	0.10	0.10	0.11	0.11	0.10	0.10	0.10
Total	1.45	5.80	1.77	1.61	2.38	1.27	1.55	2.09	2.43	7.72	1.70	1.89	1.68	1.64	4.69	1.30	1.70	1.76

Appendix D

Model fact sheet

Basic characteristics

Model name: REMix (Renewable Energy Mix)
Author: DLR – German Aerospace Center, Institute of Engineering Thermodynamics
Licence: proprietary
Model scope: development and analysis of energy supply scenarios
Model type: energy system model with cost minimization approach for capacity expansion planning and operation optimization
Technical focus: power supply and its linkages to heat and transport sector

Technical and mathematical basis

Environment: GAMS
Programming technique: linear programming, mixed-integer linear programming
Preferred solver: CPLEX
Consideration of uncertainty: scenario analysis and sensitivities
Deterministic (Y/N): Yes
Objective function: minimization of system costs
Composition of the objective function:

- annuities of all assets
- fixed and variable operational costs of all assets, including fuel costs and CO_2 emission certificate costs
- costs of unsupplied demand, if applicable

Temporal and spatial scope

Typical geographic assessment area: Europe, North Africa, and Middle East
Regional subdivision in Germany: either 18 regions of the transmission system operators' *Regionenmodell* or 16 federal states
Minimum calculation interval: 1 hour
Typical investigation period or years: 2020, 2030, 2040, 2050

Technological coverage

Considered power generation technologies:

- Thermal power plants (e.g. fossil, nuclear, biomass, geothermal, CSP)
- CHP (e.g. fossil, nuclear, biomass, geothermal)
- Other renewables: run-of-the-river hydro power, reservoir hydro power, photovoltaic and wind power

Considered power transmission technologies:

- High-voltage direct current
- High-voltage alternating current

Considered balancing technologies:

- Electricity-to-electricity storage
- Thermal energy storage
- Demand response / demand side management
- Hydrogen electrolysis and storage

Considered linkages to heat and transport sector:

- Electrical heat pumps and boilers
- Battery electric vehicles with adjustable charging and vehicle-to-grid technology
- Hydrogen production from electricity for utilization in fuel cell vehicles and industry
- Methanization and gas network feed-in

Considered system services

- Demand for and provision of secondary and tertiary reserve

Possible restrictions in the composition of the supply system:

- Definition of supply shares and ratios for specific technologies
- Definition of minimum firm power generation capacity
- Definition of domestic supply shares

Curriculum Vitae

Felix Cebulla

born on March 23, 1986

in Weimar, Germany

2012–2017	Researcher	German Aerospace Center (DLR)
2015–2017	PhD candidate	University of Stuttgart and German Aerospace Center Visiting researcher at Stanford University, Department of Civil and Environmental Engineering
2012–2015	Scholarship holder	Helmholtz Research School on Energy Scenarios
2012	Diploma	Graduation from the University of Flensburg, Energy and Environmental Management Study abroad at Victoria University of Wellington, Geographic Information Systems
2010–2011	Research assistant	Fraunhofer Institute for Systems and Innovation Research (ISI), Karlsruhe
2004	Baccalaureate	Friedrich-Schiller-Gymnasium, Weimar

Eidesstattliche Erklärung

Hiermit erkläre ich, diese Arbeit selbständig angefertigt, alle benutzten Hilfsmittel vollständig und genau angegeben sowie alles kenntlich gemacht zu haben, was aus Arbeiten anderer unverändert oder mit Abänderungen entnommen wurde.

Stuttgart, den 13.06.2017

Ort, Datum Unterschrift